2016-11

Development of Traceable Capabilities in Non-Contact Thermal Metrology

Sam Boles
Technological University Dublin

School of Physics
Dublin Institute of Technology (DIT)
Kevin Street,
D08 NF82

Development of Traceable Capabilities in Non-Contact Thermal Metrology

Sam Boles

November 2016

A thesis submitted to the Dublin Institute of Technology for the degree of

Master of Philosophy

Supervised by

Dr Suzanne Martin (DIT)

Dr Izabela Naydenova (DIT)

Dr David Fleming (National Standards Authority of Ireland, NSAI)

Mr Dubhaltach MacLochlainn (NSAI)

Abstract

Accurate temperature measurement is crucial in industry to reduce waste and environmental impact. Industrial use of Radiation Thermometers (RTs) is becoming increasingly common due to their wide market availability, fast response time, large temperature ranges, and their ability to measure temperature without contact. With this growth in use, accurate RT measurements that are traceable to the International Temperature Scale of 1990 (ITS-90) are a growing requirement. Traceable calibrations are usually performed using horizontal Blackbody Cavity Radiation Sources (BCRSs). In the work presented, a unique vertical bath-based BCRS, constructed in-house at the National Standards Authority of Ireland (NSAI), was compared over the range from -30 °C to 150 °C, against a suite of conventional horizontal bath-based BCRSs in overseas National Metrology Institutes (NMIs) and against a previous iteration of this new vertical design. Vertical bath-based BCRSs are more flexible and economical to use than horizontal BCRSs and can take advantage of existing calibration equipment.

In the comparison of BCRSs, it was found that the vertical orientation was comparable to within 0.25 °C of standard horizontal cavities for the range from -30 °C to 150 °C. It was concluded that the vertical configuration is an economical alternative for calibration of RTs within the range assessed. A conservative evaluation of the uncertainty of measurement found that it ranged from ±0.34 °C to ±0.66 °C ($k = 2$).

Alongside this comparison, the calibration of direct-reading, handheld Infrared RTs (often simply referred to as IRTs) was investigated. These are lower-cost instruments that read directly in temperature and do not give access to the unprocessed detector signal. IRTs are the most common type of RT used in industry. IRTs are known to

suffer from poor Size-of-Source Effects (SSEs), which introduce errors caused by scattered radiation from outside the IRT's nominal target area. Variation in readings due to changes in proximity of the detector to the source – the Distance Effect (DE) – has also been found to cause significant errors in IRTs. In the present work, best practice calibration procedures and uncertainty budgets were investigated for IRTs using a case study instrument. The instrument was calibrated over the range from -30 °C to 900 °C, and its SSE and Distance Effect (DE) were measured.

The test case IRT's SSE was measured at three different temperatures to determine its true field of view. The IRT was also tested at five target distances and using a variety of radiation sources to calibrate it and determine its DE. The IRT was found to exceed its specification by 3.7 °C when measuring an 800 °C BCRS and was out of specification across most of the rest of its range. At 500 °C, the IRT reading was found to vary by 1.75 °C across a 500 mm range of distances. The IRT reading was also found to drift by up to 2 °C when kept exposed to a 500 °C source for an hour.

The case study of the IRT highlighted the importance of providing detailed calibration conditions, particularly regarding calibration geometry, IRT housing temperature, and exposure duration. As well as aiding in the establishment of a fit-for-purpose high-level non-contact calibration capability at NSAI, the work presented details a method by which other NMIs can inexpensively develop RT calibration facilities without custom-built baths.

Declaration

I certify that this thesis, which I now submit for examination for the award of MPhil, is entirely my work and has not been taken from the work of others, save and to the extent that such work has been cited and acknowledged within the text of my work.

This thesis was prepared according to the Regulations for Graduate Study by Research of the Dublin Institute of Technology (DIT) and has not been submitted in whole or in part for another award in any other third level institution.

The work reported on in this thesis conforms to the principles and requirements of the DIT's guidelines for ethics in research.

DIT has permission to keep, lend or copy this thesis in whole or in part, on condition that any such use of the material of the thesis be duly acknowledged.

Signature _____ Date _____

Sam Boles

Acknowledgements

Abbreviations

ASTM	American Society for Testing and Materials
BCRS	Blackbody Cavity Radiation Source
BIPM	Bureau International des Poids et Mesures
	(International Bureau of Weights and Measures)
CCT	Consultative Committee on Thermometry of the BIPM
CIPM-MRA	International Committee for Weights and Measures-Mutual Recognition Arrangement
CMC	Calibration and Measurement Capability
CMI	Český Metrologický Institut
	(Czech Metrology Institute, Czech Republic)
CNC	Computer Numerical Control
DE	Distance Effect
DI	Designated Institute
DIT	Dublin Institute of Technology
EURAMET	European Association of National Metrology Institutes
FOV	Field of View
FPBB	Fixed Point Blackbody
GUM	Guidelines to the Expression of Uncertainty in Measurement
HPBB	Heat Pipe Blackbody
IEC	International Electrotechnical Commission
ILC	Interlaboratory Comparison
IEO	The Centre for Industrial and Engineering Optics (DIT)
IRT	Infrared Thermometer or Infrared Radiation Thermometer
ISO	International Organization for Standardization
KC	Key Comparison
LMK	Laboratorij za Metrologijo in Kakovost
	(Laboratory for Metrology and Quality, Slovenia)
LNE-CNAM	Laboratoire National de métrologie et d'Essais, Conservatoire National des Arts et Métiers
	(National Laboratory of Metrology and Testing, National Conservatory of Arts and Crafts, France)

MSL	Measurement Standards Laboratory of New Zealand
NMI	National Metrology Institute
NML	National Metrology Laboratory (Ireland)
NPL	National Physical Laboratory (UK)
NSAI	National Standards Authority of Ireland
OIML	Organisation Internationale de Métrologie Légale (International Organization of Legal Metrology)
PRT	Platinum Resistance Thermometer
PTB	Physikalisch-Technische Bundesanstalt (National Metrology Institute, Germany)
PTFE	Polytetrafluorethylene
RT	Radiation Thermometer
SI	Système International d'unités (International System of Units)
SPRT	Standard Platinum Resistance Thermometer
SSE	Size-of-Source Effect
TI	Thermal Imager
TS	Technical Specification
TPW	Triple Point of Water
TRT	Transfer Radiation Thermometer
UNC	Unified Coarse Thread
UUT	Unit Under Test
VIM	The International Vocabulary of basic and general terms in Metrology
VDI	Verein Deutscher Ingenieure (Association of German Engineers)
VDE	Verband der Elektrotechnik, Elektronik und Informationstechnik (Association for Electrical, Electronic & Information Technologies)
WG5	Working Group 5 on Non-Contact Thermometry, (since renamed Working Group for Non-Contact Thermometry or WGNCTh) of the BIPM Consultative Committee on Thermometry (CCT)

Table of Contents

List of Figures

List of Tables

Chapter 1.   Introduction

1.1   Background to Research

Metrology is the science of measurement. The National Metrology Laboratory (NML, a division of NSAI – the National Standards Authority of Ireland) is tasked with *maintaining* and *disseminating* the national representations of the SI units for Ireland. The first responsibility entails physically realising or maintaining certain units under controlled conditions and performing key comparisons with other National Metrology Institutes (NMIs). These units and their derived units are disseminated to industry via a calibration service. The calibration service involves checking client artefacts (instruments and samples) against reference measurement standards that are part of NSAI's *calibration system* and producing calibration certificates. The calibration system includes measurement standards that are traceable to international standards and that undergo regular rigorous in-house verification at pre-determined intervals.

Temperature measurement is the most widely performed and often most important type of measurement across the manufacturing industry. Accurate measurement and control of temperature underpins numerous industrial processes and is key to ensuring their safety and efficiency and reducing their environmental impact [1].

Radiation thermometry is the measurement of the temperature of an object based on knowledge of the spectral emissivity of that object and the radiant energy emitted from the object [2]. Spectral Emissivity is a dimensionless property of the object's surface relating to how it reflects radiation – at a given wavelength, an object that is perfectly reflective has an emissivity of zero whereas an object that absorbs all incident radiation

has an emissivity of one. Because a perfectly emissive object such as this appears black, it is termed a blackbody. Blackbodies emit radiation of a spectrum that depends only on temperature, according to Planck's Law, as described in section 2.5 [3]. Radiation Thermometers (RTs) are variously termed:

- Non-Contact Thermometers;

- Infrared Thermometers or Infrared Radiation Thermometers (IRTs, as in Figure 1.1 (a)), where the thermometer measures radiation entirely in the infrared spectrum and usually referring to handheld RTs (see section 2.6.1);

- Pyrometers (from *pyr*, meaning 'fire' in Greek), usually where the temperature range extends hundreds of degrees above normal room temperatures; and

- Laser Thermometers, a misnomer that is used due to confusion about the targeting apparatus of RTs, which frequently incorporate lasers, but have no other role in the measuring principle of the RT.

Intermediary and high accuracy examples of RTs are shown in Figure 1.1. (Note that the distinction between RTs and handheld IRTs is used throughout the work presented).

(a)   (b)

Figure 1.1 (a) A handheld RT, model Fluke 574 (of the kind often referred to as IRTs). Image courtesy of Fluke Corporation.
(b) A laboratory-grade RT, model Heitronics TRT IV.82.

In the field of contact thermometry, NSAI NML has published contact Calibration and Measurement Capabilities (CMCs, see 2.2.4) ranging from -75 °C to 1100 °C [4]. NML had begun to assemble some non-contact thermometry equipment prior to the commencement of the work presented in this thesis, but traceability schema had not yet been established, and there were no written procedures available to follow. This inter-NMI research was undertaken in pursuit of the eventual goal of obtaining accreditation in this field through published CMCs and thereby establishing a traceable non-contact calibration facility within NSAI NML.

In order to measure temperature, heat transfer is necessary. Traditional thermometers employ conductive or convective heat transfer through contact with the medium, be that a gas or a liquid, to measure temperature. In practice, the highest achievable calibration accuracy is generally possible via conductive transfer [5, p. 336]. However, there are some applications to which contact measurement is not suited, and measurement of temperature by radiative transfer is preferred. RTs are becoming increasingly widespread and with them comes a growing demand for traceable calibration [6].

The basic principle when calibrating an RT is to target it towards a source apparatus of known temperature. The source instrument is typically a Blackbody Cavity Radiation Source (BCRS, see 2.6.9) or a planar radiator (see section 2.7.3.5). The temperature displayed on the RT and the source reference temperature or the expected RT reading are recorded and produced in a calibration certificate. The certificate enables the user of the RT to apply corrections to the instrument's readings.
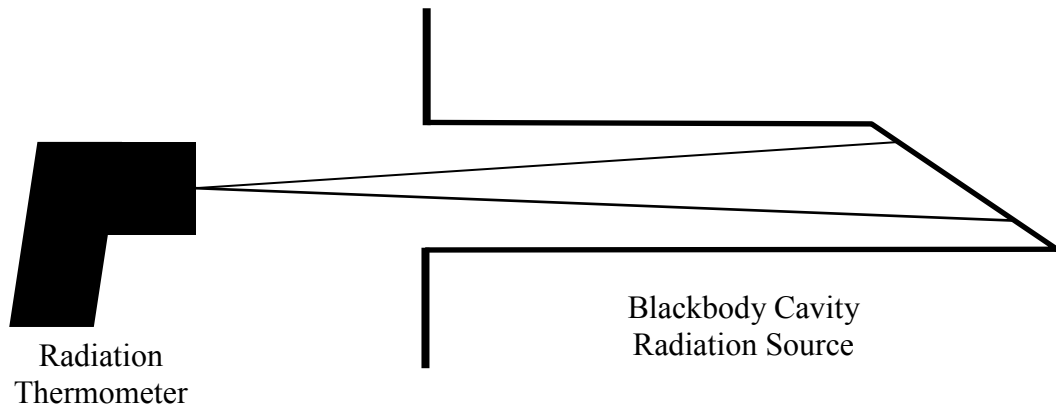
Figure 1.2 Calibration of an RT using a BCRS. The Field of View (FOV) of the RT is also shown.

The International Temperature Scale of 1990 (ITS-90, described in detail in 2.3) specifies radiation thermometry as the primary method to realise the temperature scale for high temperatures (above the freezing point of silver, 961.78 °C), where it is the most accurate means of temperature measurement [7]. The National Metrology Institutes of major industrial countries have thus had high-temperature radiation thermometry capabilities for some time [3], [8], [9]. These NMIs have been well placed to extend their calibration capabilities below the silver point to service the rapidly growing market for RTs operating in this range (above 961.78 °C). Smaller NMIs with more constrained resources must choose a selected complement of services to offer to industry. NSAI NML, in common with other comparable NMIs, has not maintained primary metrology capabilities for high temperatures above 419.527 °C (the freezing point of zinc) and therefore had little experience in non-contact thermometry. As such, providing traceability to the growing area of non-contact thermometry presents a challenge.

The foremost labs in the field operate a primary level metrology service, offering traceability for high-end RTs with low uncertainties. Some manufacturers have developed calibration equipment for low-cost RTs [10]. This equipment is designed for

the commercial (secondary level) calibration laboratory market. Intermediate institutes –
that operate occasionally at both high and low levels, depending on range or service –
do not in many cases offer any radiation thermometry capabilities. There is thus a need
to define the requirements for calibration systems that may be used to calibrate low and
mid-range RTs and RT calibrators.

Most NMIs in the European region are members of the European Association of
National Metrology Institutes (EURAMET). Through EURAMET, the Eura-Thermal
project was launched in 2015. Eura-Thermal is an international research project that
aims to strengthen thermal metrology capacity, including in radiation thermometry,
across emerging measurement institutes [11]. As a member of the Eura-Thermal
consortium, NSAI NML had the opportunity to avail of support to develop its radiation
thermometry capabilities. This project is a result of that collaboration.

1.2 Literature Review

The overview presented here reviews existing published standards and peer-reviewed
publications relevant to this topic.

1.2.1 Publications from Standard-Setting Bodies (and Calibration Guides)

A key finding of this literature review is that the area of radiation thermometry, as an
area of measurement that is developing relatively rapidly has, until recently, been
lacking with regard to standardisation [12]. The standardisation that does exist is
somewhat fragmented across different regions and standardisation bodies and, in many
cases, is not widely applied. This situation contrasts notably with measurement of

temperature by contact methods, where long-established standardisation applies to instrument design, usage procedures, evaluation of measurement uncertainty and calibration techniques [5, p. 29].

Indeed, detailed directions for the design and calibration of equipment in the form of published standards are also common in other metrological areas, for example, mass [13] and acoustics [14]. These standards enable the harmonisation of calibration methods and lay the way for legislation to refer to such measurements, where necessary. EURAMET publishes a range of calibration guidelines (previously published by European co-operation for Accreditation) for different types of instruments [15]. Some, but not all, types of thermal metrology instruments are covered – guidance for radiation thermometers is absent.

For measurement procedures and calibration techniques relating to RTs, there are, however, some recommendations, including precisely defined terminology and methodology, published in research literature sources [16]. Guidance has also been produced for inter-laboratory comparisons that can inform calibration procedures [17]. The key publications are discussed in the following subsections and their recommendations have been distilled into the NSAI calibration procedure described in section 5.2.

1.2.1.1 Consultative Committee on Thermometry Uncertainty Guide

Working Group 5 (WG5, since renamed Working Group for Non-Contact Thermometry or WGNCTh) of the BIPM Consultative Committee on Thermometry (CCT) prepared CCT-WG508-03, a comprehensive catalogue of the uncertainty components for the

calibration of 'laboratory-grade' radiation thermometers below the freezing point of silver (961.78 °C) [18]. ITS-90 gives guidance for realising the temperature scale above the silver point using radiation thermometers. However, the techniques described have limited application below this temperature because the spectral responsivity of an RT (its operating wavelength or waveband) varies according to its temperature range (see section 2.6.4). There are also difficulties associated with the direct measurement of relative spectral responsivity for the longer wavelengths required for lower temperatures. The uncertainty components are categorised by their origin:

- from the BCRS;

- from the radiation thermometer itself;

- from interpolation errors in the calibration equation; and

- from the instrumental drift after the calibration.

The document relates each of the 18 separate uncertainty components to a mathematical model of the particular physical phenomenon. The document includes estimates of the uncertainty components from the participating metrology institutes in the field. Each component includes an estimate of what can be expected as 'normal' and 'best' achievable uncertainties based on the input of the participating institutes [18]. However, only radiation thermometers that provide access to the unprocessed radiance signal output are considered, precluding the vast majority of radiation thermometers in use in industry [12].

Countries with developed RT design industries tend to have some level of standardisation in place, in particular, Germany and the US.

1.2.1.2 Verein Deutscher Ingenieure and Verband der Elektrotechnik, Elektronik und Informationstechnik 3511 Part 4

The German Verein Deutscher Ingenieure (VDI, Association of German Engineers) and Verband der Elektrotechnik, Elektronik und Informationstechnik (VDE, Association for Electrical, Electronic & Information Technologies) standardisation bodies produced some of the earlier efforts at standardising radiation thermometry, with the first part (Part 4) having been first published in 1995. Together, VDI/VDE produced a set of 5 documents under the title, 'Temperature measurement in industry − Radiation thermometry' in both English and German. This suite of standards is the most comprehensive of all the standards applying to radiation thermometry. The documents cover:

- radiation thermometry (Part 4);
- specifications of RTs (Part 4.2);
- test methods for RTs (Part 4.3);
- calibration of RTs (Part 4.4); and
- practical application of RTs (Part 4.5) [19].

Part 4 'Radiation thermometry' is intended as a primer to the area of radiation thermometry, covering theory, application, selection and issues affecting RTs [19].

Part 4.2 'Maintenance of the specification for radiation thermometers' acts as a guide for RT users, to sources of error and their avoidance, maintenance and regular testing of RTs [20].

Part 4.3 'Standard test methods for radiation thermometers with one wavelength range' describes standard test methods to determine qualities of RTs such as the Long Term Stability, Repeatability, Response Time and Spectral Range [21].

Part 4.4 'Calibration of radiation thermometers' discusses traceability schemes, set-ups, procedures, and uncertainty budgets for calibration of RTs. The latter three items are described where traceability is ensured through contact thermometers, RTs and to Tungsten ribbon lamps [22]. Tungsten ribbon lamps are used as an alternative to BCRSs for RTs with narrow spectral responsivities and narrow Fields of View (FOVs) at high temperatures (see section 2.6.7) [2].

Part 4.5 'Practical application of radiation thermometers' describes criteria for selecting RTs based on their spectral band, emissivity and SSE problems during in-use measurement, and the estimation of uncertainties applying to everyday measurements [23].

1.2.1.3 International Electrotechnical Commission Technical Specifications

These German standards, in an abridged form, have constituted the basis of International Electrotechnical Commission (IEC) Technical Specification (TS) documents. Official TS documents such as these lay out non-binding guidelines for manufacturers and test laboratories to follow. These TSs are a precursor to full IEC standardisation and are used where a field is still developing, and a consensus on best practice for design or testing has not yet been reached. Manufacturers following the TS recommendations will have an advantage if the TS becomes a binding International Standard. The following IEC TSs have been published:

- IEC TS 62492-1:2008 'Industrial process control devices - Radiation thermometers - Part 1: Technical data for radiation thermometers';

- IEC TS 62492-2:2013 'Industrial process control devices - Radiation thermometers - Part 2: Determination of the technical data for radiation thermometers'.

A third part of the standard is planned but has not been published, as the IEC working group charged with its authorship is currently engaged with the more pressing matter of developing TSs for a related and equally rapidly developing area – Thermal Imagers.

These documents place great emphasis on standardising terminology applying to the field to reduce confusion.

1.2.1.4 American Society for Testing and Manufacturing Standards

The American Society for Testing and Manufacturing (ASTM) has a subcommittee group concerned with radiation thermometry, designated E20.02. This committee has published three relevant standards:

- ASTM E1256, 'Standard Test Methods for Radiation Thermometers (Single Waveband Type)';

- ASTM E2758, 'Standard Guide for Selection and Use of Wideband, Low Temperature Infrared Thermometers';

- ASTM E2847, 'Standard Practice for Calibration and Accuracy Verification of Wideband Infrared Thermometers'.

ASTM E1256 describes standardised test methods for RTs and applies to common commercial instruments operating in the 8 µm to 14 µm waveband [24]. The test methods described are:

- Calibration Accuracy Test Method;

- Repeatability Test Method;

- Field-of-View Test Method;

- Response Time Test Method;

- Warm-Up Time Test Method;

- Long-Term Stability Test Method;

This standard was recently revised to correspond with the terminology used in IEC TS 62492-1:2008 [12].

ASTM E2758 is intended for users of RTs and describes issues that arise in their use. Test methods to determine emissivity, transmissivity, and reflected temperature, for the purpose of improving in-use measurement accuracy are included [25].

ASTM E2847 discusses the equipment requirements, traceability schemes, estimation of uncertainty for calibration of RTs below 1000 °C [26].

The uncertainty budget model discussed is similar to that in CCT-WG508-03, except that it is simplified and generalised to allow for calibration sources that are not true blackbodies (refer to 2.7.3.5). The traceability schemes are based on those used in VDI/VDE 3511 Part 4 [12].

1.2.1.5 Other Standards

Another notable guide relating to radiation thermometry is produced by the Measurement Standards Laboratory of New Zealand (MSL). This guide, which is titled 'MSL Technical Guide 22, Calibration of Low-Temperature Infrared Thermometers' and is part of a series of guides distributed free online, is intended for the calibration of handheld direct-reading RTs. RTs of this type give a reading in temperature terms only and do not give the user access to their unprocessed signal. The internal operation of RTs is discussed in terms of their measurement equation, measurement signal processing and calibration procedures. The corrections required when there is a mismatch between the source emissivity and RT emissivity setting are described in detail. It is authored by P. Saunders and references his more detailed peer-reviewed publications [27].

Table 1.1. Standards applying to radiation thermometry, categorised by scope and applicability to different measurement accuracy levels.

Body	Standard	Usage	Calibration	Uncertainty	Test Methods	NMI	High-Accuracy	Industrial
BIPM	CCT-WG508-03 IEC				■	■	□	□
IEC	IEC 62492-1	■				■	■	□
VDI	3511 Part 4	■				□	■	□
VDI	3511 Part 4.2	■				□	■	□
VDI	3511 Part 4.3				■	□	■	□
VDI	3511 Part 4.4		■	■		□	■	□
VDI	3511 Part 4.5	■		■			□	■
ASTM	E1256				■	■	■	□
ASTM	E2758	■					□	■
ASTM	E2847		■	■	■		□	■
MSL	TG22		■		□		□	■

■ Full Applicability

□ Partial Applicability

A summary of these standards and guides, as adapted from [12], is presented in Table 1.1.

The International Organization of Legal Metrology (OIML) issued an informative non-binding document that lays out the terminology and technical characteristics of total radiation pyrometers as well as requirements for their calibration. Total radiation pyrometers infer the temperature of an object based on virtually the entire spectrum, rather than using a filter to examine a spectral band [28]. The document also includes a suggested calibration procedure for radiation pyrometers. The OIML's goal is to harmonise legal metrology ultimately to facilitate trade. The organisation's aim is to enable measurements that use a common procedure and are, as such, on the same footing, rather than pursuing the highest measurement accuracy. While this document is helpful in terms of its technical definitions and approach, the methodology described is not particularly applicable to calibration of general-purpose RTs in a scientific metrology sense [29]. The document offers no discussion on uncertainty components other than repeatability and no uncertainty budget format is suggested. Furthermore, publications that are more recent provide a methodology that is more applicable to scientific and industrial calibration of RTs operating over smaller spectra.

Another source of authoritative information on calibration methods for radiation thermometers are the published protocols for the Inter-Laboratory Comparisons (ILCs) made in pursuit of Bureau International des Poids et Mesures (International Bureau of Weights and Measures or BIPM) Key Comparisons (KCs). An example is [17], for a radiation thermometry ILC covering the 156 °C to 1000 °C temperature range. This document includes calibration procedures and requirements for the presentation of calibration set-ups, results, and uncertainties. This particular KC was conducted using a

highly-accurate NMI grade RT; some requirements are not applicable to commercial instruments.

Other standards of note that apply to metrology generally include the VIM, GUM, and ISO 17025. JCGM 200:2008 'The international vocabulary of basic and general terms in metrology' (VIM) is a joint publication of the BIPM, IEC, ISO, OIML and other standards bodies and is intended to standardise the terminology used throughout metrology. Its purpose is to ensure a common approach across different metrological fields and improve the standard of communication between labs and across publications [30]. The JCGM 100:2008 'Evaluation of measurement data — Guide to the expression of uncertainty in measurement' (GUM) is a similar joint publication that aims to ensure a harmonised approach across disciplines to the way uncertainty is evaluated and expressed [31].

ISO/IEC 17025 'General Requirements for Calibration and Testing Laboratories' is a standard that lays out the procedures calibration laboratories must follow if they are to be accredited by an accreditation body [32].

1.2.2   Peer-Reviewed Research Publications and Prior Work

The majority of literature dealing with radiation thermometer calibration is focused on instruments with ranges that begin at temperatures hundreds of degrees above ambient. This is to be expected as these thermometers, being the most accurate means of temperature measurement in this range, have had a longer-established requirement for traceability. The type of equipment used and the radiation sources are different for these ranges. In many cases, the problems experienced in these high-temperature calibrations

are the same as those faced at lower temperatures but exaggerated. Emissivity errors are a prime example of this. In other respects, however, low-temperature thermometers pose greater challenges, due to a smaller radiation signal and, in many cases, due to lower quality components and construction.

A 2009 review from Physikalisch-Technische Bundesanhalt (PTB), the NMI for Germany, gives a detailed outline of the techniques developed for calibration in the fields of photometry, radiometry, and radiation thermometry. The significance and history of the field are discussed in terms of the theory, methods and equipment developed. One of the first tasks of PTB (then Physikalisch-Technische Reichsanstalt or PTR) was to investigate standard radiation sources in order to evaluate lighting equipment in development at the end of the 19th century. The theory of blackbody radiators and the development of different cavity designs are described in detail [3].

J. B. Fowler of the National Institute of Standards and Technology (NIST) in the US outlined a design of blackbody source consisting of a horizontal cavity that was built into the side of a commercially available oil temperature calibration bath in 1996. The cavity was analysed in terms of its geometry, construction, and uniformity performance and was found to offer low uncertainty in the calibration of infrared detectors, radiation thermometers, and thermal imaging systems. The cavity was a horizontally oriented 107 mm diameter cylinder with a conical base and was constructed of copper with a black surface coating. The relatively large size of the diameter and aperture were chosen to enable the calibration of instruments with a large FOV [33].

P. Saunders showed that there are particular considerations affecting direct-reading radiation thermometers in 2009. The signal processing algorithms used in RTs of this

type take advantage of assumptions about the measurement conditions to simplify the use of the RT. To a certain extent, these algorithms obscure the influence of variables that affect the expected readings. These variables include the emissivity setting on the RT (the instrumental emissivity), the emissivity of the target and the temperature of the detector. To correct for the influence of the detector temperature and reflection errors, the signal at the detector of an RT is required. A method is given to determine the detector temperature of an RT under calibration where the RT has a variable emissivity setting [6].

The dominant uncertainty component in most cases for radiation thermometers is a characteristic of the radiation thermometer optics known as the Size-of-Source Effect (SSE). The SSE is a ratio describing the dependence of the thermometer signal on the area surrounding the target area (see section 2.6.6). I. Pušnik *et al.* related the uncertainty of the SSE characteristic for direct-reading radiation thermometers to the resulting temperature uncertainty [34].

M. Bart *et al.* described a novel scanning method, employing a computer-controlled translation stage, for determining the SSE without using variable apertures. The traditional SSE techniques - the direct (variable aperture) and indirect (variable obscuration) - were also rigorously reviewed and their equivalence was demonstrated [35].

Rodriguez and Mendez-Lango described how the distance of the RT from the BCRS and focus could compound the SSE in terms of their influence on the calibration of RTs. They highlight the importance of providing reference conditions for distance and focus

on the calibration certificate. They also make several other recommendations to improve the reproducibility of calibration for RTs with both fixed and variable focus [36].

T. Kolat and F. Liebmann provided a thorough overview of the different standards that had been written applying to the field of radiation thermometry as at 2012. Each of the standards that had been written at the time is summarised in terms of content and purpose with the aim of helping the reader 'apply published standards to measurement, calibration, and testing involving radiation thermometry and infrared thermometry' [12]. Since the publication of this manuscript, further standards have been issued – IEC 62492-2 (as described in section 1.2.1.3) and VDI/VDE 3511 Part 4.5 (see section 1.2.1.2).

Finally, B. Cusack, in his DCU Applied Physics undergraduate final year project report, titled "The Design, Construction and Characterisation of an Infrared Thermometer Calibration System", outlined the NSAI vertical blackbody cavity and a preliminary characterisation of the cavity using a mid-range Fluke 574 IRT that was traceable to LMK over the temperature range 0 °C to 75 °C [37]. The cavity was constructed through a collaboration between NSAI NML and DCU to specifications chosen based on previous designs, as described in section 3.2.2. A modelling of the cavity's emissivity was performed using the integration method outlined in [38]. Preliminary thermal uniformity measurements of the cavity were also performed from 4 °C to 75 °C. This preceding report was the precursor to the present more extensive (in terms of temperature range and measurement accuracy) analysis of the cavity's performance and calibration methodology. This report provided a starting point for literature sources and RT calibration methodology in the present work.

1.3   Research Questions:

1.3.1   Performance differences of horizontal and vertical Blackbody Cavities

Numerous designs of BCRS exist, utilising stirred baths, heat pipes and fixed points (phase transitions of certain high-purity materials). Bath-based horizontal BCRSs have been demonstrated as robust sources for the calibration of RTs from -50 °C up to 300 °C [39], [40] and their use is commonplace. Vertically oriented immersible BCRSs are used for the calibration of tympanic thermometers [41], and sometimes for ice-point checks of industrial RTs [5], but are not currently used for the calibration of RTs. The key advantage of using a removable vertical cavity is flexibility. Vertical BCRS may be easily immersed in baths containing various temperature media, and may also be used below the dew point temperature, where horizontal cavities have a limitation at low temperatures due to the build-up of dew or ice on the internal walls.

The research question investigated here is whether a unique low-cost design of vertical BCRS, which was constructed in-house, is suitable for calibration use over the temperature range from -30 °C to 150 °C and whether its performance compares favourably with horizontally oriented BCRSs. The lower limit of this range corresponds to the low limit of many RTs, and the upper limit was determined by the properties of materials used in the construction of the BCRS (see section 3.2.2).

Three of the horizontal cavities used for the comparison are part of the suite of BCRSs in LMK, the national temperature standards laboratory for Slovenia. The newly constructed NSAI vertical cavity was also compared to a similar vertical cavity that had previously been constructed at LMK. In addition, measurements were made in order to

compare the new vertical NSAI cavity against the horizontal BCRSs in the Heitronics calibration laboratory, which is ISO 17025 accredited.

Note that throughout this work, when referring to the LMK BCRSs, the orientation is stated, and when referring to the NSAI BCRS, of which there is only one vertical cavity, the orientation is not stated.

1.3.2 Development of a Calibration Procedure and Investigation of the Size-of-Source and the Distance Effects

As outlined in 1.2, much of the research literature has focused on achieving better uncertainties in the calibration of high-end RTs (with some exceptions [6], [16], [42]). However, when disseminating national temperature standards, particularly for emerging metrology institutes like NSAI, the bulk of calibration work is likely to be for commercial-grade handheld IRTs. There are many challenges associated with the calibration of these lower accuracy thermometers.

Despite numerous manufacturers' guides and calibration systems being available [10], [43] there is still considerable ambiguity about the most accurate, efficient, and practical calibration approaches. There are variations on the methods of calibration, particularly with regard to ways of dealing with the heating of the IRT under test.

The research question addressed here is the significance of the various uncertainty components affecting direct-reading IRTs during calibration, particularly the Size-of-Source Effect, Distance Effect and IRT housing temperature, and whether calibration procedures need to be improved to take such effects into account.

During the course of the calibration of a commercial-grade IRT owned by NSAI, a case study into the effects of radiation scattering (SSE), variation of distance (DE), and housing heating was undertaken. The aim was to quantify each of these effects and determine if the instrument met its specification. The work also sought to investigate ways manufacturers could clarify specifications. The objective was to investigate the procedures for evaluating these effects and general RT calibration procedures.

Chapter 2. Principles of Radiation Thermometer Calibration

2.1 Introduction

Although we usually associate radiant heat with the red glow of a fire or an electric oven hob, all objects, in fact, radiate heat. This electromagnetic emission is radiated in large quantities, and it is possible to infer an object's temperature from this signal. In an age where reducing latency is a key objective across many technical fields, RTs, which can give an almost instantaneous reading, are increasingly more desirable than contact thermometers, which have a time-consuming requirement for reaching thermal equilibrium with the measurand.

RTs are very useful for making quick diagnostic measurements of hot spots, for example, in checking remote parts of vehicles or electrical installations. As the instrument specifications have improved, however, repeatable, accurate, and traceable readings are increasingly expected of RTs. This is particularly true for critical applications in medicine, food storage and process control [5].

2.2 Measurement and Traceability

2.2.1 Measurement

Measurement is defined in [30] as the 'process of experimentally obtaining one or more quantity values that can reasonably be attributed to a quantity'. A more general

definition of measurement is 'the quantitative comparison of an unknown quantity with a standard' [44].

In the case of many of the measurements in this project, one of the quantities is a source instrument (a blackbody cavity), and the other is an indicating instrument (a radiation thermometer). The relation resulting from the comparison may then be used to correct the item being measured or calibrated, often referred to as the Unit Under Test (UUT).

2.2.2 Measurement Standards and Transfer Standards

For the calibration of a UUT to have any meaning, the known quantity against which it is compared – the *measurement standard,* or *etalon* – must in turn also have been calibrated [30]. In some cases, a *transfer standard* is used [45]. An example of this would be where an indicating instrument, which has not been calibrated, is used as an intermediary instrument to transfer traceability from a calibrated source instrument. This indicating instrument may then be used to determine the value of another source.

2.2.3 The International System of Units (SI)

Measurement standards necessitate a hierarchical system whereby comparisons are conducted against increasingly well-known quantities. At the top of this chain sits the definition of an SI unit, as shown in Figure 2.1. As such, the definitions of the SI units are of the utmost importance: they must be constant as far as possible and internationally accepted [44]. Six of the seven base units of the SI (the kelvin, second, metre, mole, candela, and ampere) have a definition that can be realised anywhere in the world. The exception is the kilogram, which, at the time of writing, is still based on a physical artefact maintained in the BIPM in Paris [5].

Below the SI definition in the traceability chain, for the six units mentioned, sits the realisation of that definition, as shown in [44], [45]. The realisation can take the form of a physical standard such as an atomic clock, in the case of the second, or in the case of the kelvin, the ITS-90 scale, described in detail in 2.4.
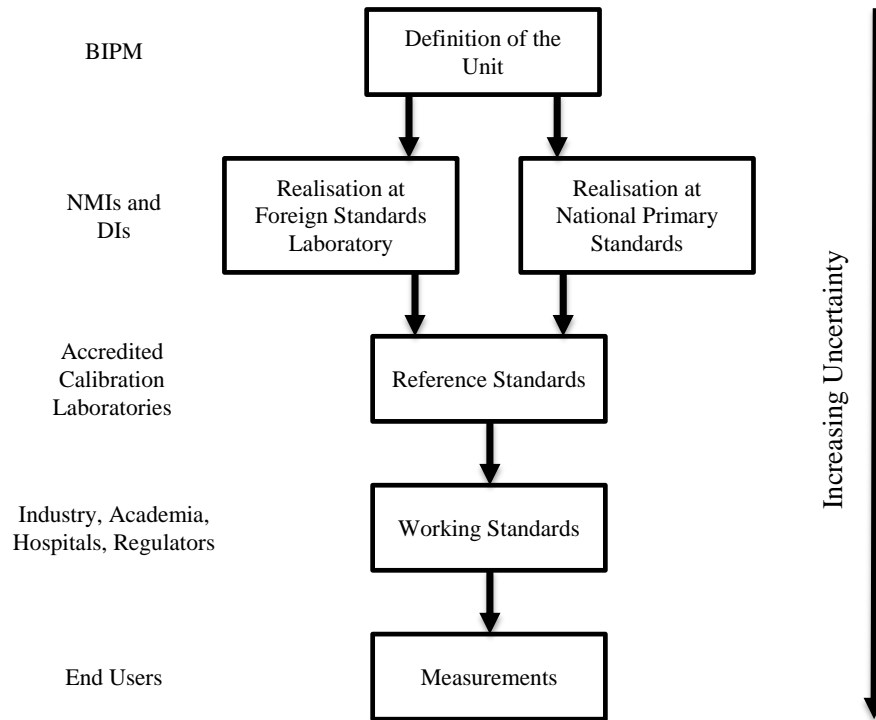
Figure 2.1 High-level chain of traceability, as adapted from [45].

2.2.4   Accreditation and Traceability

Another requirement for meaningful calibration is accreditation. Laboratories performing calibration must have their processes and procedures checked by an independent external organisation – an accreditation body. Primary laboratories operate at the highest levels and include NMIs and Designated Institutes (DIs; where different metrology capabilities are spread across a collection of institutes throughout a country). These laboratories are each accredited and receive CMCs by a peer-review process

formalised as the International Committee for Weights and Measures-Mutual Recognition Arrangement (CIPM-MRA) [45]. Secondary laboratories, which might be operating on a commercial basis, are accredited, usually by the national accreditation body in their country, according to ISO/IEC 17025 (see section 1.2.1) [32].

Calibrations are performed periodically at predetermined intervals appropriate to the UUT's long-term stability, usage conditions, and the significance of its measurements. When an instrument has been calibrated by an accredited laboratory, the instrument and measurements made with it may be said to be *traceable*, meaning that they may be traced back to internationally accepted realisations of the SI units.

2.2.5   Standardisation

For the SI to work on an international basis, terms like calibration and uncertainty must have the same meaning in one country as they do in another. The internationally recognised definitions of these metrological terms are published by the BIPM in the VIM (see section 1.2.1.5) [30]. It is important to note that in the VIM, the calibration of an instrument or artefact is considered a distinct step from the adjustment of that instrument. The principle of calibration is simply to compare two quantities against each other and report the results in a certificate.

2.3   Uncertainty of Measurement

2.3.1   Quantifying Uncertainty

In the same way that a measurement is incomplete if the appropriate unit is omitted, no measurement can be considered complete without including an estimation of the

uncertainty of that measurement. Uncertainty of measurement, in the broadest sense, is defined as 'doubt about the validity of the measurement'[31]. More specifically, the VIM defines it as the 'parameter, associated with the result of a measurement, that characterises the dispersion of the values that could reasonably be attributed to the measurand' [30]. It is important to quantify the uncertainty of a measurement so that:

- The quality of the measurement may be judged;

- Measurement results may be compared;

- Compliance with specifications may be judged; and

- Documentary standards are adhered to.

Measurement uncertainty is evaluated systematically, by appraising all of the random and systematic factors contributing to the measurement error and attempting to quantify them.

The methodology of uncertainty evaluation and its conventions are outlined in the GUM, an internationally prepared document that aims to standardize the evaluation of uncertainty so that uncertainties evaluated in any laboratory can be placed on a common footing – in the same way that the SI allows measurement best estimates to be compared on a common footing [5], [31].

The evaluation of measurement uncertainty is an extensive topic, and a thorough exploration is beyond the scope of the present work. Two examples of uncertainty contributions will be presented to illustrate some key concepts in uncertainty: repeatability and quantisation error.

2.3.2 Best Estimates, Distribution Functions and Uncertainty Budgets

If a measurement, for example of the temperature of a calibration bath determined by a Platinum Resistance Thermometer (PRT) and measuring bridge, is repeated numerous times, the result will usually vary at the least significant digits. If a histogram is prepared from the results of these repeat measurements and enough measurements are performed, a normal (or Gaussian) probability distribution function emerges, similar to that in Figure 2.2. The arithmetic mean, μ, of the repeat measurements may be taken to be the *best estimate* of the true temperature of the bath (in the vicinity of the probe, at least). The spread or repeatability may be expressed in terms of standard deviations, σ. It should be noted, however, that the mean of any finite data set is only an estimation of the true mean of the population [46].

An uncertainty budget is a table stating the:

- measurement uncertainty;
- the components of that measurement uncertainty, and
- the calculation and combination of those components [30].
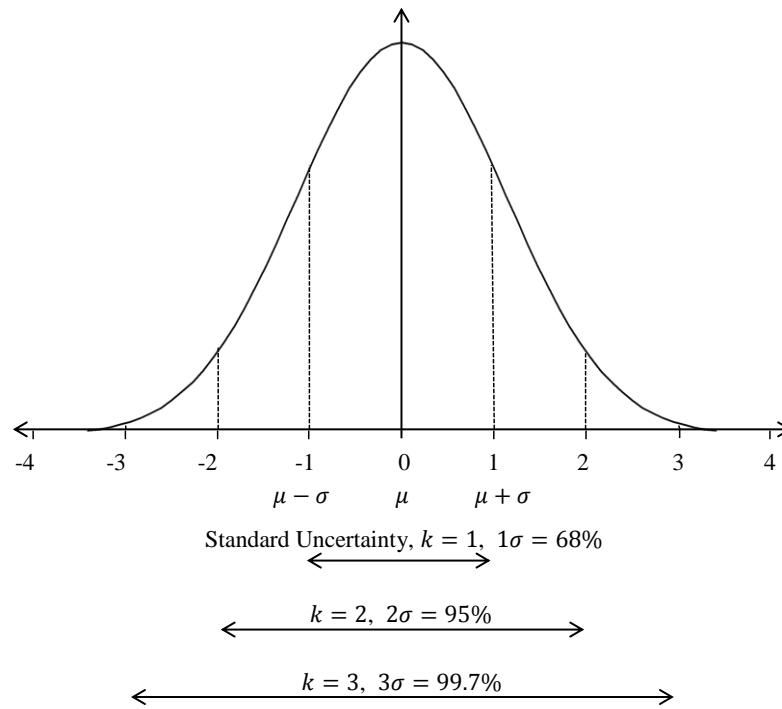
Figure 2.2 A normal probability distribution.The probability values centred about the mean (μ), coverage factors (k), number of standard deviations (σ) covered and corresponding coverage probabilities (%) are shown.

The repeatability component in the above example serves as one element of an uncertainty budget of other components contributing to the overall uncertainty. The other components, for instance, the UUT resolution or the uniformity of the bath medium, which may have differing distribution functions are ultimately combined into a single uncertainty distribution function as described in 2.3.5. Uncertainty budgets for the work presented may be seen in 5.3.

An example of an alternative distribution function is the rectangular distribution, which is so-called because it has a rectangular shape. Measurements in a rectangular distribution have uniformly distributed values that could occur with equal probability at any location between the highest and lowest values [47]. This type of distribution, unlike the normal distribution, has probabilities that have defined limits.

The UUT resolution, for example, is an uncertainty component with a rectangular distribution. The actual value measured by the UUT could lie anywhere between the smallest incremental value that the instrument can display. An RT with a resolution of 0.1 °C and displaying 100.0 °C, could, in fact, be measuring any value between 99.95 °C and 100.05 °C and rounding the reading. This is also known as a quantisation error. The range or width of the distribution is 0.1 °C in this case.

2.3.3   Type A and Type B Uncertainty Evaluations

According to conventions specified in the GUM and VIM, uncertainty components are categorised as either Type A, where the evaluation is based on statistical analysis of observations, or Type B, where the evaluation is based on other information [30], [31]. Type B evaluations may be based on information from specifications, past experience, calibration certificates, and calculations [47].

2.3.4   Coverage Probability, Coverage Factors, Confidence Intervals

Standard uncertainties are defined as covering one standard deviation on either side of the mean on the horizontal scale to give a total coverage probability of 2σ or approximately 68 % [46].

The coverage probability of an uncertainty statement is a percentage representing the probability that the measurement's actual value lies within the range represented by the uncertainty. This probability may also be referred to as a confidence level [46].

2.3.5   Combining Uncertainties

Before combining uncertainty components, the uncertainties are all placed on a common footing as standard uncertainties. To combine a uniformly distributed uncertainty with other uncertainties, the half-width of its distribution should be divided by $\sqrt{3}$ [31]. Where an uncertainty is stated with a coverage factor other than $k = 1$, the uncertainty should be divided by the coverage factor first to convert it into a standard uncertainty. When a series uncertainty of components with identical units are independent and uncorrelated, they are combined by summation in quadrature as shown in Eq. 2.1, where y is an estimate of the measurand, $(u_1(y), u_2(y), u_3(y) \dots)$ are the uncertainty components, N is the number of uncertainty components and $u_c(y)$ is the combined variance [31], [48].

$$u_c^2(y) = \sum_{j=1}^{N} u_i^2(y) \qquad\qquad \text{Eq. 2.1}$$

The combined uncertainty, U, is calculated as shown in Eq. 2.2,

$$U = k \times u_c(y), \qquad\qquad \text{Eq. 2.2}$$

where k is the coverage factor. It is convention to state the overall uncertainty as covering 2 standard deviations on either side of the mean, or in other words with a coverage factor, k, equal to 2 [47]. This corresponds to a coverage probability of 95 %; a convenient level that is only exceeded 5 % of the time. This relates to 1 observation in 20 and coincides with commonly used data set sizes [2, p. 359].

2.3.6 Discussion

The elements of an uncertainty budget mentioned in 2.3.2 are usually implemented in a spreadsheet application. With all the uncertainty components tabulated, the largest and most influential components are immediately obvious. Ultimately, the uncertainty is typically quoted as a single number along with the measurement as per Figure 2.3.

(100.002 ± 0.02) °C with a 95 % coverage probability

Or generally:

(**best estimate** $\pm$ **combined uncertainty**) [unit], statement of coverage probability
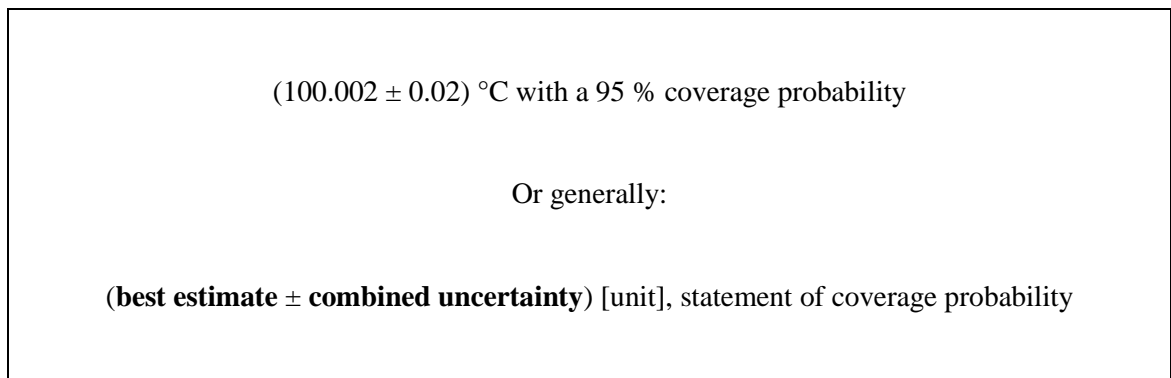
Figure 2.3 A typical uncertainty statement and the general elements of an uncertainty statement.

It is important to note the types of error that are not considered to contribute to measurement uncertainty. Uncertainties do not normally account for mistakes made during the recording of measurements or the calculation of results. It should also be remembered that uncertainties are distinct from product tolerances, which are acceptance limits. A measurement uncertainty is not a specification, but it may be used to judge compliance with such acceptance limits or specifications [47].

When each element of the error has been individually quantified and added to an uncertainty budget as with those above, the usual methodology is to focus on reducing the largest contributing factor. Following this approach has improved the accuracy of many quantities. One of the often cited successes of adhering to this method of improving accuracy is that of time – the proper functioning of GPS atomic satellite

clocks requires measurement to 1 part in 10^{13} [49]. Specific uncertainty components relating to radiation thermometry are discussed further, in detail, in 5.2.

2.4   The International Temperature Scale of 1990 (ITS-90)

2.4.1   Thermodynamic Temperature

Temperature is one of the seven base quantities of the SI. The kelvin thermodynamic temperature scale has the symbol T and the unit K and is specified in the SI as the scale underpinning all others, including Celsius and Fahrenheit, and is defined by the Triple Point of Water (TPW), 273.16 K [50]. The SI also permits the expression of temperature in Celsius with the symbol t and unit °C. The relationship between the units is shown in Eq. 2.3.

$$t/°C = T/K - 273.15 \qquad \text{Eq. 2.3}$$

 The International Temperature Scale of 1990 (ITS-90) provides a framework for establishing a practical thermodynamic temperature scale in a laboratory. It is designed to deliver a close approximation of thermodynamic temperature while being more easily reproducible than true primary thermometers. True primary thermometers avoid using additional unknown, temperature-dependant constants, and instead use a simple relation between the thermodynamic temperature and the measurand that can be explicitly stated [1]. Primary thermometers like the constant volume gas thermometer are too cumbersome and expensive to operate in all but the most well-equipped laboratories, however.

ITS-90 is the result of large-scale international co-operation and periodic revision since 1923. The scale consists of:

- Highly repeatable fixed points of defined temperature;

- Interpolating thermometers which are calibrated at the fixed points; and

- Interpolating equations for use with these thermometers [5].

ITS-90 superseded the previous scale, the International Practical Temperature Scale of 1968 (ITPS-68) (and its amendments and addendums [7]). Each successive iteration of the ITS has incorporated improved estimations of the fixed points and methods with better repeatability.

2.4.2   The Triple Point of Water

The most important fixed point of the ITS-90 is the TPW, 0.01 °C in that, as mentioned, the kelvin is defined as 1/273.16 of the thermodynamic temperature of the TPW. The TPW may be readily created in a lab anywhere in the world using a TPW cell. At the TPW, the three phases of water – ice, liquid and vapour – are in thermal equilibrium with one another [5]. The cell is a hermetically sealed vessel containing liquid water of a specified purity and under its own vapour pressure (611.73 Pa). The cell is usually constructed of glass and with a cylindrical probe opening (known as a well or re-entrant tube) into which an SPRT may be inserted [1].

When a particular procedure is followed, whereby the cell is pre-cooled in a vacuum-insulated flask of melting ice and then cooled from the well outwards, using an agent such as frozen CO_2, the liquid water in the cell forms a mantel of ice around the probe opening. By gently heating the well with a rod, the mantel is separated from the well

and left floating. The three phases of water – vapour, liquid and solid –then share a common interface and exist in equilibrium near the top of the cell's interior. A pre-cooled probe inserted into the well, along with a liquid to improve thermal contact with the cell, will be exposed to the precisely defined temperature allowing a calibration with an uncertainty as low as 40 μK. As the actual triple point only occurs near the top of the well, as shown in Figure 2.4, a simple correction is applied to account for the increased immersion depth of the probe under calibration [5], [51].
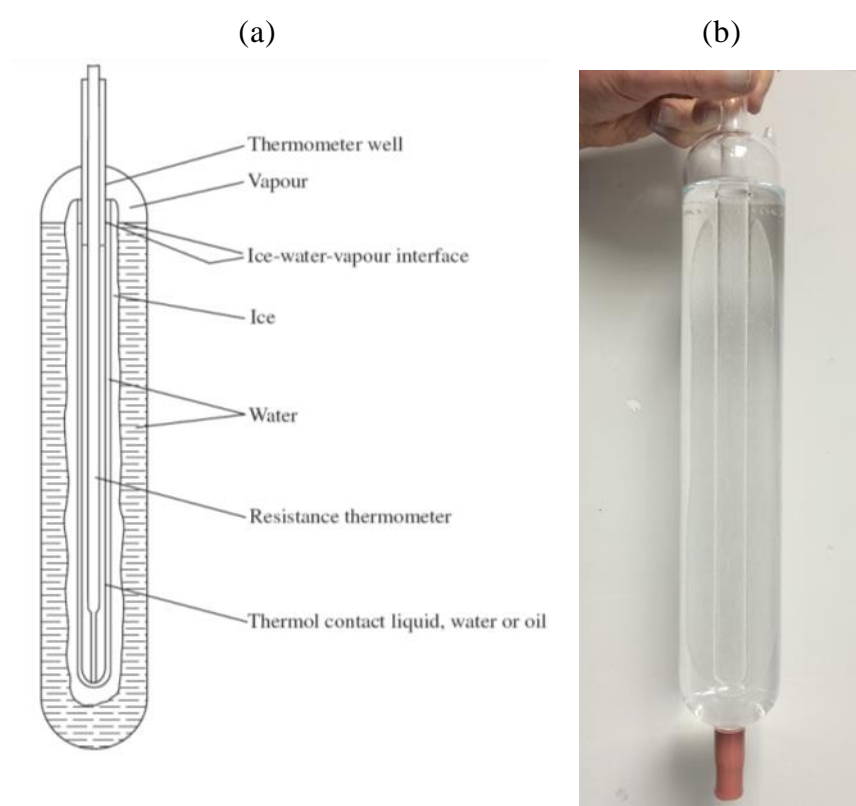
Figure 2.4 (a) Schematic of TPW cell in the triple-point state. Note the location of the ice-water-vapour interface near the top of the thermometer well. Figure from [1, p. 1083]. (b) Photo of the NML TPW cell showing ice mantel.

2.4.3 Other Fixed Points

ITS-90 consists of T_{90} temperatures assigned to 17 fixed temperature points, as shown in Figure 2.5, which are defined by very reproducible thermodynamic states of

equilibrium of highly pure compounds. The lower limit of the helium vapour pressure thermometer and hence the ITS-90 scale is 0.65 K [1, p. 1066].

Fixed Points		Interpolation Instruments
T_{90} (K)	t_{90} (°C)	
		Radiation Thermometer
1357.77	1085.62 Cu	
1337.33	1064.18 Au	
1234.93	961.78 Ag	
933.473	660.323 Al	
692.677	419.527 Zn	
505.078	231.926 Sn	
429.7485	196.5985 In	
302.9146	29.7646 Ga	Platinum Resistance
273.16	**0.01** H_2O (T_{TPW})	Thermometer
234.3156	-38.8344 Hg	
83.8058	-189.3442 Ar	
54.3584	-218.7916 O_2	
24.5561	-248.5939 Ne	
20.3	-252.85 e-H_2	
17	-256.15 e-H_2	Gas Thermometer
13.8033	-259.3467 e-H_2	
5	-268.15 He	
3	-270.15 He	He Vapour Pressure
0.65	-272.50	

Figure 2.5 Schematic of the defining fixed points and interpolating instruments of the International Temperature Scale of 1990.

The values of the of the various other fixed points relative to the TPW were based on the best estimates of repeated international experiments using true primary thermometers conducted before 1990. Improved estimates of the true values of the fixed points have been continually published since [52], although the scale has not been officially revised.

2.4.4   Interpolating Instruments and Equations

The Standard Platinum Resistance Thermometer (SPRT) is specified as the primary interpolating instrument covering the largest portion of the scale. Pure unstrained platinum − of the type used in SPRTs − gives a highly reproducible and almost linear relationship between electrical resistance and temperature. SPRTs cover the range between these fixed points from the triple point of equilibrium hydrogen (13.8033 K) to the freezing point of silver (961.78 °C) as they offer the lowest interpolation uncertainty in this range [7].

The sensing element of an SPRT is a finely wound coil of highly pure platinum wire, as shown in Figure 2.6 (a) and (c), which is encased in a protective silica, steel, or Inconel sheath. The sheath is filled with an inert gas to control the oxidation and reduce contamination of the platinum filament [5, p. 115]. The dimensions, materials (including their purity) and nominal resistance are all specified with precise tolerances. The specifications vary according to the range the SPRT covers. The combinations of ranges between the fixed points, known as sub-ranges, are also prescribed in ITS-90.

(b)

(c)
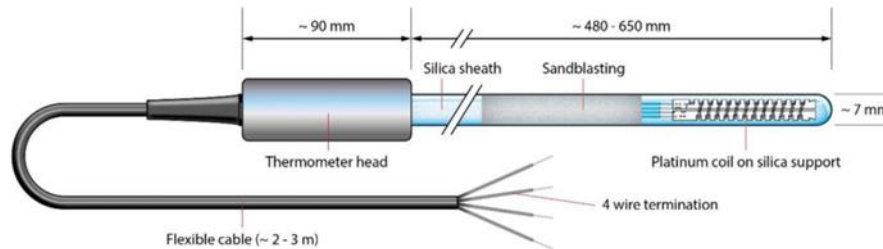
Figure 2.6 (a) The platinum coil resistive element in a glass sheath SPRT and (b) the entire SPRT assembly in its protective case. (c) Schematic diagram of an SPRT (long stem type) from [53]

For an individual SPRT, the ideal linear relationship between resistance and temperature is modelled in a standard reference function, and the departure from this ideal relationship is modelled in an individual deviation function which also follows a standardised form. The deviation equation coefficients are determined from the calibration results at the ITS-90 fixed points [1, p. 1067].

These reference and deviation functions are specified for the resistance ratio $W(T_{90})$, shown in Eq. 2.4, which is a ratio of the resistance of the SPRT at the measurement temperature, T_{90} to its resistance at the TPW. Specifying the ratio in this way allows the cancellation of the uncertainty contributed by the resistance measurements [5, p. 115].

The deviation functions are of several different forms of polynomial that depend on the subset of fixed-points (the subrange) used for the calibration. Specific subranges to be used for SPRTs and the other interpolating instruments are also mandated in ITS-90.

$$W(T_{90}) = \frac{R(T_{90})}{R(273.16 \ \text{K})}$$

Eq. 2.4

The use of these standardised equations in ITS-90 allows the deviation functions to be implemented electronically in measuring bridges, meaning that SPRTs may be used interchangeably with different equipment once the coefficients of the deviation function are known. SPRTs use a four-wire connection between the measuring element and the bridge; two wires are used to supply the current, and two wires are used for the voltage measurements. This configuration eliminates the influence of lead resistance on the measurements [46].

Below the useful range of SPRTs, the constant-volume gas thermometer is specified as the interpolating instrument due to its sensitivity advantage, and above the SPRT's range, the radiation thermometer is used. The intense heat close to and above the silver point is such that it is damaging to SPRTs [5].

It should be noted that the colour gradient on the temperature scale in Figure 2.5 approximately represents the peak wavelength of light emitted from a blackbody from 500 °C and above. The spectral distribution of radiation emitted is discussed further in 2.5.4.

2.4.5   Calibration of Industrial Contact Thermometers

SPRTs are practical for use in a calibration laboratory but are too fragile for use in industrial settings. For routine calibration of contact thermometer probes, metrology baths or dry wells are used. A metrology bath consists of a stirred liquid that is maintained at a stable temperature by a control system. The liquids are chosen so that they remain stable in composition and temperature over the desired temperature range. In NSAI for example, deionised water is used for calibration temperatures from around 5 °C to 85 °C and mineral oils are used from 85 °C to 260 °C and methanol is used from -100 °C to 15 °C [54]. Traceability is ensured by using a contact reference: a calibrated SPRT connected to a resistance measuring bridge.

2.4.6   Impending Developments in the SI

As mentioned, the best estimates of the true thermodynamic values of the ITS-90 fixed points have been continually re-measured since 1990. This is necessary because, as technology advances, the linear nature of temperature may be established more and more accurately. Improved methods may uncover previously undetectable non-linearity in the scale. The end-goal of these improved measurements is a redefinition of the kelvin, in 2018, to coincide with a wider revision of the SI.

From 2018, the SI definition of the kelvin will no longer rest on the TPW, but on a fixed value for the Boltzmann constant, k_B. The Boltzmann constant specifies the amount of energy in joules that corresponds to one kelvin. This has been made possible through multiple international measurements, using various principles, of k_B at the TPW [44].

2.5 Blackbody Radiation and Planck's Law

2.5.1 Thermal Radiation

All matter with temperature above absolute zero emits electromagnetic energy from its surface [55]. The waveband of this energy, which is emitted due to the internal heat, is termed *thermal radiation* and ranges from 10^{-1} μm to 10^{3} μm. As such it incorporates the infrared, the visible and a portion of the ultraviolet spectra [2, p. 27].
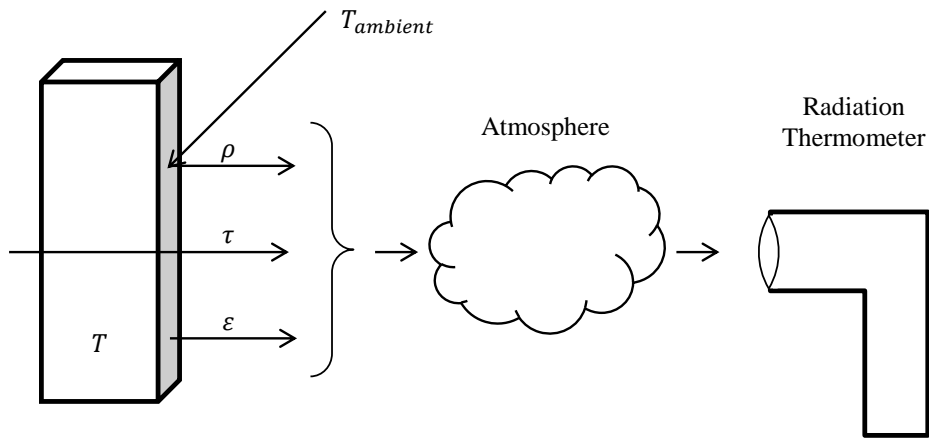
Figure 2.7 Reflectivity, transmissivity and emissivity for a sample of temperature T and atmospheric transmission.

As with visible light, any thermal radiation incident on an object must be reflected, absorbed, or transmitted, as shown on the left of Figure 2.7. This leads to Eq. 2.5, which shows the corresponding symbols for these basic optical properties of objects: reflectivity ρ, emissivity ε, and transmittance τ. The quantities for these phenomena are dimensionless ratios without units [5].

$$\rho + \varepsilon + \tau = 1 \qquad \qquad \text{Eq. 2.5}$$

The emissivity is a parameter that determines the amount of radiation emitted from an object's surface due to its temperature, T. As mentioned in 1.1, emissivity is a property of the object's surface relating to how it reflects radiation; an object that is perfectly

reflective has an emissivity of zero whereas an object that absorbs all incident radiation has an emissivity of one [2]. A more formal definition of emissivity introduces the concept of a blackbody, an opaque and non-reflective body: 'Emissivity is the ratio of the radiance of a substance to the radiance of a blackbody at the same temperature as that of the substance' [29].

Most solid objects are opaque, with τ equal to zero [5], and so in this case Eq. 2.5 simplifies to:

$$\rho + \varepsilon = 1 \qquad\qquad\qquad \text{Eq. 2.6}$$

Assuming an opaque sample as per Eq. 2.6, object temperature $T \gg T_{ambient}$, and negligible atmospheric influence, the radiation received by the RT in Figure 2.7 will depend only on T and ε.

The transmittance does, however, need to be considered when accounting for the effect of the atmosphere or with substances such as glass or silicon wafers, which may be transparent in the wavelengths of interest. This is discussed further in 2.6.4.

2.5.2   Blackbody Radiation

Blackbody radiation is the type of electromagnetic radiation within or surrounding a body in thermodynamic equilibrium with its environment, or emitted by a blackbody held at constant, uniform temperature. The radiation has a specific spectrum and intensity that depends only on the temperature of the body [3].
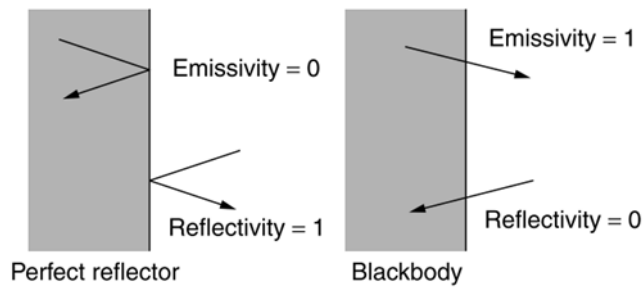
Figure 2.8 Emissivity and reflectivity for radiators and blackbodies, reproduced from [5, p. 346].

A blackbody is a theoretical structure with an emissivity of unity and therefore capable of absorbing all radiation incident to it. Figure 2.9 shows the effect of the complementary properties of emissivity and reflectivity of an ideal blackbody and for a perfect reflector. A fully sealed enclosure with a uniform temperature across all walls (isothermal, in other words) would emit blackbody radiation; this would be impractical to measure, however. A good approximation of a blackbody is a cavity with dimensions much larger than its opening.
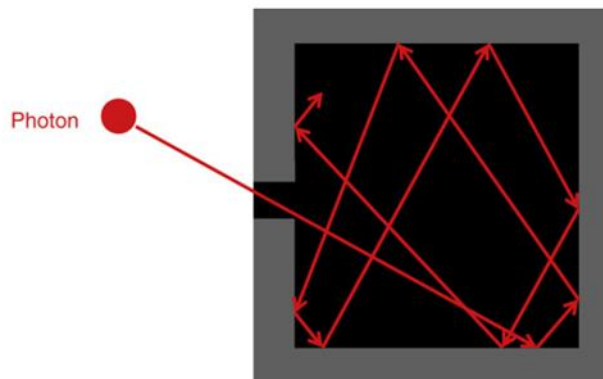
Figure 2.9 An approximation of a blackbody cavity.
Figure reproduced from [3].

A photon entering such a blackbody will undergo several reflections; it is unlikely to be re-emitted from the cavity and will most likely be fully absorbed. Similarly, any radiation that enters from outside is unlikely to exit the cavity and as such the cavity's absorption and emissivity are very high. The radiation emitted from the cavity walls is

the only radiation emitted from the cavity. The smaller the area of the hole in the cavity in relation to the total interior surface area, the better the approximation to a true blackbody [3]. The influence of cavity geometry is discussed further in 2.7.2.

2.5.3   Wien's Displacement Law and the Rayleigh-Jeans Law

Prior to Planck's elucidation of the spectral radiance of a blackbody, which launched the field of quantum mechanics, Wien and Rayleigh-Jeans had developed equations that modelled the short and long wavelength radiance respectively.

Wien's displacement law is only valid at low temperatures and short wavelengths and describes the energy emitted in a certain direction by a blackbody per unit area and wavelength interval $L_{\lambda,s}(\lambda, T)$. The approximation is given as follows [3], [5, p. 347]:

$$L_{\lambda,s}(\lambda, T) = \frac{c_1}{\lambda^5} \exp\left(-\frac{c_2}{\lambda T}\right),$$

Eq. 2.7

where c_1 and c_2 are the first and second radiation constants, with the values: $c_1 = 2hc_0^2$ and $c_2 = \frac{hc_0}{k}$ and where c_0 is the speed of light, and h and k are the Planck and Boltzmann constants.

Rayleigh and Jeans had developed their approximation, which only holds for high temperatures and long wavelengths, using classical thermodynamics and empirical observations of cavities [3]. The approximation is given as follows:

$$L_\lambda, s = \frac{c_1}{\lambda^5} \cdot \frac{\lambda T}{c_2}$$

Eq. 2.8

At low temperatures, the Rayleigh Jeans approximation is problematic and predicts an infinite spectral radiance as shown in Figure 2.10
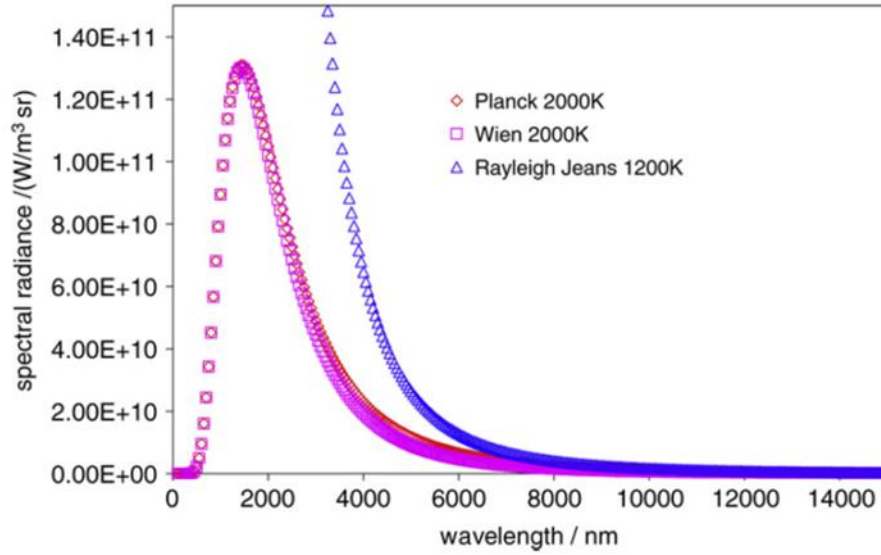
Figure 2.10 The Planck, Wien and Rayleigh Jeans curves compared. Figure from [3].

2.5.4 Planck's Distribution Law

Planck was able to unify the two approximations theoretically, giving an approximation that both models short and long wavelength radiance accurately, and also interpolates in the medium wavelength region. Mathematically, Planck's law is given as follows [3], [5, p. 345]:

$$L_{\lambda,b}(\lambda, T) = \frac{c_1}{\lambda^5 \left(e^{\frac{c_2}{\lambda T}} - 1 \right)},$$
Eq. 2.9

where $L_{\lambda,b}$ is the spectral radiance, with the subscript b indicating blackbody conditions.

Planck's Law shows that at a given wavelength, the radiant intensity from a blackbody $L_{\lambda,b}(T)$ depends only on the temperature [56]. When calculated for fixed temperatures across a range of wavelengths, Planck curves may be plotted as shown in Figure 2.11. The curves show the predicted spectral distribution of energy radiated from a blackbody.

43
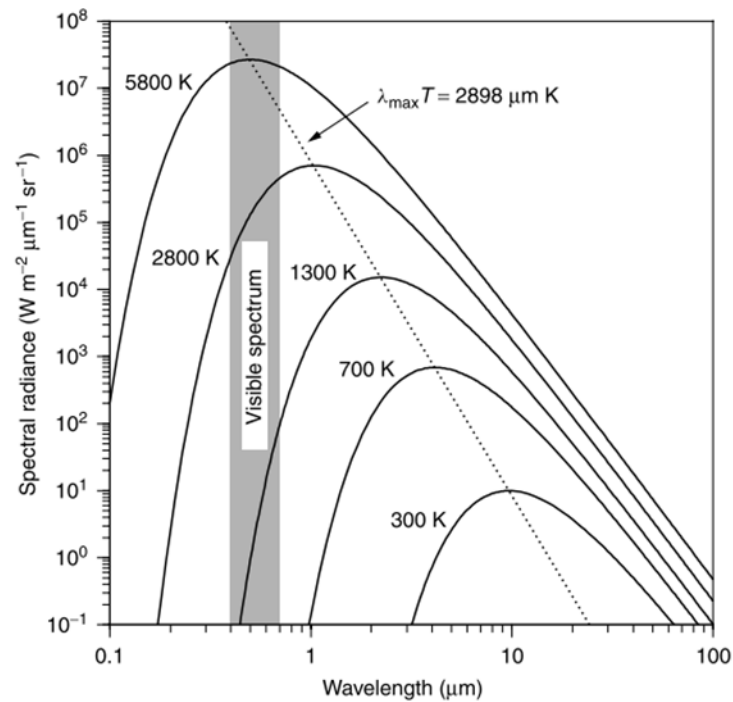
Figure 2.11 Planck curves, showing how the intensity of thermal radiation (its spectral radiance) varies with wavelength for temperatures from 300 K to 5800 K. Note that both axes are logarithmic [5, p. 344].

2.6   Non-Contact Thermometry

Radiometers are devices that measure the power (radiant flux) of electromagnetic radiation and radiation thermometers are a subset of these devices designed and calibrated especially to indicate the temperature of a target body [2]. Instruments that take measurements without any direct contact with the measurand often present particular difficulties.

RTs are distinct from contact thermometry in that they make a direct measurement of a thermodynamic property rather than an indirect measurement, where the thermometric property of a material is used [5, p. 343], [57].

Traceability for RT calibration may be provided via contact or radiometric means. An example of a traceability scheme for radiation thermometry, whereby traceability is provided through contact thermometers, is shown in Figure 2.12 (adapted from [19]).
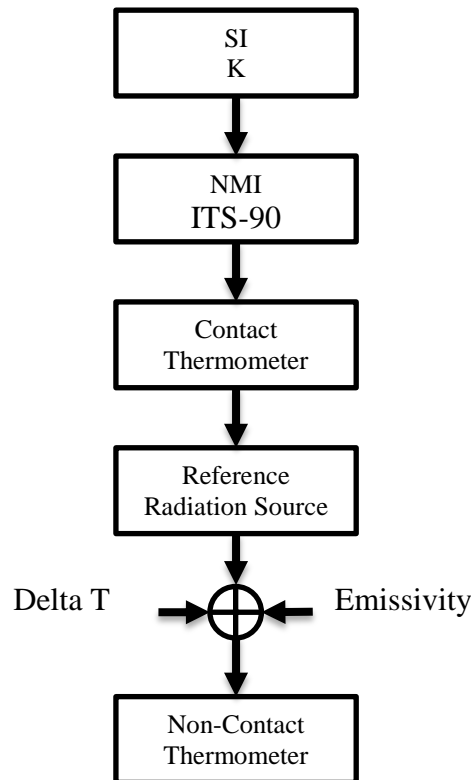
Figure 2.12 Contact traceability scheme for a reference radiation source calibrated using contact thermometry.

2.6.1   Advantages and disadvantages of Radiation Thermometers

As mentioned, RTs have proliferated in industry a great deal in recent years due to their perceived ease of use [5]. This perception is likely created by the response time, which is relatively fast when compared with contact thermometers. This fast response time is enabled by the lack of conductive heat transfer [56] which also enables measurement of very small objects high temperatures, hazardous environments and surface temperature.

On the other hand, RTs are always more expensive than contact thermometers of comparable accuracy. The most serious problem with RTs is that they require the user to have knowledge of the emissivity of the measurand's surface. This means that, in practice, many RT measurements that are made will be inaccurate due to an unmatched instrumental emissivity setting. This issue is also discussed in 2.6.9.

Another disadvantage of RTs relative to contact methods is that calibration is more difficult due to added variables such as the spectral responsivity (see section 2.6.4) and FOV (see section 2.6.6).

2.6.2 Measurement Equation

In order to calibrate any instrument, it is necessary to have an understanding of its measuring principle. Using equations to describe the phenomena associated with a measurement can help inform an uncertainty budget.

A basic schematic of an RT measuring a sample is shown in Figure 2.13. Ideally, the detector signal, S_{meas} would relate entirely to the temperature of the sample, T_s. As discussed in 2.5.1, the radiation emitted by the sample is dependent on its surface emissivity ε_s.

The complete measuring equation is given in Eq. 2.10,

$$S_{meas} = \varepsilon_S S(T_S) + (1 - \varepsilon_S)S(T_W) - S(T_D) \qquad \text{Eq. 2.10}$$

where:

- S_{meas} is the signal measured by the detector (before processing);
- ε_S is the surface emissivity of the target;

46

- $S(T_S)$ is the signal resulting from the radiance temperature of the target surface;

- $S(T_W)$ is the signal from the radiance temperature of the surroundings, T_W; and

- $S(T_D)$ is the signal resulting from the temperature of the detector, T_D.

In the first term, the signal from the sample's temperature, is scaled by the emissivity of the sample's surface. The second term accounts for the reflected ambient radiation, which is scaled by the sample's surface reflectivity, equal to $(1 - \varepsilon_S)$. The third term accounts for radiation emitted by the detector itself, which is significant at temperatures close to ambient [6], [27]

From Eq. 2.10 it is clear that in order to obtain the true target temperature, the target emissivity, ε_s, the radiance temperature of the surroundings, T_w, and the temperature of the detector, T_d, must be corrected for.
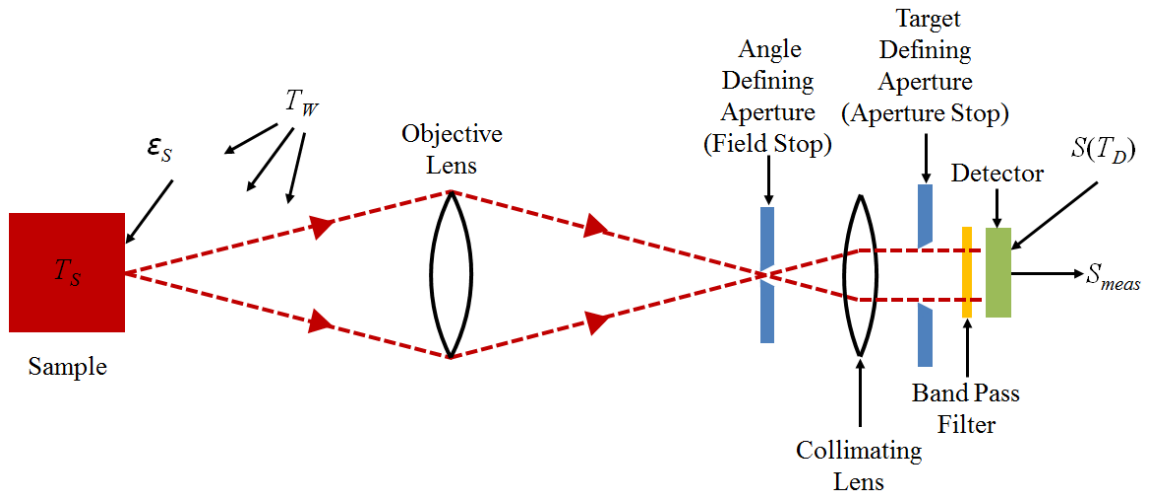
Figure 2.13 Simplified optical path of an RT, showing the parameters influencing the measurement.

2.6.3   Categories of Radiation Thermometer

According to [19], radiation thermometry instruments may be classified into three primary groups: RTs, line scanning thermometers, and thermal imagers. Another classification scheme is suggested in [28]: Partial RTs, Total RTs and Ratio or two-colour thermometers.

2.6.3.1 Optical Pyrometers

The disappearing filament optical pyrometer falls into the first group and predates most other RT designs. These devices consist of a scope that, from the operator's point of view, contains the image of a tungsten filament superimposed on the image of the target measurand. The temperature of the target is inferred by viewing it through the eyepiece and varying the current to the electrical filament. When the filament and the measurand emit light at the same wavelength, their images blend, and the filament 'disappears'. Traceability may be provided by calibration of the current using a source of known radiance such as a BCRS.

Despite the reliance on the visual sense of the operator, the method can achieve very high accuracy with a skilled operator. For example, uncertainties of $\pm$ 2.0 °C (k=2) are achievable with these instruments based on 12 measurements of a target at 800 °C.

While this method only works where the thermal radiation is in the visible spectrum, the human eye can function as an extremely sensitive photodetector with a dynamic range of about 10 decades. The most serious disadvantage of these instruments is that they are not capable of unattended operation [2, p. 345].

Optical pyrometers offered the most accurate means of measuring high temperatures for a long period, and were specified as the defining instrument above the gold point (1064.18 °C) in the International Practical Temperature Scale of 1927, the forerunner of ITS-90 [2, p. 344]. While the optical pyrometer is a useful example for illustrating the functioning of RTs, it is not expected, due to their high temperature range, that any calibration service at NSAI NML will seek to cater for these instruments.

2.6.3.2 RTs, Pyrometers and IRTs

Radiation Thermometer is the general term encompassing several types of devices. Pyrometer is a roughly equivalent term but usually applying to instruments that measure hundreds of degrees above room temperature. RTs may have fixed or variable focus and use a laser or an eyepiece for targeting. Direct-reading RTs are instruments that only give the user access to the linearized reading in temperature, rather than the unprocessed detector signal [6].

Infrared Thermometer or Infrared Radiation Thermometer (IRT) is a term applying to a subset of RTs measuring exclusively in the infrared spectrum and usually referring to direct-reading handheld devices using thermopile detectors (see section 2.6.4) [25]. An IRT is shown in Figure 1.1 (a). RTs and IRTs are the main class of instrument considered in the present work. The majority of IRTs have spectral responsivity in the 8 μm to 14 μm waveband [6] as discussed in 2.6.4.

2.6.3.3 Clinical and Tympanic Radiation Thermometers

Clinical RTs are optimised for the measurement over a narrow range of temperatures close to those of the human body. Infrared Ear Thermometers (IRETs) are designed to measure the tympanic membrane inside the ear canal as shown in Figure 2.14. Other clinical RTs are designed to measure the temperature at the forehead.

Measurement via the ear canal is preferred, as in this configuration the measured temperature is closer to the body's core temperature. The arrangement takes advantage of a natural blackbody cavity, and the effect of variations in skin emissivity is reduced [58].
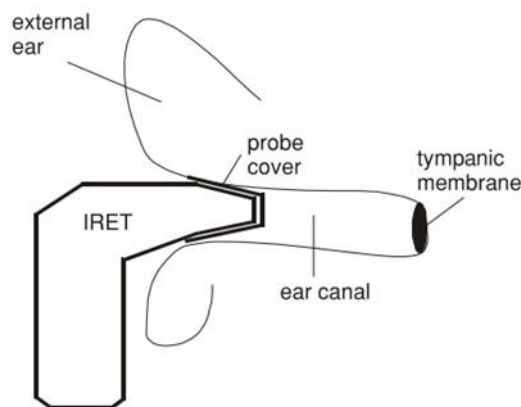
Figure 2.14 Measurement of the tympanic membrane using an IRET. Figure from [59].

2.6.3.4 Total Radiation Thermometers

These devices infer the temperature of the measurand by measuring almost the entire spectrum of emitted radiation. Total Radiation Thermometers usually use a thermopile bolometer (see section 2.6.4) [1]. These thermometers are increasingly less popular due

to the increased precision and sensitivity achievable with correctly-used spectral band RTs [28].

2.6.3.5 Line Scanners and Thermal Imagers

Line scanning RTs use a gimbal mirror to vary the location of the target area on one axis. This produces a 1-dimesional temperature profile [12].

Thermal Imagers (TIs), also known as thermographic cameras produce a two-dimensional temperature profile. TIs are useful for obtaining a qualitative indication of where relatively hot and cold areas in the FOV are located. Obtaining quantitative measurements of absolute temperature with TIs is challenging, however. Like RTs, use of TIs is growing rapidly in industry and standardisation is lagging. There are in fact no internationally recognised standards at present for TIs, although subcommittee 65B (Measurement and control devices, of IEC technical committee 65: Industrial-process measurement, control and automation) is nearing completion of a TS.

2.6.3.6 Ratio Thermometers

Ratio Thermometers, otherwise known as two-colour or two-wavelength RTs are suitable for specific applications where difficulties affecting spectral band RTs are insurmountable. These difficulties include variations in emissivity due to temperature or measurement through windows, dust or smoke [5, p. 386].

These thermometers use two wavelengths, λ_1 and λ_2, to measure the radiance allowing the following calculation:

$$R = \frac{\alpha(\lambda_1)}{\alpha(\lambda_2)} \frac{\varepsilon(\lambda_1)}{\varepsilon(\lambda_2)} \frac{L_b(\lambda_1, T_s)}{L_b(\lambda_2, T_s)} \qquad \text{Eq. 2.11}$$

If the absorption α of the atmosphere and the emissivity ε are constant at both wavelengths, then the ratio depends only on the temperature of the measurand T_s. These thermometers are usually less sensitive than spectral band thermometers [2], [60]

2.6.4 Spectral Responsivity

One of the key specifications designers provide for RTs is the spectral responsivity. This refers to the range of wavelengths that the RT responds and is determined by the optical components of the RT, including the filter, and the detector. Figure 2.11 shows the spectral distribution of radiation emitted by blackbodies at various temperatures due to Planck's distribution law. It can be seen that radiation is emitted over a range of wavelengths and that the peak wavelength varies according to the temperature.

Higher temperatures are best measured with shorter wavelengths, with common preferred bands being centred around 0.85 µm to 0.9 µm for temperatures above 500 °C and 0.65 µm above around 700 °C [1, p. 1078]. These narrowband RTs are sometimes described as being monochromatic. To ensure maximum sensitivity, it is usually preferable to use an RT operating wavelength that is as short as possible and less than λ_{max} shown in Figure 2.11 [1, p. 1078], [5, p. 347].

An RT designer does not base selection of the spectral responsivity on temperature alone because, as shown in Figure 2.15, the transmittance, τ, of the atmosphere makes certain wavelength regions unsuitable [2]. For temperatures close to ambient, a larger wavelength band must be used in order to improve the signal to noise ratio [6]. The

choice of bands is limited to two principle windows: 3 μm to 5 μm and 8 μm to 14 μm [1, p. 1078].

The choice of spectral responsivity has many implications beyond temperature range and possible targets. Laboratories may be limited in terms of the spectral responsivity of the calibration services they offer. If traceability is provided via a reference RT, i.e. radiometrically, then the responsivity of the reference RT and UUT should ideally be matched. Additional corrections may otherwise be required, particularly where sources other than true blackbodies are used (see section 2.7.3.5)
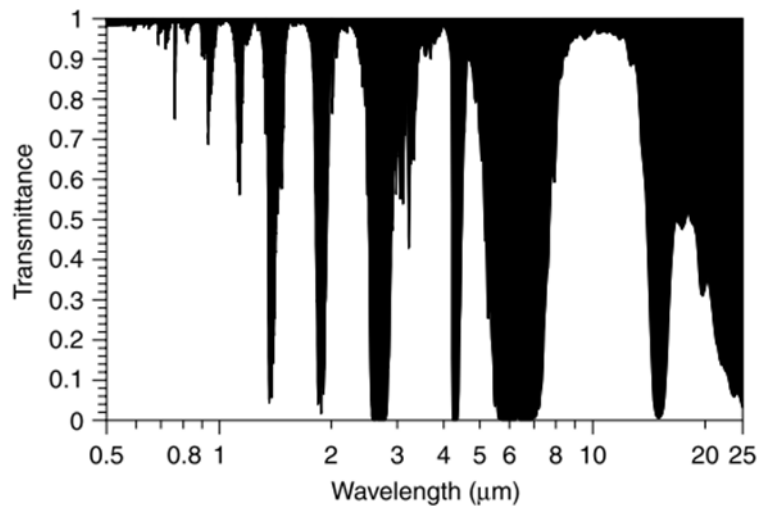
Figure 2.15 The transmittance at sea level over a distance of 300 m. The shaded areas are opaque, and the unshaded areas are transparent. Operational spectral band windows near 0.65 μm, 0.9 μm, 1.05 μm, 1.6 μm, and 8 μm to 14 μm are visible. Figure from [5, p. 361].

2.6.5 Detector Types

A variety of detector types are employed in RTs. The two overarching categories they fall into are photon (quantum) detectors and thermal detectors. Photon detectors respond to radiation quanta incident upon them, whereas thermal detectors respond to changes in temperature due to the incoming thermal radiation. Some of the frequently encountered detector types are described briefly below.

2.6.5.1 Thermopiles

The most common type of detector is the thermopile, as it is frequently used in the most common type of RT, the direct-reading IRT [12]. Thermopiles measure the temperature rise of a blackened disc [1, p. 1078] using the Seebeck thermoelectric effect employed in thermocouples. The Seebeck effect occurs where a junction of two different metals develop a voltage when exposed to a temperature gradient. These detectors consist of a number of small Thermocouples which are connected in series or series-parallel in order to increase the voltage level [2, p. 515].

Thermopiles are advantageous in that they are low-cost, DC devices. As thermocouple devices, they must use a reference junction with either a constant temperature or cold-junction compensation.

2.6.5.2 Bolometer

2.6.5.3 Thermistor Bolometer

These detectors comprise a resistive element that is made from a material with a large temperature coefficient. Made from metal films in the past, many modern microbolometers are formed from semiconductors due to larger possible temperature coefficients [61].

2.6.5.4 Pyroelectric

These are semiconductor-based detectors and rely on the pyroelectric effect. They are superior to thermopile detectors but, as AC devices, they require optical chopping. Optical chopping is achieved using a spinning wheel with slots or a similar apparatus in the optical path within the instrument [2, p. 516]. This type of detector is used in the Heitronics Transfer Radiation Thermometers (TRTs) that were used for some of the measurements in the present work as discussed in Chapter 3.

2.6.6   Sakuma-Hattori Equation

The relationship between the thermometer signal and the blackbody temperature is given by:

$$S^*(T) = \int_0^\infty R(\lambda) L_b(\lambda, T) d\lambda, \qquad \text{Eq. 2.12}$$

where $S^*(T)$ is the ideal response of a detector to blackbody radiation, $R(\lambda)$ is the absolute spectral responsivity of the thermometer and $L_b(\lambda, T)$ is the radiance spectrum emitted by a blackbody as a function of wavelength λ and temperature T [18]. The Sakuma-Hattori interpolation equation provides a good approximation of this integral [6].

In direct-reading IRTs, the Sakuma Hattori equation is, in some form, implemented internally within the IRT electronics. The equation is the response function of the thermometer and takes the output current or voltage signal from the detector, which is significantly non-linear, as its input and produces a user-friendly, linearized temperature

value on the display. The conversion to temperature is hidden from the user, who in most cases is doesn't require the detector signal [27].

The Sakuma-Hattori method can be used to calibrate RTs below the freezing point of silver and is suggested for this purpose in [18]. The principle advantage of the Sakuma-Hattori equation is that it allows for the calibration of an RT without knowledge of its spectral responsivity [18, p. 1068], [62]. The equation is given as follows [6]:

$$S^*(T) = C \left[exp \left(\frac{c_2}{AT + B} \right) - 1 \right]^{-1} \qquad \text{Eq. 2.13}$$

Where:

- A, B and C are constant parameters related to the properties of the thermometer that are determined by the manufacturer;
- c_2 is the second universal radiation constant, 14388 µm.K; and
- T is the temperature in Kelvin.

C is a proportionality constant which can be assumed to be 1 for calculation purposes. The constants A and B are calculated as follows:

$$A = \lambda_0 \left(1 - \frac{\Delta\lambda^2}{2\lambda_0^2} \right) \qquad \text{Eq. 2.14}$$

$$B = \frac{c_2 \Delta\lambda^2}{24\lambda_0^2} \qquad \text{Eq. 2.15}$$

Where:

- λ_0 is the centre wavelength of the RT's spectral response and

- $\Delta\lambda$ is the width of the RT's spectral response.

The inverse of Eq. 2.12 can be used to convert from signal values to temperature [27] as shown in Eq. 2.16.

$$T = \frac{c_2}{A\,ln\left(\frac{C}{S+1}\right)} - \frac{B}{A} \qquad\qquad \text{Eq. 2.16}$$

Examples of the results of the calculation of A and B for an 8 µm to 14 µm IRT are given in [27], as are results for the conversion between signal and temperature and vice-versa. Eq. 2.13 is suggested in [18] as a suitable underlying physical model for interpolation allowing uncertainty estimation in accordance with GUM principles [31]. It is suggested in [63], however that the assumptions about the constants A, B and C, which manufacturers do not provide for their instruments, limit its usefulness at present.

2.6.7   The Size-of-Source Effect (SSE)

The dominant source of calibration uncertainty when the emissivity is precisely known is termed the Size-of-Source Effect (SSE). The SSE results from scattered radiation from outside the radiation thermometer's nominal target area entering the FOV and affecting the reading [64].

As mentioned in 1.2.2, the SSE is a ratio describing the dependence of the thermometer on the area surrounding the nominal target area. RT manufacturers typically specify the nominal FOV as a ratio between the target distance and the diameter of the target area at that distance for the RT but it may also be specified as an angle. Manufacturers often indicate that the RT response over the FOV is rectangular in shape, but is in fact

roughly Gaussian [2, p. 505], [36]. In the case of some RTs, manufacturers specify that the indicated target area encircles a proportion, typically 90 %, of emitted energy, but this is often the only indication that the RT has an SSE.

Some RTs, particularly low-cost models, have large FOVs which call for very large BCRS apertures. The FOV often extends beyond the nominal target area due to the SSE. Under normal operation, the FOV of an RT should be overfilled, as shown in Figure 2.16 [34], [65].
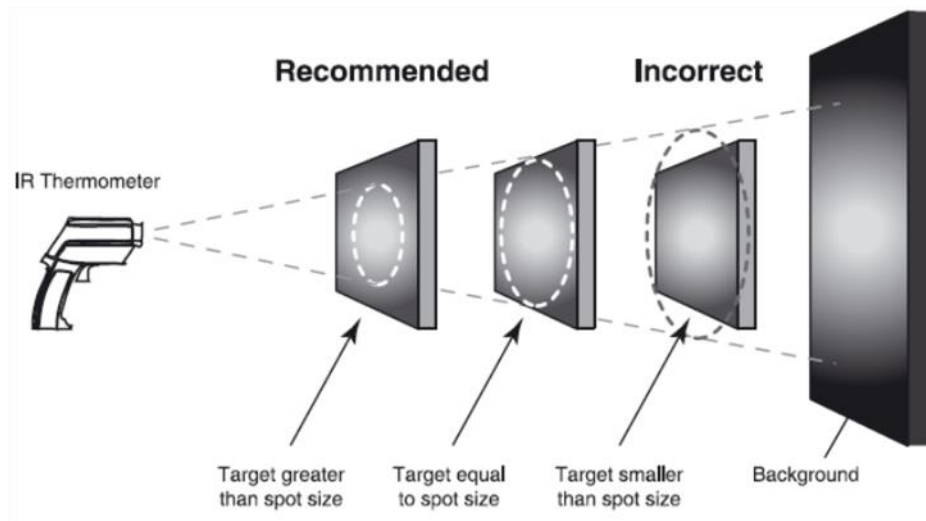
Figure 2.16 An example of guidance from a commercial RT manufacturer showing the recommended method of avoiding the SSE. Figure courtesy of Fluke Corporation [66].

The SSE is caused by radiation scattering and diffraction. Diffraction effects include inter-reflections, misalignment, imperfections and scratches on the components, dust, grease and optical aberrations in the optical components of the RT [67].

2.6.7.1 Optical Aberrations

Optical aberrations are the consequence of the real-world departure from idealised conditions [68]. There are several categories of aberrations that can affect optical

components. Two of those, chromatic and spherical aberrations, are described briefly here.

Chromatic aberrations result from the index of refraction of real lens materials varying as a function of wavelength. For example, for sunlight striking a converging lens, violet is refracted more than red as shown in Figure 2.17 (a) [68].

Spherical aberrations affect converging and diverging lenses where the surface of the lens is a section of a sphere. Rays striking the lens surface at angles far from normal are refracted more than those arriving at angles close to normal, as shown in Figure 2.17 (b) [68].

Optical aberrations have the overall effect of blurring the target image from the point of view of the RT, resulting in a target area that is not well defined [5].
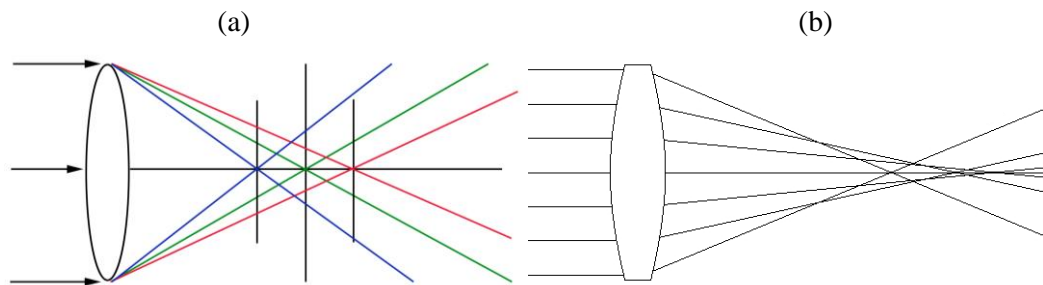
Figure 2.17 (a) Axial chromatic aberration and (b) axial spherical aberration.

2.6.7.2 SSE Determination Methods

Three main methods have been developed to quantify the SSE of RTs [35], [69]. All three rely on the target being partially obscured in the RT's FOV. These are:
- the indirect method, which uses variable obscurations;

- the direct method, which uses variable apertures; and

- the scanning method, which uses a slot-shaped aperture and a translation stage.

2.6.7.2.1   The Indirect Method

The indirect method uses a small, blackened disc, placed centrally in front of the source so that it obscures the nominal target area. The diameter of the disc is incrementally changed [69], [70]. As such, this method seeks to measure the signal resultant from the SSE in isolation from the primary thermal signal. The disc should be at a similar distance from the UUT as the source. This is an equivalent approach to that used to examine the corona of the sun using a telescope known as a coronagraph. Some optical methods used to characterise the solar rejection properties of radiation thermometers have been adopted from coronagraphy [64].

2.6.7.2.2   The Scanning Method

The scanning method, the most recently developed of the techniques, uses a slot placed in the optical path between the RT and the source to determine the influence of the SSE. This method is intended to be performed using a computer-controlled positioning stage. The advantage of this method is that it is more easily automated than a varying the aperture using plates [35].

2.6.7.2.3   The Direct Method

The direct method is the preferred means of measuring the SSE of direct-reading RTs, with their limited resolution, despite the method's lower sensitivity and susceptibility to noise relative to the other methods [35, pp. 2112–2113].

Under the direct method, the RT is focused on the centre of an aperture placed immediately in front of the radiation source. Interchangeable aperture plates are used to vary the source diameter [69]. The aperture blocks radiation from the source from entering the FOV of the RT. Comparing the RT reading for each aperture against the maximum aperture reading gives an indication of the true extent of the thermometer's FOV.

The aim of the direct method is to remove or constrain that portion of the signal that originates due to the SSE. A blackened aperture which is temperature controlled by means of internally circulated water is used. As the size of the aperture is varied, the change in the RT's output signal is observed and thus the influence of the SSE is determined. The aperture diameter is usually varied by fixing plates, with different size holes cut through their centres, onto the temperature-controlled mount.
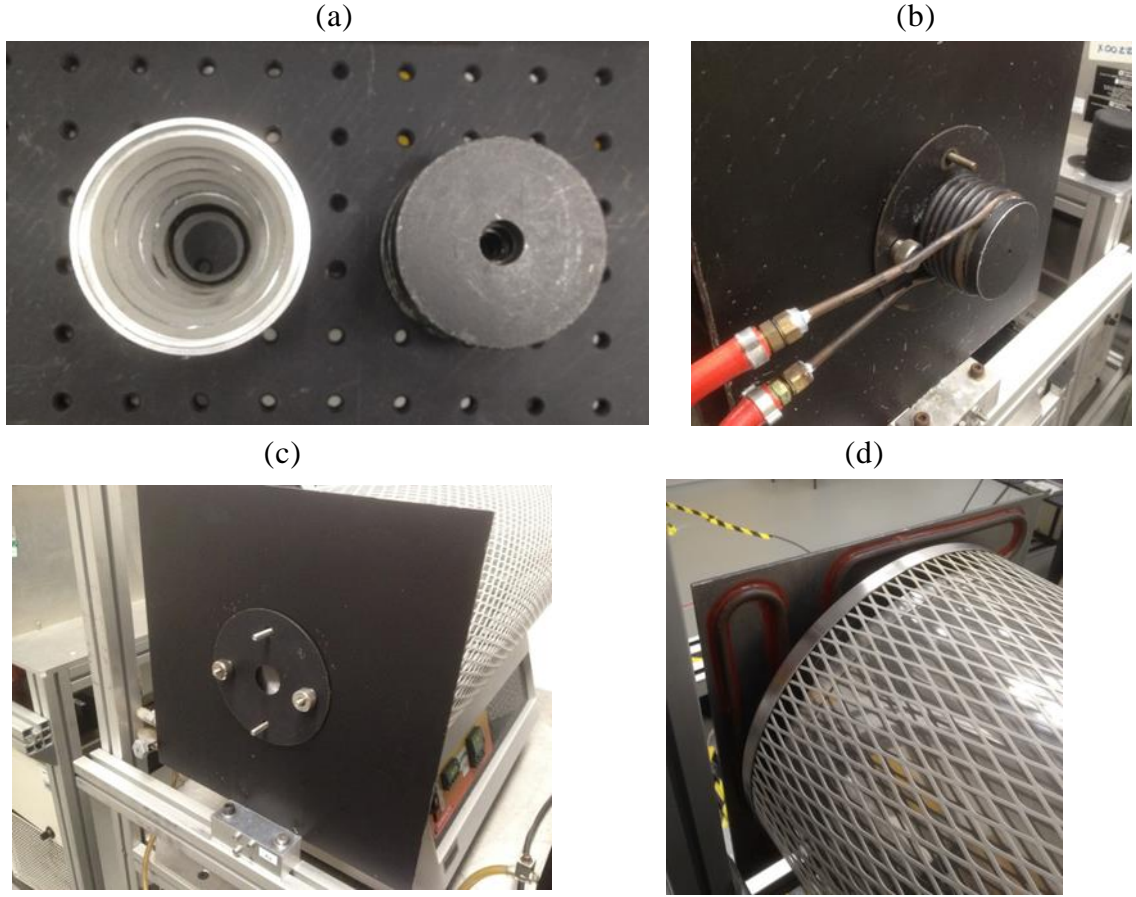
Figure 2.18 Direct-Method SSE Aparatus in the radiation thermometry laboratory in NPL. (a) Two stacks (showing the front on the left and the rear on the right) of lid-type aperture plate that slot over the cylindrical holder with helical circulating coil shown in (b). (c) shows the front of a variable aperture holder. (d) shows the rear of this holder with circulating pipe visible.

Under the direct method, the SSE is characterised as the ratio, $\sigma_s(r)$, between the RT signal where exposed to a source of radius r and radiance L, $S(r, L)$ to the signal when exposed to the same source but with infinite radius. This is shown in Eq. 2.17. As an infinite radius cannot be realised in practice, the SSE is determined as the ratio of signals with radii r and r_{max}, as shown in Eq. 2.18 [71].

$$\sigma_S(r) = \frac{S(r, L)}{S(\infty, L)}$$

<div align="right">Eq. 2.17</div>

$$\sigma_s(r, r_{max}) = \frac{\sigma_s(r)}{\sigma_s(r_{max})} = \frac{S(r, L)}{S(r_{max}, L)}$$

<div align="right">Eq. 2.18</div>

The measurements for the smaller diameter apertures are typically normalised to the reading for the maximum aperture diameter (usually the diameter of the source itself), so it is crucial that the diameter of the source is large enough to accommodate the full (true) optical extent of the RT. For low-cost RTs with large FOVs, this is difficult to achieve while still maintaining good temperature uniformity and high emissivity.
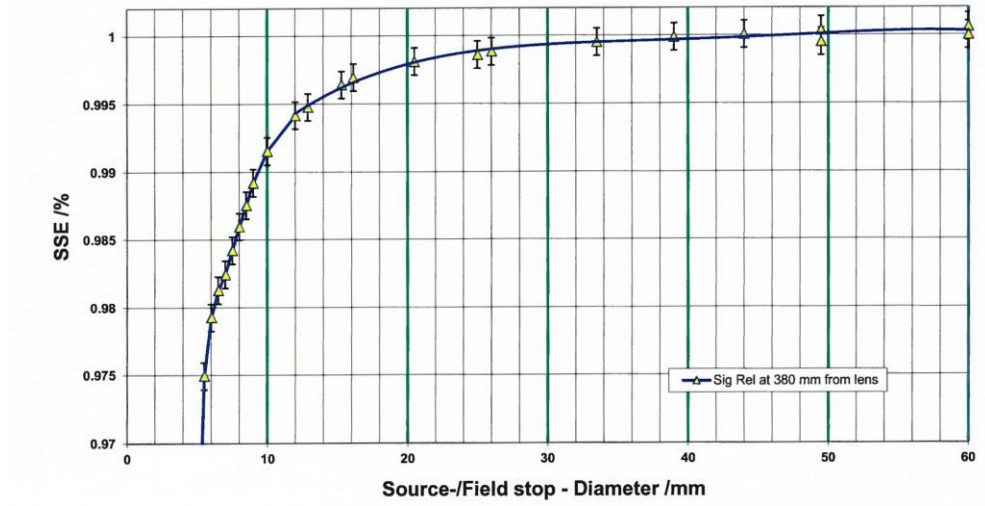
Figure 2.19 Direct method SSE results for a Heitronics TRT IV.82, showing the normalised signal percentage relative to the aperture diameter in mm.

SSE measurements from direct-reading IRTs may be converted to equivalent radiances L_{equiv} using the following method [71], [72]:

$$L_{equiv} = \frac{1}{\left(\exp\left(\frac{c_2}{\lambda_{eff}T}\right)-1\right)},$$

Eq. 2.19

where T is the temperature reading of the IRT, c_2 is the second radiation constant and λ_{eff} is the effective wavelength (assuming it is quasi-monochromatic). This conversion attempts to remove the effect of linearization performed internally in the IRT electronics and allows the expression of the SSE in terms of radiance. This is the reverse of the linearization function described in 2.6.6.

A complication of the direct SSE method is that the source behind the aperture is not at the focal length of the RT. During normal (non-SSE) calibration measurements when using cavity sources with lower uniformity, the RT is often focused on the cavity's base so that the source within the FOV has the best temperature uniformity. This is not possible when focussing on an aperture, and the source as seen from the RT will include the non-uniform cavity walls and will also be out of focus [36]. The present work considered only fixed-focus RTs as variable focus models were not encountered during the course of the work.

While the above methods offer techniques to quantify the SSE, its measurement is, in practice, of little interest to the end-user of the UUT [34]. The primary issue is to ensure that the FOV of the thermometer was filled during measurement and that the SSE did not influence the measurements at calibration points.

The main purpose of quantifying the SSE is to determine the aperture required to calibrate the RT and to calculate aperture related uncertainties [73, p. 7]. To replicate a real-world measurement in the calibration laboratory, it has been recommended that the diameter of the calibration source is at least twice the nominal target size indicated by the manufacturer at a given distance [16]. Indeed, for lower-cost thermometers with cheaper optical components and large FOVs, it is recommended that the source used is three times the nominal target size, as specified by the manufacturer [73].

2.6.8 The Distance Effect (DE)

Like the SSE, it is useful to quantify the DE if it is observed to have a significant influence on measurements. As mentioned, the DE is the influence of the distance of the

RT from the source on the measured values. When the DE of an RT is quantified, it may be included in a calibration uncertainty budget or can guide the instrument user in making measurements that are more accurate.

The method of measuring the DE is simply to vary the distance between the RT and the source and record its readings [16]. Similar to SSE measurements, a source that is large enough to fill the entire FOV at the largest measuring distance should be used. This should eliminate the influence of the SSE. Due to difficulties associated with large-area sources, however, the SSE and DE are closely related and difficult to separate.

One of the main issues encountered when measuring the DE is dealing with the radiative and convective heating of the RT housing and detector due to the source at short target distances. Methods for confronting this problem are presented in Chapter 4. Other difficulties include the emissivity and uniformity of the source, as discussed in 2.7.

2.6.9   Emissivity Corrections

Commercial direct-reading IRTs frequently have a limited number of possible emissivity settings. For example, many IRTs may have an emissivity gain adjustment fixed at 0.95 [5, p. 366], as this is appropriate for a variety of metals, wood, painted surfaces and other materials [5, p. 354]. In the case where it is not possible to match the emissivity settings with the emissivity of the source, a correction must be applied to the expected RT under test (the UUT) reading to ensure traceability. An example of this is where an RT with a 0.95 emissivity setting is calibrated using a BCRS with emissivity $\cong 1.00$. Functions for calculating such corrections are derived in [6] which are discussed

further in [27]. The equation shown in Eq. 2.20 gives the expected temperature reading on a UUT in the situation above where traceability is provided via a contact thermometer.

$$S_{UUT}(T_{Meas}) = \frac{\varepsilon_{Cavity}S_{UUT}(T_{BB}) + (1 - \varepsilon_{Cavity})S_{UUT}(T_W) - (1 - \varepsilon_{Cavity})S_{UUT}(T_D)}{\varepsilon_{Inst}} \quad \text{Eq. 2.20}$$

Where:

- S_{UUT} is the signal from the UUT;

- T_{Meas} is the temperature indicated by the UUT;

- ε_{Cavity} is the emissivity of the BCRS;

- T_{BB} is the reference temperature of the BCRS as measured by the contact thermometer;

- T_W is the temperature of the ambient surroundings;

- T_D is the temperature of the UUT's detector, determined as per Eq. 2.21;

- is the temperature of the BCRS measured by the contact thermometer;

- ε_{Inst} is the emissivity setting of the UUT;

The detector temperature of the UUT is usually not available to the user. A method is derived and presented in [6] (shown in Eq. 2.21) for determining this detector temperature, by taking two measurements T_{Meas1} and T_{Meas2} of the same target with differing emissivity settings ε_{Inst1} and ε_{Inst2}.

$$S(T_D) = \frac{\varepsilon_{Inst1}S(T_{Meas1}) - \varepsilon_{Inst2}S(T_{Meas2})}{\varepsilon_{Inst1} - \varepsilon_{Inst2}} \qquad \text{Eq. 2.21}$$

Figure 2.20 shows correction values for a cavity with $\varepsilon_{Cavity} = 1$ when calibrating a typical IRT, derived for T_D=20 °C.
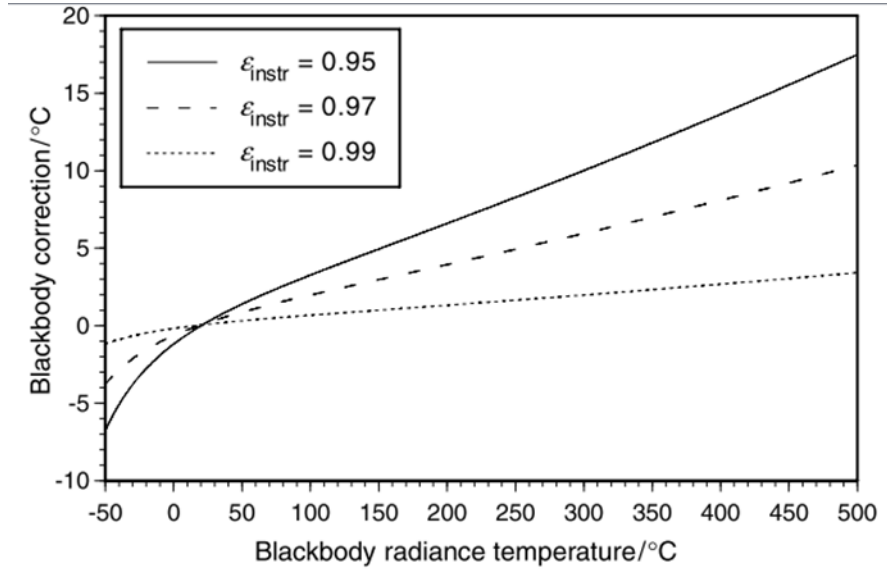
Figure 2.20 Temperature corrections required for a BCRS emissivity of unity when calibrating an RT with 8 μm to 14 μm responsivity for various emissivity settings. Figure reproduced from [6].

2.7   Blackbody Calibrators

2.7.1   Surface Treatments

In order to achieve a low calibration uncertainty when calibrating a RT, a blackbody of the highest possible overall emissivity should be used [2], [5].

A basic consideration when measuring a sample with an RT is the condition of the surface, which, along with the bulk properties of the material, determines the emissivity. In addition to the parameters emissivity ε and reflectivity ρ, introduced in 2.5.1, surfaces may be diffuse or specular. Rough surfaces reflect incident radiation diffusely,

whereas smooth surfaces, such as mirrors, reflect specularly as illustrated in Figure 2.21 [2, p. 580]. The figure shows idealised reflections from these surfaces, as well as glossy surfaces. It should be noted that real materials are neither perfectly diffuse nor perfectly specular; they contain both specular and diffuse components [2, p. 582]. Emissivity, reflectivity and specularity also vary as a function of incidence angle, wavelength and temperature in real materials [74].
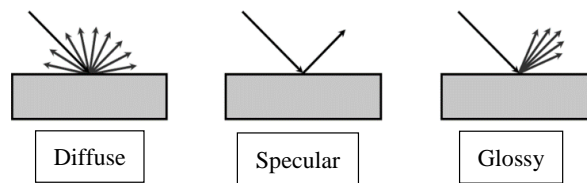
Figure 2.21 Reflection from ideally diffuse, ideally specular and glossy surfaces

The surface treatment of the material forming the walls of the cavity determines the local emissivity of the interior surface. A sample of copper with a pitted or uneven surface, for example due to oxidisation, will have a different emissivity to the same sample that is polished.

To construct a cavity with high emissivity, the treatment of the walls should be as diffuse as possible in order that the reflected radiance is reduced on each reflection.

The emissivity of many materials can vary dramatically depending on wavelength as shown for metals in Figure 2.21 [5, p. 354]. To reduce the influence of this wavelength dependency and increase the local emissivity of a radiator, special surface coatings such as Pyromark^{TM} and Nextel^{TM} are used. These dull, black coatings are rated by their manufacturers for high emissivity and reduce the uncertainty introduced by the surface condition. Creating an emissivity profile for a material similar to that in Figure 2.21

requires specialised equipment such as Fourier Transform Infrared (FTIR) spectrometers [5, p. 355], [75]. Such analyses have been performed for Nextel and Pyromark coatings applied using specified procedures [76], [77].
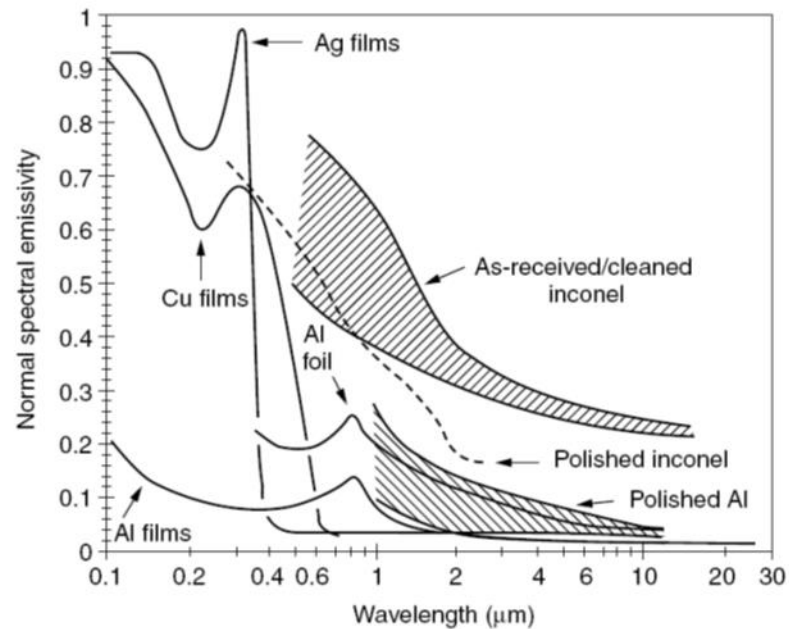
Figure 2.22 Emissivity relative to wavelength for a range of metals. The treatment of the surface has a large influence on the emissivity. Figure from [5, p. 354].

2.7.2 Cavity geometry

As mentioned in 2.5.2, the best real world approximation of a true blackbody radiator is an isothermal cavity with an opening or aperture smaller than its overall dimensions. In principal, any cavity of an enclosed shape may be used [2, p. 662]. A variety of cavity designs have been investigated by other researchers [33], [78], [79]. Cylindrical and conical shapes are most commonly used, as they can be easily constructed and can ensure a high temperature uniformity along the cavity's length.

The effective emissivity of a cavity is determined by the:

- Geometry of the cavity;

- Intrinsic or local emissivity of the cavity walls; and

69

- Temperature gradient along the cavity walls [80].

These characteristics are all interrelated; all cavity geometries face the trade-off between large openings, emissivity, and temperature uniformity. Circular cylindrical cavities that are closed at one end are an important cavity shape for practical purposes. Equation Eq. 2.22 gives an approximate method for estimating the overall emissivity of an isothermal cylindrical cavity, ε_{Cavity}, with a flat bottom perpendicular to the axis and of length l, radius r, and interior surface emissivity ε_{Wall} [3], [74]. This equation enables a quick theoretical evaluation of various cavity geometries.

$$\varepsilon_{Cavity} = 1 - \frac{1 - \varepsilon_{Wall}}{\varepsilon_{Wall}} \cdot \frac{1}{\left(1 + \frac{l^2}{r^2}\right)} \qquad \text{Eq. 2.22}$$

The second term in Eq. 2.22 models the small proportion of light reflected out of the cavity, the cavity reflectivity, ρ_{Cavity}. The key parameter in this term is the ratio of the length to the radius of the cavity, which, when carefully selected, can enhance the overall emissivity of the cavity. The emissivity for various values of $\frac{l}{r}$ is shown in Figure 2.23.

This simplification gives a quick method for determining suitable cavity dimensions for cylindrical cavities with idealised grey coatings that are wavelength independent and perfectly diffuse. For real-world cavities with surface treatments that have a specular as well as a diffuse reflective component, an end wall with a flat slope (shown in Figure 2.24) or with a cone-shape is used. More advanced emissivity estimation models take account for the specular reflections. A conical end is easy to construct if the cavity is bored out and allows simplified analysis of the emissivity, but an inclined plane is easier to construct with thin walls or using sheet materials.
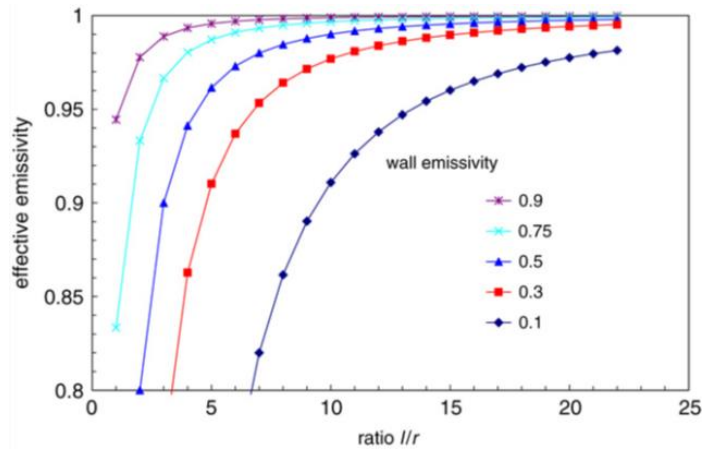
Figure 2.23 The variation in effective cavity emissivity relative to its geometry as calculated by Eq. 2.22 for various wall emissivities. Figure from [3].

More sophisticated methods for the calculation of cavity emissivities have been the subject of many articles [38], [81]–[83]. These additional methods variously take account of the temperature distribution on the walls of the cavity, the shape of the cavity end walls and model the emissivity variation due to the part of the cavity within the FOV of the measuring RT. Commercial ray-tracing software (STEEP-3.XX) is available for modelling the emissivity of cavities of various geometries [84] (although the cost was prohibitive for the present work). Free software that performs emissivity calculations has also recently become available from MSL which was used to evaluate the emissivity of the NSAI BCRS.
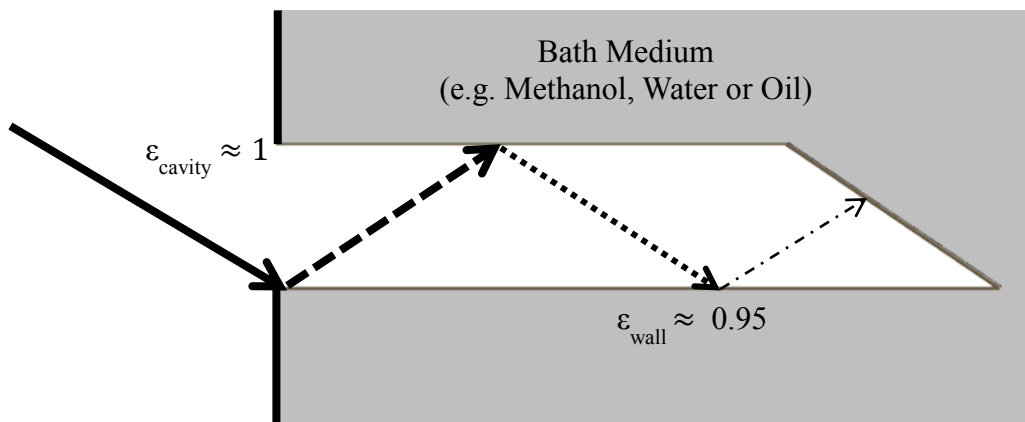
Figure 2.24 Attenuation of radiation incident on a bath-based BCRS with an inclined, flat base.

2.7.3   Cavity Designs

Most designs of cavity consist of a cavity shell where the external walls are heated using resistive electrical elements and with some mechanism to improve the uniformity. The heating elements are typically controlled using solid-state feedback controllers optimised to reduce settling time and increase stability. Some of the prominent categories of BCRS are discussed below.

Due to the desire for high temperature uniformity, metals with high heat transfer coefficients like copper are typically selected as wall materials. The selection of materials is, of course, dependent on the temperature range of the BCRS.

2.7.3.1 Heat Pipe Blackbodies (HPBBs)

A heat pipe is a passive heat transfer device that consists of a sealed vessel containing a working fluid that evaporates and condenses continually within the system. The heat transfer capabilities of heat pipes range from one hundred to several thousand times that of equivalently sized pieces of copper. When heated unevenly, for example by several electric heating elements, the process whereby the working fluid evaporates from the hotter areas of the system and condenses on the cooler walls of the heat pipe gives rise to a highly uniform temperature [85].

A Heat Pipe Black Body (HPBB), therefore, is a cavity formed within a heat pipe. Such black body cavities are typically arranged so that they fit into a cylindrical electrical furnace with the cylindrical axes of the furnace, heat pipe, and black body cavity in alignment.
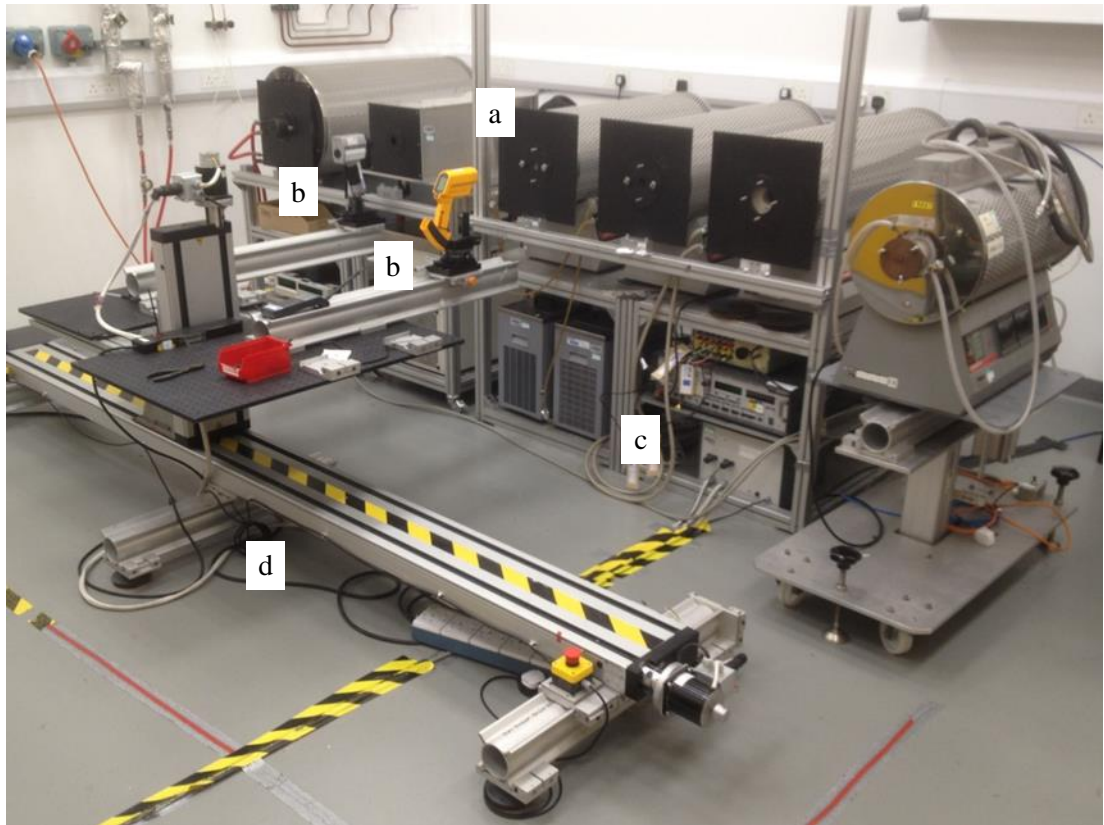
Figure 2.25 A suite of heatpipe and furnace-based BCRSs in NPL, showing cooled apertures in front of each of the cavities (black plates as at (a)), RTs mounted (b), measuring bridges for reference contact measurements (c) and Computer Numerical Control (CNC) translation stage in foreground (d).

2.7.3.2 Fixed Point Blackbodies (FPBBs)

Fixed point blackbodies are so-called as they are intended for use only at a single temperature. They are mandated as the method of defining T_{90} from the silver point (Ag, 961.78 °C) and above, at the gold and copper points (Au, 1064.18 °C and Cu, 1084.62 °C respectively) as they offer the lowest uncertainty method of establishing the scale at these temperatures. They function on the same principle as the fixed points used for establishing contact traceability in ITS-90 and take advantage of highly reproducible thermodynamic states of equilibrium.

A FPBB consists of a blackbody cavity enclosed by a fixed point cell containing the high-purity reference metal. The cell is contained in a crucible and the whole assembly

is formed of graphite in order to withstand the high temperatures. The cell, in some cases, is also contained within a heatpipe to improve the thermal uniformity. The entire assembly is mounted horizontally in the centre of an electrical furnace. The aperture of a FPBB is typically only a 2 mm to 6 mm in diameter and thus the primary level RTs calibrated by this method must have extremely small FOVs [5].
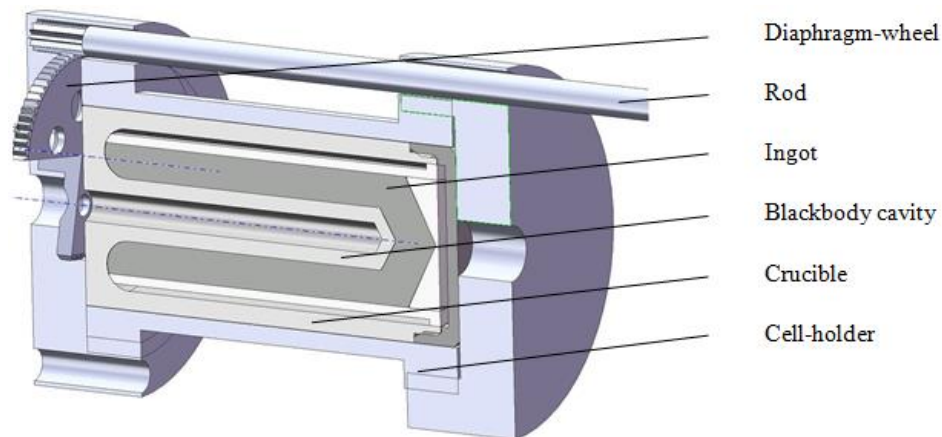
Figure 2.26 An ITS-90 FPBB designed for use at the Ag and Cu points from LNE-CNAM. Figure reproduced from [86].

The use of fixed points for radiation thermometry below the silver point is less common and different types of variable temperature blackbody are typically used with contact traceability. Some fixed points have, however been developed for use at low temperatures, for example the melting point of Gallium (29,7646 °C) [87], [88]. Some near-ambient fixed point cells also are planned for use in satellite-based calibration systems for on-orbit verification of earth observation RTs [89].

2.7.3.3 Tungsten Ribbon Lamps

Although Tungsten ribbon or strip lamps are not true blackbody radiation sources, they have long been used as calibration sources for RTs above 500 °C as they have some advantages, such as being cheaper and more compact than a blackbody cavity. These

lamps consist of a glass bulb that is either evacuated or filled with an inert gas and which contains a tungsten filament and electrical contacts.

The lamps have considerable disadvantages – as they have wavelength-dependant emissivities less than unity [3] they require calculation and corrections to be applied and frequent recalibration. Crucially, they present too small a source to fill the FOVs of many RTs. This, along with the fact that they are more suited to narrowband RTs, makes them unsuitable for calibration of many commercial RTs [2, p. 775], [5].

2.7.3.4 Bath-Based Blackbody Cavities

Thermal calibration baths – or simply metrology baths – are items of equipment common to all temperature calibration labs. They contain liquids, such as deionised water, methanol, ethanol or mineral oil blends, that are chosen to provide excellent stability and uniformity over the desired temperature range. The temperature of the bath liquid, o*r medium*, is controlled via an immersed heating coil and thermal uniformity is maximised using a stirring system. For temperatures near and below ambient a cooling coil is also used. These baths are available in a wide variety of designs depending on the type of thermometers they are designed for calibrating. In normal usage, a metrology bath is set to a temperature with reference and UUT thermometers immersed in the medium and allowed to stabilise, at which time measurements are taken [5].

Bath-based blackbodies consist of a blackbody cavity that is heated on its external walls by the liquid medium. This configuration can provide excellent temperature uniformity along the walls.
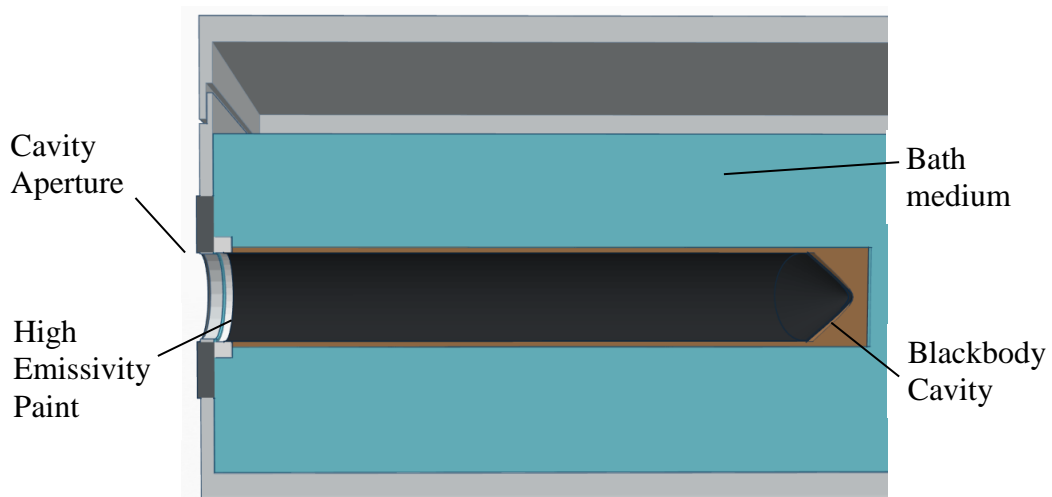
Figure 2.27 Cutaway schematic of a bath-based BCRS, similar to those used in LMK (see section 3.3.2).

The cavity may be arranged in a vertical or horizontal configuration. For the horizontal arrangement, the bath must be physically modified in order for the cavity's interior to remain dry.

Bath-based horizontal BCRSs have been demonstrated as robust sources for the calibration of RTs at primary laboratories from -50 °C up to 300 °C and have been in use for some time [33], [39], [40], [90]. Vertically oriented immersible BCRSs are used for the calibration of tympanic thermometers [41] and sometimes for ice-point checks of industrial RTs [5].

Cavities operating at temperatures below the dew point often use a purging system. These systems pass dry air or inert gas over the walls of the cavity to prevent the formation of dew or ice. The gas is usually equilibrated to the cavity's temperature setting by passing it through a heat exchanger in immersed in the bath fluid [91]. Any change in the surface condition of the walls introduces uncertainty about their emissivity and the effective emissivity of the cavity.

2.7.3.5 Planar Radiators

This type of calibration source is designed to offer a large surface area in order to fill the field of view of the UUT. Varieties with flat (often referred to as flat plate calibrators) and grooved surfaces exist and in both cases these are treated with high emissivity coatings. The large area is at the expense of the overall target emissivity, which although high, is less than that of a cavity.

Planar radiators are intended to function as greybodies. A greybody is defined as a substance with an emissivity that is less than unity and that doesn't vary with wavelength. Like blackbodies, greybodies are also theoretical substances. They can, however, be useful in modelling substances where a finite waveband is considered.

Where a UUT is calibrated using a planar radiator, the traceability should be via the radiometric route, as using contact traceability doesn't account for any drift in the surface emissivity over time. Under the radiometric regime the surface treatment and hence emissivity of the target, typically a nominal 0.95 [92], is part of the measurement system.

The surfaces of these instruments should therefore treated as delicate and should not be touched to avoid altering their value. A planar radiator may be used with a reference RT for traceability, or may be calibrated periodically and used as a calibration standard [10].

Although the emissivity of such plates may be nominally stated, manufacturers will acknowledge that this is a simplification. An example of a real emissivity profile is

shown in Figure 2.28. The manufacturer's specified nominal emissivity is 95 %. A true greybody would have a flat response across all wavelengths. The peak and trough at 8 µm and around 9 µm respectively are notable as they fall within the responsivity of many IRTs.
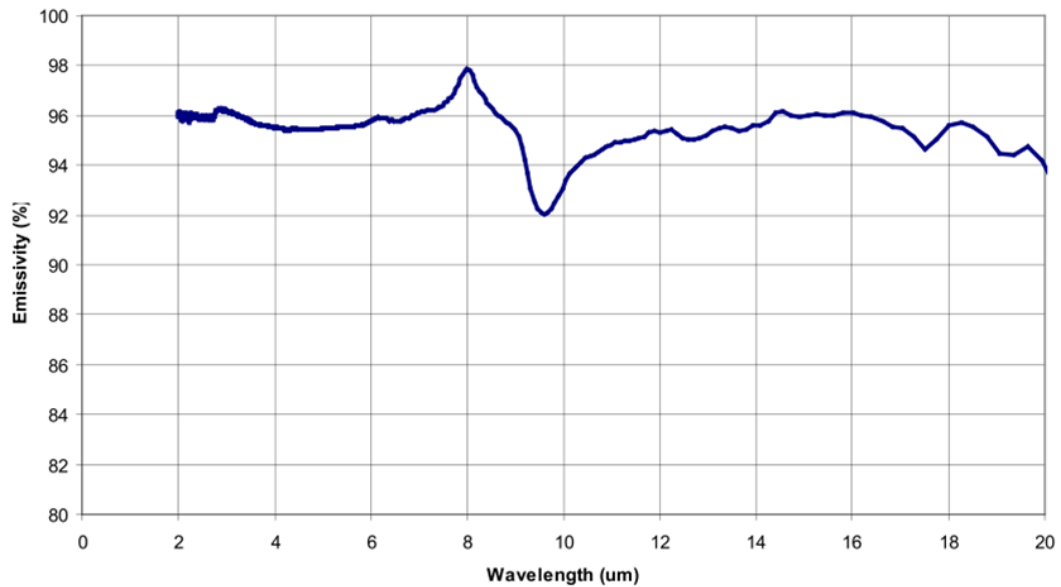
Figure 2.28 The emissivity profile of the Fluke 4181 planar radiator surface coating. Figure from [10] courtesy of Fluke Corporation.

As it is not practical to measure the spectral emissivity of a planar radiator everytime it is calibrated (if it is periodically calibrated) or even at manufacture, data such as that presented in Figure 2.28 should be treated as a type B uncertainty in an uncertainty budget [10], [93]

2.8   Summary

This chapter sought to give an overview of the various technical fields relating to the field of radiation thermometry as they arose in the course of completing the present work. The concepts of calibration traceability, particularly relating to the ITS-90 realisation of thermodynamic temperature were explained. The measuring principle of RTs, their specifications and factors affecting their selection were explained in detail. The many non-ideal influences affecting their use were introduced from a theoretical standpoint. Finally, the practical equipment types used for the calibration of RTs were described.

Chapter 3.   Comparison of Blackbody Cavities –

Measurements, Results and Analysis

3.1   Introduction

The introduction of a non-contact thermometer calibration service had been planned for some time in NSAI. To that end, an international collaboration began in 2014 between the temperature metrology laboratory at NSAI and the Laboratory of Metrology and Quality (LMK), the Slovenian DI for temperature metrology. Brian Cusack, a DCU Applied Physics undergraduate researcher at NSAI, undertook a final year project that resulted in the construction of the NSAI BCRS – an experimental, low-cost, immersible *vertical* cavity design – through this cooperation with LMK [37].

This chapter describes the development and the characterisation of the NSAI vertical BCRS, hereafter referred to as the NSAI BCRS. The cavity was characterised through a comparison with more conventional horizontal BCRSs. The comparison consisted of numerous measurements of the NSAI BCRS's radiance temperature when compared with horizontal BCRSs. Additional measurements of the uniformity of the cavity walls were carried out in order to inform the uncertainty budget described in 4.6.

This work was undertaken to investigate if the NSAI BCRS was suitable for calibration use over the temperature range from -30 °C to 150 °C, addressing the research question outlined in 1.3.1.

3.2   The NSAI Vertical BCRS

3.2.1   Design Considerations

Many RTs cover temperature ranges that span over 1000 °C. Good stability and uniformity are difficult to achieve, even in contact thermometry, over such a wide range. Blackbody sources provide improved uncertainty when optimised over narrower temperature ranges, and so an array of BCRSs is usually required. Using an array of blackbodies has other advantages like being able to calibrate at multiple temperatures in quick succession. Additionally, where two BCRS temperature ranges overlap, they can be cross-checked using an RT to improve confidence in the measurements performed.

Two key design considerations for a practical and versatile BCRS are:

- the temperature range the cavity will cover; and
- the emissivity settings and optical characteristics of the RTs that the cavity will be used to calibrate.

3.2.1.1 Filling the Field of View (FOV)

For a blackbody source to be of practical use for calibrating a given RT, the opening must be at least large enough to allow an RT's FOV to be filled. As mentioned in 2.6.6, RT manufacturers typically specify the FOV as a ratio between the target distance and the diameter of the target area at that distance for the RT, but it may also be specified as an angle. Designing a BCRS with a large aperture to accommodate large FOVs conflicts with the requirement for a small cavity opening to achieve a high cavity emissivity.
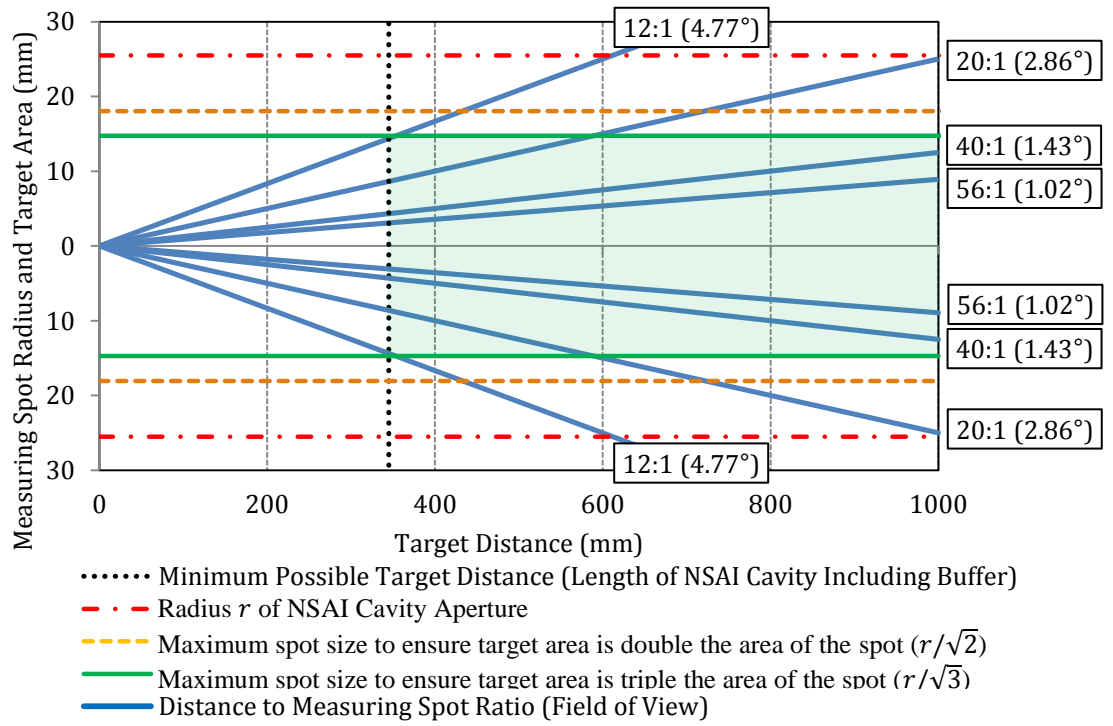
Figure 3.1 Target distances and nominal spot sizes, with a selection of commonly specified fields of view (not to scale). For illustrative purposes, the FOVs are shown with the RT lenses positioned at the origin or cavity aperture and the distance to the base of the NSAI BCRS is shown. The shaded area indicates the acceptable target distances, which may be achieved by moving the RT back away from the aperture when measuring the NSAI BCRS. The FOV of the TRT IV.82 is also shown (56:1).

Some RTs, particularly low-cost models, have large FOVs which call for very large cavity apertures. Figure 3.1 shows a selection of FOVs, including FOVs commonly available on such low-cost RT models. In addition, the FOV often extends beyond the nominal target area due to the Size-of-Source Effect (SSE), and thus a still larger source must be used so that the RT receives the full signal [34], [65]. Target areas double or triple the nominal target area have been suggested as rules-of-thumb to circumvent the SSE [71], [94]. The RT may be brought closer to the BCRS to fill its FOV, but this can present problems at extreme temperatures if convective heat transfer from the source raises or lowers the temperature of the RT's detector excessively.
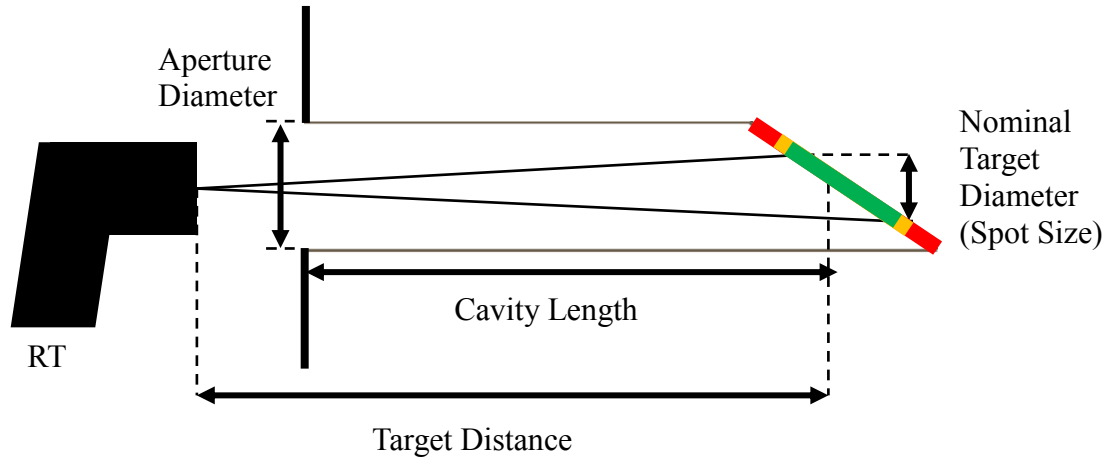
Figure 3.2 BCRS dimensions and FOV. The red, amber and green regions indicate the diameter, maximum spot size so that the target area is double and triple that of the spot respectively.

A further design consideration is whether the RT will be positioned with its focal plane at the entrance to the cavity or on the base of the cavity. Focusing on the cavity aperture requires that the cavity walls have a highly uniform temperature along their length – conditions best achieved using a heat-pipe BCRS. High thermal uniformity is necessary because the entirety of the cavity's interior is measured and the effective emissivity of the cavity in its totality is measured. The smallest errors for bath-based cavities are obtained when the RT is focused, as above, on the base, as this is where the effective emissivity is highest.

3.2.1.2 Emissivity

As mentioned in 2.7.2, calculation of emissivity is more complex for non-axisymmetric cavity shapes. Simplifying the cavity to a flat-bottomed cylinder and treating the wall emissivity as 0.93 [77] and using Eq. 2.22 yields a value of emissivity of 0.998.

Using the software from MSL (Blackbody Emissivity Version 1.3) and calculating the effective emissivity of the cavity as viewed by the TRT IV.82 (otherwise known as the integrated emissivity) under the parameters given in Table 3.1 gave an emissivity of 0.9993. The most conservative values for the uniformity (see section 3.9) and geometry of the cavity (when simplifying to a simple cylinder closed at one end) were used. The geometry of the estimation is shown in Figure 3.3.

Table 3.1 Parameters used in the MSL emissivity estimation software.

```
Cavity Type: Cylindrical, non-isothermal
Cavity length: 260 mm
Cavity diameter: 51 mm
Wall emissivity: 0.93
Base emissivity: 0.93
Mean wavelength: 11 µm
Relative bandwidth: 3
Linear temperature profile
  T at centre of base: 150.09 °C
  T at aperture: 149.27 °C
Number of divisions along each surface: 1000
Accuracy: 0.0000000000000055

Integrated Emissivity
  Diameter of aperture stop: 49 mm
  Diameter of measurement spot: 6 mm
  Working distance: 380 mm
  Distance from thermometer to front of cavity: 75 mm
  Integrated emissivity: 0.999294117503736
```
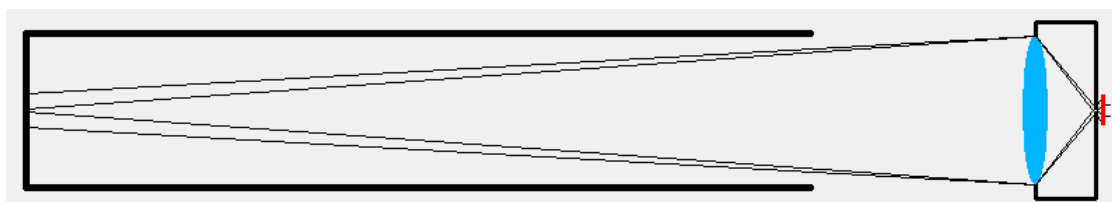

Figure 3.3 The cavity schematic as depicted in the MSL emissivity estimation software.

These estimations of emissivity gave values that tally closely with the previously calculated estimate, 0.99914[37].

3.2.1.3 Final Considerations

The size of an immersible cavity is also obviously limited by the dimensions of the available baths. The volume of liquid in the bath will also determine the response and settling time of the system.

All of the above considerations are reflected in the design of the NSAI vertical BCRS. The cavity was constructed by Brian Cusack and workshop staff in conjunction with the DCU School of Physical Sciences.

3.2.2 Assembly and Origin of the Design

The vertical NSAI BCRS was formed from commercially available copper pipe with internal diameter (d) 51 mm and wall thickness 1.3 mm. The base of the cavity was cut at an angle of 30° and sealed with a flat section of copper sheet. Figure 3.1 shows common RT FOV specifications which may be calibrated with a BCRS of these dimensions. FOVs of less than 2.86°, falling within the shaded area of the graph, may be calibrated with this cavity. Conversely, FOVs of 4.77° would need to be positioned directly at the cavity aperture to ensure the FOV is filled. Larger FOVs cannot be calibrated with this BCRS.

A high emissivity on the surface of the internal walls can be achieved by using special coatings developed for this purpose. In this temperature range, Pyromark 1200 has been shown to provide a high emissivity that is robust enough to withstand the conditions of use [77]. The NSAI cavity discussed in the present work is shown in Figure 3.4. The

walls of the cavity have been sandblasted and coated with Pyromark 1200 paint on the interior. After the last painting, the paint was dried at 100 °C for more than 24 hours.
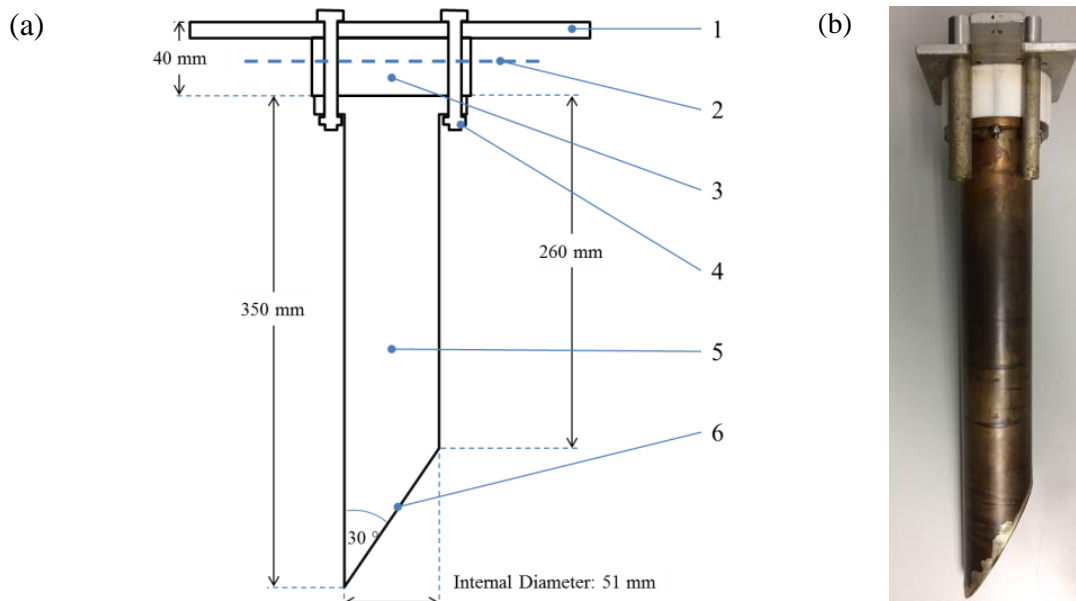
Figure 3.4 The NSAI vertical BCRS (a) and (b), showing the top mounting plate and aperture (1); immersion depth (2); PTFE buffer (3); retaining bolts connecting the mounting plate, buffer and copper flange (4); copper pipe, the interior of which is coated with high emissivity paint (5) and target area (6)

In order to increase the immersion depth of the cavity in the bath medium, a polytetrafluorethylene (PTFE) spacer is used (see Figure 3.4) in a similar approach to that in [95]. The spacer should also reduce heat conduction through the cavity to the top plate and therefore temperature gradients. The upper range limit was decided in part due to the PTFE spacer, which was found to swell slightly at temperatures above 150 °C.

The NSAI vertical BCRS is similar in its orientation, shape and use of a PTFE spacer to one described in [95] for tympanic thermometers, but larger. The cavity is also similar in terms of its shape and dimensions to the LMK vertical cavity described in 3.3.2.2, although this cavity does not feature a spacer to increase immersion. These were both pre-existing designs.

The inclined flat base of the NSAI cavity has an advantage over the cylindro-conical cavities besides being easier to construct from sheet materials. When coating the interior of the cavity, a meniscus of paint forms in the apex of the tip. With conical tips, this meniscus is in the centre of the target area of the RT, whereas with inclined, flat bases, it is located on the periphery of the target area. The meniscus may slightly increase the local specular reflectivity of the base, so it is best located away from the FOV.

The NSAI cavity, as constructed by Brian Cusack and DCU in the project preceding the present work, was used with only minor alterations. The retaining bolts connecting the mounting plate, buffer and copper flange were upgraded from iron to stainless steel to avoid contaminating the bath media. Some measurements made during the present work also used an extended top plate as described in 3.7.1.

3.3   Non-Contact Calibration Facilities Used

In most cases, non-contact calibration labs employ a variety of blackbodies to cover different temperature ranges. The blackbodies are typically horizontally oriented and arranged in a row such that mounted RTs may be moved along a rail and aligned with one cavity at a time.

3.3.1   Baths in NSAI

The methanol, water and oil baths used in NSAI were all of an up-welling design and were manufactured by Heto and were model type KB.

Upwelling baths circulate the bath liquid by stirring it through a channel. The channel contains an electrically controlled heating coil and a control PRT probe, as shown in red in Figure 3.5. Baths covering temperatures from approximately 50 °C and below also contain cooling coils which remain constantly on (shown in blue in the figure). The liquid surges over the top of a cylindrical inner well and into an outer collecting well. The working area used for contact calibration or for the immersion of a vertical BCRS comprises of the inner well.

The specifications are shown in Table 3.2.

Table 3.2 Specifications for the Heto KB Series Thermal Metrology Baths

Model Numbers:	Bath Media:
KB12	Mineral Oil
KB22	Deionised Water
KB25	Methanol
Volume	12 L
Diameter of Working Area (Inner Well)	100 mm
Depth of Working Area	500 mm
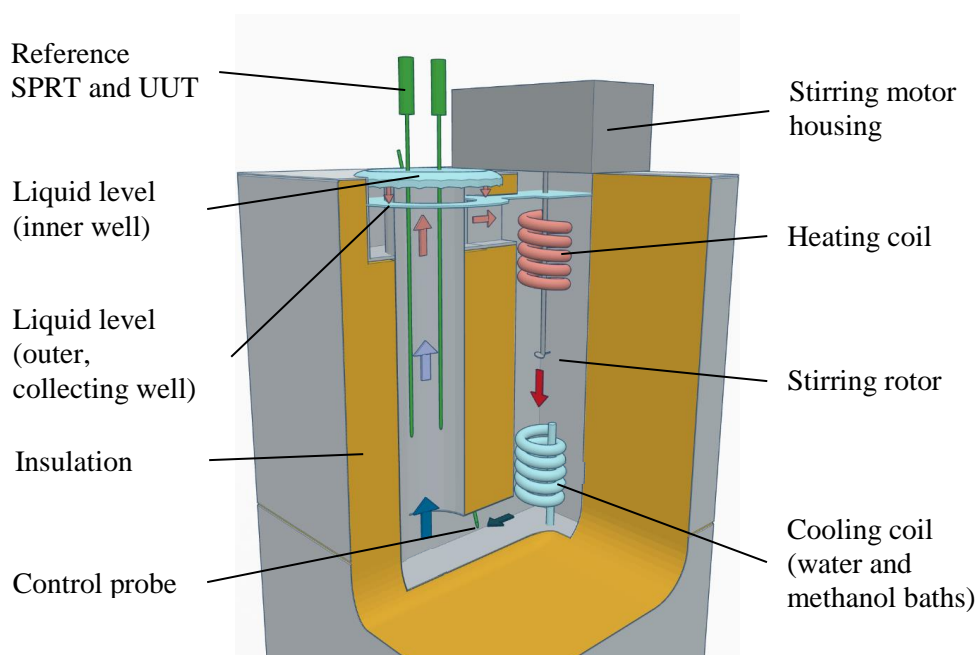
Figure 3.5 Cutaway view of an upwelling Heto bath with cooling coil as used in NSAI (not to scale). Arrows indicate the flow and the non-uniformity, which is less than 1 °C.

3.3.2 Facilities in LMK

Figure 3.6 Radiation Thermometry Laboratory in LMK.

The suite of horizontal blackbodies in LMK is shown in Figure 3.6. From left to right, three bath-based BCRSs under a fume hood may be seen, along with three furnace-based BCRSs and a large aperture bath-based BCRS for calibration of TIs (extreme right). In the foreground, the TRT II is shown mounted on a tripod, the SSE apparatus described in [71] is mounted on a tripod to the right of the TRT, and the rectangular frame of the translation stage system described in [96] is also visible. The fume hood shown is necessary to extract the vapours from the baths, as discussed in 3.3.4.

3.3.2.1 Horizontal BCRSs for use below 150 °C

The three horizontal LMK cavities used for this comparison were designed to cover the near-ambient temperature range from -30 °C to 150 °C. The horizontal cavities were cylindrical with conical ends of angle 120°, as shown in Figure 3.7. All three cavities were made of copper and were painted with high emissivity paints.

Table 3.3 Properties of the various blackbody cavities compared, including the length l, diameter d and the angle at the cavity's end θ_{tip}.

BCRS Name	l (mm)	d (mm)	Shape	θ_{tip}	Estimated ε_{Cavity}	Bath Media	Range (°C)
NSAI Vertical	390	51	Cylindrical with Inclined Flat Base	30°	0.998	Methanol, Deionised Water, Mineral Oil	-30 to 5, 5 to 80, 80 to 150
LMK Horizontal	450	60	Cylindro-conical	120°	0.999	Ethanol water mix	-30 to 5
LMK Horizontal	450	60	Cylindro-conical	120°	0.999	Deionised Water	5 to 60
LMK Horizontal	450	60	Cylindro-conical	120°	0.999	Mineral Oil	60 to 150
LMK Vertical	310	48	Cylindrical with Inclined Flat Base	30°	0.998	Methanol, Deionised Water, Mineral Oil	-30 to 20, 5 to 80, 50 to 150
SW20 Horizontal	120	40	Cylindro-conical	120°	≥0.995	Deionised Water	30 to 95
SW10C Horizontal	105	25	Cylindro-conical	120°	≥0.99	*Not bath-based*	50 to 400

The cavities are also shown in [71] in use with the LMK SSE apparatus, and in [97]. Additional LMK horizontal cavities, shown in Figure 3.6 and for use above 150 °C, are described in 4.3.1.

60 mm

410 mm

120°

386 mm

32 mm

(b)
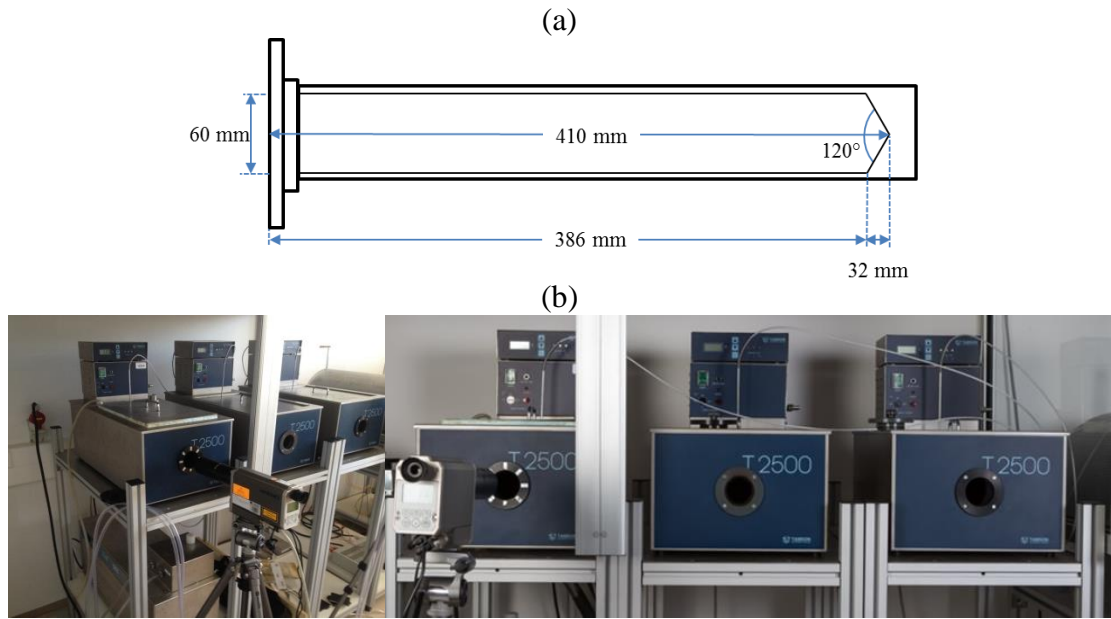
Figure 3.7 (a) Axial cross-section schematic of the LMK horizontal bath-based BCRSs and (b) photos showing the suite of bath-based BCRSs, with the transfer radiation thermometer in the foreground on the left in front of a BCRS aperture.

3.3.2.2 Vertical BCRS

The LMK immersible vertical BCRS is shown in Figure 3.8. Unlike the NSAI vertical BCRS and the horizontal cavities, the cavity is constructed out of aluminium. The cavity was painted using a similar procedure to that for the NSAI BCRS and both cavities had the same shape and equal radii to within 1.5 mm. The mounting system is visible in the photo, and consists of 3 bolts, spaced 120° apart, and normal to the cavity's cylindrical axis, and affixed through the walls of the cylindrical part and near its aperture. Brackets are attached to the bolts which allow the cavity to be mounted against the internal walls of an upwelling bath. The brackets also allow the cavity to be mounted to crossbars placed over the well, as shown in Figure 3.9.

This configuration means that the cavity may be mounted centrally in the bath's well. Unlike the NSAI BCRS's mounting design, the upper portion of the cavity is always

exposed to the air above the bath, potentially introducing a stem effect and reducing the thermal uniformity of the cavity walls near the aperture.

Figure 3.8 Photograph of the LMK vertical BCRS.

3.3.2.3 Baths in LMK

A range of baths was used with the immersible vertical BCRSs in LMK. The baths were all of an upwelling design. For negative temperatures, a Fluke/Hart Scientific bath was used and for the water and oil temperature ranges, large-diameter well Kambic baths were used. The Kambic-manufactured baths were of a custom design.

Figure 3.9 The LMK and the NSAI vertical BCRSs immersed alongside each other in a large diameter upwelling oil bath.

3.3.3 Horizontal BCRSs in the Heitronics Calibration Laboratory

As mentioned, the radiance temperature of the NSAI BCRS was also compared against two horizontal cavities in the Heitronics calibration laboratory, which was ISO 17025

accredited. Details of the SW 20 and SW 10C BCRSs, which are commercially available cavities manufactured by Heitronics, are given in Table 3.3. Note that the SW 10C cavity is a furnace-based model.

3.3.4   Safety Precautions

Appropriate safety precautions were taken as part of standard LMK and NSAI procedures, particularly regarding high temperatures and ventilation. All measurements of the ethanol, methanol and oil baths were performed under fume hoods in LMK and in fume cupboards in NSAI.

3.4   RT Alignment Materials and methods

One of the key practical disadvantages of the vertical configuration is the difficulty in mounting and aligning both reference radiation thermometers and units under test. Optical mounting equipment, from tripods for consumer cameras to optical breadboards for laboratory apparatus, is in the main, designed to accommodate horizontal mounting and targeting. Different methods and equipment used to position RTs for measurements in the work presented are discussed in this section.

3.4.1   Alignment by the Maximum RT Signal

Under ideal circumstances, the optical axis of a reference RT or an RT under test should be precisely aligned with the axis of the BCRS. To do this with a horizontal set-up, the alignment is performed only on the basis of the readings of the RT rather than using the targeting eyepiece or laser of the RT. Differences between the nominal target area

indicated by such targeting apparatus on the RT and the actual target area are sometimes observed, so the targeting system is not assumed to be accurate. These complications mostly occur where a separate optical system is used for the targeting apparatus and the measurement optics of the RT.

To align based on the readings, the RT is placed at an angle normal to the aperture of the BCRS using the lens and body of the RT and the body of the BCRS as a reference. Keeping the UUT at an angle normal to the BCRS, the RT is scanned incrementally across the aperture of the cavity on the X-axis. A change in the RT readings, either a large step (as suggested in [24]) or a specified percentage or absolute change in the readings (as suggested in [73]) is located on either side of the centre of the BCRS. The maximum reading is located centrally between these two points. This procedure is then repeated on the Y-axis, so that the RT is focused on the maximum reading in both axes. A related procedure is illustrated in 3.8.2.2.

This precise nature of this alignment method necessitates a finely graduated translation stage. The time-consuming aspect of the procedure mean that it is best performed using a CNC translation stage, as may be seen in Figure 2.25 and [96].

If a reference RT is used as a primary or secondary reference, it can be used alternately with the UUT and its axis similarly aligned with that of the BB. CNC translation stages facilitate alternating comparisons of this type by enabling the rapid and repeatable swapping of RTs.

(a)   (b)

(c)

Figure 3.10 (a) An ergonomic handheld IRT with no fixed mounting points, (b) a TRT
mounted horizontally using the ¼"-20 UNC tripod mounting thread and typical optical
mounting equipment positioned centrally below it and (c) an IRT with a thread
positioned beneath the lens (shown mounted on a tripod).

3.4.2   Mounting Features of RTs

Unfortunately, for the purposes of calibration, there are no mounting features that are
common to all radiation thermometers. While many RTs feature ¼" Unified Coarse
Thread tripod mounts (UNC - as commonly found on photographic cameras) and
occasionally other types of mounting threads, many are only designed for handheld use
by means of an ergonomic grip. Many in this latter category of RT do not have any flat,
straight edges and as such are very difficult to align. The angle that is normal to the

BCRS's entrance can only be guessed or found by a maximum signal method in this case. On those RTs which do feature mounting threads, the location of the thread can vary; 'pistol' shaped RTs may have threads under the lens or at the base of the handle.

Even when an RT is mounted using a tripod mounting thread, it is in many cases still vulnerable to twisting about the mounting point due to screwing or unscrewing. This can easily happen when operating buttons on the RT or if power or data cables connected to the RT are disturbed. Mounting features of RTs are an area where further standardisation would be welcome.

3.4.3 Handheld Alignment

Fluke, the manufacturer of the 4181 flat plate calibration system, suggest that handheld mounting of RTs is acceptable and does not contribute significantly to uncertainty [10]. Indeed, repeatable readings were found to be possible using this method [10]. This is on the assumption that the target area is at least double the size of the RT's nominal spot size, a condition that is easy to achieve with a large-area sources like planar radiators. When using targets with smaller diameters, such as conventional blackbody cavity simulators, fixed mounting is desirable.

When making handheld measurements, both hands must be used to steady the thermometer and assistance may be required to log readings. Even still, handheld positioning of RTs is imprecise, making the maximum signal method described in 3.4.1 difficult. This is especially true when using deep cavities, where alignment of the BCRS axis and the RT's optical axis is more critical. Extra noise is introduced into the RT readings while the RT is being positioned manually, making the maximum signal

method impractical. Where the maximum signal method is not practical, the targeting system of the RT is often the best available method of aligning the RT.

In order to perform a practical handheld alignment, the RT's lens is aligned centrally with the aperture of the BCRS, and the target positioned centrally on the base of the cavity.

Manual positioning can be sufficient where the RT has a good SSE characteristic and a small measuring spot relative to the diameter of the cavity. Under these circumstances, achieving a central target position with a source two to three times the size of the RT's nominal target should be realistic.

Both models of TRT (II and IV.82) fulfil these criteria; they have a small nominal spot size and a characterised SSE.

3.4.4 Development of a Mounting System

A reasonably firm mount had been designed and constructed out of extruded T-slot sections as part of the previous project [37] that allowed repeatable positioning of the Fluke 574 IRT (see section 4.2.1.1). This mount was not easily adjustable in the X or Z dimensions and thus was limited in its usefulness for mounting other thermometers.

In light of these difficulties, an exploratory approach was adopted towards designing a mounting system. Several mounting methods were trialled using a variety of optical equipment. An optical breadboard was found to give the best stability and flexibility when mounting in the horizontal configuration (mainly for measurements described in

Chapter 4). The breadboard and optical posts could also be configured to mount lightweight IRTs in the vertical configuration (as in section 4.2.1.2).

No suitable mounting system for the vertical cavity configuration was available during the measurements made in LMK, so the TRT II was positioned manually above the vertical BCRSs as shown in Figure 3.11. Two hands were used to hold the TRT in position during measurements. It was found to be possible to maintain a steady position while readings were logged and the readings were found to be stable while the TRT was manually held.
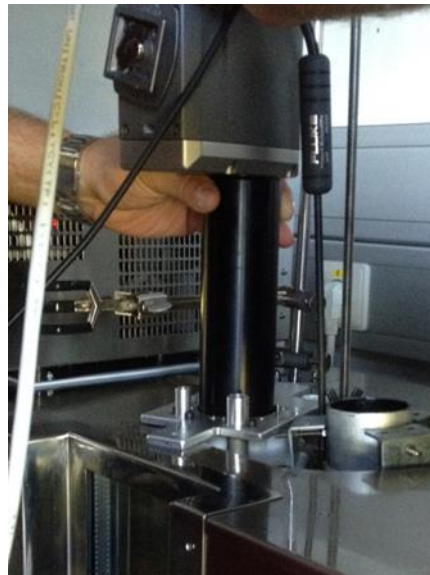
Figure 3.11 The TRT II positioned manually above the entrance to the NSAI BCRS. The BCRS is immersed in a large-diameter upwelling oil bath in LMK.

3.4.5   The NSAI Vertical RT Mount

3.4.5.1 Construction

A provisional mount to support the TRT IV.82 when measuring in the vertical configuration was assembled from readily available parts in NSAI. This mount, which

makes use of the ¼"-20 UNC tripod thread on the TRT, is shown Figure 3.10. The mount was used in all measurements of the NSAI BCRS made with the TRT IV.82 in NSAI.

The mount consists of a flat, weighted base that supports an 600 mm upright post with a rack-and-pinion adjustable stage. The stage may be fixed at any height along the post. A 400 mm horizontal post projects from the stage to a further stage that may be rotated on two axes. The TRT is mounted to this stage using the tripod thread.

(a)　　　　　　　　　　　　　　(b)

TRT

Mounting Stage

Upright Post with Rack and Pinion

Weighted Base

TRT

SPRT

NSAI BCRS Top Plate

Stirring Motor

Aperture
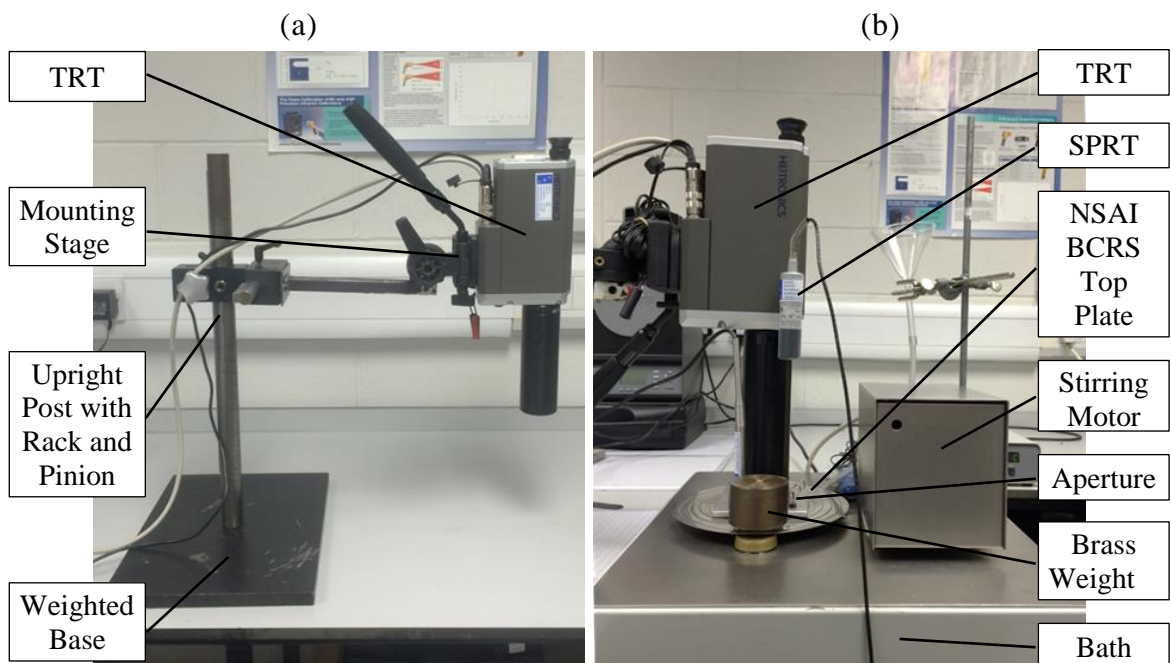
Brass Weight

Bath

Figure 3.12 (a) The TRT IV.82 mounted for measurement in the vertical orientation on the NSAI mount and (b) above the NSAI BCRS. In (b), the BCRS is immersed in the Heto bath and the aperture of the BCRS is behind a brass weight.

3.4.5.2 Usage

When using this mount, the RT was first positioned centrally over the aperture similarly to the handheld alignment method described in 3.4.3.

The central location of the laser target on the cavity base was then verified during the TRT IV.82 measurements using a smartphone camera with a light. The smartphone was positioned temporarily at the edge of the BCRS aperture so that the camera was viewing the base and the light illuminating it without obstructing the path of the TRT's laser.

In this way, the camera display showed the location of the laser target on the interior of the cavity. Even though the camera did not obscure the laser which uses the main optical system of the instrument, the TRT readings were reduced, so the camera was removed for all measurements.

The use of the camera was necessary, as the focal length of the TRT IV.82, at 380 mm, is very similar to the length of the NSAI BCRS. When in focus, the front of the TRT lens was only 35 mm from the top plate of the BCRS. The TRT lens is almost the same diameter as the BCRS aperture, so it is not possible to verify the position of the laser with the naked eye.

3.5   Reference Measurements

A selection of calibrated SPRTs and bridges were used to make contact measurements that were traceable to ITS-90.

3.5.1   SPRTs and Bridges

The SPRTs, as described in 2.4.4, were used as primary references for all measurements of the NML BCRS and LMK BCRSs under 150 °C. Under NML procedures, measurements from a primary reference are used to calculate the best measurement

estimate, unlike secondary references which are used for error-checking as described below.

A variety of measuring bridges and associated standard resistors were used with the SPRTs for the measurements in LMK and NSAI. In NSAI, Fluke/Hart Scientific model 1590 bridges were used. A four-wire connection was used in all cases between the SPRT, bridge and standard resistor.

3.5.2   Secondary References

Secondary references are used to detect any problems with the apparatus or its set-up, for example errors due to thermal contact between an SPRT and the wall of a metrology bath. The secondary references used for the NML measurements were long-stem industrial PRTs and associated indicating instruments.

3.5.2.1 T12 PRT Probes

A multichannel PRT and data acquisition system was also used for some measurements undertaken in NML, described in 3.8 to 3.10. The instrument, make and model MBW T12, consisted of 12 PRTs conforming to a EN 60751 1/10th DIN. specification connected to a multiplexing RS232 data logger.

3.5.3 Transfer Radiation Thermometers (TRTs)

3.5.3.1 Heitronics TRT II

The TRT II was used for measurements in LMK. The manufacturer's published specifications for the TRT II are given in Table 3.4. The key specifications is the spectral sensitivity from 8 μm to 14 μm in the applicable temperature range from -50 °C to 300 °C. The pyrometer has fixed-focus optics with focal length 380 mm and nominal spot size 6.8 mm.

This RT was part of the LMK radiation thermometry laboratory and was used for the measurements made there. The instrument was used as a transfer standard between the radiance temperature of the horizontal BCRSs and the vertical BCRSs. All measurements were made with an instrumental emissivity setting of 1.000.

Readings were taken via RS232 connection to a PC and logged using LMK's bespoke measurement software.
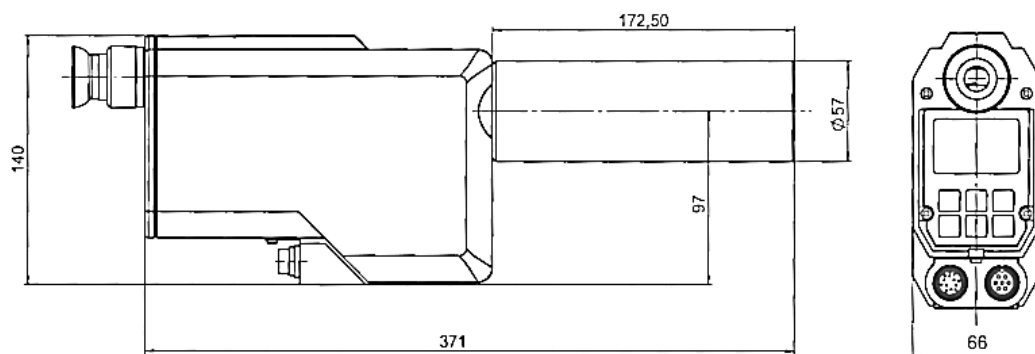
Figure 3.13 Dimensions of the TRT II, with all dimensions in milimetres [98].

Table 3.4 Heitronics TRT II Published Specifications

Value	Range I	Range II
Temperature Measuring Range	-50 °C - 300 °C	150 °C - 1000 °C
Spectral Sensitivity	8 μm - 14 μm	3.9 μm
Field of View (nominal**)	6.8 mm @ 380 mm	5.6 mm @ 390 mm
Field of View Marking	Laser marker and through-the-lens-sighting	
Lens	S977AR (Zinc Selenide)	
Detector	Pyroelectric	
Analog Output (Changeable by Software)	0 - 20 mA, 4 - 20 mA, 0 - 1 V, 0 - 10 V The output signal is linearly to the measuring temperature or linearly to the measuring radiation, depends on setting	
Resolution of the Analog Output	12 bit	
Digital Interface (RS232C)	9 600 – 115 000 bps	
Resolution of Digital Output	0.02 °C	
Response Time (90 %) [*Changeable by Software]	3 s [0.03 s ... 600 s*]	
Permissible Ambient Temperature	23 °C ± 3 °C	
Storage Temperature	-20 °C - 70 °C	
Operating Voltage	24 V DC by Power Supply T21 (80 - 230 V AC)	
Power Consumption	4.8 VA	
Weight	1.5 kg	
Protection	IP65 (NEMA 4 equivalent)	
**	Field of View and Size-of-Source Effect are individually measured by manufacturer	

3.5.3.2 Heitronics TRT IV.82

The TRT IV.82 was used for measurements in NSAI. The manufacturer's published specifications for the TRT IV.82 are given in Table 3.5.This RT is very similar to the TRT II except that it has a single temperature range from -50 °C to 1000 °C. Spectral sensitivity is again in the 8 μm to 14 μm. The optical characteristics identical to those of the TRT II described above.

This RT was used for all comparison measurements of the NSAI BCRS undertaken in NSAI. Again, all measurements were made with an instrumental emissivity setting of 1.000.

The temperature measurements of the BCRSs described in 3.7 were conducted by the TRT manufacturer as part of the TRT's initial calibration before supplying the TRT to NSAI. According to the calibration certificate for the TRT IV.82, the calibration measurements were radiometrically traceable via a reference TRT of the same model to PTB, the German NMI.

The temperature measurements undertaken in NSAI using this instrument were all logged to PCs via RS232 using the 'Easy TRT' software supplied with the instrument. This enabled the simultaneous recording of the internal reference temperature and housing temperature of the instrument. Monitoring the internal reference temperature is useful for recording when the instrument is operating in excess of its permissible rated ambient operating temperature.

It is not clear from the documentation supplied with the instrument what the housing and reference temperatures refer to. As both models of TRT use chopped pyroelectric detectors (see section 2.6.5.4), it is assumed that the reference temperature refers to the temperature of the optical chopper or another internal reference surface. Chopped radiation RTs such as these use a reference temperature measured alternately by the detector to subtract the bias signal introduced by the housing temperature from the radiation signal of the measurand.

Logging the measurements using PCs also allowed for unattended measurements as described in 3.10.

For some of the DE measurements described in Chapter 4, the TRT IV.82 was used as a standard. This instrument was acquired by NML midway through the duration of the present work.

Table 3.5: Heitronics TRT IV.82 Published Specifications

Value	Range I	Range II
Temperature Measuring Range	-50 °C - 1000 °C	not available
Spectral Sensitivity	8 μm - 14 μm	
Field of View (nominal**)	6.8 mm @ 380 mm	
Field of View Marking	Laser marker and through-the-lens-sighting	
Lens	S977AR (Zinc Selenide)	
Detector	Pyroelectric	
Analog Output (Changeable by Software)	0 - 20 mA, 4 - 20 mA, 0 - 1 V, 0 - 10 V The output signal is linearly to the measuring temperature or linearly to the measuring radiation, depends on setting	
Resolution of the Analog Output	12 bit	
Digital Interface (RS232C)	9 600 – 115 000 bps	
Resolution of Digital Output	0.02 °C	
Response Time (90 %) [*Changeable by Software]	3s [0.03 s ... 600 s*]	
Permissible Ambient Temperature	23 °C ± 3 °C	
Storage Temperature	-20 °C - 70 °C	
Operating Voltage	24 V DC by Power Supply T21 (80 - 230 V AC)	
Power Consumption	4.8 VA	
Weight	1.5 kg	
Protection	IP65 (NEMA 4 equivalent)	
**	Field of View and Size-of-Source Effect will individually be measured	
Additional specifications from user manual:		
Long-term stability:	better than 0.1 ‰ of the absolute measuring temperature in Kelvin/month	
Accuracy (provided that the emissivity has been correctly set, after a warm-up period of 15 min):	± 0.5 °C plus 0.7 % of the temperature difference between the housing containing the measuring instruments and the object to be measured or: value of temperature resolution. The higher value shall prevail.	

For both the TRT II and TRT IV.82, the cavity temperature measurements are only valid for the 8 μm to 14 μm waveband. This is not a serious limitation, as most RTs

operating in this temperature range use this waveband. The geometries of the cavities used should also minimise any corrections required if these cavities were used with RTs of another waveband.

3.5.4 Calculation of Corrections

As is customary in temperature metrology, results are presented in terms of corrections rather than errors. The corrections are calculated as:

$$t_{corr} = t_{90} - t_{meas}, \qquad \text{Eq. 3.1}$$

where t_{corr} is the correction, t_{meas} is the UUT reading and t_{90} is the reference temperature, with all values in degrees Celsius.

3.5.5 Calibration

All measurement standards used for reference measurements, including SPRTs, secondary PRTs, measuring bridges and standard resistors were within their calibration interval in accordance with NML and LMK procedures.

Similarly, it is required under IEC/ISO 17025 that all measurement standards are calibrated for measurements undertaken in the Heitronics calibration laboratory.

All measurement standards were labelled with an identification number and recalibration due date. In NML and LMK, these details were recorded electronically along with the measurement results.
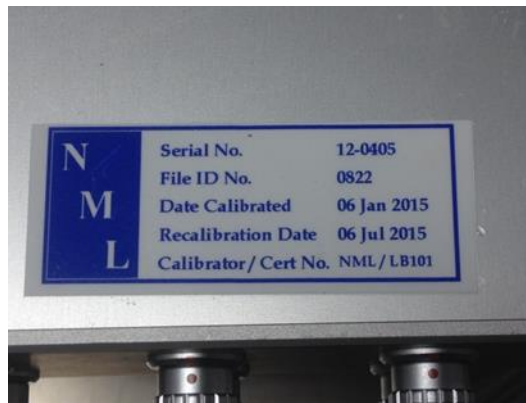
Figure 3.14 A calibration label on an instrument in the NML calibration system.

3.5.5.1 Calibration Intervals

Under NML procedures, SPRTs are checked at the start of each week at the ice point (0 °C), at six week intervals at the TPW (0.01 °C), and at two to three yearly intervals at all fixed points across their subrange [99]. In NML, the calibration label is updated after the TPW check.

The usual calibration interval for SPRTs is 6 weeks and for measuring bridges and the associated standard resistors, the interval is 1 year.

3.6   Comparison of Vertical and Horizontal BCRSs in LMK

3.6.1   Method

Comparisons were undertaken firstly in LMK and later in NSAI. The approach taken in both cases was to measure each BCRS using a TRT as if the TRT were under calibration. Traceability was provided using contact temperature measurements as described in section 3.5.

3.6.1.1 Measuring Procedure for Vertical BCRS Measurements

In order to carry out non-contact temperature measurements of the vertical cavities, they were each immersed in turn in the baths and fixed in place.

The baths were allowed to stabilise for approximately 2 hours at each of the set-points throughout the temperature range. The stability of the baths was better than ±0.01 °C at each set point. The contact temperature was monitored using SPRTs that were immersed beside the cavities such that the sensing element was within 40 mm of the target area at the base of the cavity. Secondary contact references were also used as crosschecks.

The cavities were then measured with a TRT. The optical axis of the RT was aligned with the axis of the cavity and the RT was positioned so that it was focused on the centre of the base cavity. Each measurement round consisted of ten measurements of the contact and non-contact references, recorded at 10 second intervals using data acquisition software.

To minimise the formation of condensation and ice at temperatures below the dew point, a lid was used. The lid was kept in place when the bath was stabilising and removed prior to the TRT measurements. The exterior walls of the vertical cavities were cleaned and dried after use in each media.

3.6.1.2 Measuring Procedure for Horizontal BCRS Measurements

The LMK horizontal cavities in this temperature range are all permanently sealed onto the sides of dedicated baths. The contact temperature was again monitored using SPRTs. The TRT was aligned manually in front of the cavity aperture, in a similar manner to that for the vertical measurements described in 3.6.1.1.

The low temperature LMK horizontal cavity is equipped with a gas purging system to prevent ice formation on the cavity walls at temperatures below ambient. Purging was carried using nitrogen gas of 5N purity at flow rates of approximately 1 litre per minute.

3.6.2   Results

3.6.2.1 Comparison of the NSAI Vertical Cavity with Horizontal Cavities in LMK

Figure 3.15 shows the comparison measurements made between the NSAI vertical BCRS and the suite of horizontal cavities in LMK. As in many of the graphs in the present work, the X-axis shows the reference temperature as measured with the SPRT and the Y-axis shows the corrections to be applied to the UUT (in this case, the TRT). In these graphs, horizontal dashes are used to represent measurements of horizontal cavities and triangles are used to represent measurements of vertical cavities.

The horizontal cavities were chosen according to the temperature ranges shown in Table 3.3. The uncertainty of measurement was evaluated based on the model suggested by the CCT-WG5 [18]. The difference between the errors for the cavities was less than 0.25 °C across the temperature range.
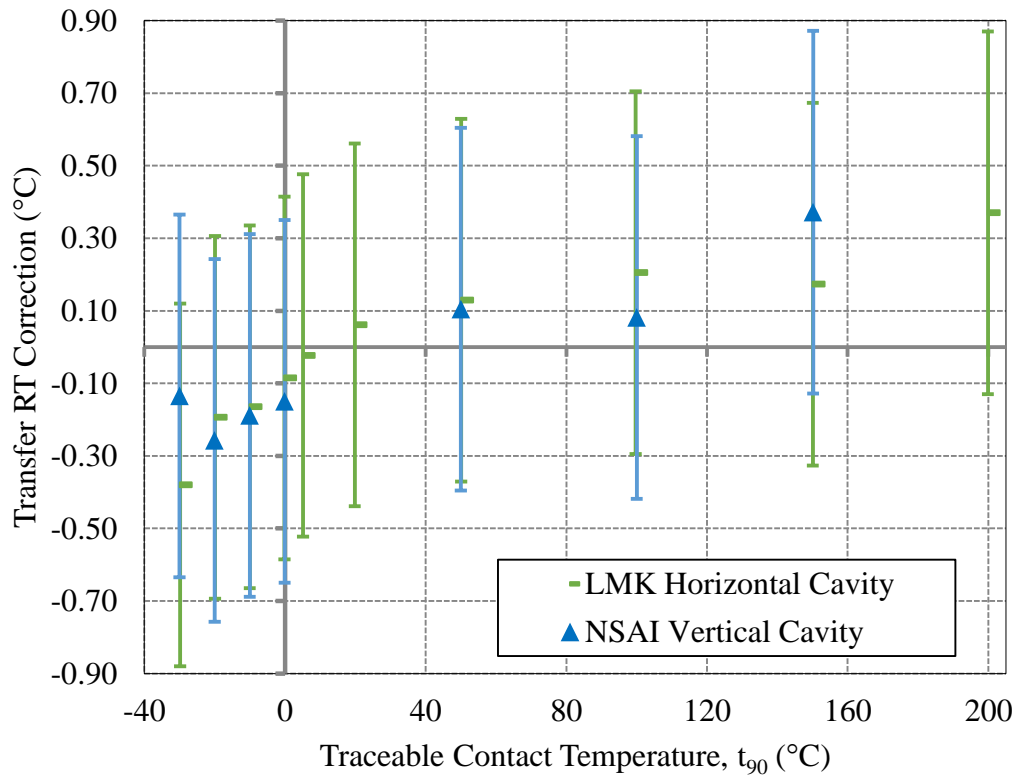
Figure 3.15 Comparison of the NSAI vertical BCRS and the horizontal LMK BCRSs in the range -30 °C to 150 °C. These measurements were made at the cavity aperture. The error bars show the estimated uncertainty ($k = 2$).

3.6.2.2 Comparison of the NSAI Vertical Cavity with Vertical Cavity in LMK

In addition to comparing the NSAI vertical cavity to horizontal cavities, it was compared to a similar vertical cavity that had previously been constructed at LMK. Both of these cavities were removable and so they could be immersed simultaneously in the same baths for the measurement experiments at the temperatures from 50 °C to 150 °C. This comparison was conducted to investigate the influences of the design differences, described in section 3.2 and 3.3, of the two cavities.

The results of the comparison are shown in Figure 3.16. The corrections for the NSAI vertical cavity were smaller than the LMK vertical cavity at each set point. The NSAI

vertical cavity benefited from an increased length, a design that improved immersion, a top plate around the aperture and a copper rather than aluminium construction.
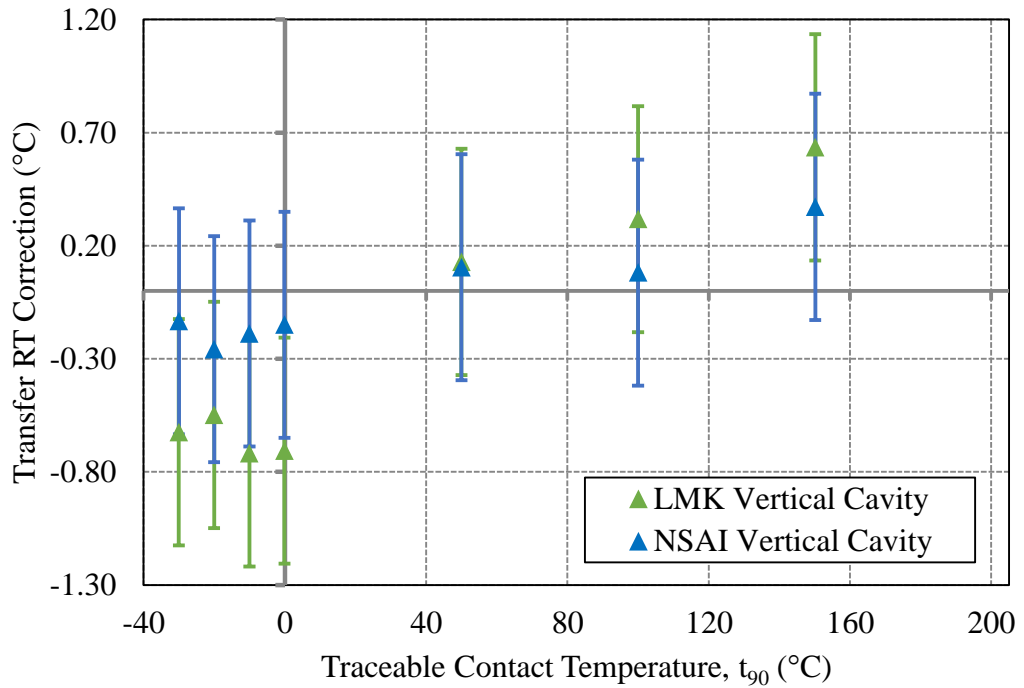
Figure 3.16 Comparison of the NSAI vertical BCRS and the vertical LMK BCRSs in the range -30 °C to 150 °C. These measurements were made at the cavity aperture. The error bars show the estimated uncertainty ($k = 2$).

3.6.3 Discussion

Overall, the results show good agreement between the horizontal and vertical configurations. Where the measured points and their associated uncertainties overlap completely, there is a 95% probability that the two configurations agree to within the stated uncertainty.

Figure 3.15 shows good agreement between the vertically and horizontally configured BCRSs at each of the temperature set points. The magnitude of the vertical cavity corrections is larger at most but not all set points. The figure indicates that the temperature corrections for the vertical cavity increase at the top end of the temperature

range. This could be indicative of an upper limit for this set-up. Use of a vertical cavity may cause problems in temperatures above the range of the comparison due to the effects of convection on the measuring RT.

Some ice did form on the walls of the vertical cavities near the aperture at temperatures below zero for the measurement experiments performed in LMK and NSAI, as shown in Figure 3.17. Ice formation near the target area, deeper within the cavity, however, was observed to be minimal. The TRT correction was usually negative below 0 °C.
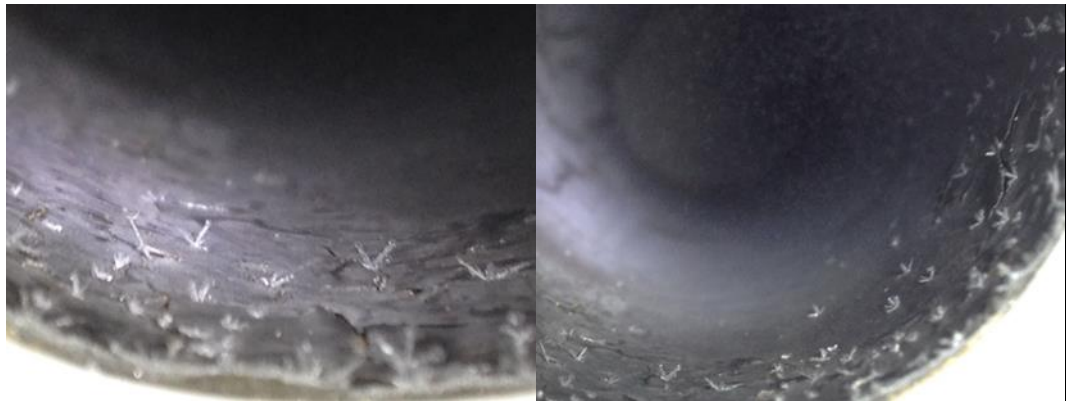
Figure 3.17 Photos of the ice crystals that formed inside the cavity near the aperture at -30 °C while the cavity lid was off.

Figure 3.16 shows that the TRT corrections for the NSAI vertical cavity were smaller than those for the LMK vertical cavity, indicating an improvement in performance. Further work is needed to determine which of the design differences described in section 3.3.2.2 had an influence on the performance improvement, which was up to 0.56 °C. The NSAI vertical cavity benefited from an increased length, a design that improved immersion and therefore temperature uniformity, a top plate around the aperture and a copper rather than aluminium construction. These are some potential reasons for the improved performance.

It should be noted that in Figure 3.15 and Figure 3.16, the exact influence of the TRT on the measurements is not known. A relative comparison of the corrections for each cavity in these figures gives an indication of this influence.

The effectiveness of the PTFE collar shown in Figure 3.4 could be improved by redesigning bolting configuration so that bolts mounting alternately from the top plate and the copper flange are used, thus eliminating heat bridges as in [95].

3.7 Comparison of NSAI Vertical BCRS Measurements against TRT Calibration Measurements

3.7.1 Method

Following the work conducted in LMK, a further comparison was made possible by NSAI's procurement of an in-house TRT. Measurements made in NSAI were compared to recent TRT calibration results received from the manufacturer.

The measurements made in NSAI were made in much the same way as those for the vertical comparisons at LMK, using upwelling baths, and traceable SPRTs and bridges. The Heto baths described in 3.3.1 were used. Two changes to the measurement procedure were made:

- A larger top plate was used, as shown in Figure 3.18, to further reduce the possibility of the bath liquid entering the cavity and limit the influence of bath vapours on the TRT lens;

- A manually positioned stand to mount the TRT vertically above the BCRS was used.

SPRT

Extended
Top Plate

Spacer

Inner Well
Liquid Level

Outer Well
Liquid Level
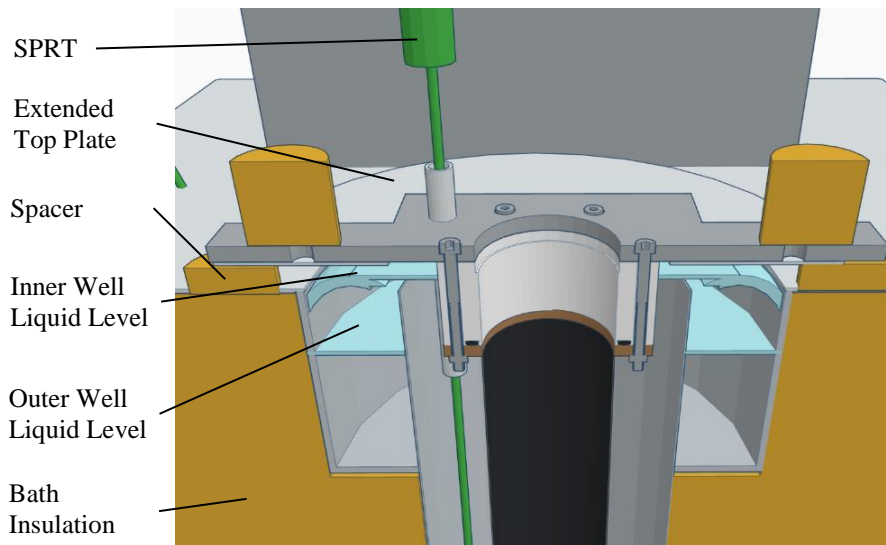
Bath
Insulation

Figure 3.18 Cutaway view of the NSAI BCRS immersed in a Heto KB series upwelling bath (not to scale).

Normally in an upwelling bath, a weir is used to maintain the liquid is at its maximum level, therefore improving the circulation of the liquid. A weir is an adjustable collar that rotates around the upper part of the bath's well, closing off side channels depending on its position. It was not possible to use a weir, as the adjusting levers would conflict with supports for the BCRS and the top plate.

Care was nonetheless taken to ensure that the level of the medium in the upwelling bath was at the maximum possible level at all times. The immersion depth is shown in Figure 3.4. This was achieved by topping up the medium using a funnel and tube passing under the top plate which is visible in Figure 3.12. Separate funnels and tubes were used for each bath medium to avoid contamination of the medium or extra cleaning.

The uncertainties evaluated in 5.3.3 are based on 5 repeat measurement runs at each of the set-points. The uncertainties were calculated for each bath medium based on the worst-case repeatability results for that medium.

3.7.2 Results and Discussion

▲ Methanol Bath   ▲ Water Bath   ▲ Oil Bath   ■ Manuf. Calibration (Horizontal), Traceable to PTB
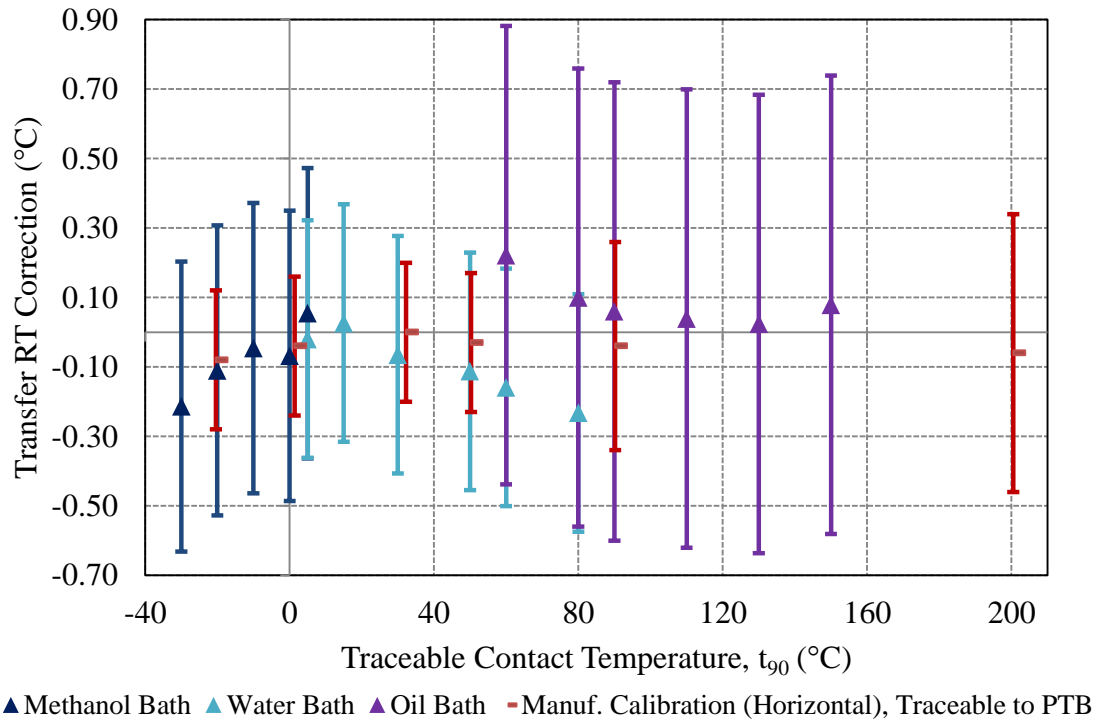
Figure 3.19 Comparison of measurements made by the RT manufacturer of horizontal BCRSs with measurements made of the NSAI vertical BCRS. The error bars show the estimated uncertainty ($k = 2$).

The results of the comparison are given in Figure 3.19 and show broad agreement between measurements for the horizontal and vertical orientations. The measurements were most repeatable for the water bath, and hence the uncertainties are lowest for this bath. The reasons for the differences in the measurement results where the temperature ranges of the baths overlap are not known. One possible explanation is effects due to bath vapours in the RT's optical path.

After these measurements were complete, an investigation into the influence of vapours from the bath media was undertaken, as described in 3.10. The influence of the vapours was found to be significant with the oil bath. It is possible that redesigned apparatus or a measurement method updated to take account of this could result in better performance at the upper limits of each of the three bath media used.

3.8 Thermal Homogeneity of the NSAI Cavity Base

In addition to measuring the linearity of the NSAI BCRS's radiance temperature, the thermal homogeneity of the cavity's base was measured in NSAI. Two methods were used:

- PRTs were attached to the base;
- The TRT IV.82 was incrementally scanned across the BCRS base in the X and Y directions.

3.8.1 PRT Measurements of the Base

3.8.1.1 Method

Ensuring good thermal contact between the T12 PRT probes (see section 3.5.2.1) and the copper walls of the BCRS without permanently modifying the cavity was found to be challenging. Mounting the probes inside the cavity on the inclined base would have proved still more difficult, and interior of the NSAI BCRS had already been painted at the commencement of the present work.

The PRTs were therefore affixed to the base's exterior to avoid damaging the interior surface coating. This allowed better thermal contact between the probes and the base. The probes were strapped to the base using rubber and copper bands as shown in Figure 3.20.

Initially two probes were used, as these uniformity measurements were being made in tandem with the axial uniformity tests described in 3.9 and not all channels were available. Later, at the extremes of the temperature range of the BCRS, five probes were attached to the base and their measurements logged.
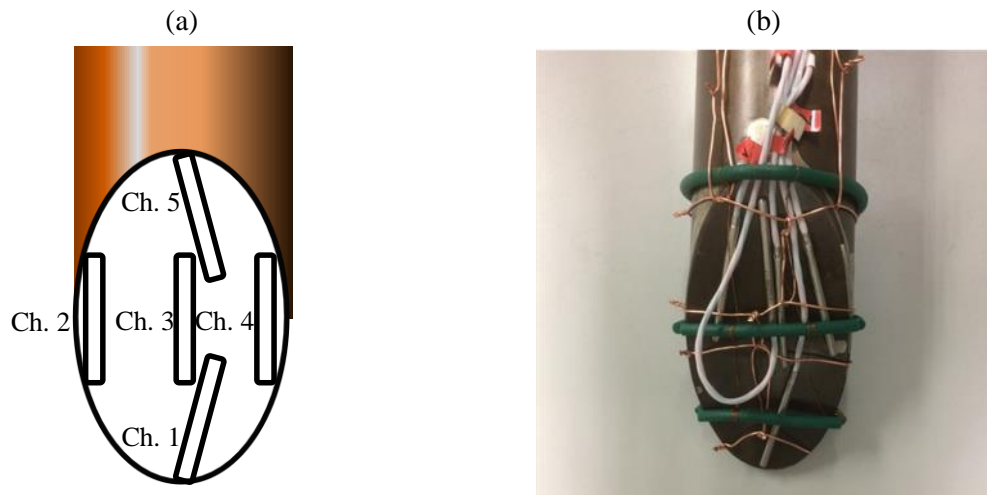
Figure 3.20 Schematic (a) and photo (b) of the five PRT probes attached to the flat, inclined cavity base.

For measurements where the uniformity was measured with two probes, the maximum difference of the two measurements was calculated over at least 10 minutes, with the measurements logged at least every minute.

For measurements using five probes, the readings were logged every ten seconds. The maximum difference between the five measurements was calculated for each set of measurements and the maximum was difference was calculated over 5 minutes.

3.8.1.2 Results

Table 3.6 Contact homogeneity measurements of NSAI BCRS base.

Temperature (°C)	Bath Medium	Thermal Homogeneity (mK)
-30	Methanol	35
5	Methanol	5*
80	Water	18*
100	Mineral Oil	59
150	Mineral Oil	63

* Denotes only 2 probes available for measurement.

3.8.1.3 Discussion

Predictably, the temperature of the base is most homogenous at temperatures close to ambient. This is presumably due to convective cooling of the interior of the cavity. The effects of convection are greater near the BCRS aperture, as discussed in 3.9.

3.8.2 Linear Scans of the Base with the TRT IV.82

3.8.2.1 Method

The TRT IV.82 was mounted on the NSAI mount described in 3.4.5. A large, printed grid was fixed to the laboratory bench under the base of the mount. The TRT was positioned initially at the presumed origin of the base (0,0) according to the procedure given in 3.4.5.2.

The grid was used to incrementally move the TRT away from the origin in 2 mm increments along the positive side of the X-axis. It was then returned to the origin point, and moved in 2 mm increments along the negative side of the X-axis.

The TRT was returned to the origin point and the process was repeated on the positive side of the y-axis and finally on the negative side of the Y-axis.

3.8.2.2 Results and Discussion

Figure 3.21 shows the results of moving the Heitronics TRT IV.82 horizontally across the aperture of the NSAI BCRS. The graph shows an area of uniform temperature within the cavity between from -8 mm to 10 mm on both axes.

(a)

(b)
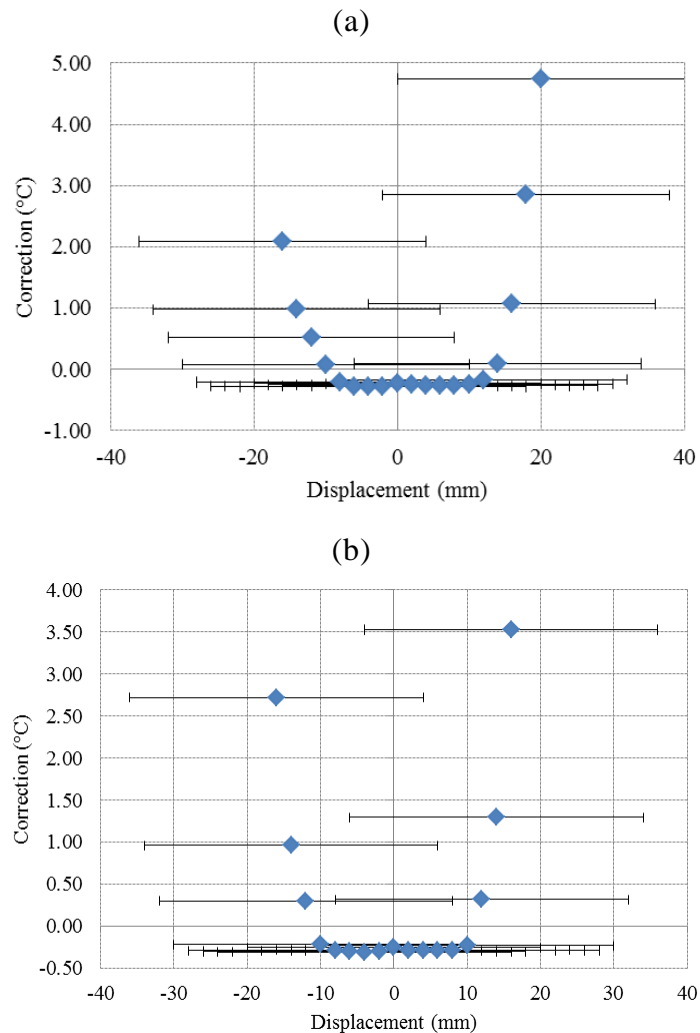
Figure 3.21 Scan across the base of the NSAI BCRS in the X and Y directions (a and b, respectively). The error bars indicate the approximate target area of the TRT IV.82.

This area of relative uniform temperature in the X direction is highlighted in Figure 3.22.
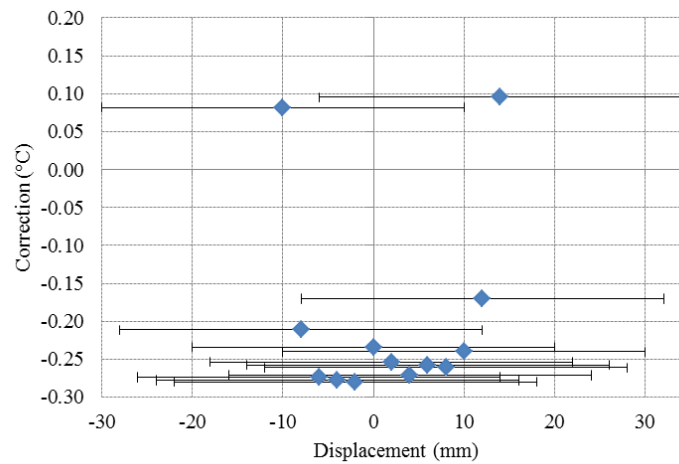
Figure 3.22 Homogeneity of the base across the X-axis, focussing only on the points where the SSE of the TRT IV.82 do not affect the measurement. The error bars indicate the approximate target area of the TRT IV.82.

The scan of the base in the X direction is less complete on the left of Figure 3.21 (a). The SPRT monitoring the reference temperature was mounted through the re-entrant well on the BCRS top plate. This conflicted with the lens of the TRT, limiting its travel in one direction.

In any case, the measured values on the outside of the relatively homogenous region (-8 mm to 10 mm on both axes) are of limited use due to the influence of the TRT's SSE and the aperture of the BCRS. The SSE of this individual instrument is shown in Figure 2.18, as measured by the manufacturer during commissioning tests. The error bars in the figures show that the TRT is actually measuring the temperature of the out-of-focus image of the BCRS aperture. The aperture, at 51 mm, covers from approximately -24.5 mm to 26.5 mm on the horizontal axis in these figures.

The asymmetry of the homogeneous region reveals that the thermometer was not correctly centred and the origin was misjudged by roughly 1 mm. As stated, the error bars in these figures show the target size of the TRT IV.82. The nominal target size of the TRT is specified as 6 mm at 380 mm, however Figure 2.18 shows that the a target of approximately 40 mm is required to receive the maximum signal from the TRT and avoid its SSE entirely. This limits its usefulness for measuring the thermal uniformity of small targets.

3.9   Axial Uniformity of the NSAI BCRS and Convection

3.9.1   Method

The thermal uniformity of the NSAI BCRS along the cylindrical axis was investigated by mounting the small T12 PRT probes mounted along the length of the copper portion of the BCRS on the external walls. The PRTs were placed on the base (similar to 3.8.1), at the upper flange and at the midway part of the cylindrical section of the cavity, as shown in Figure 3.23.

The configuration of the probes was:

- 3 PRTs equally spaced around the cylinder 60 mm below the top plate (around the top and in contact with the copper flange);
- 3 PRTs equally spaced around the cylinder 170 mm below the top plate (midway along the cylindrical section);
- 2 PRTs on the base, 345 mm below the top plate.

The BCRS was immersed such that the top of the top plate was typically 20 mm above the surface of the bath medium.

Figure 3.23 Photo of the NSAI BCRS with PRT probes attached to monitor the thermal uniformity of the cavity walls. Six probes were attached to the copper cylindrical portion of the cavity (in contact with the mounting flange and halfway along the length) and five probes were attached to the base.

The bath was allowed to stabilise and readings from the PRTs were logged every 10 seconds. The average reading of the three groups of probes at each of the locations 60 mm, 170 mm and 345 mm below the top plate was calculated over at least 2 minutes. These distances correspond to 285 mm, 175 mm and 0 mm from the centre of the cavity base, respectively. This procedure was performed at temperature set points at the limits of the mineral oil and methanol temperature media. The lid was removed during these measurements to see a representative uniformity profile.

The effect of natural air convection on the cooling of the internal cavity walls was investigated using a similar arrangement of probes as for the axial uniformity measurements. It was expected that the lid would significantly reduce the effect of this

convection. As such, the uniformity was measured with the cavity lid on and off, as per [88]. The same probe locations were used as described above.

3.9.2 Results

Table 3.7 The variation of temperature with distance from the cavity base with the lid removed

Temperature of Base (°C)	Medium	Temperature Difference between the Base and the Wall at the Given Distance from Base (°C)		
		0 mm	175 mm	285 mm
150.09	Mineral Oil	0.00	-0.28	-0.81
100.03	Mineral Oil	0.00	-0.25	-0.65
80.00	Mineral Oil	0.00	-0.22	-0.53
5.00	Methanol	0.00	0.02	0.03
0.02	Methanol	0.00	0.02	0.04
-29.98	Methanol	0.00	0.03	0.05

■ 150 °C Mineral Oil ◆ 100 °C Mineral Oil ▲ 80 °C Mineral Oil
✕ 5 °C Methanol   ✳ 0 °C Methanol   ● -30 °C Methanol
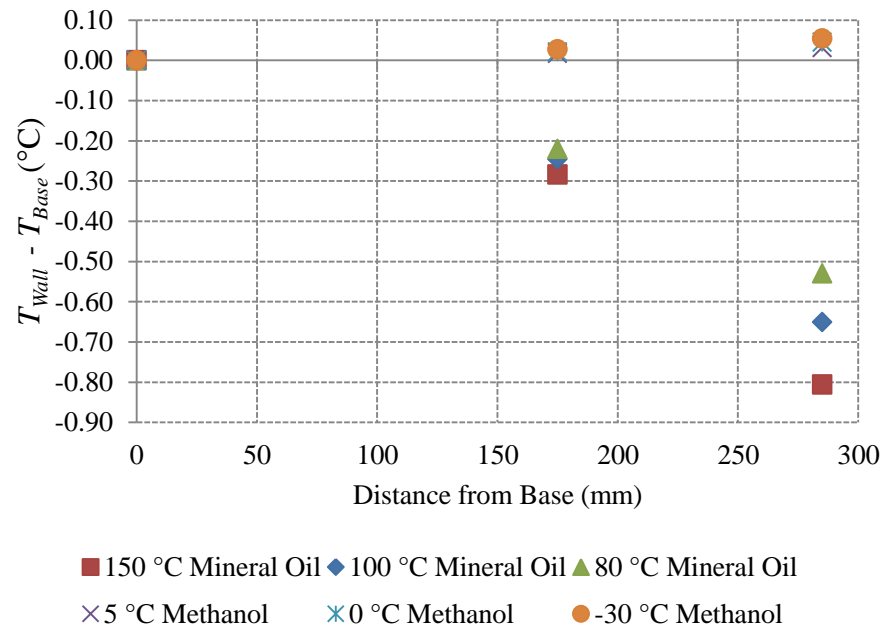
Figure 3.24 Variation of temperature along the walls of the NSAI BCRS.
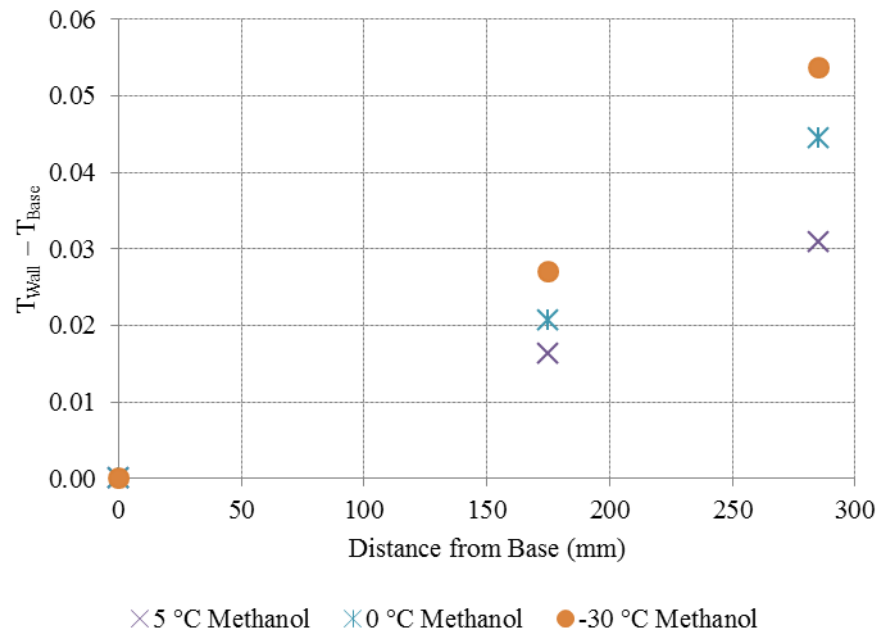
Figure 3.25 Variation of temperature along the walls of the NSAI BCRS, concentrating on the below ambient temperatures.

The results from the T12 multichannel logging thermometer system during the removal of the BCRS lid are shown in Figure 3.26 (a) and (b). These results are for immersion of the BCRS in the oil bath at temperatures of 80 °C and 150 °C respectively.

Figure 3.26 (a) shows a drop in the temperatures recorded by the probe channels nearest the aperture that coincides with the removal of the cavity lid on the left of the figure. The temperatures then stabilised with the channels near the aperture settling approximately 0.4 °C below their earlier level. The channels midway along the cavity walls showed a drop of 0.14 °C with the removal of the lid. The temperature took 8 to 10 minutes to stabilise after the removal of the lid. At the right of (a), the lid was replaced and temperatures of these channels returned to their original levels.

(a)

(b)
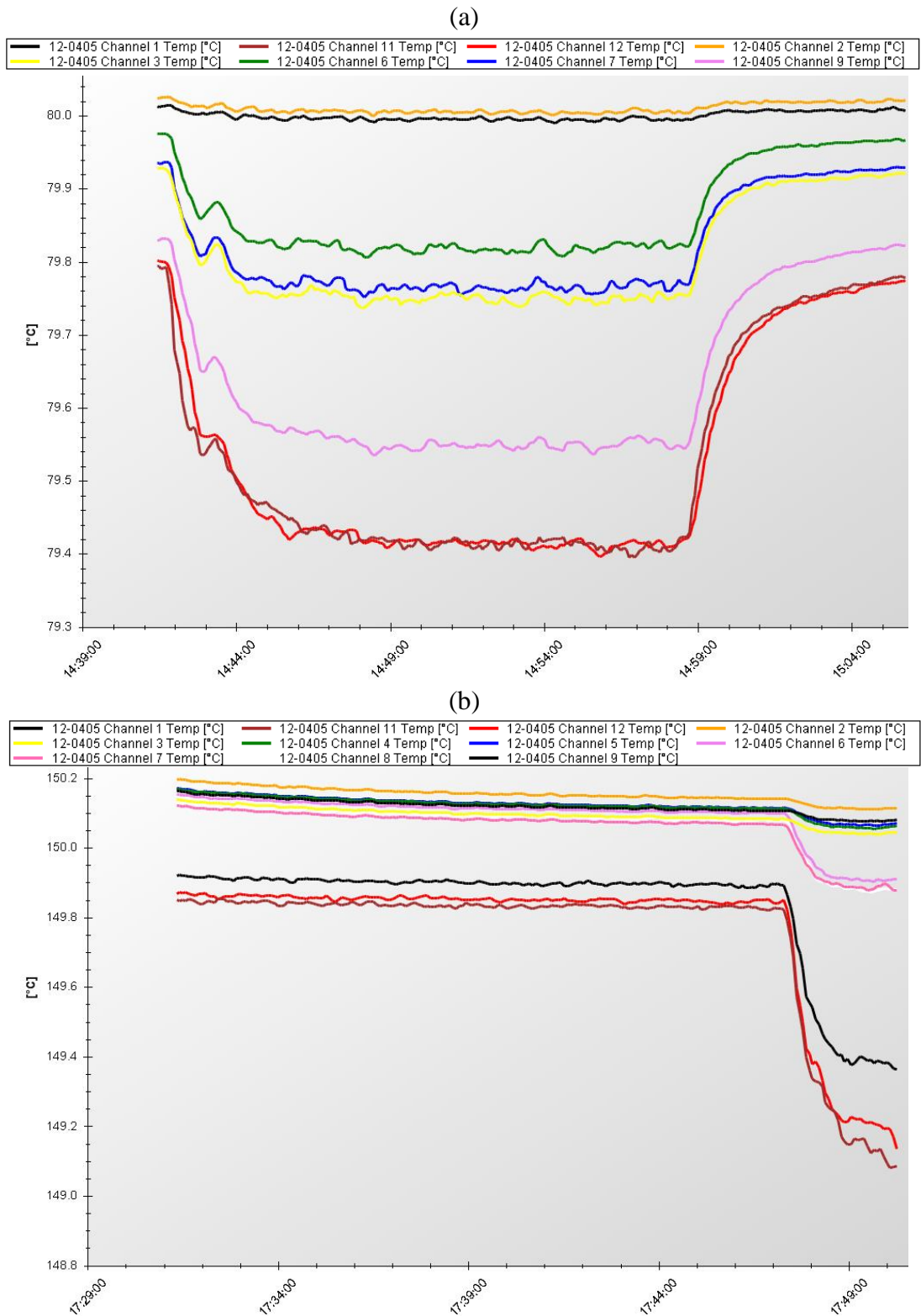
Figure 3.26 Screen captures from the T12 logging software showing the variation of temperature over time. The disturbance coincides with the removal of the lid from the NSAI BCRS at (a) 80 °C and (b) 150 °C. The largest drop in temperature is in the three channels closest to the aperture. In (a) the probes near the aperture are shown by the brown, red and pink traces and in (b) the brown red and black traces.

In Figure 3.26 (b), the temperature was stable apart from at the right edge of the plot. This coincided with the removal of the cavity lid. A temperature drop of approximately 0.7 °C occurred in the channels near the aperture. A drop of 0.2 °C occurred in the channels midway along the cavity walls. These temperature drops are slightly smaller than those recorded in Table 3.7.

In Figure 3.26 (a), 8 channels were used as described in 3.9.1. In Figure 3.26 (b), three additional probes were fixed to the base.

3.9.3 Discussion

The axial uniformity of the cavity decreases near the aperture of the cavity, as might be expected. BCRS apertures are exposed to ambient temperatures and the area of a BCRS near the aperture exchanges heat with room temperature air through convection. This is also the case with horizontal cavities [73]. Similar cavities have shown temperature drops of approximately -0.5 °C near the aperture at 150 °C.

The temperature drops shown in Figure 3.26 (a) and (b) are very likely due to increased air convection when the lid is removed. The temperature uniformity is reduced with the removal of the lid. More surface area was exposed to ambient temperatures when the lid was removed. The change in the temperature of the cavity's base was not significant, however.

Unfortunately, due to an error in setting the logging interval for the T12 logging software, the measurements of the influence of the lid were not logged in full. The

screen captures shown in Figure 3.26 (a) and (b) are the only data available that clearly shows the temperature change associated with the removal of the lid.

Figure 3.26 (b) shows an incomplete temperature profile and not enough time was allowed for the aperture temperatures to settle. The time required for the thermal uniformity of the cavity to settle after the removal of the lid is important in the context of writing a procedure, as in Chapter 5.

3.10   Influence of Vapour on the TRT IV.82 Lens

3.10.1 Method

During the course of the measurement experiments described above, the repeatability of measurements of the cavity made using the TRT was observed to be worse at high temperatures. It was detected that temperatures measured near 150 °C with the cavity in the oil bath were less repeatable results than those at lower temperatures. It was also observed that readings appeared to be drifting over time with extended exposure to the BCRS. To investigate this issue, extended measurements of the cavity were performed over periods of approximately 15 and later 72 hours.

The procedure followed was similar to that used in 3.7, except that, after set-up and before the final measurement points, these measurements were run unattended. Owing to the duration of these measurements, the SPRTs were removed during the unattended portions of the measurements.

With extended exposure to high temperatures, oxidation occurs on the platinum element of an SPRT, thus altering its resistance and linearity. This oxidation may be reversed by annealing the probes, but they must be recalibrated after annealing [5]. As such, it is normal practice to limit the exposure of SPRTs to high temperatures. The multiple T12 PT100 PRT probes, which were still attached to the BCRS following the tests described in 3.9, were in use as secondary references. These were kept immersed and logging throughout the measurements.

Readings were taken with the SPRTs at the start and end of these measurement runs for comparison with the readings from the PT100 probes.

At the end of both measuring periods, a large reduction in the TRT readings was observed. On the supposition that this change in reading was due to the condensation of bath vapours on the lens, the lens was cleaned with the TRT kept in-situ.

The cleaning of the lens was performed in accordance with the procedure given in the manufacturer's documentation: a lint-free lens wipe was gently rubbed over the lens. Three lens cleanings were performed over 10 minutes, allowing the TRT reading to settle and be checked between cleanings.

The 72-hour measurement was performed with a glass collar placed around the aperture of the NSAI BCRS. The collar was added to investigate if it was possible to shield the TRT lens from the bath vapours using materials to hand.

The lens was also wiped at the end of the end of the 72-hour measurement, this time in six stages.

It should be noted that at 150 °C, no vapours from the mineral oil bath are visible with the naked eye.

3.10.2 Results

Figure 3.27 shows the TRT IV.82 reading decreasing due to the lens fogging up over the 15 hour measurement run. The oil bath reference temperature was measured at the start and the end of the run using an SPRT. The readings were 149.9989 °C at the start and 149.9922 °C at the end. This confirmed that the sensitivity of the T12 probes, whose logs also indicated that the temperature was relatively constant, had not drifted during the measurement.

(a)

(b)
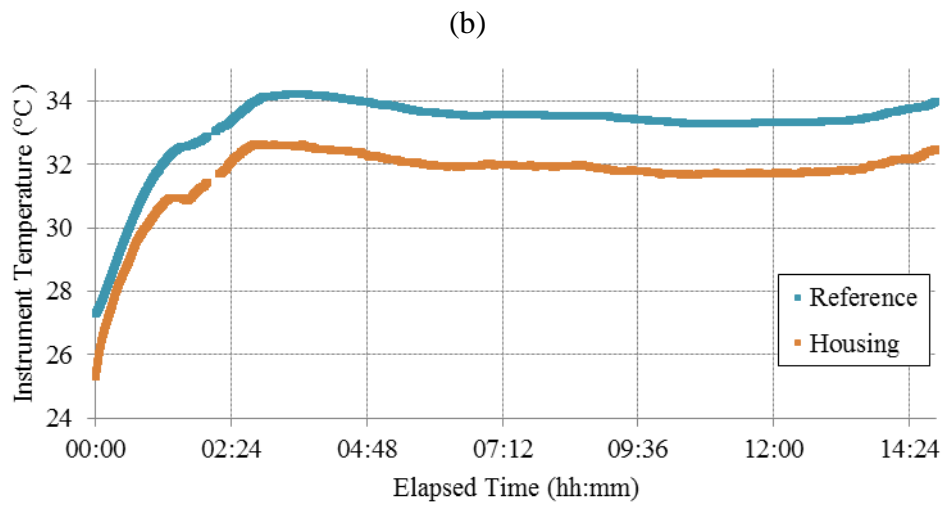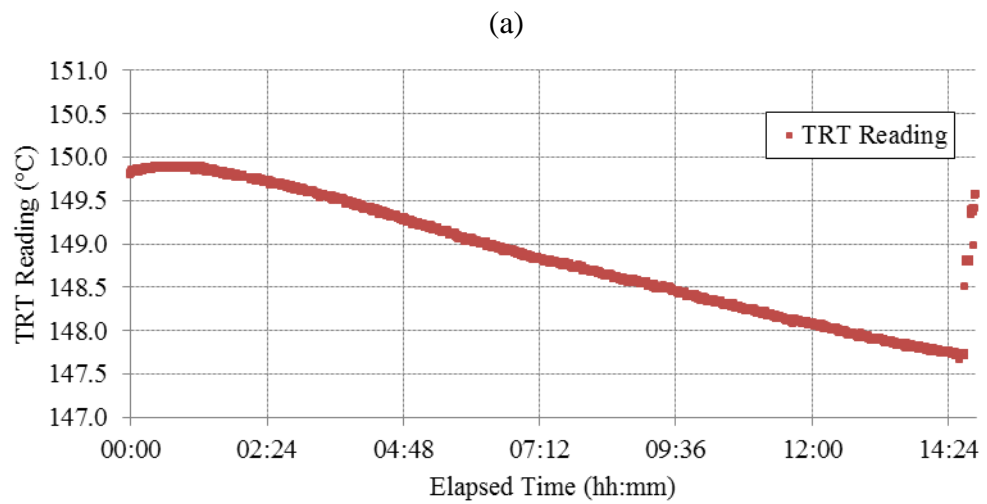
Figure 3.27 Variation in the logged TRT reading (a) and logged TRT reference and housing temperatures (b) over almost 15 hours.
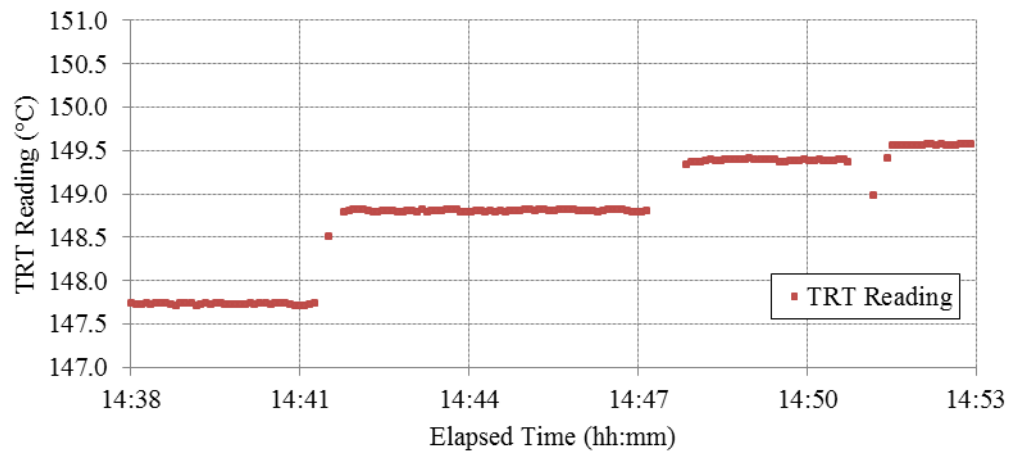
Figure 3.28 TRT readings over time, as per Figure 3.27, but showing only the last 15 minutes of the approximately 15 hour measurement.

Figure 3.28 shows the logged TRT readings at the end of Figure 3.27, coinciding with the cleaning the lens. The lens was wiped three times. The TRT's FOV was obscured during the lens cleaning, and this is visible in the figure as gaps in measurement.

Figure 3.29 shows an increase of approximately 0.05 °C in the TRT reading at the start of the 15-hour measurement run. This increase coincides with the rising internal TRT temperatures.

(a)

(b)
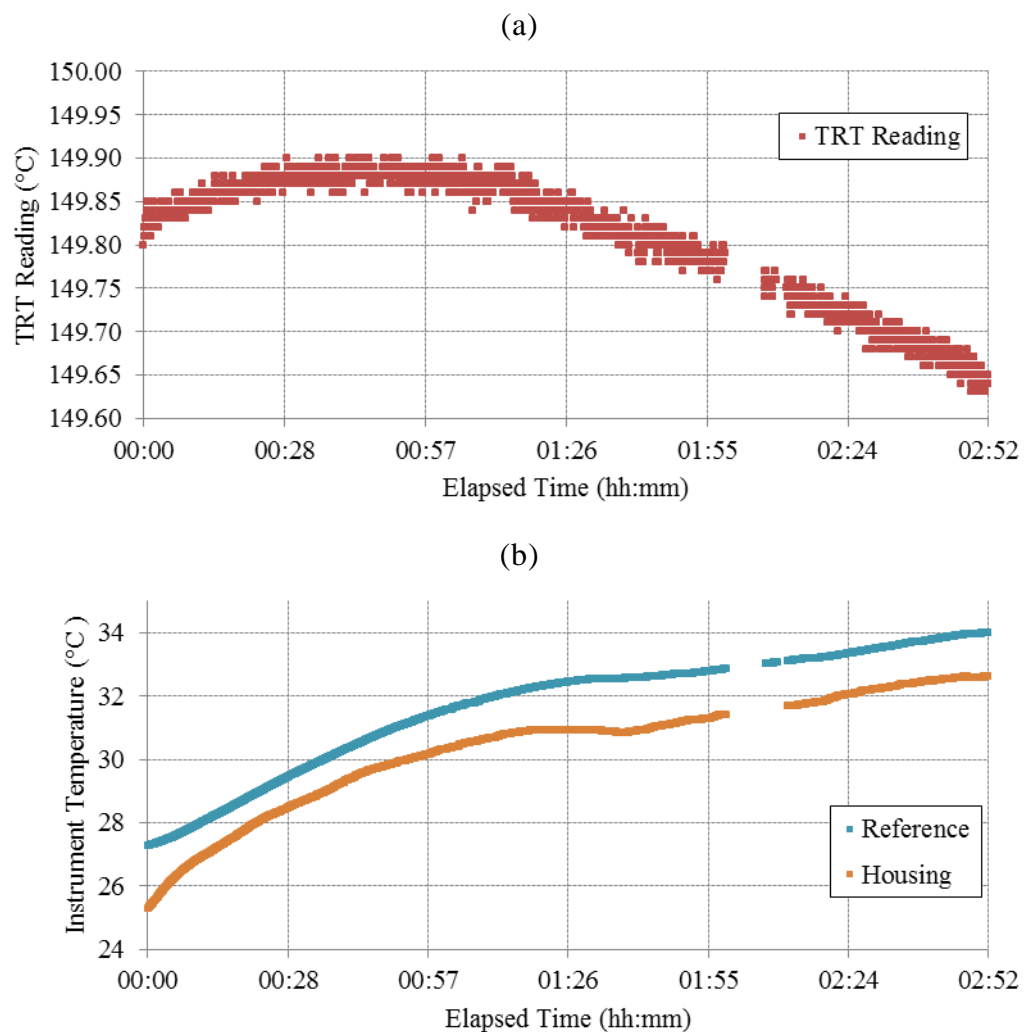
Figure 3.29 (a) TRT readings and (b) internal temperatures over time, as per Figure 3.27, but showing only the first 3 hours of the approximately 15 hour measurement. The gap in the measurement is due to a change in the PC used for logging. The quantisation of the TRT readings is visible in (a).

(a)

(b)
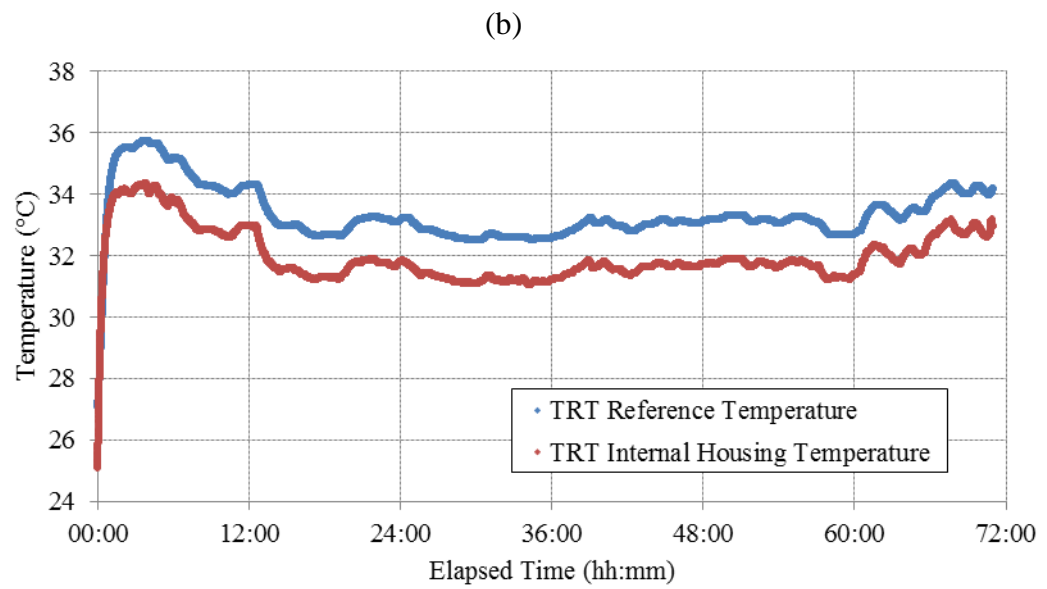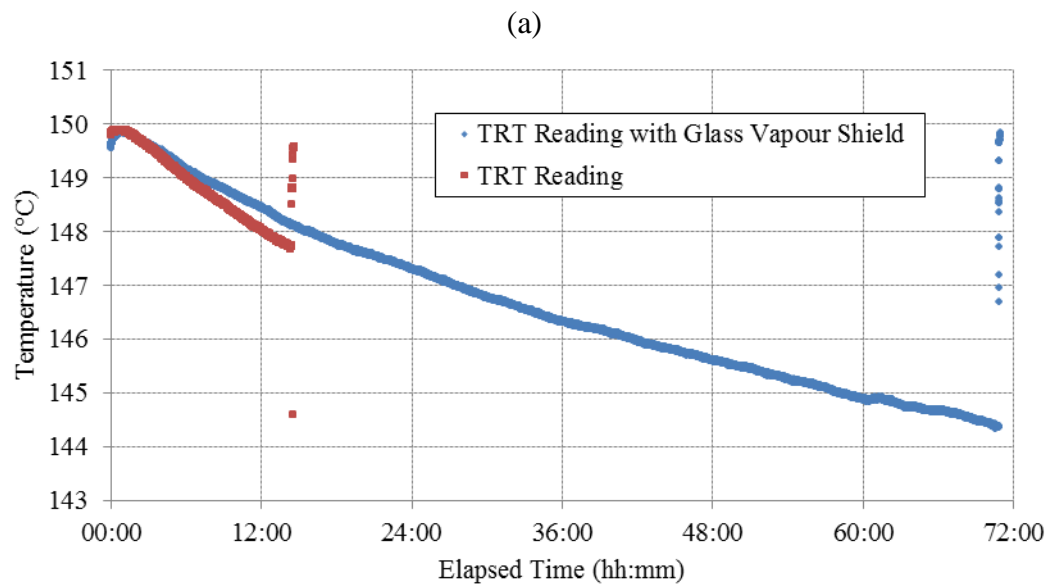
Figure 3.30 Variation in the logged TRT reading (a) and logged TRT reference and housing temperatures for the vapour shield measurement (b) over 72 hours. The 15 hour measurement is also shown in red in (a) for comparison.
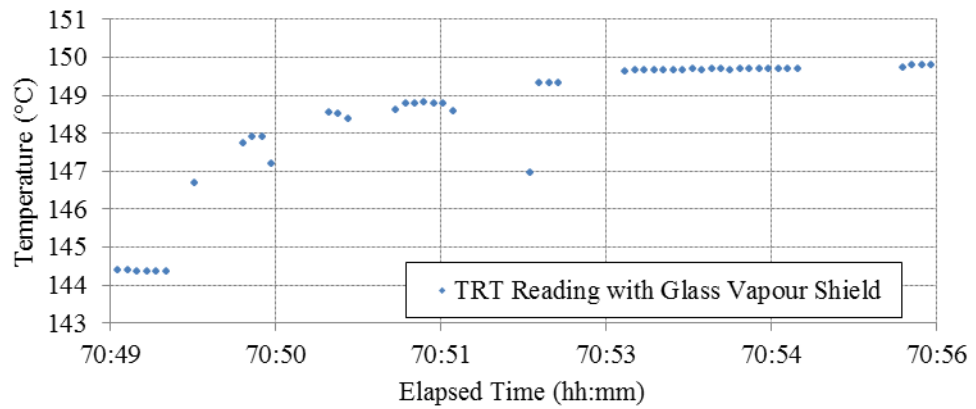
Figure 3.31 TRT readings over time, as per Figure 3.30, but showing only a 17 minute portion at the end of the 72 hour measurement where the lens was cleaned in 6 stages.

(a)
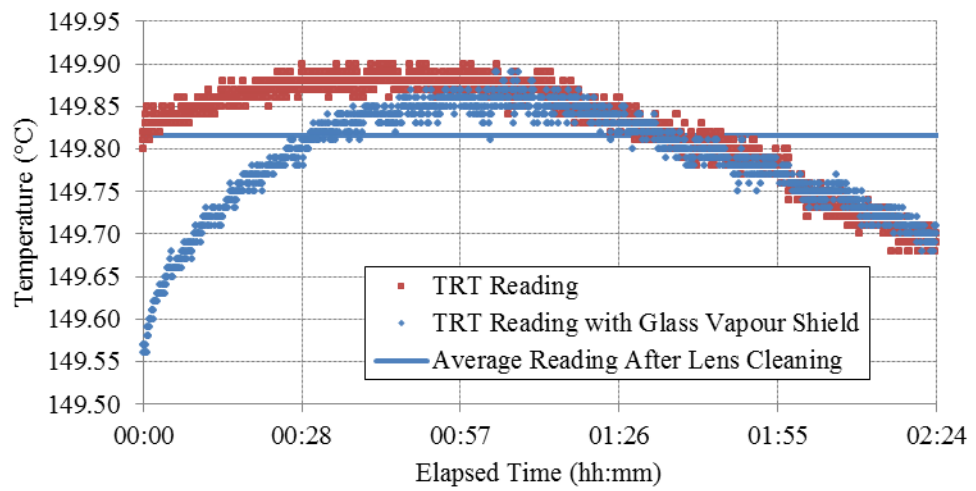
(b)
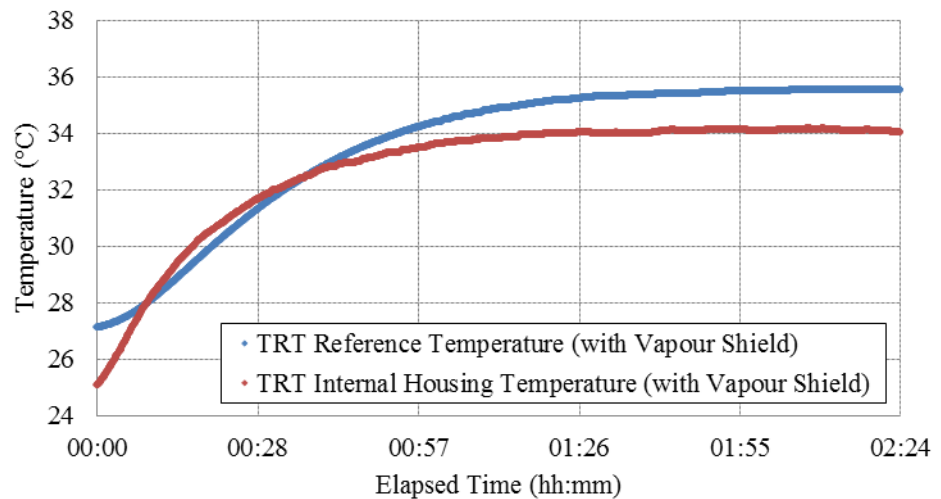
Figure 3.32 TRT readings over time (a) and internal temperatures (b), as per Figure 3.30, but showing only the initial 2 hours of the of the 72 and 15 hour measurements. During this period, the instrument reading varied with the internal temperatures.

3.10.3 Discussion

Figure 3.29 shows an initial rise in the TRT readings while the internal temperatures were also rising but before the vapours influenced the measurement. This indicates that the TRT does not compensate totally for the influence of its own temperature.

It was anticipated that the glass collar (the vapour shield) would significantly reduce any deposition of vapour on the lens, as any vapours rising off the oil in the bath would have to drop down above the level of the shield to condense on the lens. Figure 3.30 shows a small improvement over the 15-hour measurement.

The glass shield also appears to have increased the rate of heating of the TRT when Figure 3.29 and Figure 3.32 are compared. This could be because the glass was closer to the TRT and had equilibrated with the aperture of the BCRS.

The above results show the importance of checking the condition of the lens before measurement. Unfortunately, due to the small distance between the lens and the blackbody aperture, it was not possible to inspect the lens or take photos at the end of the measurement run and before cleaning. Performing such an inspection would have disturbed the position of the RT and thus the measurement of the influence of the bath vapour on the lens.

Further work is required to determine if the depositions would be visible upon inspection and to investigate if they would naturally evaporate to any extent.

These results show that management of vapours on the lens is a key consideration for vertical bath-based BCRSs. The cleanliness of the environment and the treatment of lenses is given careful consideration in other laboratories. Some laboratories are known to use clean-room environments for the lowest uncertainty measurements to reduce these issues, even for horizontally oriented BCRSs [91].

It should be noted, however, that the effect is only significant for prolonged exposure to the vapours, well in excess of what is necessary for an accurate measurement. An improved design of top plate for the cavity to further limit the effects of vapours from metrology baths is suggested in 6.2. Use of PTFE seals around the PRTs in the re-entrant wells should also reduce the effects. Finally, fitting lens caps to RTs between measurements of the NSAI BCRS should further reduce this issue.

3.11 Conclusions

In summary, this unique vertical BCRS was evaluated and found to have performance on a par with horizontal bath-based BCRSs. The cavity was found to offer a flexible, low-cost alternative to purpose-built horizontal cavities. The new design was also found to be an improvement over the previous vertical cavity constructed at LMK. It is expected that such vertical cavities could be of use to other calibration laboratories wishing to extend the temperature range of their non-contact capabilities. A vertical orientation may also assist in the assessment of prototype cavities with different dimensions or provide additional cavities to reduce turnaround times, or for crosschecks.

The NSAI BCRS was also characterised in terms of the temperature uniformity of its base and along the cylindrical axis. Phenomena relating to convection and effects arising from using the TRT vertically above a bath were investigated.

The measurements raised issues that helped to inform the procedures discussed in 5.2. These experiments also served to improve the estimation of the uncertainty as discussed in 5.3.

Chapter 4.   A Case Study of a Direct-Reading IRT

4.1   Introduction

This chapter describes measurement experiments conducted on the Fluke 574, a test case commercial-grade, direct-reading IRT (see section 4.2.1.1). A number of experiments were carried out with this instrument with the aim of conducting a preliminary characterisation of the NSAI BCRS. These experiments were performed prior to the receipt of the TRT IV.82. These initial experiments revealed the limitations of the test case instrument.

The most immediately notable issue was the repeatability of the readings. When the same measurement was repeated under the same conditions, there was a large spread of resultant measured values. This was a problem using NSAI's vertical BCRS and flat plate calibrator (4.5.1.1). A discussion of these repeatability issues is given in this chapter.

Later, in tandem with the comparison of cavity orientations undertaken in LMK discussed in Chapter 3, a full calibration of this IRT was carried out. Measurements were also performed of the size-of-source and distance effects of this instrument. This was undertaken to investigate the causes of poor repeatability and to explore the dominant uncertainty components for this instrument.

As part of the work presented, visits were undertaken to the laboratories at NPL, LMK, and CMI. The non-contact facilities in these temperature laboratories comprise a combination of bath-based blackbodies and HPBBs. The measurement experiments

conducted during these visits, described in this chapter and the previous one, supported the development of the NSAI calibration procedure (see section 5.2).

4.2 Preliminary Investigation of the Distance Effect and Repeatability of the Test Case IRT

There are a number of difficulties that arise when attempting to make repeatable measurements with an RT during calibration. The selection of calibration equipment and design of procedures require careful consideration. The initial exercise of the present work was a calibration of the test case IRT using the NSAI vertical BCRS over the range 4 °C to 160 °C. A large set of calibration measurements were gathered. These measurements were performed at four target distances in order to investigate the distance effect. Numerous repeat measurements were performed over several days, which served as an investigation of the repeatability of the instrument.

4.2.1 Materials

4.2.1.1 The Fluke 574 Close Focus (CF) Test Case IRT

The Fluke 574 CF is a commercial direct-reading handheld IRT, of the type described in 2.6.3.2, with a plastic, pistol-shaped housing. The instrument is shown in Figure 1.1 (a) and the specifications are given in Table 4.1. The instrument may be considered average among RTs in terms of cost, quality, and accuracy. It should be noted that no lens cap is supplied with the instrument.

Table 4.1 Manufacturer's published specificaitons for the Fluke 574 IRT [66].

Temperature Range	-30 °C to 900 °C
Spectral Response	8 μm to 14 μm
D:S (Distance to spot size ratio)	50:1 Fixed, Close Focus
Emissivity Adjustment	Adjustable in 0.01 increments from 0.10 to 1.00
Display Accuracy	± 0.75 % of reading or ± 0.75 °C, whichever is greater at 25 °C ambient temperature. ± 2 °C for targets below -5 °C.
Ambient Derating	< 0.05 °C/°C or < 0.05 %/°C, whichever is greater at + 25 °C ± 25 °C
Minimum Measurement Diameter	6 mm at 300 mm
Power	2 x 1.5 V Alkaline Type AA
Battery Life	13 hrs. (50 % laser and 50 % backlight on)
Power supply (External)	7.5 V > 200 mA(Using the power supply the display automatically switches on)
Dimensions	200 x 170 x 50 mm (7.9 x 6.7 x 2 inches)
Tripod Mount	¼"-20 UNC

The manufacturer's optical specifications of the IRT are shown in Figure 4.1. The instrument has converging optics.
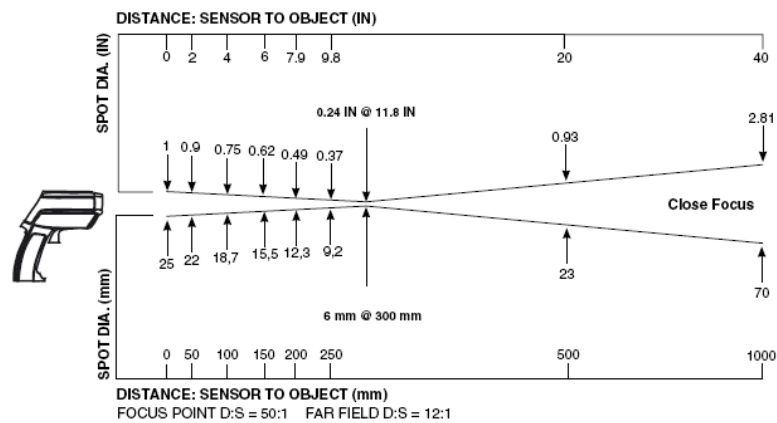
Figure 4.1 The optical specification of the Fluke 574 CF IRT. Reproduced from [66].

The distance to spot size (D:S) ratios for the focus point and the far field given in Figure 4.1 (50:1 and 12:1) are a simplification. The actual ratios vary with the distance from the sensor to the object as shown in Table 4.2.

Table 4.2 Distance to spot size specifications as given in Figure 4.1

Sensor to Object (mm)	Spot Diameter (mm)	Distance to Spot Diameter Ratio (D:S)
0	25	-
50	22	2:1
100	18.7	5.3:1
150	15.5	9.7:1
200	12.3	16.3:1
250	9.2	27.2:1
300	6	50:1
500	23	22:1
1000	70	14:1

The ambient derating specification is also detailed in a slightly opaque manner. It is stated in terms of the absolute difference from ambient temperature. By plotting it for different ambient temperatures, the specification may be interpreted more readily, as shown in Figure 4.2.
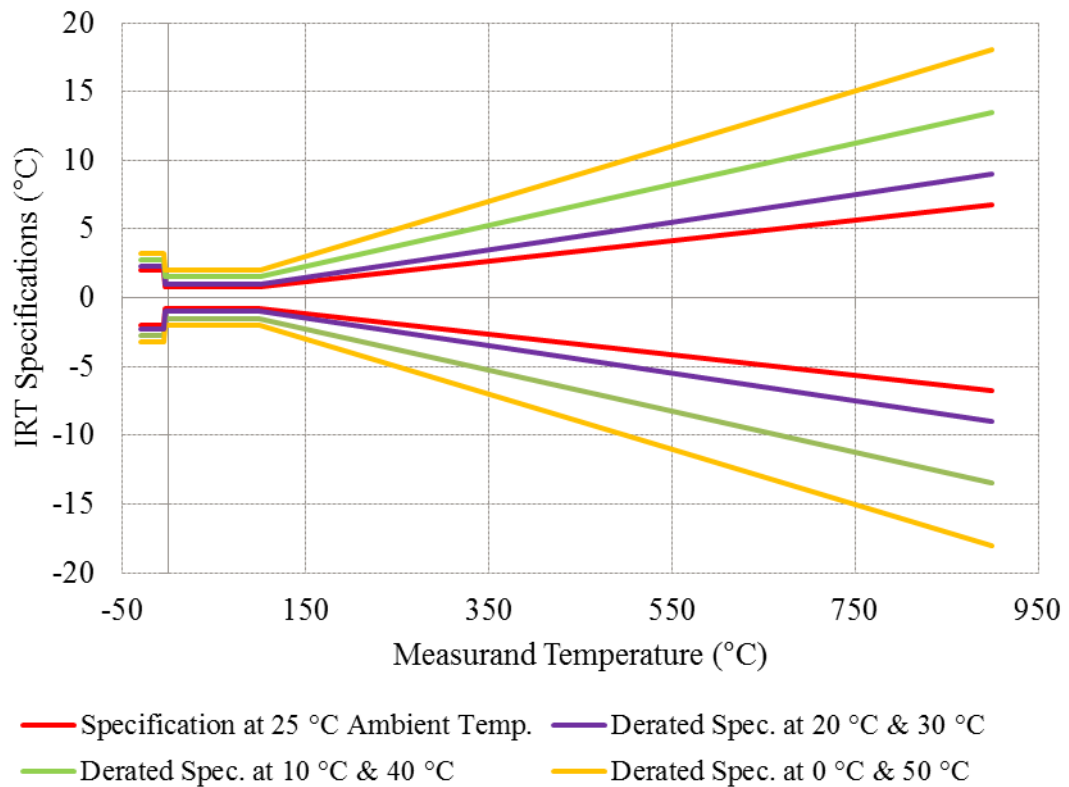
Figure 4.2 The specification of the Fluke 574 IRT for 25 °C and varous non-ambient temperatures.

4.2.1.2 NSAI Vertical BCRS and Mount

The NSAI vertical BCRS, as described in 3.2.2, was used for these measurements. The test case IRT was mounted in a vertical orientation from a post mounted to an optical breadboard. The IRT was also mounted using a tripod for some tests. The tripod was arranged carefully so the IRT could point downwards as shown in Figure 4.3.

This was necessary, as the NSAI vertical mount described in 3.4.5 had not been constructed at this stage. The NSAI mount is, in any case, incompatible with this IRT due to the unsuitable location of the IRT's ¼"-20 UNC mounting thread.

(a)   (b)
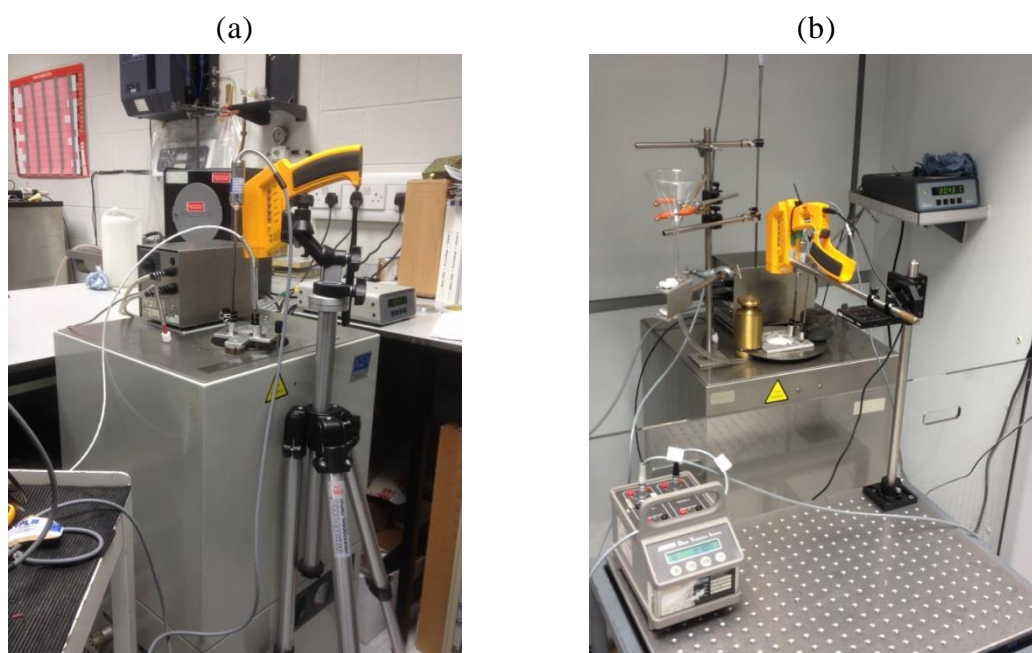
Figure 4.3 The test case IRT mounted on a tripod (a) and using an optical breadboard (b). In (b), from left to right, a secondary reference thermometer readout, glass funnel, the IRT and the bath controller may be seen.

4.2.2 Method

For these measurements, the BCRS was immersed in the deionised water and mineral oil baths in turn, with traceability to ITS-90 via SPRTs in both cases as per 3.6.1.1. The

positioning procedure was similar to the method described in 3.4.3 except that the IRT was mounted on a different stand during the measurements. The measurements were made without the enlarged top plate described in 3.7.1. The instrumental emissivity of the IRT was set to 1.00 for all measurements.

The primary set of measurements were made with a distance of 500 mm between the lens of the IRT and the midpoint of the bottom of the NSAI cavity, giving a nominal target diameter of 23 mm at the base of the cavity according to Figure 4.1. These measurements were undertaken to investigate repeatability.

Due to the difficulty in aligning the IRT in the vertical orientation, it was kept in position during the stabilisation of the baths in several cases. The measurements at the various distances were made with a minimum of repositioning for the same reason. This means that measurements might go by the following order at one temperature set point: (345 mm, 500 mm, 600 mm, 700 mm) and then: (700 mm, 600, mm, 500 mm, 345 mm) at the next set point, and so on. The condition of the lens was not monitored where the IRT was kept in position.

Further measurements were made at distances of 365 mm, 600 mm and at 700 mm. The nominal target diameters at these distances were approximately 11.4 mm, 33 mm and 42.2 mm. At 365 mm to the midpoint BCRS base, the IRT was only 20 mm from the aperture of the NSAI BCRS. This is as close as was practical to measure the base. Measurements at this distance were only carried out below 50 °C.

For each measurement point, twelve readings were taken of each of the reference and test instruments at 10-second intervals and recorded in a database.

4.2.3 Results

The largest set of measurements was made at 500 mm from the base of the BCRS. This set of measurements is shown in Figure 4.4 and the entire set of measurements made in NSAI NML is shown in Figure 4.5.
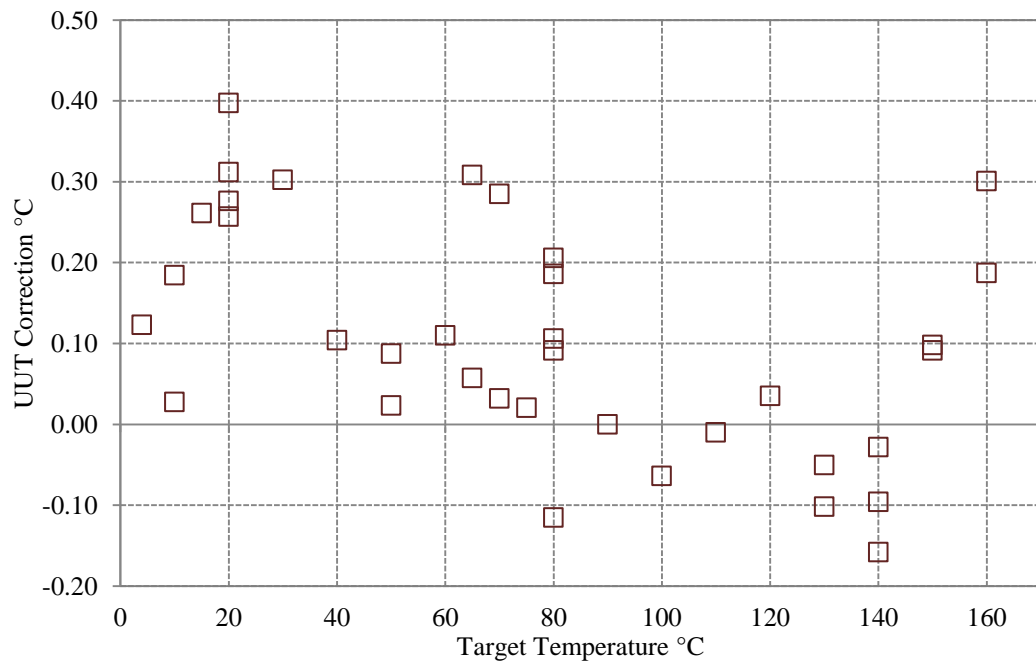
Figure 4.4 Corrections for the test case IRT using the NSAI vertical BCRS with a target distance of 500 mm
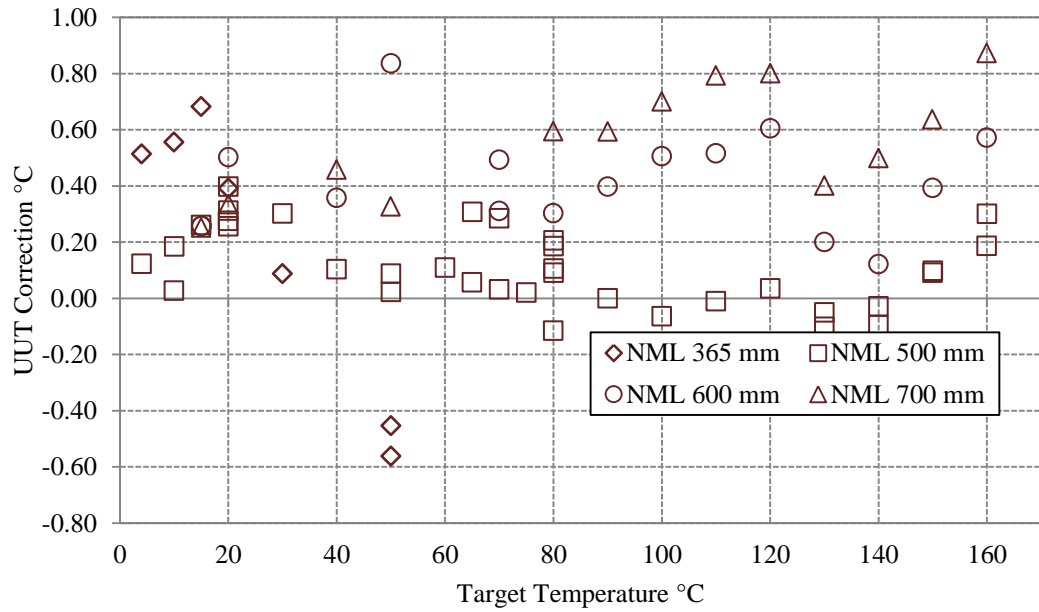
Figure 4.5 As per Figure 4.4, but also showing corrections for target distances of 365 mm, 600 mm and 700 mm.

The measurement points are shown separated by the target distance and the date on which they were performed in Figure 4.6, Figure 4.7 and Figure 4.8.
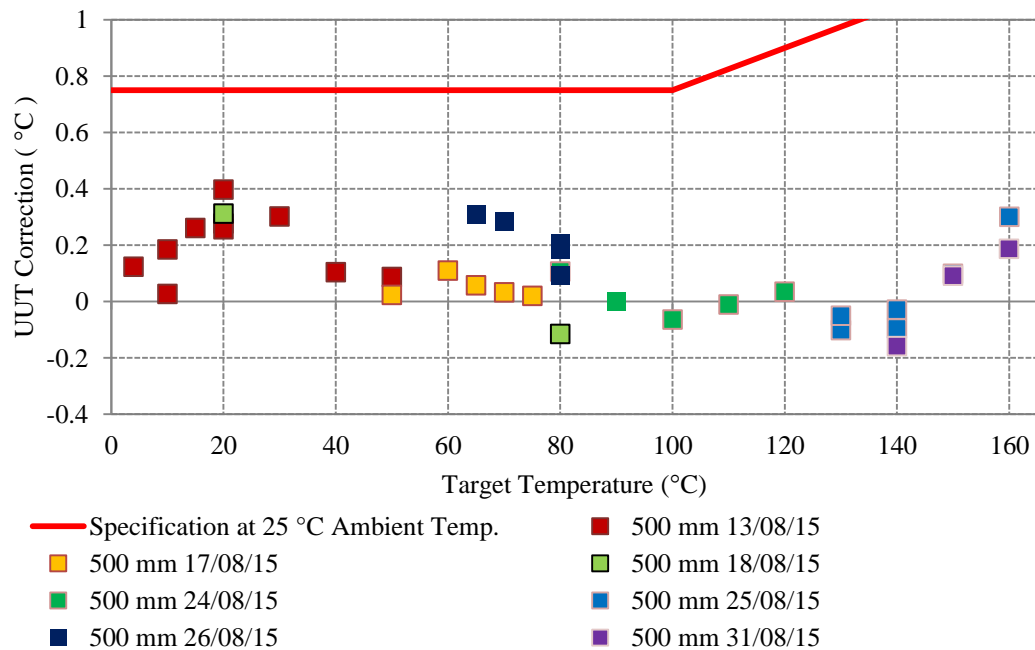
Figure 4.6 The calibration at a target distance of 500 mm, as in Figure 4.4, but separated in colour by the date on which they were performed.
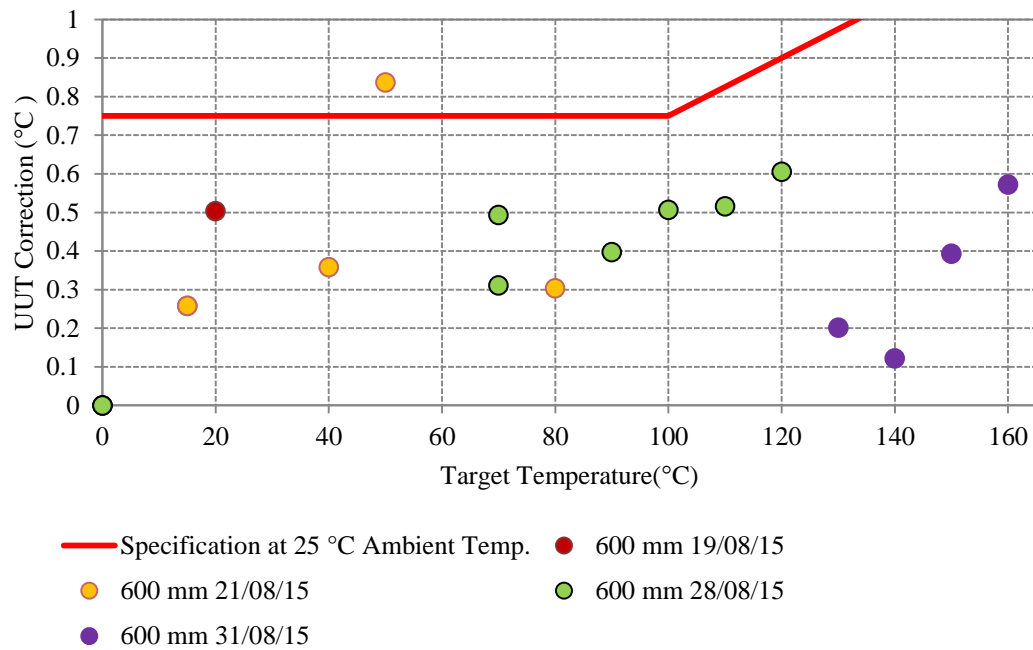
Figure 4.7 As per Figure 4.6, but showing measurements at a target distance of 600 mm.
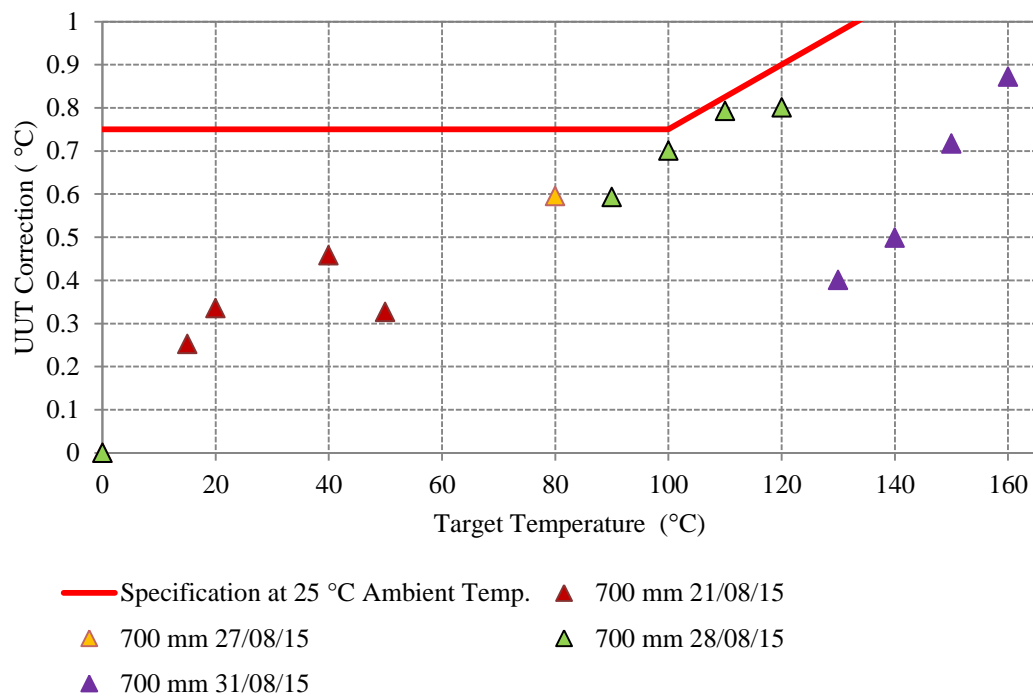
Figure 4.8 As per Figure 4.6, but showing measurements at a target distance of 700 mm.

4.2.4 Discussion

When the measurement points are separated by the target distance and the date on which they were performed, as in Figure 4.6, Figure 4.7 and Figure 4.8, there appears to be a

pattern to the magnitude of the corrections. The pattern is more pronounced at larger target distances, as in the latter two figures. On each date, the measurements were performed in order of increasing temperature, and thus it appears that the corrections were increasing with time, particularly at greater distances.

The positioning of the IRT was performed with the utmost care for these measurements. The large variation in the corrections observed is therefore likely due only to a combination of the repeatability of the instrument, the SSE, DE and the influence of bath vapours.

Due to the difficulty in aligning the IRT and obtaining repeatable measurements, and to the fact that the bath vapours are virtually invisible, the influence of vapours was overlooked at the time of the measurements. The duration of exposure of the IRT to the top of the bath was, unfortunately, not recorded. The experiment conducted into bath vapours in 3.10, however, can be considered a more definitive evaluation of this influence, albeit for a higher accuracy instrument.

The increase in the IRT correction at greater target distances is most probably due to the SSE. Optical scattering, and therefore the SSE, would very likely increase with any deposits on the IRT lens (see section 2.6.7). It has a larger effect where the source appears small in the IRT's FOV. This could also explain why the IRT corrections increase with exposure duration by a larger amount at 700 mm than at 500 mm. Measurements of the IRT's SSE and DE are given in 4.4 and 4.5 respectively.

If the variation in the readings of the test case IRT is due to the condensation of vapours on the lens, this condensation may have evaporated of its own accord. No cleaning of

the lens took place between 28/08/15 and 31/08/15, yet the readings reduced to a similar level as before the extended duration exposure to the bath (as seen in both Figure 4.7 and Figure 4.8).

The investigation of the DE of the test case IRT presented here is only relevant for the vertical orientation. Taking account of convective heating, the issue is different for horizontal sources. For this reason, repeatability measurements for the horizontal orientation were carried out as part of the full (horizontal) calibration of this IRT carried out in LMK (see section 4.3 below). The DE was also measured in the horizontal orientation as described in 4.5.

In order to improve the repeatability of RT readings in this range, the possibility of bath vapours influencing the measurement was reduced. Using the larger top plate with the NSAI BCRS, as was used for the TRT measurements in 3.7.1, would have improved the repeatability of the UUT readings in this range. Other measures that could reduce the influence of bath vapours include use of lens caps and improved mounts that permit removal of the UUT between measurements as was possible with the NSAI vertical mount in 3.4.5.

4.3   Calibration of the Test Case IRT in LMK

The IRT was calibrated in the range from -30 °C to 900 °C with a range of horizontal blackbody cavity sources in LMK.

4.3.1 Materials

The measurements undertaken at LMK used the BCRSs described in 3.3.2.1 for temperatures of 150 °C and below and additional cavities for higher temperatures. The relevant details of the high temperature BCRSs are given in Table 4.3 and the cavities are pictured in Figure 3.6 and Figure 4.9.

Table 4.3 The high temperature BCRSs at LMK used for the test case IRT calibration.

Make and Model	l (mm)	d (mm)	Shape	θ_{tip}	Estimated ε_{Cavity}	Range (°C)
Caesium Heat Pipe	500	55	Cylindro-conical	120°	0.9994	300 to 600
ACT Sodium Heat Pipe, 1312958	500	40	Cylindro-conical	120°	0.9994	600 to 1000

Figure 4.9 The test case IRT mounted in front of the sodium heat pipe BCRS at 800 °C during calibration in the LMK radiation thermometry laboratory.

4.3.2 Methods

The lens of the IRT and the TRT were inspected prior to measurements and found to be clean.

The IRT was mounted on a tripod and aligned manually in front of the BCRSs.

The BCRSs were allowed several hours to stabilise for each set point and their temperature was measured using SPRTs or TCs, which also provided traceability to ITS-90.

The optical axis of the IRT under test was aligned with that of the BCRS and the IRT was positioned such that its target area was on the base of the BCRS. The laser target on the IRT was used for coarse positioning, the RT was then scanned across the aperture of the BCRS manually, and the approximate maximum reading was used as the centre.

At higher temperatures, a larger distance was needed between the IRT and the source. This was to prevent the BB heating the IRT excessively. The distance from the front of the IRT to the base of the BCRS was 450 mm below 150 °C and 800 mm above 150 °C.

Ten measurements were taken of each of the reference and test instruments at 10-second intervals and logged using the LMK calibration management software.

4.3.3   Results

The measurements of the various sources are shown in Figure 4.10 across the full temperature range. The near-ambient measurements are shown in more detail in Figure 4.11. The previous calibration measurements from 2014 are also shown.
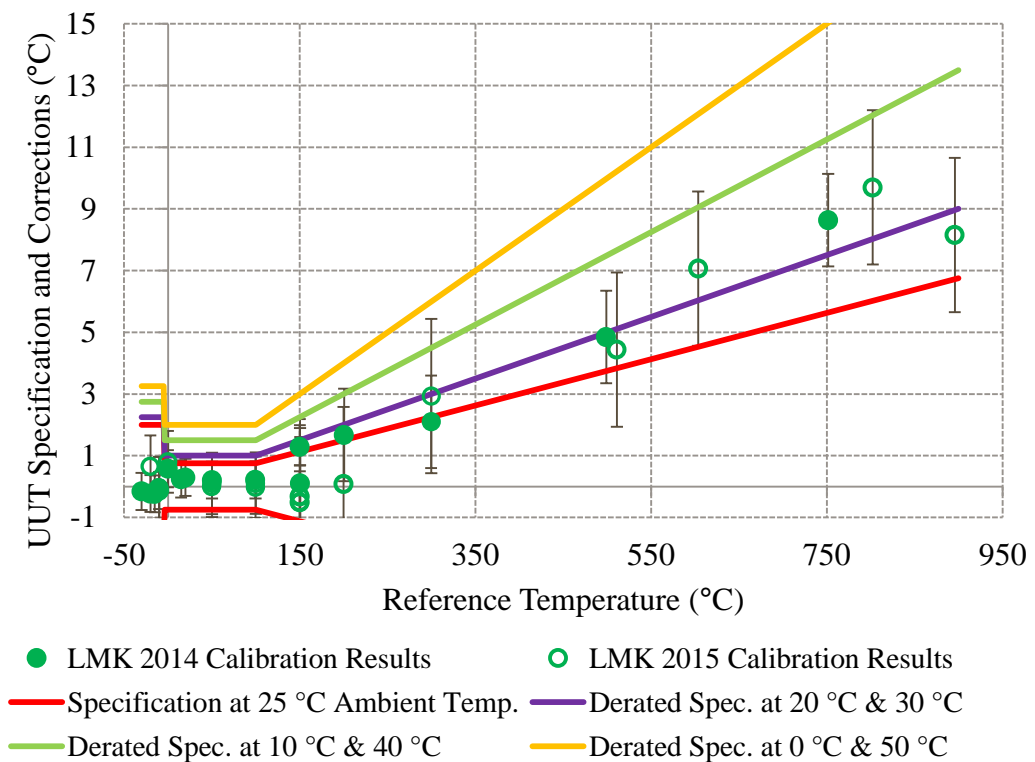
Figure 4.10 The calibration results for the test case IRT across the full temperature range in 2014 and 2015, showing the specificaiton of the instrument.
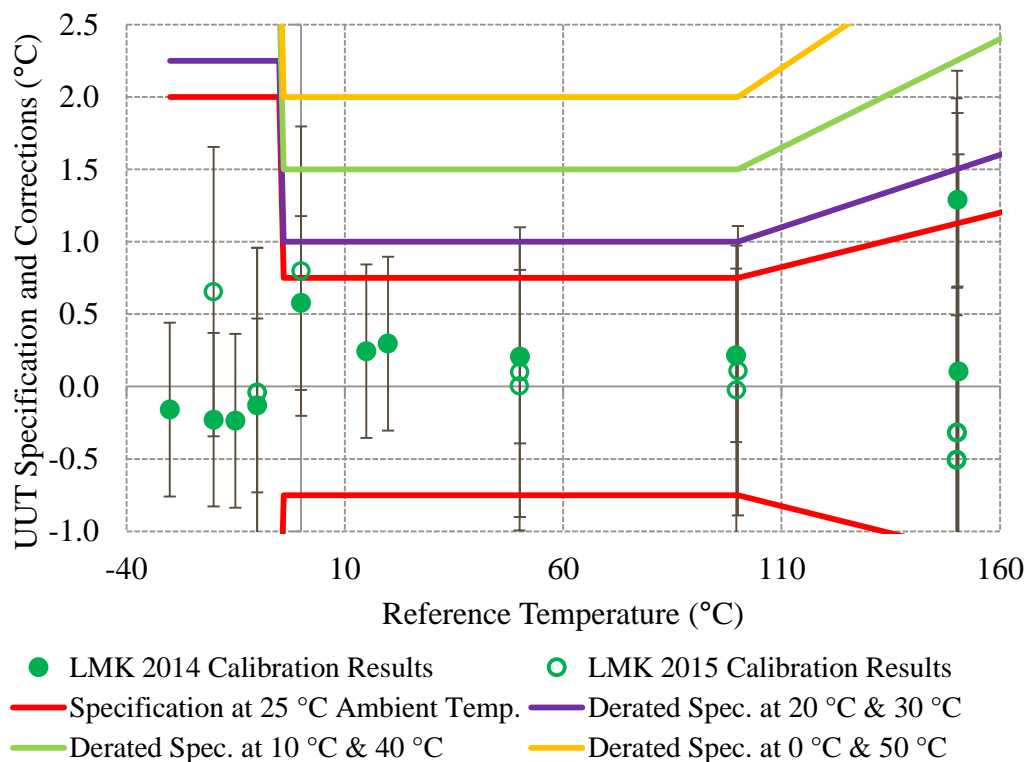
Figure 4.11 As per Figure 4.10, but concentrating on the near-ambient test points.

The results as reported in the LMK certificate are given in Table 4.4 and Table 4.5.

Table 4.4 Calibration results as stated in the 2015 LMK certificate for the bath-based BCRS range.

t_{90} (°C)	t (°C)	Correction (°C)	Uncertainty (°C)
-30	-30.4	0.4	1.0
-20	-20.4	0.4	1.0
-10	-10.3	0.3	1.0
0	-0.3	0.3	1.0
50	49.9	0.1	1.0
100	100.1	-0.1	1.0
150	150.3	-0.3	1.0

Table 4.5 Calibration results as stated in the 2015 LMK certificate for temperatures of 150 °C and above.

t_{90} (°C)	t (°C)	Correction (°C)	Uncertainty (°C)
150	150.0	-0.0	2.5
200	199.4	0.6	2.5
300	298.1	1.9	2.5
500	495.4	4.6	2.5
600	594.1	5.9	2.5
800	791.4	8.6	2.5
900	890.1	9.9	2.5

4.3.4 Discussion

The results shown above are taken directly from the calibration certificates produced at LMK. The reported results are based on regression through the measured values.

It should be noted that due to the large uncertainties (of up to ±2.5 °C), most of the measurements are marginal to the manufacturer's specification at 25 °C ambient temperature. The measurements at 600 °C and 800 °C are outside the 25 °C ambient specification and are marginal to the specification at 30 °C ambient temperature. It is likely that the IRT was being heated by the BCRS at these temperatures, with the larger derated specification applying as shown in Figure 4.2. Without access to the internal temperature of the IRT via a readout or via supplemental internal probes (as in 4.5), it is not possible to determine what temperature the IRT was.

When using a BCRS with $\varepsilon_{cavity} \approx 1$, the detector temperature of the instrument should not influence the measurement as there should be no reflection errors [27]. The UUT corrections were mostly negative for temperatures above 0 °C and were mostly positive at readings above 0 °C. This indicates that the signal received by the IRT detector had a systematic error related to the ambient temperature. This error can most likely be attributed to the SSE, whereby radiation emitted and reflected from the area surrounding the BCRS aperture reduced the magnitude of the signal from the BCRS.

4.4   Measurement of SSE of the Test Case IRT

4.4.1   Introduction

Prior to the work presented, a set of SSE aperture plates had been prepared for use in NSAI [37]. These plates were designed to be placed in front of the flat plate calibrator and were large enough to obscure the plate's entire surface except for the central aperture. As part of the work presented, the plates were painted on the RT-facing side with Pyromark 1200 paint using the same procedure as that used to paint the NSAI BCRS. Coated plates of this type are described in ASTM E1256 to enable the tests described in the document to be performed [24].

SSE measurements are best performed with a horizontal blackbody cavity. The suitability of the vertical orientation for SSE measurements is unproven and would require further experiments. Furthermore, no cooling system was developed for the NSAI system of plates, and the requirements for cooling aperture plates covering such a large area source could be difficult to meet. It was decided in the early stages of the present work that developing a cooled SSE apparatus was a non-trivial matter and was

beyond the scope of this project. The well-designed and documented systems in NPL and LMK were therefore used instead.

During the calibration measurements in LMK, measurements of the SSE and DE were undertaken to ascertain the causes of the measured errors. The direct (variable aperture) method was used to measure the SSE. Measurements were also made in NPL using a similar apparatus.

4.4.2   Materials

4.4.2.1 LMK SSE Apparatus

An SSE apparatus as described in [71] was used to measure the SSE of the test case IRT. The apparatus is partially shown in Figure 4.12 and consisted of 14 aperture plates with different aperture diameters and a water-cooled holder for the plates. The aperture plates were painted with high emissivity paint and placed over the unpainted copper portion of the holder. The two screws on either side of the aperture were tightened ensuring good thermal contact between the plates and the cooled holder.
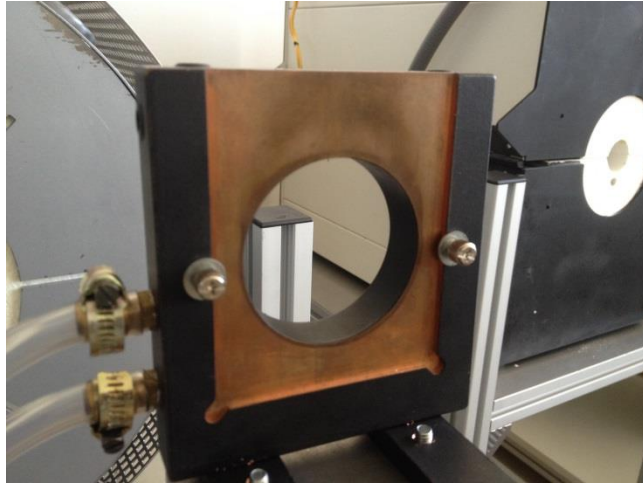
Figure 4.12 The LMK water-cooled direct-method SSE aperture plate holder.

4.4.2.2 NPL SSE Apparatus

The NPL SSE apparatus used for these measurements is shown in Figure 2.18 (a) and (b) in 2.6.7.2.3.

This apparatus used cooled water circulated through a helical coil. The coil wrapped around a drum-shaped aperture holder which was 60 mm in diameter. The aperture plates were made of aluminium and were lid-shaped, which allowed them to be placed onto the drum in quick succession. There were fourteen aluminium plates and they were all coated on the outer surface with high emissivity paint. An additional uncooled baffle, also coated in high emissivity paint and with a 60 mm aperture, was placed behind the drum.

4.4.3   Methods

With both types of apparatus, the IRT was carefully positioned by locating the maximum signal.

The SSE measurements undertaken in LMK were made in a single measurement run. The largest aperture plate was used first and replaced with smaller and smaller plates in turn. The measurements were performed at 50 °C and 150 °C with the IRT at distances of 300 mm and 330 mm from the aperture respectively.

In NPL, the IRT was positioned by the maximum signal with the smallest aperture plate in place. The SSE measurements were performed in three runs and the average UUT reading was calculated for each aperture diameter. The measurements were performed at 500 °C with the IRT 300 mm from the aperture. The lid-type apertures were designed for rapid swapping and measurements were taken approximately every 10 seconds. This allowed the SSE measurement to be performed before the UUT heated up significantly due to the source

4.4.4 Results

A plot of the SSE as obtained for this instrument in NPL and LMK is shown in Figure 4.13. The readings were converted into radiance values using Eq. 2.19. The results were normalised in both cases to relative radiance based on the UUT readings when exposed to the source with a 60 mm aperture plate in place.
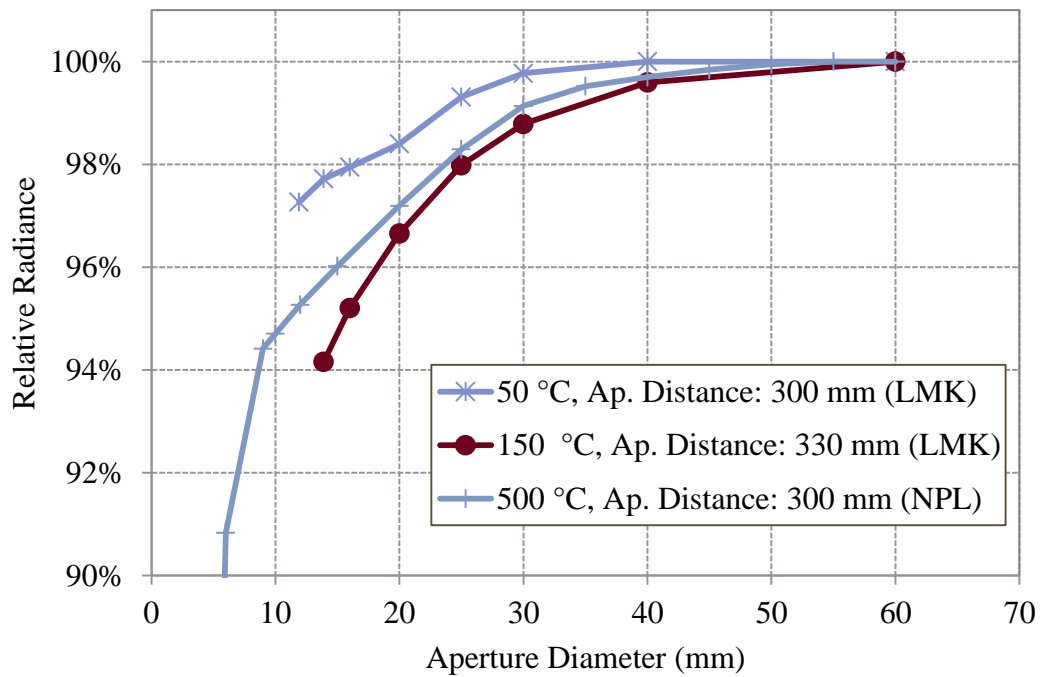
Figure 4.13 The SSE as measured in LMK and NPL.

4.4.5 Discussion

SSE specifications provided by manufacturers are usually quite limited in detail, with many manufacturers stating that the stated nominal target area of the RT accounts for 90 % or 95 % of the energy radiated from within that area. The test case IRT specifications do not include any statement about the SSE. The nominal target sizes are shown in Figure 4.1. At a distance of 300 mm, the nominal target size of the IRT is 6 mm and at 330 mm, the nominal target size should be approximately 8.2 mm. Figure 4.13 shows that the actual diameter of the area needed to give a signal of 95 % of the maximum at these distances are considerably larger than that. At 500 °C, a source size of approximately 14 mm in diameter causes the IRT to give a reading that is 95 % of its maximum reading for that temperature. An area 6 mm in diameter gives a reading that is 90 % of the maximum reading for the 500 °C target.

SSE measurements such as these are most useful where the location of a sharp decrease in relative radiance is detected. This can inform the instrument user as to how much it is necessary to overfill the RT's FOV.

It should be noted that unfortunately, during the LMK measurement, the 50 mm aperture could not be located and hence these measurements were not performed. It should also be noted that the LMK aperture holder is smaller in area than the NPL equivalent. At larger distances, the holding plate may not fill the FOV of an IRT.

Ideally, the SSE as measured through the direct method is the dependence of UUT readings on the target size alone. Theoretically, an infinitely large source with perfect uniformity and an emissivity of unity would be used and the detector temperature of the UUT would be maintained at ambient temperature. This could be accomplished using a temperature-controlled baffle or in a cooling jacket. The influence of focus and distance would also be negated.

In reality, however, many labs in this field use bespoke cavities and aperture apparatus with a wide variety of geometric constraints, making directly comparable measurements difficult. Standardised test equipment designs and procedures, if they were widely adopted, would aid repeatable measurements in different labs. Such standards would also be helpful for encouraging the publication of SSE characteristics of RTs by their manufacturers.

An indicative temperature of the IRT's internal temperature during the measurement would also be useful for such measurements to ensure the instrument is at ambient temperature. Such readouts are seldom made available to the end-user, however [6].

4.5   Characterisation of the Distance Effect of the Test Case IRT

Following the measurements in LMK, additional measurements were undertaken in NSAI of the RT's DE. As mentioned in 2.6.8, the DE is the dependence of the RT reading on the distance from the BCRS. Measurements of the DE call for a large-area target, and because no large horizontal BBs were available in NSAI, a flat plate calibrator was used to measure the DE.

4.5.1   Materials

4.5.1.1 The Fluke 4181 Flat Plate Calibrator

This instrument is a planar radiation source with a flat surface as described in 2.7.3.5. The instrument is shown on the left of Figure 4.14 and the manufacturer's published specifications are given in Table 4.6. Traceability was provided for these measurements using the TRT IV.82 (see section 3.5.3.2).
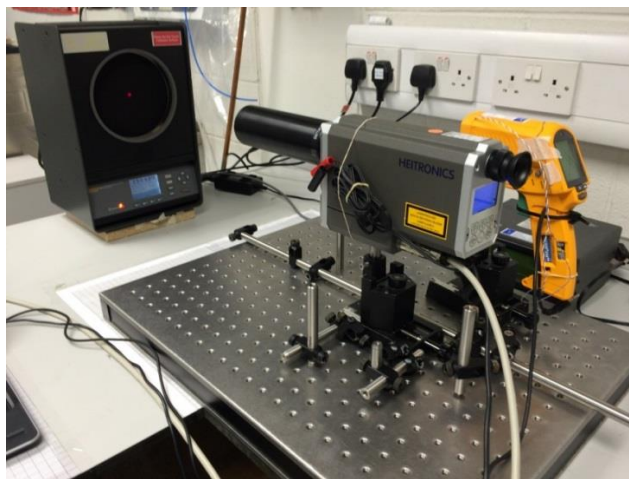
Figure 4.14 The calibration set up, showing, from left to right, the Fluke 4181 flat plate source, the TRT IV.82 and the UUT. The Chub E4 Thermometer Readout (with white and blue label on top) is also visible behind the UUT.

Table 4.6 Manufacturer's published specifications for the Fluke 4181 flat plate calibrator.

Description	Specification
Temperature range (@ 23 °C ambient, 0.95 emissivity)	35 °C to 500 °C
Display accuracy[1]	± 0.35 °C at 35 °C ± 0.50 °C at 100 °C ± 0.70 °C at 200 °C ± 1.20 °C at 350 °C ± 1.60 °C at 500 °C
Stability	± 0.05 °C at 35 °C ± 0.20 °C at 200 °C ± 0.40 °C at 500 °C
Uniformity[2], 5.0 in (127 mm) diameter of centre of target	± 0.10 °C at 35 °C ± 0.50 °C at 200 °C ± 1.00 °C at 500 °C
Uniformity[2], 2.0 in (51 mm) diameter of centre of target	± 0.10 °C at 35 °C ± 0.25 °C at 200 °C ± 0.50 °C at 500 °C
Heating time	20 min: 35 °C to 500 °C
Cooling time	100 min: 500 °C to 35 °C 40 min: 500 °C to 100 °C
Stabilization time	10 minutes
Nominal emissivity[3]	0.95
Thermometer emissivity compensation	0.9 to 1.0
Target diameter	152.4 mm (6 in)
Computer interface	RS-232
Power	115 V ac (± 10 %), 10 A, 50/60 Hz, 1000 W 230 V a (± 10 %), 5 A, 50/60 Hz, 1000 W
Fuse(s)	115 V ac 10 A, 250 V, fast blow 230 V ac 5 A, 250 V, F
Size (HxWxD)	356 mm x 241 mm x 216 mm (14 in x 9.5 in x 8.5 in)
Weight	9.5 kg (21 lb)
Safety	EN 61010-1:2001, CAN/CSA C22.2 No. 61010.1-04

[1] For 8 μm to 14 μm spectral band thermometers with emissivity set between 0.9 and 1.0
[2] The uniformity specification refers to how IR thermometers with different spot sizes both focused at the centre of the target will measure the same temperature.
[3] The target has a nominal emissivity of 0.95; however, it is radiometrically calibrated to minimize emissivity related uncertainties.

4.5.1.2 Thermocouple Probes

Two Thermocouple (TC) probes were mounted inside the test case IRT as shown in Figure 4.15. The voltage from these probes was measured using a Hart Scientific Chub E4 thermometer readout and the readings were logged over RS232 using Fluke 'Logware' PC software. TCs were chosen because of their small size. The small size allowed for unobtrusive insertion into the case of the IRT and a minimal thermal mass. The TCs therefore provided a fast response and limited influence on the measurement of the internal temperatures. The small size also enabled good thermal contact with the surfaces of the internal components of the IRT.

The wire length was chosen as 50 cm to improve the accuracy of the measurements. The wire was cut, welded and the proper connections attached. The probes were then calibrated at 20 °C, 30 °C, and 40 °C in a drywell calibrator before being inserted into the IRT.
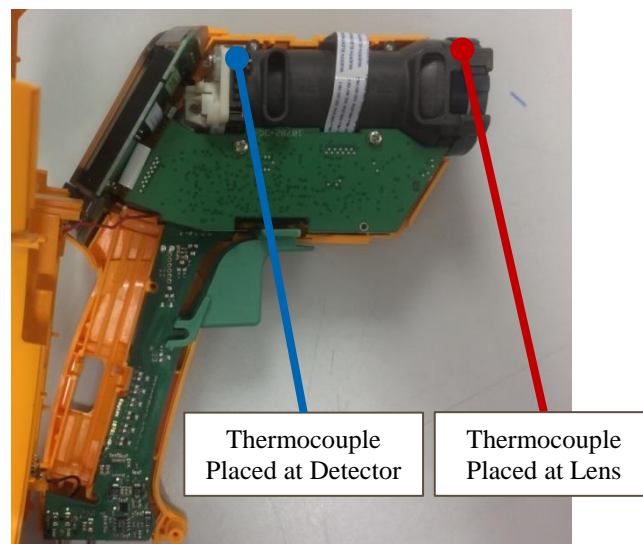
Figure 4.15 The interior of the UUT showing the mounting locations of the thermocouple probes inserted for testing purposes.

4.5.1.3 Baffle

A freestanding white, cardboard baffle was used as a shutter for these measurement experiments. The baffle was placed between the source and the IRT while the source was stabilising. It was removed rapidly to allow the effect of instantaneous exposure to a source to be measured.

4.5.2   Methods

The flat plate calibrator was used in an area free of forced air convection. Such convection could reduce the uniformity of the surface. The calibrator was also positioned such that there were no sources of infrared radiation facing it, such as windows or lights, which could cause reflection errors.

No published method of obtaining the test case RTs detector temperature could be located, so the TC probes described in 4.5.1.2 were placed inside the IRT housing. The probes were placed in thermal contact with the components using thermally conductive (heatsink) paste and were positioned as close as possible the detector and lens respectively. The TC probe at the plastic lens was placed in contact with its extreme edge, outside the optical path. Care was taken not to upset the alignment of the IRT optics. Openings were made in the casing of the IRT that were just big enough to allow the TC wires to pass through. The IRT was reassembled so that it could be used as usual.

The lens of the IRT and the TRT were inspected prior to measurements and found to be clean.

The TRT was used only at its focal length of 380 mm for all reference measurements. The TRT and IRT were manually aligned such that their optical axes were normal to the surface of the flat plate calibrator. The instruments were swapped between reference and UUT measurements. The targeting lasers of the instruments were positioned centrally on the plate using a mark made on the protective lid of the flat plate. The lid was removed for all measurements.

Both instruments were mounted on movable optical bases and were positioned on an optical breadboard. Carefully adjusted fixtures were attached to the breadboard to allow for quick and accurate exchanging of the TRT and IRT.

Measurements were made of the flat plate at distances of 300 mm, 500 mm, and 800 mm. The nominal target diameters for the test RT at these distances were approximately 6 mm, 23.8 mm and 51.4 mm respectively, so the FOV of the RT should have been overfilled by the source's 152.4 mm diameter flat plate.

As per Table 4.6, the nominal emissivity of the flat plate was 0.95 and both the TRT and the UUT were set to match this. The laboratory's ambient temperature was 21 °C ± 1 °C for all measurements.

The flat plate was allowed at least thirty minutes to fully stabilise at each set point in addition to the usual stable indication of the source (signalled by a beep).

4.5.2.1 Measurements Controlled for IRT Temperature

With the TC probes in place, measurements of the DE were possible while ensuring that the maximum housing temperature was within certain limits. The housing temperature was logged simultaneously with the IRT measurements, both at 1-second intervals.

Following the measurement runs, the acquired data were inspected. Twelve measurements were selected from the data where the readings of the temperature probes were within 24 °C ± 1.5 °C. The results of these measurements are shown in Figure 4.16.

4.5.2.2 Measurements of Lens and Detector Temperatures over Time

For two measurement runs at 300 mm and 500 mm and a flat plate temperature of 500 °C, the measurement was run for an extended duration until the IRT equilibrated with the heat from the source.

Twelve measurements of the flat plate radiance temperature at 10-second intervals were made using the TRT IV.82 before and after the long duration measurement runs. Readings were recorded during these measurement runs of both the flat plate's internal controller temperature (which is intended for use as a secondary laboratory standard with the flat plate) and the TRT measurements of the flat plate's temperature. This ensured that the flat plate temperature and its radiance temperature were very stable throughout these long-duration measurements.

4.5.3 Results and Discussion
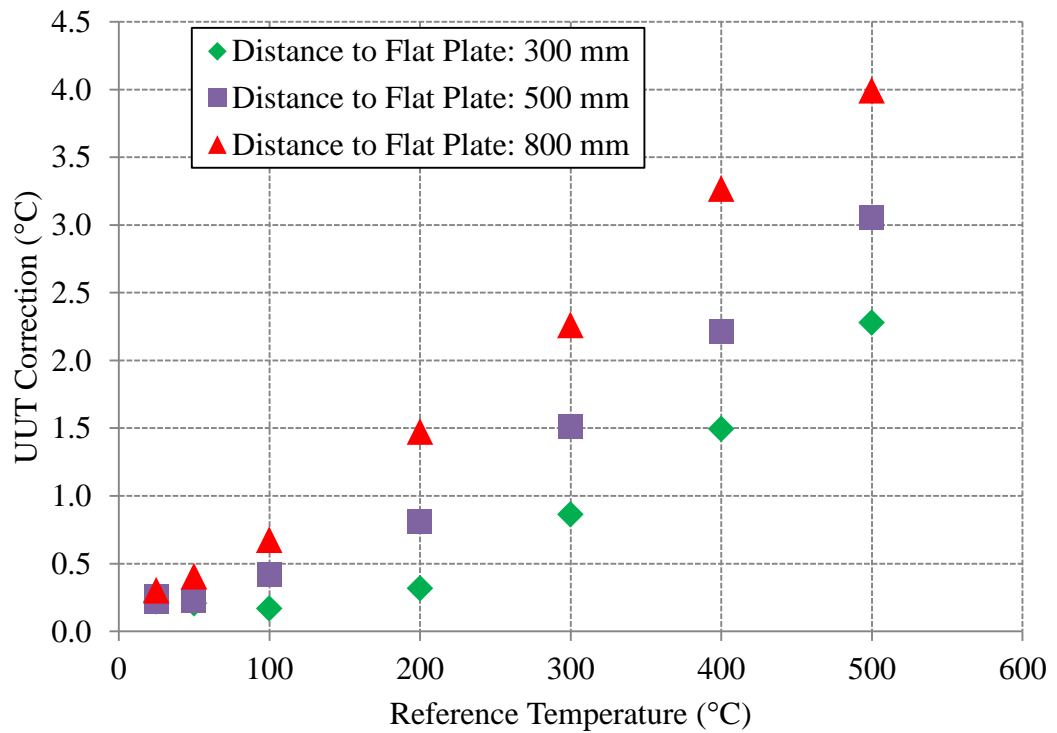
Figure 4.16 Corrections for the test case IRT at three distances from the flat plate source. These measurements were made with the internal temperatures (as measured by the TC probes) within 24 °C ± 1.5 °C.

The corrections were smaller for shorter target distances at all temperature set points, irrespective of the measurement duration as shown in Figure 4.16. This is particularly notable for the long-exposure measurement, shown in Figure 4.17. Although the lens and detector temperatures of the UUT increased further during measurement at 300 mm target distance, with a larger specification applying as per Figure 4.2, the UUT correction was smaller than the 500 mm measurement.
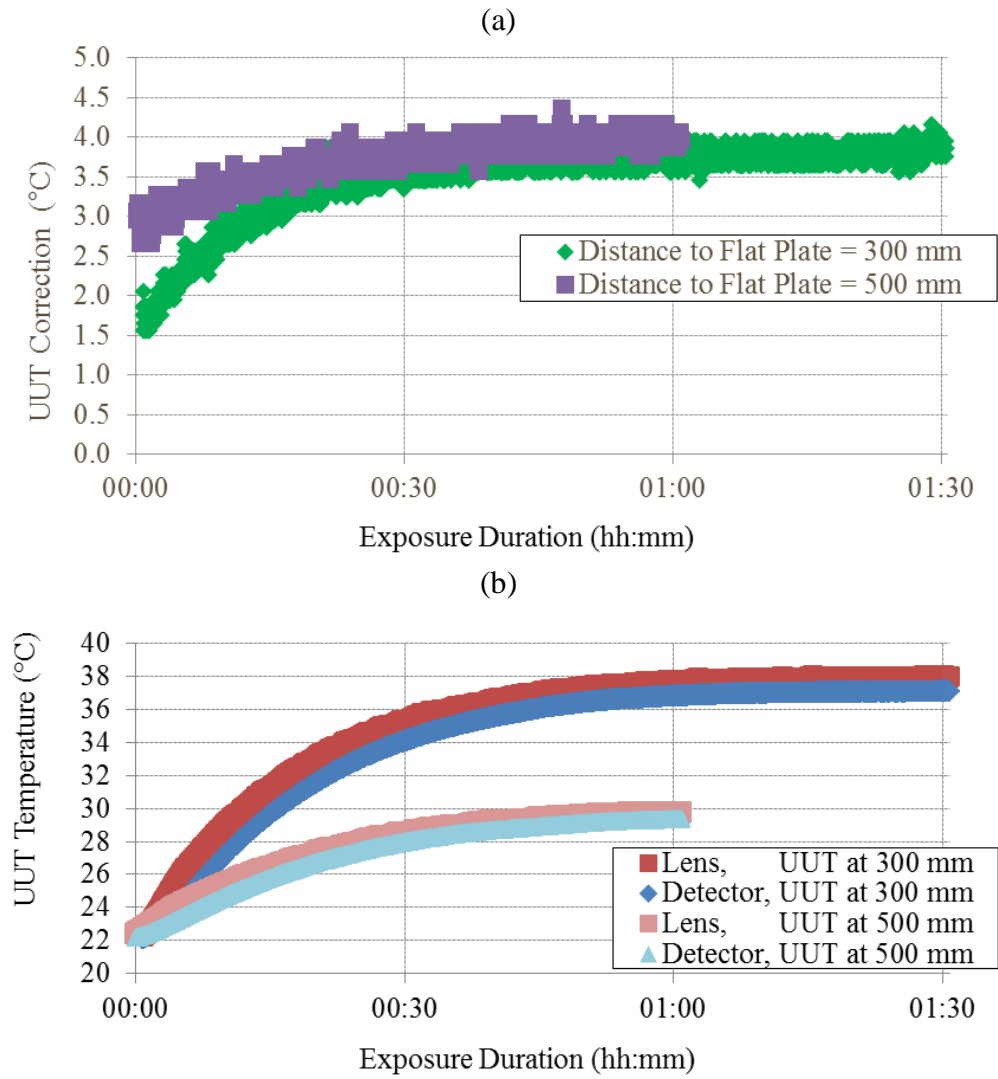
Figure 4.17 Corrections (a) and internal temperatures (b) over time for the test case IRT. The two target distances are shown for a calibration temperature of 500 °C. The measurement at 500 mm lasted 1 hour, and the measurement at 300 mm lasted 1 hour 30 minutes.

These larger corrections for the instantaneous measurements at 500 mm and 800 mm (shown in Figure 4.16) may have been due, in part, to both the SSE of the IRT and the non-uniformity of the flat plate. The FOVs of the TRT IV.82 and the test case IRT were different. As mentioned, the TRT was used at a fixed distance and with a target size of 6.8 mm. The IRT, on the other hand, had larger target sizes at the further distances which could have been influenced by a larger portion of the flat plate. The only information about the uniformity of the flat plate comes from its specification, given in Table 4.6, as the uniformity was not measured as part of this experiment.

In any case, the results highlight that accurate measurements may be made with short target distances but that the heating effects of the UUT at these short distances are problematic. The IRT is subject to a thermal shock upon exposure to the radiation from the flat plate (when the baffle is removed).

The technical guide for the flat plate states, 'If an IR thermometer is suddenly introduced to significantly different ambient conditions, it should be allowed time to reach thermal equilibrium' [10]. Such ambient conditions could be taken to include sources of thermal radiation, such as the flat plate. The UUT corrections were smallest before the IRT had equilibrated with the source, however. The technical guide for the flat plate also cautions that extended use at the high temperatures in its range will increase the rate of drift of the high emissivity coating [10]. The long duration measurements at 500 °C were thus limited to two.

Performing measurements lasting an hour or more would also make routine calibration of these instruments prohibitively expensive. It may, however, be the most representative type of calibration measurement if the instrument is permanently mounted or otherwise exposed for long durations to high-temperature sources. If on the other hand, the measurements are to be performed before equilibration, the exact moment to carry out the measurement that will be reported is not easy to determine.

The ambient derating specifications for the instrument do take account errors caused by the heating of the housing by the calibration source. However, it is possible, due to the complexity of the specification given in 4.2.1.1, that many users would not be aware of the issue. The user manual and other guides from manufacturers do not draw sufficient attention to ambient deratings. It would be helpful if:

- The derating specification was given in diagram form, similar to Figure 4.2;

- The RT's detector temperature was accessible to the user as has previously been suggested in [6];

- The RT could give a warning indication for extreme detector temperatures or even show the specification for a given measurement on the display along with the reading.

With regard to the exposure duration of the RT to the measurand, special care clearly should be taken when calibrating instruments that have uncooled detectors and no detector temperature display. This extra care is necessary to ensure that the calibration conditions are representative of the usage conditions. It is proposed that detailed information is requested from the client and relevant questions to that effect are given in 5.2.3.

The DE is not well defined in the literature. It is not clear whether heating of the RT under test from the calibration source is an element of the DE, or whether it should be excluded. Excluding RT heating from the DE is problematic because the best approach to follow will depend on how the instrument is used. It has also been suggested that the DE is simply another manifestation of the SSE [100] caused by the reduced angular size of the source in the FOV of the RT.

4.6   Discussion and Conclusions

Ideally, the TRT measurements comparing the cavity orientations described in Chapter 3 would have been conducted first, and the test case calibration using the NSAI BCRS, discussed in 4.2, would have been carried out later. The TRT measurements that

revealed and confirmed the issues with vapour (3.10) were not possible until the NSAI's TRT IV.82 had been purchased. The measurements showing the influence of distance and heating were also performed after the preliminary vertical calibration of the test case IRT. Following the improved procedure that was developed during the work presented (see section 5.2) could result in more repeatable measurements. Other potential future investigations of test case IRTs are discussed in 6.2.

The DE, SSE, and calibration of the test case IRT described were discussed in this chapter, along with the method, results, and analysis of the various measurement experiments. Manufacturers could provide improved guidance on the use of RTs to remove ambiguity and ensure that these effects are minimised. A discussion on the need for more detailed specifications and conditions of use, as detailed by the users of RTs, aiding calibrations that are more accurate, was also given. The considerations pertaining to the developed calibration procedure described in 5.2 were also presented.

Chapter 5.   Development of an NSAI Calibration Procedure and Uncertainty Budget

5.1   Introduction

In a calibration laboratory, it is required under ISO 17025 and the CIPM-MRA (see sections 1.2.1 and 2.2.4) that controlled, written procedures be followed for the calibration of instruments [32]. Individual procedures are tailored to cover categories of instruments and are stored in a document control system to ensure accountability.

Even though NSAI NML may not be accredited under the CIPM-MRA for radiation thermometry for some time, it is required under its ISO 9001:2008 accreditation to have a procedure covering any calibration work undertaken.

A record of the methodology used for the calculation of uncertainty must also be made. This is typically accomplished using a master uncertainty budget that may be tailored to individual calibrations.

In many fields of calibration, procedures are well established, and best practice guides are published by international metrology organisations such as Euramet. These may be used as the starting point for an in-house procedure.

Calibration laboratories maintain in-house procedures that are tailored to the specific types of work typically undertaken there. In-house procedures reference the equipment available and the methods typically used. Records are also kept of personnel trained in

the various procedures. Periodic internal audits and external audits (by the accreditation body or peer-review) are a normal part of ISO 17025 and the CIPM-MRA, through which various aspects of the Quality Management System (QMS) are examined.

This section presents the procedure and uncertainty budgets – developed in NSAI as work packages of this project – for calibration of radiation thermometers and incorporates discussion on some of the points. The calibration procedure itself is presented in Appendix II.

5.2   Development of an NSAI Calibration Procedure

5.2.1   Standardisation of RTs and Sources for a Procedure

In the absence of guides from metrology organisations, standardised testing procedures published by ISO, IEC or other international standardisation bodies can be of help. These guides are, however, often geared towards product testing by manufacturers or type-approval bodies rather than towards metrology or calibration. While applied standardisation in the field of radiation thermometry has been somewhat lacking, as mentioned in 1.2.1, there are some sources upon which a calibration procedure may be based.

The availability of IEC Technical Specification 62492 parts 1 and 2 (see section1.2.1.3) is welcome, however, these are non-binding technical specification documents, rather than fully adopted standards and this limits their usefulness. With adopted IEC and ISO standards, manufacturers state compliance or type-approval to a standard by quoting the standard on the instruments and in promotional material. Currently, in radiation

thermometry, there is still no standard for manufacturers to state compliance with, and so users of RTs may be largely unaware of this (and the other) standards. As such, many low quality instruments are available on the market and there is no simple way to distinguish them from good quality instruments.

Since the introduction of part 1 (technical data for RTs) of IEC TS 62492, the declaration of specifications has nevertheless improved. For example, in the specification of RT FOVs, many manufacturers now state that a given target size accounts only for a percentage of the FOV, thus indicating that the instrument has an SSE. It is too soon to determine the impact of part 2 (determination of technical data), which was introduced in 2013.

Many manufacturers still only partially follow part 1, often resulting in incomplete specifications. Commercial manufacturers have an interest in presenting their instruments in the best light, so in some cases, the capabilities of instruments may be overstated. This situation makes calibration difficult, particularly for clients hoping to verify that their instrument is within its specification.

Other sources which serve as a useful basis for the NSAI calibration procedure are ASTM 2847 [26], VDI/VDE 3511 Part 4.4 [22] and MSL Technical Guide 22 [27] which were discussed in 1.2.1.

Finally, experience of procedures gained during laboratory visits to NPL, LMK, and CMI serves to inform the NSAI procedure.

5.2.2   The Scope of the Calibration Service

The radiation thermometry calibration service offered by NSAI will be tailored towards the most prominent types of instrument in use in industry. As mentioned in 2.6.3.2, handheld IRTs have been given most consideration in the present work. This is due to their prevalence in industry (which in turn, is due to the lower cost of these instruments) and due to the types of enquiries received from clients to date. Calibration equipment for these instruments is also more widely available.

Based on this and the equipment purchased to date, the NSAI service will cater primarily to IRTs operating in the 8 μm to 14 μm waveband with a total temperature range from -30 °C to 500 °C using the Fluke 4181 flat plate source and the NSAI BCRS. Traceability will be provided by SPRT over the range of the NSAI BCRS (--30 °C to 150 °C) and by the TRT IV.82 over the range of the Fluke 4181 (35 °C to 500 °C). It will be possible to calibrate RTs with spectral responsivities other than 8 μm to 14 μm over the range of the NSAI BCRS, although such RTs are uncommon.

The service is not expected to cover clinical IRTs. It is expected that most RTs received for calibration will be handheld IRTs and that many will have large FOVs.

5.2.3   Quoting for a Radiation Thermometer

Under normal circumstances, a quotation is issued to a prospective client when an enquiry concerning calibration is received. At this stage, prior to the instrument's receipt in the laboratory, it should be verified that the calibration requirement for the RT

falls within the scope of the service and that NSAI is capable of calibrating the instrument.

When preparing a quotation, the manufacturer's specifications should be studied to determine, where possible, the IRT's:

- accuracy;

- range;

- spectral responsivity;

- FOV;

- emissivity settings; and

- mounting options.

As mentioned in section 4.5, it is recommended that questions be asked of the client at this stage to determine the usage of the instrument. Some relevant questions are:

- Has the RT been calibrated before and, if so, is can the previous certificate be supplied?

- What is the usage environment of the RT and what is its exposure to dust, dirt and grease?

- What is the RT typically used to measure and what sizes of targets are used?

  - What is the most common measurement distance?

  - What emissivity settings are used?

  - What range of temperatures is encountered?

- What accessories (including power supplies and any thermal-shielding apparatus) are normally used with the RT?

- What is the instrument user's approach to lens cleaning?

The calibration points are also normally agreed at this time.

5.2.4 Calibration Points

The selection of calibration set points depends on:

- The temperature range of the UUT;

- The ranges available from the calibration sources;

- Whether the UUT is direct-reading or not;

- The range of temperatures that the client typically uses the UUT to measure.

The CCT-WG508-03 document (see section 1.2.1.1) specifies that 'at least three temperature–signal pairs are required' in order to calibrate an RT [18]. This assumes that the RT is to be calibrated by calculation of the Sakuma-Hattori parameters (see section 2.6.6), which may not be the case for direct-reading RTs. This document only applies to instruments that give access to the unlinearised detector signal, and thus precludes most IRTs which give direct temperature readings.

When calibrating any instrument, it is normal practice to choose set-points near the top and bottom of its most accurate operating range. If some intermediary points are added, this can serve to determine if the instrument is operating linearly. In the case of a non-linear response, the number of set-points will improve the accuracy of a fit if a calibration equation is applied [5]. Thermometers may be calibrated either over their entire range or only over the client's range of normal use.

For contact thermometers, the extremes of the range may include temperatures that could damage the thermometer or where only limited exposure is recommended [5]. For RTs at reasonable distances from the source, damage is less likely, and indeed, the scope of the NSAI service will not cover the total range of many RTs. In any case, for both contact and non-contact thermometers, the specification of the instrument often increases at the peripheries of the range. Figure 4.2 serves as an example of this for a representative RT.

For a quick and cost effective calibration, it is sensible to limit the calibration range to that which satisfies the client's needs [5]. Direct-reading IRTs should, in theory, produce a temperature reading that has already been linearized. ASTM E2847 suggests that a single point may suffice where an IRT is used over a narrow range of temperatures but mandates a minimum three points for use over a wide range [26]. MSL TG22 does not make any recommendations regarding the number of points [27]. In light of these considerations, three or more points are recommended in the NSAI procedure.

5.2.5 Preliminary Inspection and Ambient Conditions

Upon receipt, the RT should be checked to confirm it matches the instrument quoted for and that the items in 5.2.3 that were determined from the specification are correct. The procedure recommends that the RT is also checked with respect to its lens condition and general operation and that 'relevant anomalies, particularly the condition of the optics should be recorded.'

As with all instruments received for calibration, RTs should be allowed enough time to equilibrate with the conditions in the laboratory. ASTM E2847 suggests that

'experimentation may need to be done to determine the proper time for the device to thermally stabilize' [26].

The temperature and humidity of all laboratories are monitored and recorded automatically as a matter of course in NSAI NML. The NSAI procedure restates that the temperature is recorded at the start of each measurement run.

5.2.6   Lens Cleaning

Any dirt, grease, or scratches on the lens of the RTs could potentially attenuate the signal reaching the detector or increase the SSE of the IRT.

As already mentioned in 3.10.3, different laboratories take different approaches to the cleaning of RT optics. Fluke recommend that the lenses of all IRTs are cleaned prior to calibration with the Fluke 4181 flat plate calibrator [10]. LMK, however, take a more conservative approach in their procedure, where the lens is only cleaned where it is deemed necessary by the laboratory. Where the lens is cleaned, a check measurement is performed at one temperature set-point [101]. In the ASTM E2847 standard, it is only recommended that lenses are cleaned in accordance with manufacturer's instructions.

Because the optical components form a vulnerable and exposed part of the RT's measuring system they should be approached with care. The NSAI procedure notes that the 'condition of the lens of an RT received for calibration should be checked upon receipt. Any anomalies should be noted, be they scratches or deposits of dirt'.

Cleaning of lenses represents an adjustment of the measuring system, and so, if it is performed, measurements may be required before and after. After inspecting the condition of the optics, the procedure notes that 'calibration technicians should avoid contact with IRT lenses. Cleaning should only be undertaken in accordance with manufacturer's instructions and by agreement of the instrument owner.'

5.2.7   Emissivity Settings

Great care is needed with regard to selection and recording of emissivity settings. The NSAI procedure states that 'the reference IRT and UUT emissivity settings should be set as close as possible to the reference emissivity value for the calibration source'.

For calibration using either the NSAI BCRS and the Fluke 4181 flat plate calibrator as detailed below, the instrumental emissivity setting ε_{Inst} (the setting of the UUT), should be recorded with each the measurement run. The reference emissivity value for the source ε_S may also be recorded. Note that where it is not possible to match the instrumental emissivity with that of the source, a correction should be applied.' The correction is calculated using the formulae and spreadsheet specified in [27].

5.2.8   Selection of a Target Distance

ASTM E2847 terms the selection of a target distance 'Z-axis alignment'. No recommendations are made in either the ASTM or MSL calibration guides about the selection of target distance. This is a key drawback of using these documents. The ASTM guide, however, describes how the distance is measured and states that it must

be shown on the calibration certificate and this has been adopted into the NSAI procedure.

The ASTM guide specifies the target distance as the distance from the base of a cavity or from a flat plate source to the front of an IRT and terms it d_{meas}. This standard does not clarify ways of dealing with instruments that specify another location to measure the target distance from. This may be indicated in the manual of some RTs or as a datum mark (ϕ) on the body of an RT as shown in Figure 5.1.
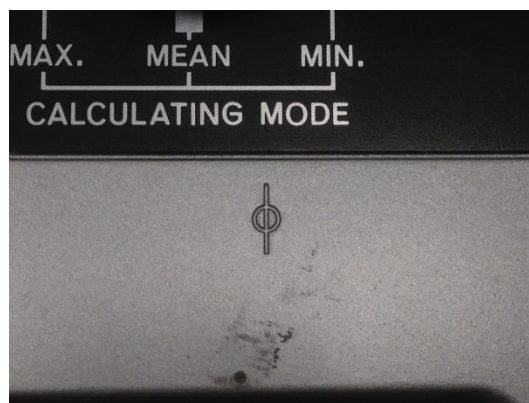
Figure 5.1 A datum mark on a handheld IRT.

As such the NSAI procedure specifies that 'the target distance (TD) is the distance between the radiation source and the optics of the IRT. This distance may be measured from another point, for example a datum mark ϕ, if indicated in the manufacturer's manual. On the other end, at the radiation source, the distance is measured from the base of a BCRS or from the surface of a flat plate calibrator.'

The other critical considerations are the diameter of the measurement spot and the heating of the IRT due to the source. These are dealt with in the NSAI procedure as follows:

'For an IRT with converging optics such as the Fluke 574 CF, there is a minimum target area (spot size) that occurs at a particular TD (300 mm in the case of the Fluke 574). IRTs with diverging optics will have target area that increases with TD. Wherever possible, the TD should be chosen such that the UUT's target area is less than half the area of the calibration source.

If the TD is too small, the IRT may heat up due to convection and radiation from the source. IRTs use measurements of their internal temperature to calculate the indicated temperature of the source. As such, the body of the IRT should be maintained, to the best extent possible, at room temperature.

The TD should be recorded with each of the measurement runs.'

5.2.9   Positioning of the RT

As discussed in 3.4, there are different approaches taken to the positioning of RTs under calibration depending on the accuracy of the UUT and the equipment available. Careful positioning of high-accuracy RTs is essential, as these instruments are capable of highly repeatable measurements. When positioning low-accuracy handheld IRTs in front of large-area sources, the same level of attention is not justified, particularly where the instruments will be used for handheld measurements by their users. Using high-accuracy methods with low accuracy instruments would make the cost of calibration prohibitive and will not necessarily reduce the uncertainty of the calibration measurements. Furthermore, the uncertainty of the in-use measurements by the end user could be an order of magnitude higher.

Alignment methods using the either the RT targeting system or the maximum signal level are described in the ASTM guide. Both methods are permitted, with the maximum signal method being preferred.

Bearing the above in mind, the best positioning technique practical should be used given the equipment available. The positioning method should be stated on the certificate. Use of the NSAI vertical mount (which was shown in Figure 3.12) is recommended with vertical measurements, and tripods or the optical breadboard and horizontal stands are recommended for use with the flat plate calibrator.

5.2.10 Calibration Geometry

Ideally, an RT with $\varepsilon_{Inst} = 1$ measuring two different BCRSs at the same temperature will give the same reading for each. In practice, the instrument will often display results that are quite different. This is largely due to the SSE of the RT.

IRTs are calibrated using a certain geometry and procedure at manufacture. This may not, however, be an accredited calibration and a certificate may not be issued. In order to determine how much the instrument has drifted since its previous calibration, the geometry of the calibration should be replicated as closely as possible given the available equipment in the laboratory. This is often not possible where the manufacturer or previous calibration laboratory does not make this information available. With BCRSs of differing lengths or radii, it may be impossible to obtain the comparable results.

The ASTM E2847 calibration guide defines parameters relating to the geometry of sources and the target and aperture distances. It also recommends that 'the measuring distance, the emissivity setting of the infrared thermometer, the diameter of the source, the ambient temperature, a description of the aperture including aperture distance (if used), and the measurement uncertainties' are included in the calibration certificate [26].

It doesn't directly address the issues relating to reproducing geometries, but if its recommendations are followed in other laboratories, these issues will be more understandable for instrument users. If the details are available, it may also enable different laboratories to perform comparable calibrations. The NSAI procedure has thus adopted these proposals.

5.2.11 Exposure Duration

Instruments received for calibration are likely to have a wide array of optical configurations. As discussed in 2.7.2, these configurations will decide which sources can be used and thus the temperature range of calibration. The key consideration is the distance to the calibration source. In practice, RTs may be used over a range of distances and the magnitude of the SSE will depend on the distance chosen. In order to eliminate the influence of the SSE, the FOV must be overfilled two or three times. The target distance must be small enough that the RT FOV is sufficiently filled but large enough that the RT housing temperature is reasonably stable and within the manufacturer's specification.

When measuring below approximately 200 °C the radiation emitted by the detector is significant and is corrected by an internally referenced temperature measurement. If the RT is heated too much, the uncertainty in this reference temperature measurement will increase (see section 5.3.3.2.9). The instrument's filter and detector responsivity may have a temperature dependence, as may the amplifier [102].

Temperature stability of the RT housing is ideally achieved by allowing the RT to equilibrate with the source over a long period. The RT user, however, may not use the instrument in this way in practice. These stable conditions may also create a condition where the housing temperature is outside the optimum operating temperature limits specified by the manufacturer, as occurred in 4.5.3. The alternative approach is to take readings upon instantaneous exposure to the source before the UUT reaches equilibrium (similar to the method in 4.5.2.1)

A third approach is to control the UUT temperature by placing it behind a temperature-controlled baffle or within a cooling jacket. This is not possible with the current equipment in NSAI.

The approach to controlling the UUT temperature should, in any case be carefully chosen to match that used by the instrument user or else to repeat that carried out in previous calibrations. This may not be possible depending on the detail supplied by the client or the previous calibration laboratory. The equipment or accessories available at the time of calibration may also restrict the methods possible. As such, the default method used is to use the instantaneous exposure technique. Care should be taken to ensure the UUT readings have stabilised and are not excessively time-dependent. The

exposure duration should be recorded and the instrument allowed to equilibrate to the laboratory temperature between measurements.

5.2.12 Using an Immersible Vertical BCRS

An abridged version of the section of the procedure relating to measurements using vertical BCRSs is given here with some discussion. The procedure is written to permit usage of the NSAI vertical BCRS, the smaller immersible BCRS, which is designed for use with tympanic thermometers or other BCRSs acquired in the future.

Calibration of IRTs with large FOVs or SSEs using the NSAI vertical BCRS has been found to be challenging. These instruments must be carefully aligned, placed very close to the source aperture and must have the duration of their exposure limited to avoid heating. It is therefore recommended that such instruments, with FOVs of 20:1 or larger, are calibrated using the flat plate at temperatures more than 15 °C from ambient.

The BCRS is used from the lowest temperature set point in order of increasing temperature in accordance with recommendations from the ASTM calibration procedure [26]. The liquid level is set as high as the bath will permit to give an immersion as per Figure 3.4. It is noted in the NSAI procedure that the lid may be used to avoid any contact with the cavity surface from solids or liquids when measurements are not in progress. The lid should be used at temperatures below the dew point to prevent the formation of dew or ice. The procedure also notes that 'a stabilisation period should be allowed after removing the cavity lid'.

The following instruction is given regarding emissivity settings: 'The reference RT and UUT … should be set as close as possible to the reference emissivity value for the BCRS.' The procedure also gives instructions on the correction methods mentioned in 2.6.9 and points to a spreadsheet where they are implemented.

In order to minimise the difference between the SPRT measurement and the temperature of the base of the cavity, it is suggested that 'the immersed tips of both the SPRT and secondary reference should be as close as possible to the centre point of the base of the BCRS'.

Targeting instructions are given as per the discussion given in 5.2.9. The requirements for recording the data are also given: 'The source type, ambient conditions in the lab, the TD and the emissivity settings of the UUT and the reference RT (where used) should be recorded.'

5.2.13 Using the Fluke 4181 Flat Plate Calibrator

The flat plate measurement procedure cautions against usage of the flat plate in the presence of additional sources of radiation which may cause reflection errors. The optical axes of both the TRT and the UUT are, in turn, placed normal to the surface of the plate. The relevant data required to be recorded are given: 'ambient temperature of the lab, the TD, and the emissivity settings of the reference RT and the UUT'. The procedure then describes options for the order of measurements.

5.2.14 Calibration Intervals

The calibration intervals used for UUTs are at the discretion of clients. NSAI can advise clients of appropriate intervals based on past accumulated experience of instrument models.

The recalibration intervals of SPRTs were discussed in 3.5.5.1. The TRT IV.82 calibration interval is currently set at 1 year based on the manufacturer's specification for long-term stability given in 3.5.3.2. Periodic monitoring of the TRT drift is possible with the NSAI BCRS.

5.2.15 Calibration Certificate

A calibration certificate is produced in accordance with standard procedure. In addition to the usual elements of the certificate, the certificate should include:

- The source temperature (or corrected source temperature);
- The corresponding instrument readings and corrections;
- The target distance used;
- The length and aperture diameter of the BCRS or the diameter of the plate;
- The emissivity setting of the instrument;

These recommendations are as per the ASTM E2847 guide [26].

5.3 Uncertainty Budgets

5.3.1 Traceability

As discussed in 2.6, a calibration is not valid unless there is an unbroken chain of traceability. Non-contact thermometry measurements follow either one of two schemes, shown in Figure 5.2 [22], [26].

In the context of the sources used in NSAI, these schemes correspond to:

- Using the NSAI cavity with contact traceability through SPRTs (Scheme I);
- Using the flat plate source with radiometric traceability via the TRT IV.82 (Scheme II).

In both cases, the components of an uncertainty budget may be categorised according to whether they originate with:

- the reference instrument;
- the calibration source; or
- the UUT.

<table>
<tr><td>(a)</td><td>(b)</td></tr>
<tr><td>Scheme I</td><td>Scheme II</td></tr>
</table>
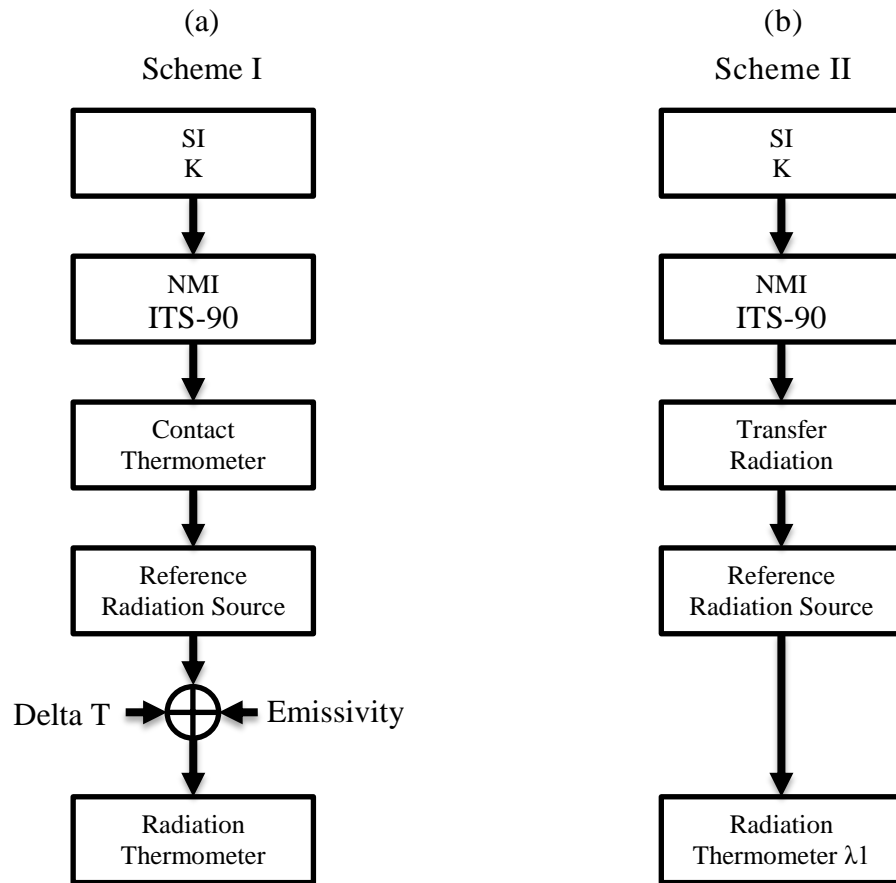
Figure 5.2 Traceability schemes for RTs where traceability is provided via contact thermometry (a) or via a transfer radiation thermometer with spectral responsivity λ1 (b).

The reference instrument may be an SPRT or the TRT for calibrations undertaken with an immersible BCRS or with the flat plate respectively. The calibration source is either the immersible BCRS or the flat plate. The UUT is an RT under calibration.

5.3.2   Sample Uncertainty Budget Structures

There are several sources for information on RT calibration uncertainty budgets. ASTM E2847 features relevant example budgets, as does the BIPM CCT-WG5/08-03 document [18], [26]. The procedure used at LMK, LMK_CP_RADT_06.01, also contains relevant uncertainty budgets [101]. The Fluke 4181 Flat Plate Technical Guide also includes a sample budget.

The CCT-WG5/08-03 budget is specifically tailored for use below the silver point and is the accepted method of achieving the lowest RT calibration uncertainties. It follows a generalised approach covering wideband RTs, with spectral responses of 8 μm to 14 μm, as well as narrowband RTs, with centre wavelengths of 1.6 μm and 3.9 μm. It gives examples of best-case and 'normal' uncertainties for the components in each applicable case. It also covers the use of FPBBs below the silver point. As previously mentioned, however, it precludes direct-reading RTs. In any case, much more conservative uncertainties are appropriate for such instruments.

The sample budgets were therefore adapted take account of the specifics of the NSAI service. These adaptations were required because of the use of a vertically oriented cavity in the case of the BCRS, calibration of direct-reading RTs, and using the flat plate with traceability to the TRT.

Sensitivity coefficients (as defined in the GUM [31]) have been omitted from the uncertainty budgets presented as all coefficients were 1.

5.3.3 Uncertainty Budgets for the NSAI Vertical BCRS with Contact Traceability

5.3.3.1 Uncertainty of the Reference Instrument

The reference instrument in this case is an SPRT. The uncertainty components associated with the SPRT are given in Table 5.1. The uncertainty of the measurements made with the SPRT is calculated separately. The result of this calculation is included in the budget for the BCRS.

Table 5.1 Uncertainty budget for reference measurements of bath temperature using the SPRT.

Denot.	Source of uncertainty	value ± mK	Probability distribution	Divisor	U_i ( ) ± mK
Uc	Calibration Unc. of SPRT	1	Normal	2	0.50
U_{drift}	SPRT Stability/Year	3	Rectangular	$\sqrt{3}$	1.73
U_{RB}	Bridge Tolerance	0.27	Rectangular	$\sqrt{3}$	0.16
U_{SR}	Std. Resistor Cal. Unc.	0.50	Normal	2	0.25
U_{TR}	Std. Resistor Temp Coeff.	0.1	Rectangular	$\sqrt{3}$	0.06
U_{RD}	Std. Resistor Drift	0.4	Rectangular	$\sqrt{3}$	0.23
$U_{B\Sigma}$	Temp. Medium Stability	10	Rectangular	$\sqrt{3}$	5.77
$U_{B\Gamma}$	Temp. Medium Gradients	20	Rectangular	$\sqrt{3}$	11.55
U_c ( )	Combined Standard Uncertainty		Normal		13.04
U	Expanded Uncertainty ($k = 2$)		Normal k=2		26.08

A description of each of the components follows:

5.3.3.1.1   Calibration Uncertainty of SPRT, Uc

This is the uncertainty arising from the calibration of the SPRT against laboratory fixed points [103]. Since the value comes from a calibration certificate and was stated with k=2, a divisor of 2 is used to convert it to a standard uncertainty.

5.3.3.1.2   SPRT Stability/Year, U_{drift}

This component accounts for the annual drift of the SPRT probe. The drift is monitored at weekly ice point checks and 6 week TPW checks [103].

5.3.3.1.3   Bridge Tolerance, U_{RB}

The tolerance associated with the resistance measuring bridge is taken from the manufacturer's specifications. The SPRT readings are taken with the bridge, which is

referenced to a calibrated standard resistor [103]. As it is a tolerance with defined limits, it follows a rectangular distribution.

5.3.3.1.4   Standard Resistor Calibration Uncertainty, U_{SR}

This is based on the estimated uncertainty in the calibration certificate for the standard resistor from the NSAI NML electrical laboratory. Again, as an uncertainty from another certificate, this component is stated with k=2.

5.3.3.1.5   Standard Resistor Temperature Coefficient, U_{TR}

This is the best measurement estimate of the coefficient representing the variation of the resistance value with temperature. It is based 'on temperature monitoring of the resistor during calibration, the manufacturer's original specification, calibration data from NML's Electrical Laboratory and the ambient conditions of the laboratory which are recorded daily' [103].

5.3.3.1.6   Standard Resistor Drift, U_{RD}

This component accounts for the long-term drift of the resistor between annual calibrations.

5.3.3.1.7   Temperature Medium Stability, $U_{B\Sigma}$

This component accounts for the stability of the bath medium and is estimated based on previous experiments performed on the baths. A rectangular distribution is used.

5.3.3.1.8   Temperature Medium Gradients, U_{BT}

This component accounts for gradients in the bath medium measured previously using

SPRTs. It uses a rectangular distribution.

5.3.3.2 Uncertainty of the Blackbody and RT

All uncertainty components in this section are from the CCT-WG5/08-03 document

unless otherwise stated. Estimates from this document are used where measurements of

the respective phenomena were not possible using the equipment in NSAI. Where

values from this document are used, the most conservative estimate for 8 µm to 14 µm

RTs (referred to in the document as 10 µm RTs) is used.

Table 5.2 Uncertainty budget for the NSAI BCRS as measured with the TRT IV.82 over the range of water bath temperatures (5 °C to 80 °C)

Source of Uncertainty	Value ± mK	Probability distribution	Divisor	Type	U_i ± mK
BCRS Components					
NML Contact Unc. of Measurement [†]	26	Normal	2	A	13
Blackbody Emissivity	42	Normal	1	B	42
Reflected Ambient Radiation	49	Normal	1	B	49
Cavity Bottom Heat Exchange	15	Rectangular	$\sqrt{3}$	B	9
Convection Heat Loss	29	Rectangular	$\sqrt{3}$	B	17
Cavity Bottom Uniformity [†]	63	Normal	1	A	63
Blackbody Ambient Conditions	58	Normal	1	B	58
RT Components					
Size-of-Source Effect	44	Rectangular	$\sqrt{3}$	B	25
Reference Temperature	100	Normal	1	B	100
Ambient Temperature	51	Normal	1	B	51
Atmospheric Absorption *	33	Normal	1	B	33
Repeatability [†]	76	Rectangular	$\sqrt{3}$	A	44
Readout Resolution	50	Rectangular	$\sqrt{3}$	B	29
Combined Standard Uncertainty		Normal			171
Expanded Uncertainty ($k = 2$)		Normal			342

[†] indicates values based on measurements in NSAI
* indicates values from ASTM E2487

5.3.3.2.1 NML Contact Uncertainty of Measurement

This element arises from the result of the budget given in 5.3.3.1 and, as such, the value is not from CCT-WG5/08-03. As this component is already stated with a coverage factor of 2, it is divided by 2 to convert it to a standard uncertainty for the purposes of calculation in this budget.

5.3.3.2.2 Blackbody Emissivity

This component accounts for uncertainty due to the isothermal and non-isothermal emissivities of the BCRS, as defined in sections 4.1.4.2 and 4.1.5 of CCT-WG5/08-03 [18]. These respectively take account of the geometric and thermal departures from ideal blackbody conditions.

The values used here are a combined value from the 'normal' estimates from tables 6 and 7 in CCT-WG5/08-03. Given that the RT is focused only on the base of the NSAI BCRS for the TRT measurements and in most other cases, this is most likely a conservative estimate.

5.3.3.2.3 Reflected Ambient Radiation

This component represents the signal from the external environment reflecting off the internal BCRS walls and reaching the RT, as defined in section 4.1.6 of CCT-WG5/08-03. The values are based on table 8 in that document.

5.3.3.2.4   Cavity Bottom Heat Exchange

This component accounts for the heat loss due to radiation from the base of the BCRS and the resulting temperature difference between the SPRT and the base. The value is based on table 10 and derived from a model in section 4.1.7.1 in CCT-WG5/08-03.

5.3.3.2.5   Convection Heat Loss

This is the heat-exchange effect caused by the airflow between the cavity and the laboratory, as defined in section 4.1.7.2 of CCT-WG5/08-03. The values from CCT-WG5/08-03 are for a horizontal 60 mm cavity of length 525 mm [18]. Such losses are most significant at temperatures above the upper limit of the NSAI BCRS. It is expected that the vertical orientation will reduce convective losses at temperatures below the dew point. The values are based on table 11 in CCT-WG5/08-03.

5.3.3.2.6   Cavity Bottom Uniformity

This component is based on the worst-case uniformity measurement of the base of the cavity as described in section 3.8 of the present work. The figure for the highest temperature is used across the range to give the most conservative estimate.

5.3.3.2.7   Blackbody Ambient Conditions

This component accounts for the noise in the temperature of the bath caused by the influence of ambient conditions, as defined in section 4.1.9 of CCT-WG5/08-03. The values are from table 13 in that document.

5.3.3.2.8   Size-of-Source Effect

SSE is the first of five uncertainty components associated with the RT under test. Values from table 14 in CCT-WG5/08-03 are used. In the case of the TRT IV.82 measurements, the FOV was overfilled with the base of the BCRS, even accounting for the measured SSE, so these values are thought to be conservative.

5.3.3.2.9   Reference Temperature

Detectors employing a chopper, such as that in the TRT IV.82, measure the radiation signal from the measurand alternately with that of an internal reference surface. The temperature of the surface is measured and used as a reference temperature to compensate for the radiation emitted by the detector enclosure and other components of the RT. This component represents the uncertainty in the output temperature resulting from possible errors in the internal measurement of the reference temperature. Values from table 16 in section 4.2.3.1 of CCT-WG5/08-03 are used.

5.3.3.2.10   Ambient Temperature

This component accounts for the drift in the internal temperature of the RT due to heating from the source, as defined in section 4.2.3.1 of CCT-WG5/08-03. As seen in section 4.5, the RT reading may depend strongly on its internal temperature. This is a net effect as it is based on the thermal drift of the different components of the RT, such as the detector, amplifier, and optics. As such, it is assigned a normal distribution. The worst-case value from table 17 of CCT-WG5/08-03 is used across the temperature range.

5.3.3.2.11   Atmospheric Absorption

This component represents the attenuation introduced by the atmosphere. According to section 4.2.4 of the CCT-WG5/08-03 document, losses due to the transmission of radiation in the atmosphere are negligible for RTs in most cases [18]. This is because these instruments use bandwidths specifically chosen to maximise transmission (see section 2.6.4).

The values used here are based on estimates from table X1.1 in the ASTM E2847 document which are more conservative than those in CCT-WG5/08-03.

5.3.3.2.12   Repeatability

This is a measure of the agreement between identical repeated measurements [30]. As this component was measurable in NSAI, it is based on measurement data. A repeat measurement is taken over a short period of time but not as part of a single measurement run. The repeatability would often be represented by a standard deviation and assigned a normal distribution as it includes several contributions. In this case, it was decided to use the half the span of the repeatability measurements and therefore assign a rectangular distribution. This approach was chosen to give a more conservative estimate.

For the TRT IV.82 measurements made in NSAI which these uncertainty budgets represent, at least 5 repeat measurements were made at each point (see Figure 3.19). The largest span for each bath was chosen as the 'worst-case' repeatability for that medium and temperature range.

The CCT-WG5/08-03 document considers several additional components applicable to RTs. These include the non-linearity of the instrument, gain ratios and noise. As mentioned in section 5.3.2, this approach takes account of a different class of instruments. These components are less applicable for direct-reading RTs and are not easily measureable. In the ASTM E2487 document, these are all accounted for as 'Noise'. The NML uncertainty budget follows the ASTM structure in this case.

5.3.3.2.13   Readout Resolution

This component accounts for the quantisation error introduced by the display of the UUT. It is defined as having half the range of the least significant digit on the display and has a rectangular distribution.

Table 5.3 Uncertainty values for the NSAI BCRS measured with the TRT IV.82 over the three ranges of thermal medium.

Source of uncertainty	Methanol -30 to 5 °C ± mK	Water 5 to 80 °C ± mK	Oil 80 to 150 °C ± mK
BCRS Components			
NML Contact Uncertainty of Measurement [†]	13	13	13
Blackbody Emissivity	42	42	78
Reflected Ambient Radiation	99	49	29
Cavity Bottom Heat Exchange	0	9	9
Convection Heat Loss	17	17	33
Cavity Bottom Uniformity [†]	63	63	63
Blackbody Ambient Conditions	58	58	58
RT Components			
Size-of-Source Effect	25	25	25
Reference Temperature	100	100	100
Ambient Temperature	51	51	51
Atmospheric Absorption *	33	33	59
Repeatability [†]	95	44	275
Readout Resolution	29	29	29
Combined Standard Uncertainty	209	171	330
Expanded Uncertainty ($k = 2$)	418	342	660

[†] indicates values based on measurements in NSAI
* indicates values from ASTM E2487

5.3.4 Uncertainty Budget for the Flat Plate Calibrator with Radiometric Traceability

A sample uncertainty budget is included in the technical guide for the flat plate calibrator [10]. This budget is written from the point of view of using the calibrator as a laboratory standard. Some customisation of the budget was necessary, given that the TRT would be used as the laboratory standard rather than the calibrator itself.

Table 5.4 Uncertainty budget for the Fluke 4181 flat plate calibrator using the TRT IV.82 as a reference at 150 °C.

Source of uncertainty	Value $\pm$ °C	Probability distribution	Divisor	U_i $\pm$ °C
Flat Plate Calibrator Uncertainties				
Calibration Uncertainty	0.300	normal	2	0.150
Stability (Long Term)	0.050	normal	2	0.025
Uniformity	0.145	rectangular	$\sqrt{3}$	0.084
Noise	0.150	rectangular	$\sqrt{3}$	0.087
Display Resolution	0.050	rectangular	$\sqrt{3}$	0.029
IR Thermometer Uncertainties (UUT)				
Readout Resolution	0.050	rectangular	$\sqrt{3}$	0.029
Ambient Temperature	0.030	rectangular	$\sqrt{3}$	0.017
Noise	0.250	rectangular	$\sqrt{3}$	0.144
Atmospheric Losses	0.200	normal	2	0.100
Angular Displacement	0.030	rectangular	$\sqrt{3}$	0.017
Background Temperature	0.700	rectangular	$\sqrt{3}$	0.404
Spectral Variation	0.200	normal	2	0.100
Combined Standard Uncertainty		Normal		0.494
Expanded Uncertainty ($k = 2$)		Normal		0.988

A description of each of the components follows:

5.3.4.1 Calibration Uncertainty

The uncertainty of the calibration comes from the TRT IV.82 calibration certificate. It is assumed to follow a normal distribution, as it is a combination of other components, and is divided by 2 to convert it to a standard uncertainty.

5.3.4.2 Stability (Long Term)

This contribution accounts for the possible drift of the TRT between calibrations. As it results from a number of influences, it is expected to follow a normal distribution.

5.3.4.3 Uniformity

This component represents the uniformity of the surface of the plate of the calibrator. It is based on a specification from the manufacturer and therefore follows a rectangular distribution.

5.3.4.4 Noise

This is the contribution of noise or flicker in the readings of the TRT. It is based on measured data and is therefore a type A uncertainty.

5.3.4.5 Display Resolution

This component is as per 5.3.3.2.13 and accounts for the quantisation error of the TRT.

5.3.4.6 Readout Resolution

This component is as per 5.3.3.2.13 and accounts for the quantisation error introduced by the UUT.

5.3.4.7 Ambient Temperature

This contribution comes from the possible range of ambient temperatures. Values used come from the ASTM E2847 standard [26].

5.3.4.8 Noise

This component represents the flicker in the readings of the UUT, similar to 5.3.4.4.

5.3.4.9 Atmospheric Losses

According to the CCT-WG5/08-03 document, losses due to the transmission of radiation in the atmosphere are negligible for RTs in most cases [18]. This is because these instruments use bandwidths specifically chosen to maximise transmission (see section 2.6.4).

The values used here are based on those given by the manufacturer which come from several sources and hence a normal distribution is used.

5.3.4.10 *Angular Displacement*

This component accounts for variation in the plate's surface emissivity because of the RT not being at an angle normal to the surface of the flat plate.

5.3.4.11 *Background Temperature*

Changes in temperature of surfaces facing the plate are represented by this component. This mainly consists of the laboratory walls. The temperature of the laboratory falls within a limited band, so a rectangular distribution is applied.

5.3.4.12 *Spectral Variation*

The flat plate surface is nominally 0.95, but actually varies with wavelength. An example of the spectral response of the surface of this model of flat plate was shown in Figure 2.28. The response of the UUT is also taken into account. A normal distribution is therefore used.

5.4 Discussion and Summary

Several RTs were received for calibration during the present work and calibration was undertaken (outside of the scope of the CIPM-MRA). Some of the certificates for these calibrations are included (with client information redacted) in Appendix III.

It is potentially possible to calibrate instruments with spectral responsivities other than 8 μm to 14 μm using the flat plate with traceability to the TRT IV.82 [92], [104]. This

was not attempted as part of the present work, as all of the IRTs encountered in NSAI had a responsivity of 8 µm to 14 µm.

Even though low-uncertainty measurements may be possible with direct-reading IRTs in the laboratory, the control over conditions possible with laboratory measurements may be artificial in comparison with in-use conditions. By stating small uncertainties, there is a risk that clients will develop unrealistic expectations of the capabilities of these instruments. Manufacturers, NMIs, and secondary calibration laboratories have a role to play in educating users of these instruments and informing them of the standards discussed in 1.2.1. If accurate non-contact measurements are important to users, instruments must be carefully selected and appropriate measuring procedures designed and followed.

In this chapter, the documentary requirements for calibration procedures were introduced, leading to a examination of each of the considerations required for an NSAI procedure. The theory and experimental results given in the previous two chapters informed this discussion. Details of the procedures for calibration using the NSAI vertical BCRS and the flat plate calibrator were given.

Finally, the uncertainty budgets for both sources were described. Each of the uncertainty components was briefly explained, and the overall uncertainty budgets were shown.

Chapter 6. Discussion and Conclusion

6.1 Introduction

The overall aim of this work was to improve calibration facilities for Radiation Thermometers; in particular, to provide a method for laboratories to develop calibration capabilities for the increased numbers of lower-cost RTs appearing on the market.

Specifically, this work sought to investigate the performance of vertical BCRSs and establish whether they are suitable for use as calibration sources for RTs. A comparison of vertical cavities and conventional horizontal BCRSs was undertaken to that end.

The calibration of handheld direct-reading IRTs was also investigated. Significant problems were found relating to the calibration of these instruments. Further to the summaries and conclusions in each chapter, a brief discussion of potential items of future work is given here along with some closing comments.

6.2 Limitations and Future Work

The key limitations of the horizontal and vertical cavity comparison measurements were:

- The use of manual positioning and the lack of a graduated translation stage for vertical cavity measurements
- The potential influence of vapours on the lens

The limitations of the measurements of the test-case IRT are similar to those for the comparison of BCRS orientations. For the initial vertical measurements, the measurements were made with the IRT in place over the bath for extended periods. As such, there may have been a large influence on these measurements due to bath vapours.

More research is needed into the repeatability component of the TRT IV.82 measurements of the NSAI vertical BCRS. The repeatability of the measurements, particularly for the oil bath range of temperatures, could be improved through the use of a redesigned top plate.

A new top plate could be designed to limit the egress of vapour from the bath by enclosing the entire area of the bath's well. A viewing port in the top plate would be desirable in this case, to ensure that the bath fluid was at its maximum level and that the cavity was immersed as far as possible. A small, sealable opening could also be made in the redesigned top plate for re-filling the bath using a tube and funnel, allowing the liquid level to be increased without removing the cavity.

As mentioned in 3.6.3, the effectiveness of the PTFE collar, shown in Figure 3.4 (a), could also be improved by redesigning the bolting configuration so that bolts mounting alternately from the top plate and the copper flange below it are used, thus eliminating heat bridges as in [95]. This would improve the thermal uniformity of the BCRS, especially at high temperatures.

Further work of this type could also improve the repeatability of measurements of the vertical BCRS made with IRTs similar to the test case thermometer. Use of a graduated translation stage could improve the repeatability of positioning of all categories of RT.

This could, therefore, improve the repeatability of measurements. Improved repeatability would be beneficial for measurements in both horizontal and vertical orientations.

6.3 Key Findings

6.3.1 Performance Differences of Horizontal and Vertical BCRSs

An extensive set of measurements, over the temperature range from -30 °C to 150 °C and comparing horizontal and vertical BCRSs, was made in LMK through an international collaboration. Further comparisons were made by comparing RT measurements of a vertical cavity in NSAI with recent calibration data for the thermometer from the manufacturer's laboratory. The uncertainty of the measurements ($k = 2$) was evaluated according to best practice and found to range from 0.34 °C to 0.66 °C.

Vertical BCRSs have not been described in the literature to any great extent, and a comprehensive literature survey found no articles investigating their use or comparing them with horizontal BCRSs. The use of immersible vertical BCRSs is of interest because they are a flexible and economical alternative to existing methods.

Suites of purpose-built horizontal BCRS systems with smaller temperature ranges are generally used for RT calibration. However, with a single immersible vertical cavity, measurements may be made in commonplace stirred calibration baths with different temperature media across a wider range.

It has been concluded from the present work that vertical BCRSs are an acceptable means of providing traceability to ITS-90 for the range from -30 °C to 150 °C. The uncertainty of measurement has been evaluated according to best practice, and it has been found that uncertainties of the same order of magnitude as for the horizontal orientation are achievable in this temperature range. The most important considerations for the vertical orientation were identified. These include the need to:

- Limit any bath vapours in the optical path
- Limit any increase in the temperature of the RT housing
- Ensure maximum immersion in the bath

6.3.2   Investigation into the Calibration of Direct-Reading RTs

Best practice procedures and uncertainty budgets relating to handheld direct-reading RTs were examined and applied. A case-study instrument of this type was tested in three NMIs and found to be outside its specification over a large part of its range and to be affected by a substantial SSE and DE.

This case-study highlights the difficulty in choosing an appropriate target distance during calibration. The effect of UUT heating due to the BCRS was found to be unsatisfactorily addressed in literature and standards presenting calibration procedures. It was also found that manufacturers do not draw sufficient attention to RT derating specifications and the effects of heating from the measurand.

The ambient temperature of an RT was found to be critically important for low-temperature measurements. It was also important for measurements where temperature

compensation is used due to target emissivities of less than 1. As such, the duration of exposure of RTs to the source was found to be critical to ensuring repeatable measurements. The approach to exposure duration should be reported with the measurements for instruments if an instrument is suspected to be operating near its ambient temperature limits or to have a strong dependence on ambient temperature.

6.4   Summary

The overall output from this work has been the establishment of a fit-for-purpose high-level non-contact calibration capability at NSAI. This capability was developed inexpensively for use with existing calibration baths. It is hoped that this work provides a method by which such facilities can be implemented with relative ease in any metrology laboratory. Although it was found that some additional care is needed regarding vapours and heating of the RT, the vertical BCRS offers advantages in terms of lower cost and increased flexibility and yet provides similar performance to custom-made horizontal BRCSs when used for calibration.

References

[1]   J. Fischer and B. Fellmuth, "Temperature metrology," *Reports Prog. Phys.*, vol. 68, no. 5, pp. 1043–1094, 2005.

[2]   D. P. DeWitt and G. D. Nutter, *Theory and Practice of Radiation Thermometry*, 1st ed. Wiley, 1988.

[3]   J. Hartmann, "High-temperature measurement techniques for the application in photometry, radiometry and thermometry," *Phys. Rep.*, vol. 469, no. 5–6, pp. 205–269, 2009.

[4]   BIPM, "BIPM - Calibration and Measurement Capabilities - CMCs - NSAI NML," *Key comparison database*, 2013. [Online]. Available: http://kcdb.bipm.org/appendixC/T/IE/T_IE.pdf. [Accessed: 01-Jun-2015].

[5]   J. V. Nicholas and D. R. White, *Traceable Temperatures*, 2nd ed. John Wiley & Sons Ltd, 2001.

[6]   P. Saunders, "Calibration and use of low-temperature direct-reading radiation thermometers," *Meas. Sci. Technol.*, vol. 20, no. 2, p. 025104, 2009.

[7]   H. Preston-Thomas, "The International Temperature Scale of 1990 (ITS-90)," *Metrologia*, vol. 27, no. 1, pp. 3–10, Jan. 1990.

[8]   C. E. Gibson, B. K. Tsai, and A. C. Parr, "Radiance Temperature Calibrations." NIST, Gaithersburg, MD, 1998.

[9]   G. Machin, T. Ricolfi, M. Battuello, and G. Negro, "Comparison of the ITS-90 using a transfer standard infrared radiation thermometer between seven EU national metrological institutes," *Metrologia*, no. 33, pp. 197–206, 1996.

[10]   "Fluke 4180, 4181 Precision Infrared Calibrator Technical Guide." Fluke Corporation, American Fork, Utah, 2007.

[11]   "Eura-Thermal: Developing traceable capabilities in thermal metrology." [Online]. Available: http://www.eura-thermal.org/. [Accessed: 07-Feb-2016].

[12]   T. Kolat and F. Liebmann, "Standards for Radiation Thermometry," in *NCSL International Workshop and Symposium*, 2012.

[13]   OIML, "International Recommendation OIML R 111-1 Edition 2004 (E)," vol. 2004, p. 80, 2004.

[14]   "IEC 61672-3:2013 Electroacoustics - Sound level meters -- Part 3 : Periodic tests." IEC, Geneva, 2013.

[15]   "Calibration Guides and Technical Guides - EURAMET." [Online]. Available: http://www.euramet.org/publications-media-centre/calibration-guides-and-technical-guides/. [Accessed: 01-Jul-2015].

[16]   K. D. Hill and D. J. Woods, "Exploring the size-of-source and distance effects of

radiation thermometers," in *TEMPMEKO*, 2004, no. October, pp. 599–604.

[17] H. McEvoy and R. Underwood, "Protocol for Euromet 658 Extension: Project To Examine Underlying Parameters in Radiance Temperature Scale Realisation from 156 ° C to 1000 ° C." London, pp. 1–11, 2007.

[18] P. Saunders, J. Fischer, M. Sadli, M. Battuello, C. W. Park, Z. Yuan, H. W. Yoon, W. Li, E. Van Der Ham, F. Sakuma, J. Ishii, M. Ballico, G. Machin, N. Fox, J. Hollandt, M. Matveyev, P. Bloembergen, and S. Ugur, "CCT-WG5/08-03 Uncertainty budgets for calibration of radiation thermometers below the silver point," Paris, 2008.

[19] "VDI/VDE 3511 Part 4 Radiation thermometry," no. December. VDI/VDE, Dusseldorf, pp. 3–6, 2011.

[20] "VDI/VDE 3511 Part 4.2 Maintenance of the specification for radiation thermometers," no. February. VDI/VDE, Dusseldorf, 2014.

[21] "VDI/VDE 3511 Part 4.3 Standard test methods for radiation thermometers with one wavelength range," no. July. VDI/VDE, Dusseldorf, 2005.

[22] "VDI/VDE 3511 Part 4.4 Calibration of radiation thermometers," no. July. VDI/VDE, Dusseldorf, pp. 1–2, 2005.

[23] "VDI/VDE 3511 Part 4.5 Practical application of radiation thermometers." VDI/VDE, Dusseldorf, 2015.

[24] "ASTM E1256 − 15 Standard Test Methods for Radiation Thermometers (Single Waveband Type)." West Conshohocken, PA, 2015.

[25] "ASTM E2758 − 15a Standard Guide for Selection and Use of Wideband, Low Temperature Infrared Thermometers." West Conshohocken, PA, 2015.

[26] "ASTM E2847 − 14 Standard Test Method for Calibration and Accuracy Verification of Wideband Infrared Thermometers." West Conshohocken, PA, 2014.

[27] P. Saunders, "MSL Technical Guide 22 Calibration of Infrared Thermometers," vol. 64, no. 1, pp. 1–8, 2009.

[28] J. Dixon, "Radiation thermometry," *J. Phys. E.*, vol. 21, no. 5, pp. 425–436, 1988.

[29] "OIML Document D24," vol. 2007. BIPM, Paris, 1996.

[30] "JCGM 200:2008 The international vocabulary of basic and general terms in metrology." BIPM, Paris, 2008.

[31] "JCGM 100:2008 Evaluation of measurement data — Guide to the expression of uncertainty in measurement," 2008.

[32] "ISO/IEC 17025:2005 General requirements for the competence of testing and calibration laboratories," *International Standard*, vol. 2005. ISO, pp. 1–36, 2005.

[33] J. B. Fowler, "An Oil-Bath-Based 293 K to 473 K Blackbody Source," *J. Res. NIST*, vol. 101, no. 5, pp. 629–637, 1996.

[34]   I. Pušnik, G. Grgić, and J. Drnovšek, "Calculated uncertainty of temperature due to the size-of-source effect in commercial radiation thermometers," *Int. J. Thermophys.*, vol. 29, no. 1, pp. 322–329, 2008.

[35]   M. Bart, E. van der Ham, and P. Saunders, "A new method to determine the size-of-source effect," *Int. J. Thermophys.*, vol. 28, no. 6, pp. 2111–2117, 2007.

[36]   H. Rodriguez and E. Mendez-Lango, "The Influence of Distance and Focus on the Calibration of Infrared Radiation Thermometers," *Int. J. Thermophys.*, vol. 30, no. 1, pp. 179–191, 2009.

[37]   B. Cusack, "The Design, Construction and Characterisation of an Infrared Thermometer Calibration System," DCU, Dublin, 2015.

[38]   T. J. Quinn, "The calculation of the emissivity of cylindrical cavities giving near black-body radiation," *Br. J. Appl. Phys.*, vol. 18, no. 8, pp. 1105–1113, 1967.

[39]   K. D. Hill, "The NRC Blackbody-Based Radiation Thermometer Calibration Facility," *AIP Conf. Proc.*, vol. 684, no. January, pp. 669–674, 2003.

[40]   P. R. Dekker and E. Van Der Ham, "ITS-90 scale realization on the new radiation thermometer calibration facility at NMi VSL," *Int. J. Thermophys.*, vol. 29, no. 3, pp. 1001–1013, 2008.

[41]   R. Simpson, G. Machin, H. McEvoy, and R. Rusby, "Traceability and calibration in temperature measurement: a clinical necessity," *J. Med. Eng. Technol.*, vol. 30, no. 4, pp. 212–7, 2006.

[42]   L. Kňazovická and L. Šindelářová, "Different blackbody geometry and distance of measurement influence on the calibration results of hand infrared thermometers," 2015.

[43]   "Basic Principles of Non-Contact Temperature Measurement." Optris GmbH, Berlin, pp. 1–32, 2009.

[44]   M. de Podesta, "Rethinking the kelvin," *Nat. Phys.*, vol. 12, no. 1, pp. 104–104, 2016.

[45]   F. (National P. L. Redgrave and P. (Danish F. M. L. Howarth, *Metrology – In Short 3rd Edition*. 2008.

[46]   Fluke Corporation., *Fluke - Calibration Philosophy in practice*, 2nd ed. Fluke Corp, 1994.

[47]   S. Bell, *NPL Good Practice Guide No. 11 Introductory Guide to Uncertainty of Measurement*, no. 11. London: NPL, 2001.

[48]   "EA-4/02M:2013 Evaluation of the Uncertainty of Measurement in Calibration," no. September. European Co-operation for Accreditaion, p. 75, 2013.

[49]   L. Kirkup and R. B. Frenkel, *An Introduction to Uncertainty in Measurement*. Cambridge: Cambridge University Press, 2006.

[50]   H. Preston-Thomas, "The International Temperature Scale of 1990(ITS-90)," *Metrologia*, vol. 27, no. 1, pp. 3–10, 1990.

[51] D. Mac Lochlainn, D. Fleming, P. Cromwell, and M. White, "TP-NM-10: Rev.1.4 Triple Point of Water Cell." NSAI National Metrology Laboratory, 2016.

[52] J. Fischer, M. De Podesta, K. D. Hill, M. R. Moldover, L. Pitre, R. Rusby, P. Steur, O. Tamura, D. R. White, and L. Wolber, "Present estimates of the differences between thermodynamic temperatures and the ITS-90," *Int. J. Thermophys.*, vol. 32, no. 1–2, pp. 12–25, 2011.

[53] A. Peruzzi, E. Mendez-Lango, J. Zhang, M. Kalemci, F. Points, A. Peruzzi, E. Mendez-Lango, J. Zhang, and M. Kalemci, "Guide to the Realization of the ITS-90." BIPM, Paris, pp. 1–15, 2015.

[54] D. Mac Lochlainn, D. Fleming, P. Cromwell, M. Wolf, and M. White, "TP-NM-90: Calibration of Thermometers in liquid mediums from -100C to 550C." NSAI National Metrology Laboratory, Dublin, 2016.

[55] T. Husmann and C. S. Magnus, "Thermography in incremental forming processes at elevated temperatures," *Measurement*, vol. 77, pp. 16–28, 2016.

[56] R. Rusby, *Introduction to Temperature Measurement*, no. 125. 2016.

[57] H. E. Sostmann and P. D. Metz, "Fundamentals of Thermometry," *Isotech Journal of Thermometry*, vol. 6, no. 2, 1995.

[58] I. Pušnik and A. Miklavec, "Dilemmas in Measurement of Human Body Temperature," *Instrumentation, Sci. Technol.*, vol. 37, no. 913571838, pp. 516–530, 2009.

[59] I. Pušnik and J. Drnovsek, "Infrared ear thermometers--parameters influencing their reading and accuracy.," *Physiol. Meas.*, vol. 26, no. 6, pp. 1075–84, 2005.

[60] P. Saunders, "Analysis of the Potential Accuracy of Thermodynamic Measurement Using the Double-Wavelength Technique," *Int. J. Thermophys.*, vol. 35, no. 3–4, pp. 417–437, 2014.

[61] A. Rogalski, "Infrared detectors: An overview," *Infrared Phys. Technol.*, vol. 43, no. 3–5, pp. 187–210, 2002.

[62] P. Saunders and D. R. White, "Physical basis of interpolation equations for radiation thermometry," *Metrologia*, vol. 40, no. 4, pp. 195–203, 2003.

[63] F. Liebmann, "Uncertainty Budgets for IR Temperature Measurement – An Overview," *Proceedings of Thermal Solutions*. Fluke, 2008.

[64] H. W. Yoon, D. W. Allen, and R. D. Saunders, "Methods to reduce the size-of-source effect in radiometers," *Metrologia*, vol. 42, pp. 89–96, 2005.

[65] Y. Yamada and J. Ishii, "Toward Reliable Industrial Radiation Thermometry," *Int. J. Thermophys.*, no. April, pp. 1699–1712, 2015.

[66] "Fluke 574 Infrared Thermometer User Manual," no. March. Fluke Corporation, 2005.

[67] G. Machin, "The Size of Source Effect (SSE)." NPL, London, 1999.

[68] E. Hecht, *Optics*. Pearson, 2012.

[69] D. H. Lowe, M. Battuello, G. Machin, and F. Girard, "A Comparison of Size of Source Effect Measurements of Radiation Thermometers between IMGC and NPL," *AIP Conf. Proc.*, vol. 684, no. 1, pp. 625–630, 2003.

[70] X. Hao, Z. Yuan, X. Lu, and W. Zhao, "Size-of-source effect difference between direct and indirect methods of radiation thermometers," *Int. J. Thermophys.*, vol. 32, no. 7–8, pp. 1655–1663, 2011.

[71] I. Pušnik, G. Grgić, and J. Drnovšek, "System for the determination of the size-of-source effect of radiation thermometers with the direct reading of temperature," *Meas. Sci. Technol.*, vol. 17, no. 6, pp. 1330–1336, 2006.

[72] G. Machin and M. Ibrahim, "Size of source effect and temperature uncertainty: I. High temperature systems," in *TEMPMEKO*, 1999, pp. 681–686.

[73] F. Liebmann, "Traceability and Quality Control in a Radiation Thermometry Laboratory," in *NCSL International Workshop and Symposium*, 2011.

[74] G. Bauer and K. Bischoff, "Evaluation of the emissivity of a cavity source by reflection measurements.," *Appl. Opt.*, vol. 10, no. 12, pp. 2639–2643, 1971.

[75] "Measurement of Spectral Emissivity by a FTIR Spectrometer, S. Clausen, Tempmeko, 2001.pdf." .

[76] C. J. Donlon, W. Wimmer, I. Robinson, G. Fisher, M. Ferlet, T. Nightingale, and B. Bras, "A second-generation blackbody system for the calibration and verification of seagoing infrared radiometers," *J. Atmos. Ocean. Technol.*, vol. 31, no. 5, pp. 1104–1127, 2014.

[77] X. Song, K. Huan, W. Dong, J. Wang, Y. Zang, and X. Shi, "Research on infrared radiation characteristics of Pyromark 1200 high-temperature coating," in *International Symposium on Optoelectronic Technology and Application 2014*, 2014, p. 93001S.

[78] R. Castrejón-García, J. R. Castrejón-Pita, and A. A. Castrejón-Pita, "Design, development, and evaluation of a simple blackbody radiative source," *Rev. Sci. Instrum.*, vol. 81, no. 5, 2010.

[79] J. B. Fowler, "A Third Generation Water Bath Based Blackbody Source," *J. Res. NIST*, vol. 100, no. 5, pp. 591–599, 1995.

[80] K. D. Hill and D. J. Woods, "Characterizing the NRC blackbody sources for radiation thermometry from 150 °C to 962 °C," *Int. J. Thermophys.*, vol. 30, no. 1, pp. 105–123, 2009.

[81] O. Kozlova, S. Briaudeau, L. Rongione, F. Bourson, S. Guimier, S. Kosmalski, and M. Sadli, "Calibration of Radiation Thermometers up to 3000 °C: Effective Emissivity of the Source," *Int. J. Thermophys.*, vol. 36, no. 8, pp. 1726–1742, 2015.

[82] V. I. Sapritsky and A. V. Prokhorov, "Calculation of the Effective Emissivities of Specular-Diffuse Cavities by the Monte Carlo Method," *Metrologia*, vol. 29, no. 1, pp. 9–14, 1992.

[83] J. De Lucas, "A Simple Geometrical Model for Calculation of the Effective

Emissivity in Blackbody Cylindrical Cavities," *Int. J. Thermophys.*, vol. 36, no. 2–3, pp. 267–282, 2015.

[84]   H. McEvoy, M. Sadli, F. Bourson, S. Briaudeau, and B. Rougié, "A comparison of the NPL and LNE-Cnam silver and copper fixed-point blackbody sources, and measurement of the silver/copper temperature interval," *Metrologia*, vol. 50, no. 6, pp. 559–571, 2013.

[85]   X. Yang, Y. Y. Yan, and D. Mullen, "Recent developments of lightweight, high performance heat pipes," *Appl. Therm. Eng.*, vol. 33–34, no. 1, pp. 1–14, 2012.

[86]   F. Bourson, M. Sadli, B. Rougié, S. Briaudeau, and O. Kozlova, "Influence of the Opening of a Blackbody Cavity Measured at the Ag and Cu ITS-90 Fixed Points," *Int. J. Thermophys.*, vol. 35, no. 3–4, pp. 516–525, 2014.

[87]   V. B. Khromchenko, S. N. Mekhontsev, and L. M. Hanssen, "Design and evaluation of large-aperture gallium fixed-point blackbody," *Int. J. Thermophys.*, vol. 30, no. 1, pp. 9–19, 2009.

[88]   D. Cárdenas-García, "Design and construction of a gallium fixed-point blackbody at CENAM," vol. 61, no. APRIL, pp. 74–76, 2015.

[89]   B. A. Wielicki, D. F. Young, M. G. Mlynczak, K. J. Thome, S. Leroy, J. Corliss, J. G. Anderson, C. O. Ao, R. Bantges, F. Best, K. Bowman, H. Brindley, J. J. Butler, W. Collins, J. A. Dykema, D. R. Doelling, D. R. Feldman, N. Fox, X. Huang, R. Holz, Y. Huang, Z. Jin, D. Jennings, D. G. Johnson, K. Jucks, S. Kato, D. B. Kirk-Davidoff, R. Knuteson, G. Kopp, D. P. Kratz, X. Liu, C. Lukashin, A. J. Mannucci, N. Phojanamongkolkij, P. Pilewskie, V. Ramaswamy, H. Revercomb, J. Rice, Y. Roberts, C. M. Roithmayr, F. Rose, S. Sandford, E. L. Shirley, W. L. Smith, B. Soden, P. W. Speth, W. Sun, P. C. Taylor, D. Tobin, and X. Xiong, "Achieving climate change absolute accuracy in orbit," *Bull. Am. Meteorol. Soc.*, vol. 94, no. 10, pp. 1519–1539, 2013.

[90]   B. Chu, H. McEvoy, and J. W. Andrews, "The NPL reference sources of blackbody radiation," *Meas. Sci. Technol.*, vol. 5, no. 1, p. 12, 1994.

[91]   S. A. Ogarev, M. L. Samoylov, N. A. Parfentyev, and V. I. Sapritsky, "Low-temperature blackbodies for IR calibrations in a medium-background environment," *Int. J. Thermophys.*, vol. 30, no. 1, pp. 77–97, 2009.

[92]   D. Cárdenas-García and E. Méndez-Lango, "The influence of the spectral emissivity of flat-plate calibrators on the calibration of IR thermometers," vol. 8, pp. 752–756, 2013.

[93]   F. Liebmann, "A Study on the Effects of Bandwidth of IR Thermometry Measurements," in *NCSL International Workshop and Symposium*, 2009.

[94]   F. Liebmann, "Infrared Thermometer Calibration," *Cal Lab Int. J. Metrol.*, pp. 20–22, 2011.

[95]   "EN 12470-5: Clinical thermometers - Part 5: Performance of infra-red ear thermometers (with maximum device)." CEN, Brussels, 2003.

[96]   A. Miklavec, V. Batagelj, J. Bojkovski, I. Pusnik, and J. Drnovšek, "Automated

Calibration Bench for Calibration of Radiation Thermometers," in *XIX IMEKO World Congress Fundamental and Applied Metrology*, 2009, pp. 1154–1157.

[97] I. Pusnik, J. Bojkovski, V. Batagelj, and J. Dmovsek, "TRACEABILITY OF RADIATION THERMOMETRY IN SLOVENIA," in *TEMPMEKO*, 2001, pp. 747–750.

[98] O. Struß, "Transfer radiation thermometer covering the temperature range from -50 ˚C to 1000 ˚C," *AIP Conf. Proc.*, vol. 684, pp. 565–570, 2003.

[99] D. Mac Lochlainn, D. Fleming, P. Cromwell, and M. White, "TP-NM-33 Rev.1.4: Calibration and routine monitoring of standard PRTs." NSAI National Metrology Laboratory, Dublin, 2016.

[100] P. Saunders, "Dealing with the size-of-source effect in the calibration of direct-reading radiation thermometers," in *AIP Conf. Proc.*, 2013, vol. 619, pp. 619–624.

[101] Drnovšek, Janko, I. Pusnik, and J. Bojkovski, "LMK _CP_RADT_06.01 Procedure for calibration of radiation thermometers and thermal imagers." Laboratory of Metrology and Quality, University of Ljubljana, Ljubljana, 2012.

[102] P. Saunders, J. Fischer, M. Sadli, M. Battuello, C. W. Park, Z. Yuan, H. W. Yoon, W. Li, E. Van Der Ham, F. Sakuma, J. Ishii, M. Ballico, G. Machin, N. Fox, J. Hollandt, M. Matveyev, P. Bloembergen, S. Ugur, P. Saunders, M. Sadli, M. Battuello, C. W. Park, Y. Zundong, H. W. Yoon, W. Li, E. Van Der Ham, F. Sakuma, Y. Yamada, M. Ballico, G. Machin, J. Hollandt, M. Matveyev, P. Bloembergen, S. Ugur, J. Fischer, M. Sadli, M. Battuello, C. W. Park, Z. Yuan, H. W. Yoon, W. Li, E. Van Der Ham, F. Sakuma, J. Ishii, M. Ballico, G. Machin, N. Fox, J. Hollandt, M. Matveyev, P. Bloembergen, and S. Ugur, "Uncertainty budgets for calibration of radiation thermometers below the silver point," *Int. J. Thermophys.*, vol. 29, no. 3, pp. 1066–1083, 2008.

[103] D. Mac Lochlainn, D. Fleming, P. Cromwell, M. Wolf, and M. White, "TP-NM-66 Estimation of Measurement Uncertainty for Typical Temperation Comparison." NSAI National Metrology Laboratory, Dublin, 2016.

[104] D. Cárdenas-García and E. Méndez-Lango, "Use of Radiometrically Calibrated Flat-Plate Calibrators in Calibration of Radiation Thermometers," *Int. J. Thermophys.*, vol. 36, no. 8, pp. 1775–1783, 2015.

Appendix I.   Publications and Presentations

Oral Presentations:

S. Boles, D. Mac Lochlainn, D. Fleming, I. Naydenova, S. Martin, "Developing Traceable Capabilities in Non-Contact Thermal Metrology", Annual Evaluation, DIT, Dublin, 13th May 2016.

S. Boles, I. Pušnik, D. Mac Lochlainn, D. Fleming, "A Comparison Of Blackbody Cavities in the range from -30 °C to 150 °C", Tempmeko 2016, Zakopane, Poland, 27-30th June 2016.

Poster Presentation:

S. Boles, I. Pušnik, D. Mac Lochlainn, D. Fleming, "A Case Study of the Distance Effect on a Commercial Direct-Reading Radiation Thermometer", Tempmeko 2016, Zakopane, Poland, 27-30th June 2016.

Journal Publication (pending):

S. Boles, I. Pušnik, D. Mac Lochlainn, D. Fleming, I. Naydenova, S. Martin, "Development and Characterisation of a Bath-Based Vertical Blackbody Cavity Calibration Source for the Range -30 °C to 150 °C", Elsevier Measurement, Submitted June 2016.

Development and Characterisation of a Bath-Based Vertical Blackbody Cavity Calibration Source for the Range -30 °C to 150 °C

S. Boles [a, b, *], I. Pušnik [c], D. Mac Lochlainn [a], D. Fleming [a], I. Naydenova [b], S. Martin [b]

[a] *National Standards Authority Ireland (NSAI), Dublin, Ireland*
[b] *Centre for Industrial and Engineering Optics, School of Physics, Dublin Institute of Technology, Dublin, Ireland*
[c] *Metrology Institute of the Republic of Slovenia/University of Ljubljana-Faculty of Electrical Engineering/Laboratory of Metrology and Quality (MIRS/UL-FE/LMK), Ljubljana, Slovenia*

* Corresponding author. Tel.: +353 1 808 2674; *E-mail:* Sam.Boles@NSAI.ie

A B S T R A C T

Industrial use of Radiation Thermometers (RTs) is becoming increasingly common due to the perceived advantages and wide market availability. Blackbody Cavity Radiation Sources (BCRSs) are typically used for calibration of these instruments, and these cavities are oriented horizontally in most cases. For BCRSs based in thermal baths, this necessitates the use of custom-built baths with side openings. This paper presents a unique design of vertical bath-based BCRS that may be immersed in conventional calibration baths without modifications to the baths. The method, results, and analysis of an international comparison comparing this vertical BCRS, standard horizontal BCRSs, and a previous iteration of the vertical design of BCRS are also presented. The comparison was conducted through collaboration between the Laboratory of Metrology and Quality, Slovenia (LMK) and the National Standards Authority Ireland (NSAI), with the intention of evaluating the suitability of the vertical orientation for calibration work. Transfer pyrometers and Standard Platinum Resistance Thermometers (SPRTs) were used as comparison standards. The transfer pyrometers used have spectral sensitivity from 8 μm to 14 μm in this temperature range. It was found that the vertical orientation was comparable to within 0.25 °C throughout the range to standard horizontal cavities. It was concluded that a vertical configuration is an economical alternative for calibration of RTs within the range assessed.

1. Introduction

Thermometric traceability to the International Temperature Scale of 1990 (ITS-90) is becoming a more and more common requirement for Radiation Thermometers (RTs). The principal method of linking radiation temperature measurements to contact methods is through the use of blackbody radiation sources of known emissivity. The temperature of these blackbody sources may be monitored by using conventional Standard Platinum Resistance Thermometers (SPRTs) and thermocouples in thermal contact with the source, or by using a radiation thermometer. In either case, instruments with traceability to ITS-90 are used.

Emissivity – a dimensionless quantity with values ranging from zero, for perfectly reflective surfaces, to unity for bodies that absorb all incident radiation – is a key parameter in radiation thermometry [1]. The performance of a practical BCRS is measured in terms of its spectral emissivity, ε_{cavity}, which is a ratio comparing the spectral radiance of the real body to that of an ideal blackbody, having an emissivity of unity. In order to achieve a low calibration uncertainty when calibrating a RT, a blackbody of the highest possible overall emissivity should be used. To realize such a blackbody source with a total emissivity close to unity, a blackbody cavity should have a high temperature uniformity and an opening much smaller than the cavity volume [2].

Numerous designs of BCRS exist that fulfil these requirements, utilising stirred baths, heat pipes and fixed points (phase transitions of certain high-purity materials). Cylindrical and conical shapes are most commonly used, as they can ensure a high temperature uniformity along the cavity's length. Bath-based horizontal BCRSs have been demonstrated as robust sources for the calibration of RTs

from -50 °C up to 300 °C [3,4]. Vertically oriented immersible BCRSs are used for the calibration of tympanic thermometers [5] and sometimes for ice-point checks of industrial RTs [6].

The principal advantage of using a removable immersible vertical cavity is flexibility. The BCRS may be immersed in different baths containing various temperature media. This enables the use of conventional calibration baths already in widespread use in temperature calibration labs, thus significantly reducing the cost of establishing in-house traceability of RTs to contact methods over the cavity's temperature range.

Another potential advantage of the vertical orientation relates to its use below the ambient dew point temperature. Horizontal cavities have a limitation at low temperatures due to the build-up of dew or ice on the internal walls. Typically purging with an inert gas is required to reduce this effect. In the vertical orientation, it has been observed that there is comparably less dew or ice formation, possibly due to stagnation of the air within the cavity.

Vertical cavities covering temperatures above and below those used for tympanic thermometers seem to have been largely avoided, presumably due to expected problems with convection at high temperatures, although after an extensive literature survey, no data was available to support this.

The present work was undertaken to investigate if a unique low-cost design of vertical BCRS, constructed in-house to take advantage of equipment already in-situ at NSAI, was suitable for calibration use over the temperature range from -30 °C to 150 °C. A reference RT was used to compare vertical and horizontal cavities in order to determine whether measurements from the two orientations were in agreement, once their associated uncertainties were accounted for. The two RTs used in the comparison, which were both manufactured by Heitronics (models TRT II and TRT IV.82), allowed measurements with an uncertainty ranging from 0.34 °C to 0.66 °C ($k = 2$) to be made over the temperature range of interest.

Three of the horizontal cavities used for the comparison are part of the suite of BCRSs in LMK, the national temperature standards laboratory for Slovenia. The newly-constructed NSAI vertical cavity was also compared to a similar vertical cavity that had previously been constructed at LMK. In addition, measurements were made to compare the new vertical NSAI cavity against the horizontal BCRSs in the Heitronics calibration laboratory, which is ISO 17025 accredited.

The results reported should facilitate the establishment of measurement capabilities for the calibration of RTs in NSAI and other National Metrology Institutes (NMIs).

2. Materials and Methods

2.1 BCRS Design considerations

Many RTs cover temperature ranges that span over 1000 °C. It is difficult to achieve good stability and uniformity within calibration media, even in contact thermometry, over such a wide range. Blackbody sources provide improved uncertainty and may be designed and constructed more practically when optimised over narrower temperature ranges and so an array of blackbodies is usually required. Using an array of blackbodies has other advantages like being able to calibrate at multiple temperatures simultaneously.

Two key design considerations for a practical and versatile BCRS are:

- the temperature range the cavity will cover; and
- the emissivity settings and optical characteristics of the RTs that the cavity will be used to calibrate.

RTs commonly have a limited number of emissivity settings. These settings are intended to correspond to the surface emissivity of common materials with the most commonly available setting being 0.95. If using a BCRS with an unmatched emissivity, corrections must be applied to account for this difference [7].

2.1.1 Filling the Field of View (FOV)

For a blackbody source to be of practical use for calibrating a given RT, the opening must be at least large enough to allow a RT's FOV to be filled. RT manufacturers typically specify the FOV as a ratio between the target distance and the diameter of the RT's measuring spot (spot size) at that distance, but it may also be specified as an angle. Designing a BCRS with a large aperture to accommodate large FOVs conflicts with the requirement for a small cavity opening to achieve a high cavity emissivity.
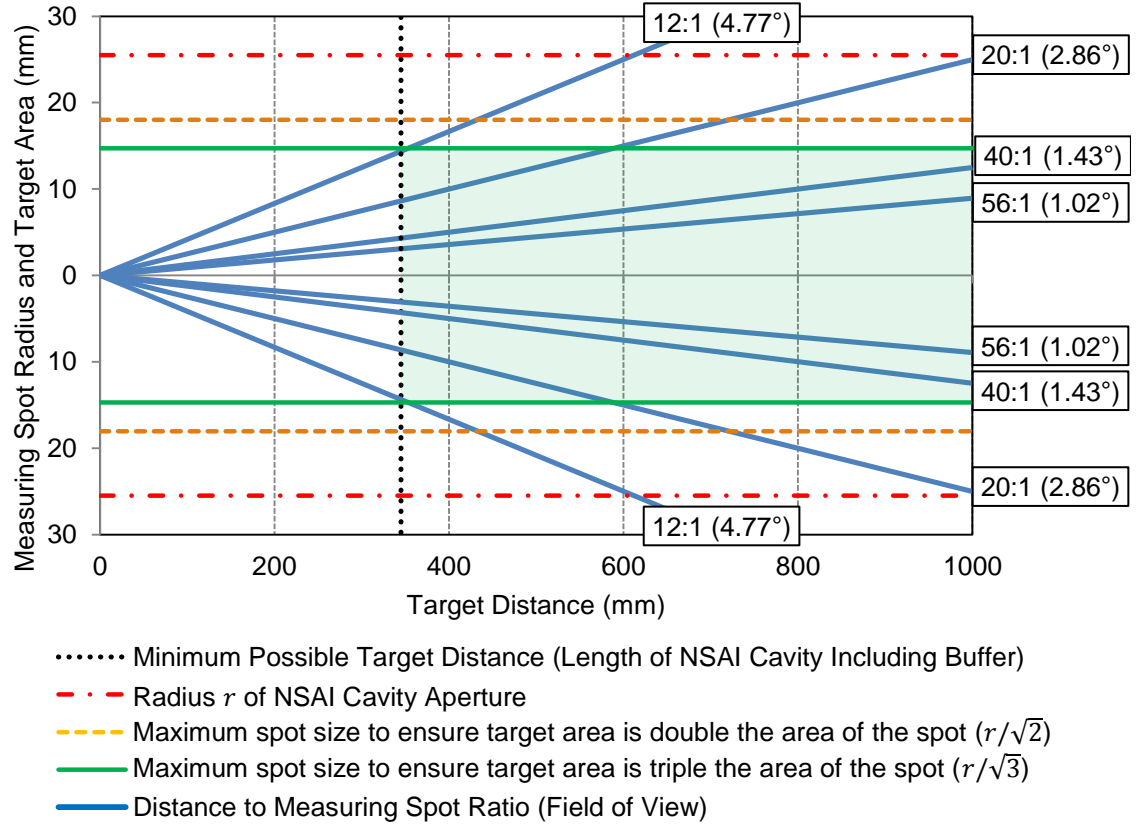
Fig. 1. Target distances and nominal spot sizes, with a selection of commonly specified fields of view (not to scale). For illustrative purposes, the FOVs are shown with the RT lenses positioned at the origin or cavity aperture and the distance to the base of the NSAI BCRS is shown. The shaded area indicates the acceptable target distances, which may be achieved by moving the RT back away from the aperture, when measuring the NSAI BCRS. The FOV of the TRT IV.82 is also shown (56:1).

Some RTs, particularly low-cost models, have large FOVs which call for very large cavity apertures. Fig. 1 shows a selection of FOVs, including FOVs commonly available on such low-cost RT models. In addition, the FOV always extends beyond the nominal spot size due to the Size-of-Source Effect (SSE), and thus a still larger source must be used so the RT receives the full signal [8,9]. Target areas double or triple the nominal spot size have been suggested as rules-of-thumb to circumvent the SSE [10,11]. The RT may be brought closer to the BCRS in order to fill its FOV, but this can present problems at extreme temperatures if convective heat transfer from the source raises or lowers the temperature of the RT's detector excessively.

A further design consideration is whether the RT will be positioned with its focal plane at the entrance to the cavity or on the cavity bottom. Focussing on the cavity aperture requires that the cavity walls have a highly uniform temperature along their length - conditions best achieved using a heat-pipe BCRS. This is because the entirety of the cavity's interior is measured and the effective emissivity of the cavity in its totality is measured. The smallest errors for bath-based cavities are often obtained when the RT is focused, as above, on the cavity bottom, as this is where the FOV is filled and the effective emissivity is highest [12].

In order to reduce the specular reflectivity of the end of the cavity, a cone shape or an inclined plane is typically used. A conical end is easy to construct if the cavity is bored out and allows simplified analysis of the emissivity, but an inclined plane is easier to construct with thin walls or using sheet materials.

2.2 The NSAI BCRS

The NSAI cavity discussed in this paper is shown in Fig. 2. The vertical NSAI BCRS was formed from commercially available copper pipe of length (l) 350 mm, with internal diameter (d) 51 mm and wall thickness 1.3 mm. The cavity bottom was cut at an angle and sealed with a flat section of copper sheet.

Fig. 1 shows common RT FOV specifications which may be calibrated with a BCRS of these dimensions. RTs with FOVs of less than 4.77°, falling within the shaded area of the graph, may be calibrated with this cavity. RTs with such large FOVs would, however, need to be positioned directly at the cavity aperture to ensure the FOV is filled. RTs with larger FOVs cannot be calibrated with this BCRS. Due to difficulties associated with calibrating RTs directly at the aperture, the NSAI BCRS is recommended for calibration of RTs with FOVs of approximately 2.86° or less.

A high emissivity on the surface of the internal walls can be achieved by using special coatings developed for this purpose. In this temperature range, Pyromark 1200 has been shown to provide a high emissivity that is robust enough to withstand the conditions of use [13]. The walls of the cavity have been sandblasted and coated with Pyromark 1200 paint on the interior. After the last painting, the paint was dried at 100 °C for more than 24 hours.

In order to increase the immersion of the cavity in the bath medium, a polytetrafluorethylene (PTFE) spacer is used in a similar approach to that in [14]. The upper range limit was decided in part due to the PTFE spacer, which was found to swell slightly at temperatures above 150 °C.
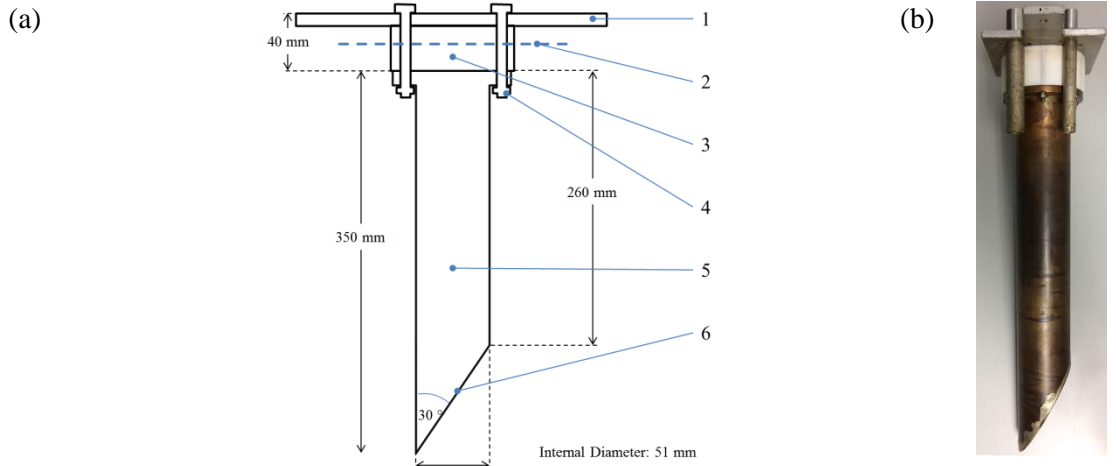
Fig. 2. The NSAI vertical BCRS (a) and (b), showing the top mounting plate and aperture (1); immersion depth (2); PTFE buffer (3); retaining bolts connecting the mounting plate, buffer and copper flange (4); copper pipe, the interior of which is coated with high emissivity paint (5) and target area (6)
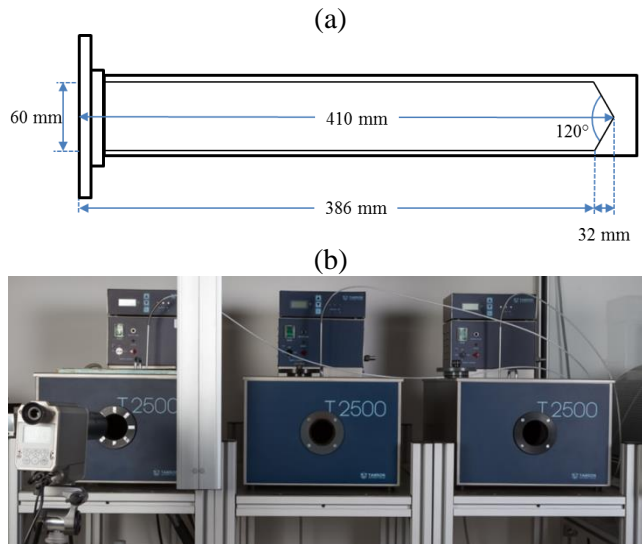
Fig. 3. Design of the LMK horizontal cavity (a) and photo showing the suite of BCRS, with the transfer radiation thermometer in the foreground on the left (b).

2.3 Description of the Comparison Cavities

The details of the baths and cavities used for the comparison are given in Table 1. Including the NSAI BCRS, two vertical cavities and five horizontal cavities were compared in terms of their radiance temperature. The vertical cavities were cylindrical with 30° inclined bottoms.

The LMK cavities were designed to cover the low temperature range from -30 °C to 150 °C. The horizontal cavities were cylindrical with conical bottoms of angle 120°. All cavities were painted with high emissivity paints and all were made of copper, apart from the LMK vertical cavity which was made of aluminium.

Besides its aluminium construction, the LMK vertical BCRS differs from the NSAI cavity in that it is slightly smaller and lacks the upper mounting plate and PTFE buffer shown in Fig. 1. The LMK vertical cavity is normally mounted with the upper part of the aluminium walls projecting 30 mm to 40 mm above the liquid level of the bath to prevent the ingress of liquid. Both vertical cavities had the same shape and equal radii to within 1.5 mm.

The TRT manufacturer used two commercially available blackbody cavities (Heitronics SW20 and SW10C) to perform the initial calibration of the TRT. These cavities produced stable temperatures and the radiance temperature was measured by the TRT. A calibration certificate was produced and supplied with the TRT to NSAI. The calibration measurements are traceable via another TRT of the same model (TRT IV.82) to Physikalisch-Technische Bundesanstalt (PTB), the German NMI. These calibration measurements were also used in the comparison.

Table 1

Properties of the various blackbody cavities compared, including the length l, diameter d and the angle at the cavity's end θ_{tip}.

BCRS Name	l (mm)	d (mm)	Shape	θ_{tip}	Estimated ε_{cavity}	Bath Medium	Range (°C)
NSAI Vertical	350	51	Cylindrical with Inclined Flat Bottom	30°	0.998	Methanol, Deionised Water, Mineral Oil	-30 to 5, 5 to 80, 80 to 150
LMK Horizontal	450	60	Cylindro-conical	120°	0.999	Ethanol water mix	-30 to 5
LMK Horizontal	450	60	Cylindro-conical	120°	0.999	Deionised Water	5 to 60
LMK Horizontal	450	60	Cylindro-conical	120°	0.999	Mineral Oil	60 to 150
LMK Vertical	310	48	Cylindrical with Inclined Flat Bottom	30°	0.998	Methanol, Deionised Water, Mineral Oil	-30 to 20, 5 to 80, 50 to 150
SW20 Horizontal	120	40	Cylindro-conical	120°	≥0.995	Deionised Water	30 to 95
SW10C Horizontal	105	25	Cylindro-conical	120°	≥0.99	*Not bath-based*	50 to 400

2.4 Comparison Method

Comparisons were undertaken firstly in LMK and later in NSAI. As with a regular RT calibration, the TRT was pointed at the BCRSs and the RT reading t_{TRT} and the traceable contact temperature t_{90} of the cavity bottom were recorded. TRT corrections were calculated as $t_{corr.} = t_{90} - t_{TRT}$.

The measurements in LMK were made with a single TRT measuring a variety of BCRSs in-house over the course of a week. The measurements in NSAI were made with a different TRT over the course of two months, starting one month after the TRT's initial calibration by the manufacturer.

For each of the measurements undertaken in LMK and NSAI, the RT was manually aligned with the axis of the BCRS using a variety of mounts to replicate practical usage conditions. The RT was positioned such that its lens was 35 mm from the aperture of the BCRS. As such, for measurements of the NSAI BCRS, the RT was focused on centre of the cavity bottom. For measurements of the LMK horizontal BCRSs, the RT's focal plane was midway along the cavity, 65 mm from the bottom. Measurements were made with the cavity diameters given in Table 1 as the defining apertures and cooled apertures were not used.

The measurements in the Heitronics laboratory were made with the RT focused on the BCRS aperture, and 36 mm and 24 mm aperture plates were used with the SW20 and SW10C BCRSs respectively.

2.5 Comparison Thermometers

The following comparison standards were used:

- The TRT II was used for measurements in LMK. The applicable temperature range of this RT is from -50 °C to 300 °C with spectral sensitivity from 8 µm to 14 µm. The pyrometer has fixed-focus optics with focal length 380 mm and nominal spot size 6.8 mm. The SSE characteristic of the RT was measured by the manufacturer using the direct method. At a target distance of 380 mm, it was found that the instrument received 99% of the signal from a 10 mm diameter target relative to the signal measured from a 50 mm diameter target.
- The TRT IV.82 was used for measurements in NSAI. This RT has a single temperature range from -50 °C to 1000 °C and spectral sensitivity from 8 µm to 14 µm. The optical characteristics are identical to those of the TRT II described above.
- A selection of calibrated SPRTs and bridges were used to make contact thermometry measurements that were traceable to ITS-90.

2.6 Vertical Cavity Measurements

In order to carry out non-contact temperature measurements of the vertical cavities, they were each immersed in turn in the baths and fixed in place.

The baths were allowed to stabilise for approximately 2 hours at each of the set-points throughout the temperature range. The stability of the baths was better than ± 0.01 °C at each set point. The bath temperature was monitored using SPRTs that were immersed beside the cavities such that the sensing element was within 40 mm of the target area at the cavity bottom. Secondary contact thermometer references were also used as crosschecks.

The cavities were then measured with a TRT. The optical axis of the RT was aligned with the axis of the cavity and the RT was positioned so that it was focused on the centre of the cavity bottom. Each measurement round consisted of ten measurements of the contact temperature and non-contact temperature references, recorded at 10 second intervals using data acquisition software.

To minimise the formation of condensation and ice at temperatures below ambient, a lid was used. The lid was kept in place when the bath was stabilising and removed prior to the TRT measurements. The exterior walls of the vertical cavities were cleaned and dried after use in each media.

2.7 Horizontal Cavity Measurements at LMK

The LMK horizontal cavities are all permanently sealed onto the sides of dedicated baths. The contact temperature was again monitored using SPRTs. The TRT was aligned manually in front of the cavity aperture, in a similar manner to that for the vertical measurements described in section 2.6.

The low temperature LMK horizontal cavity is equipped with a gas purging system to prevent ice formation on the cavity walls at temperatures below ambient. Purging was carried using nitrogen gas of 5N purity at flow rates of approximately 1 litre per minute.

3. Comparison Results

3.1 Comparison of the NSAI Vertical Cavity with Horizontal Cavities in LMK

Fig. 4 shows the comparison measurements made between the NSAI vertical BCRS and the suite of horizontal cavities in LMK. The horizontal cavities were chosen according to the temperature ranges shown in Table 1. The uncertainty of measurement was estimated based on the model suggested by the CCT-WG5 [15]. The difference between the magnitude of the TRT corrections for the vertical

8

and horizontal cavities $|t_{corr.\ vertical}| - |t_{corr.\ horizontal}|$ was less than 0.25 °C across the temperature range.
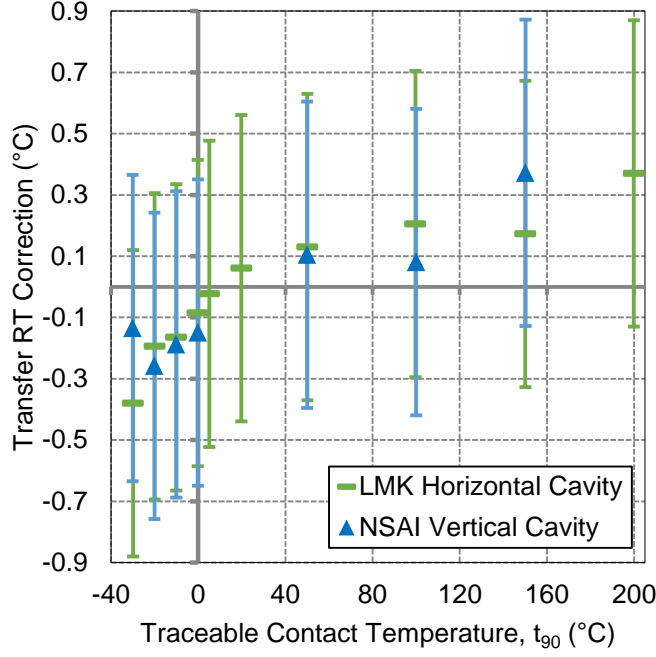
Fig. 4. Comparison of the NSAI vertical BCRS and the horizontal LMK BCRSs in the range -30 °C to 150 °C. The error bars show the estimated uncertainty ($k = 2$).

3.2 Comparison of the NSAI Vertical Cavity with Vertical Cavity in LMK

In addition to comparing the NSAI vertical cavity to horizontal cavities, it was compared to a similar vertical cavity that had previously been constructed at LMK. Both of these cavities were removable and so they could be immersed simultaneously in the same baths for the measurement experiments at the temperatures from 50 °C to 150 °C. This comparison was conducted to investigate the influences of the design differences, described in section 1.2, of the two cavities.

The results of the comparison are shown in Fig. 5. The corrections for the NSAI cavity were smaller than the LMK vertical cavity at each set point.
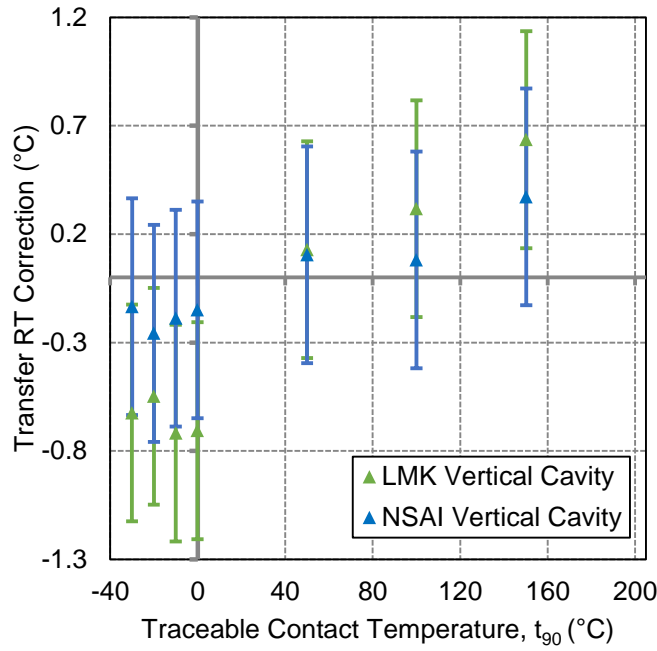
Fig. 5. Comparison of the NSAI vertical BCRS and the vertical LMK BCRSs in the range -30 °C to 150 °C. The error bars show the estimated uncertainty ($k = 2$).

3.3 Comparison of the NSAI Vertical Cavity against TRT Manufacturer's Measurements

Following the work conducted in LMK, a further comparison was made possible by NSAI's procurement of an in-house TRT. Measurements made in NSAI were compared to recent TRT calibration results received from the manufacturer.

The measurements made in NSAI were made in much the same way as those for the vertical comparisons at LMK, using upwelling baths, and traceable SPRTs and bridges. Two changes to the measurement procedure were made:

- A larger top plate was used to further reduce the possibility of the bath liquid entering the cavity and limit the influence of bath vapours on the TRT lens;
- A manually-positioned stand to mount the TRT vertically above the BCRS was used.

A summary of the uncertainty components used for the measurements made in NSAI is given in Table 2. The simplified budget follows the structure used in the CCT-WG5/08-03 document [15], with the exception of the contributions due to blackbody emissivity and repeatability, where aggregate components are used. The blackbody emissivity component comprises the isothermal and non-isothermal emissivity contributions. Values for the other contributions which were not measured are the sourced from CCT-WG5/08-03 and ASTM E2847 [16] with the most conservative values being used.

The uncertainty was evaluated in order to give a conservative estimate. The most conservative value for each of the measured components was used across the range of a given bath media. In the case of the contact measurement and cavity bottom uniformity components, the most conservative estimate was applied across the entire temperature range.

Table 2
Uncertainty values for the NSAI BCRS measured with the TRT IV.82 over the three ranges of thermal medium.

Source of uncertainty	Methanol -30 to 5 °C ± mK	Water 5 to 80 °C ± mK	Oil 80 to 150 °C ± mK
BCRS Components			
NML Contact Uncertainty of Measurement [†]	13	13	13
Blackbody Emissivity	42	42	78
Reflected Ambient Radiation	99	49	29
Cavity Bottom Heat Exchange	0	9	9
Convection Heat Loss	17	17	33
Cavity Bottom Uniformity [†]	63	63	63
Blackbody Ambient Conditions	58	58	58
RT Components			
Size-of-Source Effect	25	25	25
Reference Temperature	100	100	100
Ambient Temperature	51	51	51
Atmospheric Absorption *	33	33	59
Repeatability [†]	95	44	275
Readout Resolution	29	29	29
Combined Standard Uncertainty	209	171	330
Expanded Uncertainty ($k = 2$)	418	342	660

[†] indicates values based on measurements in NSAI
* indicates values from ASTM E2487

▲ Methanol Bath
▲ Water Bath
▲ Oil Bath
- Manuf. Calibration (Horizontal), Traceable to PTB

Fig. 6. Comparison of measurements made by the RT manufacturer of horizontal BCRSs with measurements made of the NSAI vertical BCRS. The error bars show the estimated uncertainty ($k = 2$).

4. Discussion

Overall, the results show agreement between the horizontal and vertical configurations in this temperature range.

Fig. 4 shows good agreement between the vertically and horizontally configured BCRSs at each of the temperature set points. The magnitude of the TRT corrections for the vertical cavity is larger at most but not all set points. The figure indicates that the corrections for the vertical cavity increase at

the top end of the temperature range. This could be indicative of an upper limit for this set-up. Use of a vertical cavity may cause problems in temperatures above the range of the comparison due to the effects of convection on the measuring RT.

Some ice did form on the walls of the vertical cavities near the aperture at temperatures below zero for the measurement experiments performed in LMK and NSAI. Ice formation near the target area, deeper within the cavity, however, was observed to be minimal. The TRT correction was usually negative below 0 °C.

Fig. 5 shows that the TRT corrections for the NSAI vertical cavity were smaller than those for the LMK vertical cavity, indicating an improvement in performance. Further work is needed to determine which of the design differences described in section 2.3 had an influence on the performance improvement, which was up to 0.56 °C. The NSAI vertical cavity benefited from an increased length, a design that improved immersion and therefore uniformity, a top plate around the aperture and a copper rather than aluminium construction. These are some potential reasons for the improved performance.

It should be noted that in each of the comparison figures 4, 5 and 6, any intrinsic influence on the measurements due to the TRT is not known. A relative comparison of the TRT corrections for each cavity in Fig. 4 and Fig. 5 gives an indication of this influence.

The effectiveness of the PTFE collar shown in Fig. 2 could be improved by redesigning bolting configuration so that bolts mounting alternately from the top plate and the copper flange are used, thus eliminating heat bridges as in [14].

5. Conclusions

In summary, a vertical BCRS was designed, constructed, and evaluated. The cavity was found to offer a flexible, low-cost alternative to purpose-built horizontal cavities. The new design was also found to be an improvement over the previous vertical cavity constructed at LMK. It is expected that such vertical cavities could be of use to other calibration laboratories wishing to extend the temperature range of their non-contact capabilities. A vertical orientation may also assist in the assessment of prototype cavities with different dimensions or provide additional cavities to reduce turnaround times, or for crosschecks.

The evaluated expanded uncertainties ($k = 2$) ranged from 0.66 °C when the cavity was immersed in the oil bath to 0.34 °C when immersed in the water bath. The key outcome is that the use of vertically oriented cavities is a valid method for achieving repeatable measurement traceable to ITS-90.

Acknowledgements

12

References

[1] D.P. DeWitt, G.D. Nutter, Theory and Practice of Radiation Thermometry, 1st ed., Wiley, 1988. doi:10.1002/9780470172575.

[2] J. Hartmann, High-temperature measurement techniques for the application in photometry, radiometry and thermometry, Phys. Rep. 469 (2009) 205–269. doi:10.1016/j.physrep.2008.09.001.

[3] K.D. Hill, The NRC Blackbody-Based Radiation Thermometer Calibration Facility, AIP Conf. Proc. 684 (2003) 669–674. doi:10.1063/1.1627204.

[4] P.R. Dekker, E. Van Der Ham, ITS-90 scale realization on the new radiation thermometer calibration facility at NMi VSL, Int. J. Thermophys. 29 (2008) 1001–1013. doi:10.1007/s10765-008-0420-2.

[5] R. Simpson, G. Machin, H. McEvoy, R. Rusby, Traceability and calibration in temperature measurement: a clinical necessity, J. Med. Eng. Technol. 30 (2006) 212–7. doi:10.1080/03091900600711530.

[6] J.V. Nicholas, D.R. White, Traceable Temperatures, 2nd ed., John Wiley & Sons Ltd, 2001.

[7] P. Saunders, MSL Technical Guide 22 Calibration of Infrared Thermometers, 64 (2009) 1–8.

[8] Y. Yamada, J. Ishii, Toward Reliable Industrial Radiation Thermometry, Int. J. Thermophys. (2015) 1699–1712. doi:10.1007/s10765-015-1870-y.

[9] I. Pušnik, G. Grgić, J. Drnovšek, Calculated uncertainty of temperature due to the size-of-source effect in commercial radiation thermometers, Int. J. Thermophys. 29 (2008) 322–329. doi:10.1007/s10765-007-0330-8.

[10] I. Pušnik, G. Grgić, J. Drnovšek, System for the determination of the size-of-source effect of radiation thermometers with the direct reading of temperature, Meas. Sci. Technol. 17 (2006) 1330–1336. doi:10.1088/0957-0233/17/6/007.

[11] F. Liebmann, Infrared Thermometer Calibration, Cal Lab Int. J. Metrol. (2011) 20–22. doi:10.1126/science.189.4201.483.

[12] R.E. Bedford, I. Introduction, Design of an isothermal cavity with nonuniform local instrinsic emissivities to give true blackbody radiant characteristics, (1992) 3213–3216.

[13] X. Song, K. Huan, W. Dong, J. Wang, Y. Zang, X. Shi, Research on infrared radiation characteristics of Pyromark 1200 high-temperature coating, in: M. Guina, H. Gong, Z. Niu, J. Lu (Eds.), Int. Symp. Optoelectron. Technol. Appl. 2014, International Society for Optics and Photonics, 2014: p. 93001S. doi:10.1117/12.2072577.

[14] EN 12470-5: Clinical thermometers - Part 5: Performance of infra-red ear thermometers (with maximum device), (2003).

[15] P. Saunders, J. Fischer, M. Sadli, M. Battuello, C.W. Park, Z. Yuan, H.W. Yoon, W. Li, E. Van Der Ham, F. Sakuma, J. Ishii, M. Ballico, G. Machin, N. Fox, J. Hollandt, M. Matveyev, P. Bloembergen, S. Ugur, CCT-WG5/08-03 Uncertainty budgets for calibration of radiation thermometers below the silver point, Paris, 2008. doi:10.1007/s10765-008-0385-1.

[16] ASTM E2847 − 14 Standard Test Method for Calibration and Accuracy Verification of Wideband Infrared Thermometers, i (2014) 1–17. doi:10.1520/E2847.

A Case Study of the Distance Effect on a Commercial Direct-Reading Radiation Thermometer

S. Boles [1, 2], I. Pušnik [3], D. Mac Lochlainn [1], D. Fleming [1]

[1] *National Standards Authority of Ireland (NSAI), Dublin, Ireland*
[2] *Dublin Institute of Technology (DIT), Dublin, Ireland*
[3] *Metrology Institute of the Republic of Slovenia/University of Ljubljana-Faculty of Electrical Engineering/Laboratory of Metrology and Quality (MIRS/UL-FE/LMK), Ljubljana, Slovenia*
E-mail (corresponding author): Sam.Boles@nsai.ie

1. Introduction

Despite selection, calibration and testing guides for Radiation Thermometers (RTs) being available [1,2], including some regional standards [3,4], there is no accepted standardised approach for:

- presentation of detailed RT specifications;
- determination of measurement anomalies;
- separation of these intrinsic anomalies.

- Data presented here was recorded in three different NMIs with a variety of different instrumentation.
- Different procedural approaches were observed in this study.

Size of Source (SSE) and Distance Effects (DE)

- SSE is the result of scattered radiation outside the nominal target area of the RT entering its field of view and affecting the reading.
- DE is the variation in readings due to changes in proximity of the RT's detector to the source, and has been found to have a significant influence on measurements.
- When the SSE/DE of an RT is quantified, it may be included in a calibration uncertainty budget and can facilitate more accurate measurements.

Quantification of SSE and DE

- Typically, RT is focused on the centre of an aperture placed immediately in front of the radiation source.
- Interchangeable aperture plates are used to vary the source diameter [5], and determine the Field of View (FOV).
- By varying the distance of the RT to a stable source, it is possible to quantify the DE.
- Radiative and convective heating of the RT housing and detector requires investigation.
- A filled FOV is required for both SSE and DE measurements.

Research Questions

- Can we quantify the SSE and DE of a commercial grade direct-reading RT?
- How can manufacturers clarify their specifications?

2. Materials and Methods

- A common commercial direct-reading RT was used as a test case (see specifications).
- Calibration range: -30 °C to 900 °C, 45 cm to 80 cm
- Source emissivity, ε=1. RT set to match this. Traceable SPRTs TCs used throughout.
- Transfer Radiation Thermometer (TRT) used as a check standard.
- Apparatus as described in [6] was used to measure the SSE of the Unit Under Test (UUT).

DE method

- Flat plate calibrator of ε=0.95 used to measure the DE. RT ε set to match. Laboratory ambient temperature: 21 °C ± 1 °C.
- Calibration range: 50 °C to 500 °C; 300 mm, 500 mm and 800 mm.
- Nominal UUT target diameters: 6 mm, 23 mm and 45 mm.
- Plate diameter: 150 mm (RT FOV should have been overfilled).
- Traceable TRT (Heitronics IV.82) used throughout.
- To monitor the RT's internal temperature, TC probes were placed inside the RT housing.
- Probes were placed as close as possible to the detector and lens.
- With TC probes in place, measurements of the DE were possible while ensuring that the housing temperature was within 25 °C ± 2 °C.

UUT Specifications

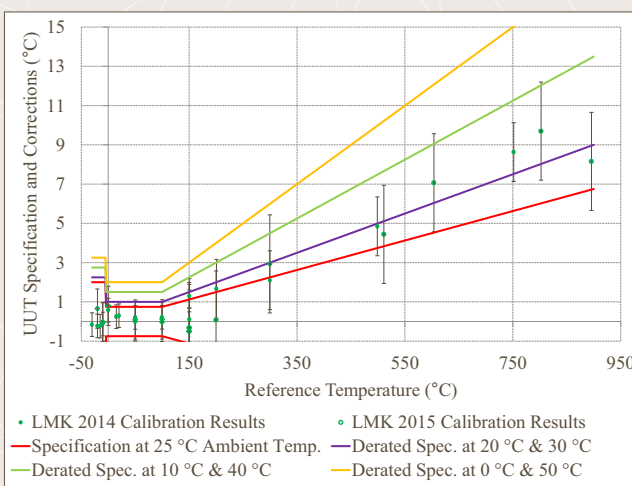| UUT Specifications	
Temperature Range	-30 °C to 900 °C
Spectral Response	8 µm to 14 µm
D:S (Distance to measurement spot diameter ratio)	50:1 (Fixed, close focus)
Min. Measurement Diameter	6 mm at 300 mm
Emissivity Setting	Adjustable in 0.01 increments from 0.10 to 1.00
Display Accuracy	± 0.75% of reading or ± 0.75 °C, whichever is greater at 25 °C ambient temperature. ± 2 °C for targets below -5 °C.
Ambient Temperature Derating	< 0.05 °C/°C or < 0.05%/°C, whichever is greater at + 25 °C ± 25 °C
Ambient Operating Range	0 °C to 50 °C

3. Results

LMK 2014 Calibration Results • LMK 2015 Calibration Results
Specification at 25 °C Ambient Temp. — Derated Spec. at 20 °C & 30 °C
Derated Spec. at 10 °C & 40 °C — Derated Spec. at 0 °C & 50 °C

Fig. 1: Graphical Spec. & Calibration Points
Outside specification above 150 °C.

50 °C, Ap. Distance: 300 mm (LMK)
150 °C, Ap. Distance: 330 mm (LMK)
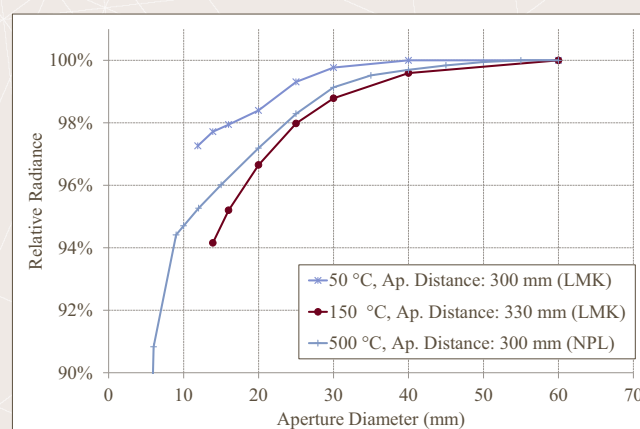500 °C, Ap. Distance: 300 mm (NPL)

Fig. 2: Size-of-Source-Effect Results
Carried out in both LMK and NPL (UK). To minimise scatter, target size must be > 30 mm, 5 times the nominal specification.
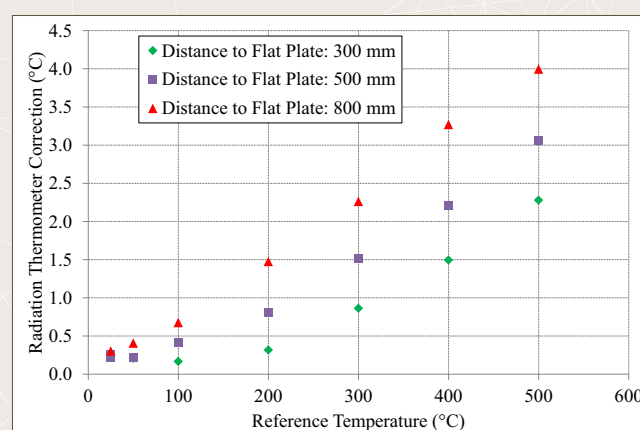

Distance to Flat Plate: 300 mm
Distance to Flat Plate: 500 mm
Distance to Flat Plate: 800 mm

Fig. 3: Distance Effect Results
DE results before equilibrium reached.

Thermocouple Placed at Detector   Thermocouple Placed at Lens

Figure 4: RT Housing

Distance to Flat Plate = 300 mm
Distance to Flat Plate = 500 mm

Lens, UUT at 300 mm
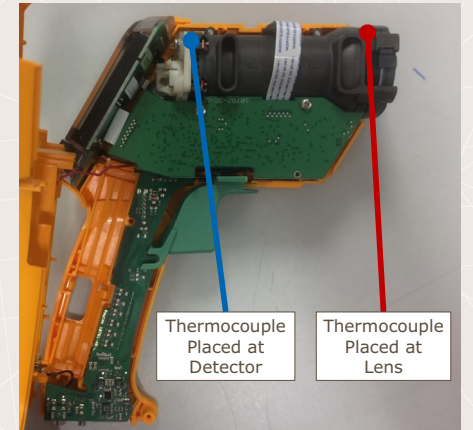Detector, UUT at 300 mm
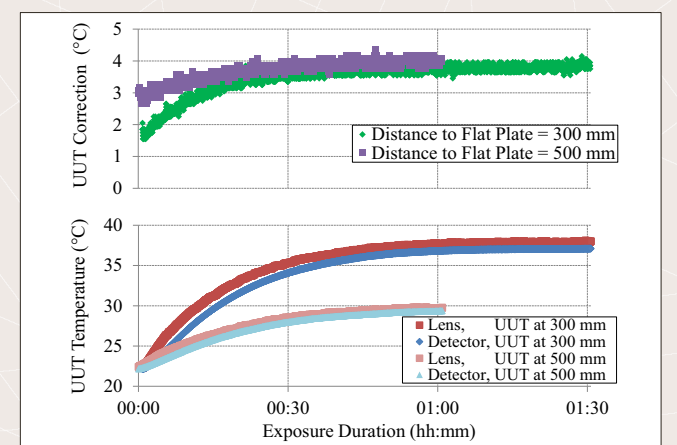Lens, UUT at 500 mm
Detector, UUT at 500 mm

Fig. 5: RT Heating Results
Corrections during equilibration with 500 °C source

4. Conclusions

- UUT demonstrated significant errors attributable to DE.
- Effects of equilibration require careful consideration.
- Good agreement shown between SSE methods.

Recommendations to Manufacturers

- RT detector temperature should be accessible to the user [7] to emphasise problems of measuring at housing temperatures above and below ambient.
- Ambient derating specifications should be clearer, for example, using graphical form (similar to Fig. 1).
- Detailed SSE specifications should be provided by manufacturers.

Recommendations for Calibration

The following questions should be asked of the client:
- What is the instrument typically used to measure and over what temperature ranges and distances?
- What is the RT exposure duration (< 1 hour or permanent) to elevated temperatures?

Different approaches were observed at NMIs due to:
- bespoke cavities and aperture apparatus utilised with a wide variety of geometries;
- use of cooled apertures for non-SSE measurements;
- inconsistent determination of the target focal plane;
- various grades of equipment received for calibration, with ambiguous specifications provided by manufacturers.

- A standardised approach for calibrating direct-reading RTs is required.
- Furthermore, measurement complexities associated with these various approaches could be limited if comprehensive specifications were provided by manufacturers.
- Ultimately, design standards specifying the minimum optical performance would be helpful to encourage the use of RTs with small FOVs and good SSE characteristics.

References

[1] Basic Principles of Non-Contact Temperature Measurement, (2009) 1–32. doi:10.1016/B978-0-12-386984-5.00002-3.
[2] Fluke 418C, 4181 Precision Infrared Calibrator Technical Guide, (2007).
[3] ASTM E2758 – 15a Standard Guide for Selection and Use of Wideband, Low Temperature Infrared Thermometers, 44 (2015).
[4] ASTM E2847 – 14 Standard Test Method for Calibration and Accuracy Verification of Wideband Infrared Thermometers, I (2014) 1–17. doi:10.1520/E2847.
[5] D. Lowe, M. Battuello, G. Machin, F. Girard, A Comparison of Size of Source Effect Measurements of Radiation Thermometers between IMGC and NPL, AIP Conf. Proc. 684 (2003) 625–630. doi:10.1063/1.1627197.
[6] I. Pušnik, G. Grgić, J. Drnovšek, System for the determination of the size-of-source effect of radiation thermometers with the direct reading of temperature, Meas. Sci. Technol. 17 (2006) 1330–1336. doi:10.1088/0957-0233/17/6/007.
[7] P. Saunders, Calibration and use of low-temperature direct-reading radiation thermometers, Meas. Sci. Technol. 20 (2009) 025104. doi:10.1088/0957-0233/20/2/025104.

Appendix II. Calibration Procedure

Calibration of Infrared Thermometers

1. Scope

This document describes the calibration of client Radiation Thermometers (RTs) using one or both of the following sources and traceability routes:

    i)   Immersible Blackbody Cavity Radiation Source (BCRS) by comparison with NML's SPRT for the range -30 °C to 160 °C.

    ii) Flat plate RT calibrator by comparison with reference RT for the range 35 °C to 500°C.

2. Applicable Documents

Manufacturer's manual for the operation of the Kambic/Heto/ASL Baths and BCRS used in the calibration.

TP-NM-89 Safety precautions when using the Liquid Baths in NML's Temperature Laboratory
TP-NM-54 Calibration of Thermometers at the Ice Point

Manufacturer's instruction manual for the Heitronics TRT IV.82 reference RT.

Manufacturer's instruction manual for the Fluke 4181 Infrared Calibration Source.

Supplemental Documents:

MSL Technical Guide 22 – Calibration of Low-Temperature Infrared Thermometers

ASTM E2847 − 14 Standard Test Method for Calibration and Accuracy Verification of Wideband Infrared Thermometers

3. Outline of Calibration Methods

The methods chosen for calibrating a given RT depend on the selected calibration points, the optical configuration of the RT, the spectral range of the RT and the ranges of the available calibration sources.

3.1 Using Immersible BCRS

The calibration is carried out at a number of temperatures by setting the bath to a specific set point and measuring the stabilised temperature of the BCRS with the reference RT and Unit Under Test (UUT) while the Standard Platinum Resistance Thermometer (SPRT) measures the bath liquid temperature for traceability. In order to do so, the SPRT is connected to one of NML's reference temperature meters. The BCRS may be used with RTs of any spectral responsivity.

3.2 Using Flat Plate RT Calibrator

For higher temperatures and for RTs with a larger Field of View (FOV), a flat plate calibration source is used. The calibrator consists of a vertically mounted flat plate with a black coating of known emissivity. Traceability is to a reference RT. Measurements are taken using the reference RT for comparison with the thermometer under calibration. The flat plate calibration source is designed for use with RTs with a spectral responsivity of 8 μm to 14 μm. The

NSAI NML

SOP Temperature		Reference	TP-NM-94
		Page	Page 2 of 6
Process Leader	Technical Manager	Revision	1.2
Calibration of Infrared Thermometers		Approved	P. Hetherington

spectral responsivity reference RT and UUT must match this (unless a correction is applied, but this is beyond the scope of this procedure).

4. Equipment

- Heitronics TRT IV.82 (or similar) Reference RT
- Calibrated SPRT
- Reference Temperature Meter
- Calibration Bath
- Immersible BCRS(s)
- Secondary Reference
- Ancillary rail/rack mounting equipment
- Fluke 4181 Precision Infrared (Flat Plate) Calibrator

5. Traceability

Before commencing the calibration, check calibration label on all measuring equipment and standards to ensure each item is in calibration.

6. Calibration Points and Client Questionnaire

Three calibration points are recommended as a minimum. The calibration points should be evenly spaced throughout the UUT range unless otherwise specified by the client.

In order to tailor the calibration procedure to suit the client's needs, the following questions are suggested:
- Has the RT been calibrated before and, if so, is can the previous certificate be supplied?
- What is the usage environment of the RT and what is its exposure to dust, dirt and grease?
- What is the RT typically used to measure and what sizes of targets are used?
    - What is the most common measurement distance?
    - What emissivity settings are used?
    - What range of temperatures is encountered?
- What accessories (including power supplies and any thermal-shielding apparatus) are normally used with the RT?
    What is the instrument user's approach to lens cleaning?

7. Calibration Procedure

7.1 Preliminary Inspection of RT Under Test

The UUT should be checked with respect to its available emissivity settings, lens condition, general operation, target distance to target diameter ratio(s) (also known as distance to spot or D:S ratio) and possible mounting configurations. Relevant anomalies, particularly the condition of the optics should be recorded. Calibration technicians should avoid contact with RT lenses. Cleaning should only be undertaken in accordance with manufacturer's instructions and by agreement of the instrument owner.

7.2 Emissivity Settings

The reference RT and UUT emissivity settings should be set as close as possible to the reference emissivity value for the calibration source.

For both types of calibration detailed below, the instrumental emissivity setting $\varepsilon_{\text{instr}}$ (the setting of the UUT), should be recorded with each the measurement run. The reference emissivity value for the source ε_{s} may also be recorded. Note that where it is not possible to match the instrumental emissivity with that of the source, a correction should be applied. The correction at each required temperature may be calculated using the spreadsheet:

S:_Special Access\TEMPERATURE\Infrared Thermometry\tg22-blackbodycorrections.xls

7.3 Selecting a Target Distance

The Target Distance (TD) is the distance between the radiation source and the optics of the RT. This distance may be measured from another point, for example a datum mark ϕ, if indicated in the manufacturer's manual. On the other end, at the radiation source, the distance is measured from the base of a BCRS or from the surface of a flat plate calibrator.

Note that the surface of the flat plate should never be touched. A recessed area at the base of the cavity, which is at the same depth relative to the housing as the plate, may be used for the purposes of measuring the TD.

For an RT with a converging optical region such as the Fluke 574 CF, there is a minimum target area (spot size) that occurs at a particular TD (300 mm in the case of the 574). Beyond this TD, the target area increases. RTs with diverging optics will have target area that only increases with TD. Wherever possible, the TD should be chosen such that the UUT's target area is less than half the area of the calibration source.

If the TD is too small, the RT may heat up due to convection and radiation from the source. RTs use measurements of their internal temperature to calculate the indicated temperature of the source. As such, the body of the RT should be maintained, to the best extent possible, at room temperature.

If the RT is calibrated over a wide range, more than one TD may be used. For example, a short TD may be used for low temperature test points and a large TD may be used for higher test points.

The TD should be recorded with each of the measurement runs.

7.4 Mounting

Use of the NSAI vertical mount is recommended with vertical measurements, and tripods or the optical breadboard and horizontal stands are recommended for use with the flat plate calibrator. Handheld use is also acceptable where the source is large with respect to the FOV of the RT.

7.5 Exposure Duration

The RT is assumed to be operated in an instantaneous manner unless otherwise indicated by the client. As such, in most cases, measurements should be taken instantaneously before the RT equilibrates with the source. If the RT reading is found to change predictably with exposure duration, the exposure duration should recorded and should be quoted on the certificate with a concise outline of the method for the calibration.

The duration of the measurement will influence the type of mounting used and a larger

NSAI NML

SOP Temperature		Reference	TP-NM-94
		Page	Page 4 of 6
Process Leader	Technical Manager	Revision	1.2
Calibration of Infrared Thermometers		Approved	P. Hetherington

specification may apply, depending on the instrument temperature.

7.6 Using Immersible Black Body Calibration Source

The lid of the cavity may be kept in place when measurements are not in progress. Particular care should be taken when changing the level of liquid in the bath or moving wet contact probes in the vicinity of the BCRS to ensure that no liquids or solid objects make contact with the cavity surface. Care should also be taken to ensure the cavity aperture is kept covered at temperatures below the dew point to prevent the formation of dew or ice inside the cavity.

A stabilisation period should be allowed after removing the cavity lid. This may be up to 15 minutes at 150 °C, depending on the SSE of the UUT. The temperature near the base will remain relatively constant after removing the lid but the temperature of the cavity near the aperture will need some time to equilibrate.

The Bath/BCRS should be operated in accordance with the manufacturer's instruction manual. The bath should be filled with the correct liquid, to an appropriate depth, not above the BCRS edge while the bath is in operation.

Set the bath temperature controller to the first required temperature set point, usually the lowest. Allow for expansion of the liquid to ensure it does not accidentally overflow into the BCRS.

The reference RT and UUT emissivity settings should be set as close as possible to the reference emissivity value for the BCRS.

Note that if a nominal reference temperature is desired and there is a mismatch between the source emissivity value and the available emissivity settings on the UUT, the set point temperature should be corrected for emissivity differences before measuring. For example, where the highest emissivity setting for the UUT is 0.95, and the reference value for the calibration source is 1.00, the corrected reference temperature at 50 °C is 51.26 °C (where spectral bandwidth = 8 – 14 μm; $T_{ambient} = T_{detector} = 22.0$ °C).

The SPRT and Bridge are operated in accordance with the manufacturer's instructions. The SPRT should be placed just next to the immersible BCRS in the bath to a minimum immersion depth of 200 mm, or at the minimum immersion depth advised by the manufacturer. Where the BCRS is used at the ice point, procedure TP-NM-54 should be followed and the cavity should be sufficiently immersed in the ice. The secondary reference should be situated in the liquid/ice next to the BCRS. The immersed tips of both the SPRT and secondary reference should be as close as possible to the centre point of the base of the BCRS.

The bath temperature is set to the first calibration point and the controls are fine-tuned until the thermometer under test indicates a reading near to the first set point.

The UUT is positioned above the entrance to the cavity at a distance such that its target area is less than half the area of the base. The optical axis of the UUT should pass through the centre of the entrance to the BCRS to the centre of the base. Coarse positioning may be achieved using the laser or optical sighting of the UUT. More precise positioning may be possible using the UUT indication. This may be necessary where the UUT's targeting system is not aligned with the sensor optics.

With the UUT permanently switched on, the UUT indication may be used for positioning as

follows:
1. Note the location of a sharp change in indicated temperature on the left hand edge of the cavity entrance.
2. Note the location the same sharp change in indicated temperature on the right hand edge of the cavity entrance. Use the midpoint for the left-right axis.
3. Repeat the previous two steps for the upper and lower edges of the cavity entrance.

UUTs with a trigger-type push-button may be permanently switched on by depressing the switch with a reusable cable tie.

The source type, ambient conditions in the lab, the TD and the emissivity settings of the UUT and the reference RT (where used) should be recorded.

When the reference thermometer reading has stabilised, and with the cavity lid removed, a set of at least 5 readings are taken from the Bridge/SPRT, the reference RT (where used) and the UUT.

The procedure detailed above is repeated for the remaining calibration points falling within the range of the Bath/BCRS.

7.7 Using Flat Plate RT Calibration Source

Note: The surface of the flat plate is delicate and exposed part of the calibration system. It should not be touched as to do so could alter its spectral emissivity.

The flat plate should be positioned such that it is not facing a window or any other sources of radiation. Any radiation other than room temperature radiation reflecting off of the plate will contribute to error in the measurement.

The flat plate calibrator is switched on and set to the lowest chosen set point. A mounting configuration should be chosen such that the reference RT is aligned with its optical axis normal to the centre of the flat plate. The flat plate cover, which has a mark to indicate the centre, may be used for this purpose. The reference RT should be positioned at the TD selected as per 7.3. A similar mounting configuration should be arranged for the UUT.

The comparison measurements may be taken with the reference RT and the UUT being moved into position in alternately, or both RTs may be positioned adjacent to and either side of the axis normal to the flat plate's centre (so long as in both cases the FOV is overfilled). In some cases, the flat plate may be used as a transfer standard, where the reference RT is used to measure the flat plate temperature before and after the UUT measurements, with the temperature reading on the flat plate recorded throughout. The method used should be noted.

The ambient temperature of the lab, the TD and the emissivity settings of the reference RT and the UUT should be recorded.

When both the flat plate's internal thermometer and both RTs have stabilised at the set point, the lid is removed and a set of at least 5 readings are taken from the reference RT and the UUT. Reading(s) from the flat plate's internal thermometer may also be recorded.

The procedure detailed above is repeated for the remaining calibration points to be performed using the flat plate calibrator.

7.8 Size of Source Effect Measurement

Where SSE data for an RT model are known, it may be included as a component in the uncertainty budget.

8. Calibration Certificate

Calibration certificates should state the source temperature (or the corrected source temperature), RT readings, the TD, the emissivity setting of the RT and the diameter of the source.

9. Uncertainty

The uncertainty budgets associated with the calibration can be found in the excel documents on sharepoint associated with this procedure.

Link to document.

Appendix III. Calibration Certificates

Certificate of Calibration

Issued to	Sample Company
	Sample Address 1
	Sample Address 2
Attention	Sample Customer

Certificate Number	Sample Certificate Number
Date Received	Sample Date
Manufacturer	Testo
Instrument	Thermometer
Model	810
Serial Number	Sample Serial Number
Client ID Number	Sample ID Number
Instrument Range	-30 °C to +300 °C (Infrared Sensor)
Calibrated Range	+30 to +90 °C
Resolution	0.1 °C
D : S Ratio	6 : 1
Order Number	Sample Order Number
NML Procedure Number	TP-NM-94
Calibration Standards	Heitronics TRT IV.82, ID: 0237, Due Date: 18 Jan 2017

Calibrated by	Sam Boles	Approved by	Paul Hetherington
	Dubhaltach Mac Lochlainn		
Date of Calibration	18 Feb 2016	Date of Issue	

Standard Terms & Conditions for Calibration, Testing and Consultancy Assignments

1. Reports issued by the National Metrology Laboratory Division of NSAI are copyright to NSAI and shall not be used, either in whole or in part, for the purposes of advertising, publicity or litigation without the written consent of the Chief Executive or his nominee.

2. No action or legal proceeding shall be taken (except in the case of wilful neglect or default) against NSAI or the Board or any member of the Board or any committee appointed by the Board or any officer or servant of NSAI, by reason of or arising out of the carrying out of any research, investigation, test or analysis or the publication of the results thereof in the name of NSAI.

3. NSAI will not release any information received from or provided to the client in relation to this report except as may be required by law, including the Freedom of Information Act 1997, or as specified by the client.

4. This certificate relates only to the item(s) described on the front page and shall not be reproduced, except in full.

5. This contract is governed by the laws of Ireland whose courts shall have exclusive jurisdiction.

Specifications

Instrument Specification ±2 °C from -30 °C to +100 °C
±2 % of reading (rest of range)

Results

Reference Reading (°C)	UUT Reading (°C)	Correction (°C)	Uncertainty (°C)
29.98	30.2	-0.22	1.1
59.97	59.9	0.07	1.1
90.00	89.3	0.70	1.1

Comments

A 25 Ω SPRT was placed adjacent to an immersible blackbody cavity source in a stabilised calibration bath. The UUT was aligned and placed a distance of 50 mm away from the centre of the cavity's 50 mm aperture.

The emissivity of the UUT was set to 0.99 to match the manufacturer's estimated emissivity value of the blackbody cavity.

The correction should be added algebraically to the instrument reading.

The reported expanded uncertainty of measurement (which includes the uncertainty of the reference temperature) is stated as the standard uncertainty of measurement multiplied by the coverage factor $k = 2$, which for a normal distribution corresponds to a coverage probability of approximately 95 %. The standard uncertainty of measurement has been determined in accordance with ISO "Guide to the expression of uncertainty in measurement".

This calibration was undertaken at an ambient laboratory temperature of 22 °C ± 4 °C

This certificate provides traceability of measurement to recognised national standards, and to the units of measurement realised at the NSAI National Metrology Laboratory (NML) or other recognised national standards laboratories in accordance with the International Temperature Scale of ITS-90.

Certificate of Calibration

Issued to	Sample Company
	Sample Address 1
	Sample Address 2
Attention	Sample Customer

Certificate Number	Sample Certificate Number
Date Received	Sample Date
Manufacturer	VWR Traceable
Instrument	Infrared Thermometer
Model	6202101
Serial Number	Sample Serial Number
Client ID Number	Sample ID Number
Instrument Range	-20 °C to 420 °C (Infrared Sensor)
Calibrated Range	35 °C to 70 °C
Resolution	1 °C
D : S Ratio	8 : 1
Order Number	Sample Order Number
NML Procedure Number	TP-NM-94
Calibration Standards	Heitronics TRT IV.82, ID: 0237, Due Date: 18 Jan 2017

Calibrated by	Sam Boles	Approved by	Paul Hetherington
	Dubhaltach Mac Lochlainn		
Date of Calibration	18 May 2016	Date of Issue	

Standard Terms & Conditions for Calibration, Testing and Consultancy Assignments

1. Reports issued by the National Metrology Laboratory Division of NSAI are copyright to NSAI and shall not be used, either in whole or in part, for the purposes of advertising, publicity or litigation without the written consent of the Chief Executive or his nominee.

2. No action or legal proceeding shall be taken (except in the case of wilful neglect or default) against NSAI or the Board or any member of the Board or any committee appointed by the Board or any officer or servant of NSAI, by reason of or arising out of the carrying out of any research, investigation, test or analysis or the publication of the results thereof in the name of NSAI.

3. NSAI will not release any information received from or provided to the client in relation to this report except as may be required by law, including the Freedom of Information Act 1997, or as specified by the client.

4. This certificate relates only to the item(s) described on the front page and shall not be reproduced, except in full.

5. This contract is governed by the laws of Ireland whose courts shall have exclusive jurisdiction.

Specifications

Instrument Specification   ±2 °C or ± 2%

Results

Reference Reading (°C)	UUT Reading (°C)	Correction (°C)	Uncertainty (± °C)
34.9	35	-0.1	1.1
50.1	50	+0.1	1.1
70.0	70	0.0	1.1

Comments

The instrument with probe was found to meet the manufacturer's specifications at the set points calibrated.

The UUT was aligned and placed a distance of approximately 112 mm away from the centre of the radiation source, which had a diameter of 150 mm. The reference radiation thermometer was placed at its focal length of approximately 380 mm from the same source.

The emissivity of the UUT was set to 0.95 to match the manufacturer's estimated emissivity value of the radiation source.

The correction should be added algebraically to the instrument reading.

This reported expanded uncertainty of measurement (which includes the uncertainty of the reference temperature) is stated as the standard uncertainty of measurement multiplied by the coverage factor $k = 2$, which for a normal distribution corresponds to a coverage probability of approximately 95 %. The standard uncertainty of measurement has been determined in accordance with ISO "Guide to the expression of uncertainty in measurement".

This calibration was undertaken at an ambient laboratory temperature of 22 °C ± 2 °C

This certificate provides traceability of measurement to recognised national standards, and to the units of measurement realised at the NSAI National Metrology Laboratory (NML) or other recognised national standards laboratories in accordance with the International Temperature Scale of ITS-90.